Transcriptional profiling of human pancreatic ductal adenocarcinoma cells in response to 10 nM 1,25-dihydroxyvitamin D_3 supplementation.

by

Shuaib Hadia

807108

Dissertation

Submitted in fulfilment of the requirements for the degree

Master of Science

in

Molecular and Cell Biology

in the Faculty of Science, University of the Witwatersrand, Johannesburg, South Africa

Supervisor: Dr Vanessa Meyer

Co-supervisor: Dr Nikki Gentle

June 2022

Table of Contents

Declaration

I, Shuaib Hadia (807108), am a student registered for the degree of Master of Science (MSc) by research in the academic year 2022. I hereby declare the following:

● I am aware that plagiarism (the use of someone else's work without their permission and/or without acknowledging the original source) is wrong.

● I confirm that the work submitted for assessment for the above degree is my own unaided work except where explicitly indicated otherwise and acknowledged.

● I have not submitted this work before for any other degree or examination at this or any other University.

● The information used in the Dissertation has not been obtained by me while employed by, or working under the aegis of, any person or organisation other than the University.

● I have followed the required conventions in referencing the thoughts and ideas of others.

● I understand that the University of the Witwatersrand may take disciplinary action against me if there is a belief that this is not my own unaided work or that I have failed to acknowledge the source of the ideas or words in my writing.

Signature: 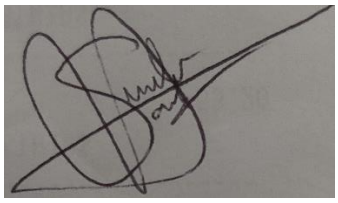 **Date:** 09 June 2022

Acknowledgements

I would like to thank my supervisors Dr Vanessa Meyer and Dr Nikki Gentle for help in conceptualising this study, and providing encouragement, advice and guidance throughout my research work. I am grateful for the opportunities that you both have provided me and hope that my work has made you proud.

Dr Meyer, I am grateful for your understanding and kindness. You made research so much fun when I joined your lab and I could not have wished for a better supervisor and mentor. Thank You.

Dr Gentle, you guided me through this bioinformatics journey and helped me develop new skill sets. Thank you.

I would like to thank my laboratory colleagues D Govender, C A Gaza, K Nyamupangedengu, M Gibson, D Cosser, and D Moonsamy for assisting me with research work, providing support and encouragement.

I would like to thank all my friends that in some way assisted me throughout my tertiary education, special mention to Luqmaan and Muhammed Yusuf.

I would like to thank the NRF for funding my MSc – grant number 122955

I would like to thank my family at large, especially my brothers, Yusuf for always supporting and helping me, and Zaydaan for thinking I'm the smartest person in the world. Most of all, I would like to thank my parents, who have supported me through all my life and encouraged and made possible for me to pursue my dreams. You both have made many sacrifices for my education, and I am so immensely grateful for you. Thank you dad for all the effort you've made and the love you've given me. Thank you mum for the love you've given me, and thank you for sharing science with me. I would not be here today without you two. The love and support of my family has carried me through my education.

To my wife Azraa, I cannot put into words how much your support and understanding meant to me through my time as a student. You have assisted me in every way possible, you calmed me when I was stressed and encouraged me when I was down. I could not have managed this research without you by my side. I am so incredibly grateful for you, my wife. Thank you.

List of figures

Figure 3.9 KEGG calcium signalling pathway linked to cell proliferation with general down-regulation of pathway constituents.

Figure 3.10 KEGG antigen processing and presentation signalling pathway linked to initiating and assisting in immune responses with general up-regulation of pathway constituents.

Figure S1 Mean estimate dispersion plots show that the DESeq2 algorithm had effectively shrunk gene estimates to reduce variance between the samples.

Figure S2 M (log ratio) A (mean average) plots show shrunken log2-fold changes shrinkage towards zero with a relatively symmetrical distribution of up and down regulated genes.

List of tables

List of abbreviations

AS	Alternative spliced
BP	Biological process
CAFs	Cancer associated fibroblasts
CC	Cellular component
CDK	Cyclin dependent kinase
cDNA	Complimentary DNA
CSCs	Cancer stem cells
DE	Differentially expressed
DEGs	Differentially expressed genes
DGE	Differential gene expression
DMSO	Dimethyl sulfoxide
DNA	Deoxyribonucleic acid
DNMT	DNA methyltransferase
E	Epithelial
ECM	Extracellular matrix
EGF	Epidermal growth factor
EMT	Epithelial-mesenchymal transition
FCS	Functional class scoring
GFs	Growth factors
GFRs	Growth factor receptors
GO	Gene ontology
GSEA	Gene set enrichment analysis

HIF	Hypoxia-inducible transcription factor
HLA	Human leukocyte antigen
IGF	Insulin-like growth factor
KEGG	Kyoto Encyclopaedia of Genes and Genomes
LFC	Log2 fold change
M	Mesenchymal
MAPK	Mitogen-activated protein kinase
MDSCs	Myeloid-derived suppressor cells
MF	Molecular function
MHC	Major histocompatibility complex class
MMP	Matrix metalloproteinases
mRNA	Messenger ribonucleic acid
miRNA	Micro ribonucleic acid
ncRNA	Non-coding RNA
NFκB	Nuclear transcription factor κB
NK	Natural killer
ORA	Over-representation analysis
PC	Pancreatic cancer
PDAC	Pancreatic ductal adenocarcinoma
PanIN	Pancreatic intraepithelial neoplasia
PanNET	Pancreatic neuroendocrine tumour
PCA	Principal component analysis
PI3K/AKT	Phosphatidylinositol 3-kinase–AKT pathway

PSCs	Pancreatic stellate cells
QC	Quality control
QM	Quasi-mesenchymal
RAF	Rapidly accelerated fibrosarcoma
RNA	Ribonucleic acid
RNA-Seq	RNA sequencing
SA	Suffix array
SVA	Surrogate variable analysis
TF	Transcription factor
TGF-β	Transforming growth factor β
TME	Tumour microenvironment
TNF-α	Tumour necrosis factor-α
TSGs	Tumour suppressor genes
$1,25(OH)_2D_3$	1,25-dihydroxyvitamin D_3;
$1,25D_3$	$1,25(OH)_2D_3$
VDR	Vitamin D receptor
VDREs	Vitamin D response elements
VEGF	Vascular endothelial growth factor

Abstract

Pancreatic cancer (PC) is the 11th most common cancer globally and the 7th leading cause of cancer related deaths worldwide. The incidence of PC is expected to rise, especially in the developing world. The most common type of PC is pancreatic ductal adenocarcinoma (PDAC), accounting for more than 85% of all PC cases. PDAC is an aggressive malignancy, presenting with a 5-year survival rate of only 9%. Transcriptional profiling has sorted PDAC into distinct subtypes with the majority being classified as either classical epithelial (E) or quasi-mesenchymal (QM). Research has shown the two subtypes to exist on a continuum with features of both subtypes present in PDAC cells, suggesting an interconversion between the cell states. This interconversion has been linked to PDAC plasticity and a heterogeneous tumour, which together contribute to the poor clinical outcome of PDAC. Vitamin D and its receptor, the vitamin D receptor (VDR), function as a transcription factor and regulator of gene expression. Vitamin D deficiency has been associated with an increased risk of developing PC. Vitamin D supplementation has been shown to modulate PDAC E and QM subtypes, and hence PDAC plasticity. Here we look at the transcriptional profile of PDAC cells taken from PDAC patients, supplemented with 10 nM biologically active vitamin D - 1,25$(OH)_2D_3$. We quantified transcript and gene-level abundance estimates from publicly available RNA-sequence data, and then performed differential gene expression (DGE) and pathway analysis on the RNA expression profiles of the PDAC samples (E: n = 3; QM n = 3). We identified genes differentially expressed in each PDAC subtype, as well as biological processes enriched from these differentially expressed genes in response to 10 nM 1,25$(OH)_2D_3$ supplementation. In total, DGE analysis yielded 1991 and 1744 DEGs (Wald Test p-value < 0.05) in the E and QM subtypes respectively in response to 10 nM 1,25$(OH)_2D_3$ supplementation. Comparing the DEGs of the PDAC subtypes revealed 335 commonly DEGs, of which 270 were contra-regulated, indicating a differential response to 1,25$(OH)_2D_3$ between the subtypes. Notably, the gene encoding the vitamin D metabolising enzyme, *CYP24A1*, was up-regulated in the E subtype in response to 1,25$(OH)_2D_3$ supplementation only. *CYP24A1* contains a vitamin D response element (VDRE) and is known to be a direct transcriptional target of liganded VDR. Various cancer-related genes, including *RAS* family genes, the *MYC* oncogene, *TGFB1* and *TGFB2*, *HIF1A* and *CCND2* were differentially expressed in both the E and QM PDAC subtypes, in response to 1,25$(OH)_2D_3$ supplementation. Biological pathways relating to activating immune

responses were up-regulated from the DEGs of both subtypes, and pathways relating to down-regulation of cell cycle were enriched from the DEGs of the E subtype. Both subtypes presented with mixed expression of epithelial and mesenchymal markers in response to $1,25(OH)_2D_3$ supplementation, showing $1,25(OH)_2D_3$ to not promote the intrinsic cell type markers of that subtype only. We noted the down-regulation of *TGFB1* and *TGFB2* in the E subtype, but up-regulation of *TGFB2* in the QM subtype. This suggests that differential *TGFB* gene expression may possibly modulate the differential response to $1,25(OH)_2D_3$ observed between the E and QM PDAC subtypes, through differential regulation of the *VDR* and EMT-related transcription factors.

Chapter 1: Literature review

1.1 Epidemiology, risk factors, and management of pancreatic cancer.

1.1.1 *Epidemiology of pancreatic cancer*

Pancreatic cancer (PC) results from pancreatic cells multiplying uncontrollably, leading to the formation of the PC mass. These PC cells have the ability to migrate to and invade other parts of the body. PC is mainly divided into two groups- cancers of the exocrine pancreas referred to pancreatic intra-epithelial neoplasia (PanIN), and cancers of the endocrine pancreas referred to as pancreatic neuroendocrine tumour (PanNET). PanINs develop from the exocrine pancreas, responsible for producing and secreting digestive enzymes and bicarbonate ions into the small intestine. PanINs account for 95% of all PC cancer cases. One particular type of PanIN, pancreatic ductal adenocarcinoma (PDAC), accounts for 90% of all PanIN cases (Bray et al., 2018). PDAC is the most malignant form of PC. PanNETs develop from the hormone producing neuroendocrine cells of the pancreas. These cells are responsible for the production and secretion of hormones including insulin, glucagon and gastrin into the bloodstream. PanNETs account for only 5% of all PC cases and present with a much better prognosis than PanINs (Bray et al., 2018; Hidalgo et al., 2015). PC is the 11th most common cancer globally (Globocan, 2018), and 24th most common cancer in South Africa (SA; National Cancer Registry, 2014). South Africa has seen a four-fold increase in the prevalence of PC from 0.46% of newly diagnosed cancer cases in 2014 to 1.9% of new cancer cases in 2018 (WHO Global Cancer Observatory, 2019; NICD, 2014). PC is the 7th leading cause of cancer related deaths worldwide (WHO Global Cancer Observatory, 2019), and its contribution to cancer related deaths is expected to increase (Pourshams et al., 2019).

PC incidence varies between countries. There is a greater prevalence of PC in more developed countries and regions with higher income (Fig. 1 A and B). Regions across Europe, North America and Australia, which are more developed and have a higher net income, present with greater age-standardised PC incidence. Regions across the less developed and poorer Africa and South-Central Asia present with a lower age-standardised PC incidence, but the PC mortality rate in these regions is much closer to its incidence (Fig. 1A). The age-standardised rate of PC incidence is greatest in Europe and North America, affecting 7.7- and 7.6 - per 100 000 people respectively (Bray et al.,

2018). The lowest rate of age-standardised PC incidence is observed in Africa, where it is estimated that PC affects only 2.2 per 100 000 people; more than three times less than what is observed in Europe and North America (Bray et al., 2018). PC is also slightly more common in men than in women, globally, affecting 5.5- and 4- per 100 000 people respectively (Bray et al., 2018). PC incidence also increases with age (*Cancer Statistics Review, 1975-2015*). Most PC cases are recorded in patients older than 55 years, with the greatest PC incidence reported in patients 70 years and older (Malvezzi *et al.*, 2016, Bosetti *et al.*, 2012). Like the majority of cancers, PC affects older people more than younger people. The age-standardised mortality rates match closely with the incidence rates of PC, reflecting the poor prognosis and fatality of the disease. PC is seldom diagnosed early enough for the effective administration of treatment, and most PC cases are detected during autopsies (Avgerinos and Björnsson, 2001, Sens *et al.*, 2009). This is because of the lack of specific early symptoms of PC development, and the difficulty and cost of tests relating to PC development screening. The majority of PC cases are diagnosed at an already advanced stage of the disease, when tumour resection and chemotherapy are less effective, adding to the poor prognosis of PC (Oberstein and Olive, 2013).

Analysis of cancer statistics have shown an increase in the incidence of PC cases and mortality, in the previous decade. An increase in PC cases in people aged between 20- and 29 years old has also been observed (Bray et al., 2018). This possibly points to PC becoming more common in younger people, as opposed to it being only common in older people, historically. GLOBOCAN estimates present a daunting PC incidence trend. GLOBOCAN estimates that PC incidence and mortality will increase significantly between now and 2040, with the greatest increases in incidence and mortality forecast for Africa, Latin America and the Caribbean, and the lowest forecast for Europe (Bray et al., 2018).

PC prognosis is poor- the five year survival rate of patients diagnosed with PC was 5 %, this increased to 9% between 2014 and 2018 (Bray et al., 2018). This shows that progress regarding PC management has been made, but there is still much to do to improve the survival rate. Despite PC being more prevalent in more developed and higher income-earning regions than less developed and lower-earning regions, the survival rates barely differ across all regions (Fig. 1B, Oberstein and Olive, 2013, Levi *et al.*, 2003). PC survival rate is influenced by many factors,

including age, sex, PC cancer type, size of the tumour at diagnosis, treatment and access to healthcare and general health and lifestyle.

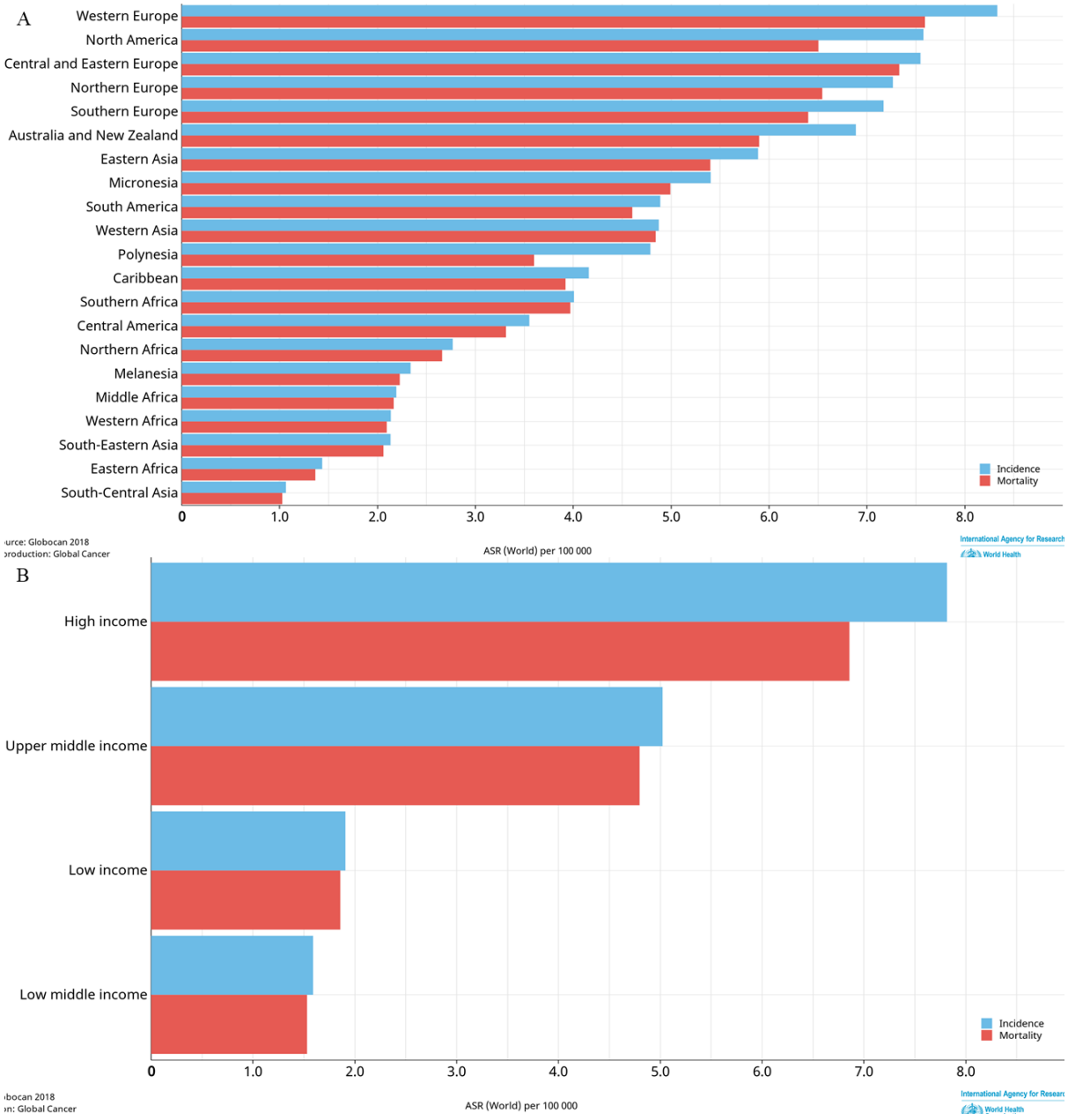

Figure 1.1 Pancreatic cancer incidence is more common in the more developed and higher-earning regions of the world. Estimated age-standardized incidence and mortality rates for pancreatic cancer across world areas (A) and income groups (B) in 2018, including both sexes and all ages (reproduced from http://globocan.iarc.fr/).

Exact reasons for the observed differences in PC incidence between the developed and less developed world remain unclear, but associations with lifestyle, PC risk factors and the environment have been made. These reasons may contribute to the observed geographical and income difference observed in PC incidence. It is also possible that detecting PC in the less developed countries is more difficult and less common, leading to a lower proportion of actual PC cases being recorded (Avgerinos and Björnsson, 2001, Mathers *et al.*, 2005). These reasons may also contribute to the expected trends in PC incidence, globally.

1.1.2 *Risk factors associated with pancreatic cancer*

PC etiology has been extensively studied, even though the relatively low incidence and survival rate of PC have posed challenges with regards to identifying PC risk factors. The majority of PC associated risk factors can be described as either modifiable or non-modifiable risk factors. The modifiable risk factors, which are lifestyle-based, include smoking, excessive alcohol consumption, diet and obesity, and occupational exposure to carcinogens. The non-modifiable PC risk factors include sex, age, ethnicity, diabetes mellitus, family history of PC and genetic factors, blood group, and chronic pancreatitis.

Tobacco smoking is considered to be the most important modifiable risk factor associated with developing PC. Multiple studies have shown strong positive associations between smoking and PC. Smokers are almost two times more likely to develop PC than non-smokers, and the risk for smoker's increases with duration of smoking and the amount of cigarettes smoked per day (Ezzati et al., 2005). Smoking prevalence has decreased in the more developed world, but remains high in the less developed countries and is increasing amongst women (Kuzmickiene et al., 2013; Mizuno et al., 2014). Various studies have made positive associations between excessive alcohol consumption and the risk of developing PC, but no association with low to moderate alcohol consumption (Wang et al., 2016). Some studies have shown > 30 g/day and > 60 g/day of alcohol to increase the risk of developing PC (Genkinger et al., 2009; Michaud et al., 2010). There is also an increased risk of developing PC in moderate alcohol consumers who also smoke tobacco (Rahman et al., 2015).

It is plausible that dietary factors would influence the risk of digestive system related diseases, including PC. Certain foods like red and processed meats, fried and nitrosamine-containing foods, and foods rich in cholesterol may increase the risk of PC (Michaud et al., 2005). Processed meats and red meat cooked at high temperatures appear most dangerous. It is possible that the nitrite compounds (and other curing agents) used to preserve processed meats and carcinogenic compounds formed on the surface of red meat cooked at high temperatures might be responsible for this (Stolzenberg-Solomon et al., 2007). Another dietary and lifestyle associated factor, obesity, has been linked to increased risks of developing various cancers, including PC. The prevalence of obesity is increasing worldwide, and studies have associated obesity with an increased risk of developing PC (Berrington de Gonzalez et al., 2003; Calle et al., 2003). Some studies have linked being overweight or obese during early adult years to an increased risk of developing PC, and that obesity in older ages is associated with a lower survival rate (Li et al., 2009). It is possible that the increasing incidence of PC is associated with the rising prevalence of obesity.

The last of the documented modifiable PC risk factors is occupational exposure to chemical carcinogens. It is approximated that 12% of PC cases are linked to exposure to metals and chemical pesticides (Bosch de Basea et al., 2011; Hartwig et al., 1994). Studies have reported increased risks of PC development linked to nickel, cadmium and arsenic exposure (Ojajärvi et al., 2000). Nickel is a carcinogenic metal, involved in the inhibition of DNA repair and generation of reactive oxygen species (Hartwig et al., 1994). Cadmium, a carcinogenic metal, has been observed to accumulate in the pancreas (Luckett et al., 2012). Cadmium is involved in the inhibition of DNA repair, in influencing the regulation of cancer associated genes, and contributes to an unstable genome. Arsenic, a carcinogenic metalloid, is toxic and can induce oxidative stress, inhibit DNA repair and mediate methylation pattern changes in cancer related genes (Reichard and Puga, 2010). Well designed, high-quality studies linking environmental, occupational and lifestyle factors and the effect it has on gene expression and PC are needed to gain deeper insight into how modifiable risk factors influence PC etiology.

The non-modifiable PC risk factors include sex, age, ethnicity, diabetes mellitus, family history of PC and genetic factors, infection, blood group, and chronic pancreatitis.

The risk of developing PC is higher in men than in women (Bray et al., 2018). The exact reasons for this observation are unknown. It is speculated that lifestyle, environmental and occupational

factors associated with PC are more commonly observed with men. These factors include smoking and excessive alcohol consumption, and increased exposure to carcinogens in the work environment. It is also possible that men have an increased genetic predisposition to developing PC, but this remains undiscovered. The risk of developing PC is also greater amongst older people, and this risk increases with age. It remains unknown why this is so. Cancer has, historically, been a disease associated with age. Knudson's two-hit hypothesis for cancer development requires loss-of-function mutations in both tumour suppressor genes, as well as oncogene activation, and this has classically been accepted to happen over time (Conroy *et al.*, 2011)(Laconi *et al.*, 2020). Certain races are also more at risk of developing PC, where studies have been conducted. Studies conducted in the United States of America found African Americans to be more at risk than Caucasian Americans, with the lowest PC incidence found in Pacific Islanders and Asian Americans (Midha et al., 2016a). The observed differences in risk and incidence of PC between the race groups have in some way been attributed to differential exposure to modifiable risk factors like diet, vitamin D insufficiency, tobacco smoking and increased alcohol consumption (Pernick et al., 2003; Silverman et al., 2003). However, certain studies have also shown PC patients of different races to have different expressions of the cancer-associated *KRAS* and *p53* genes, where biomarker immune expression and cancer-associated gene mutations were studied across Asian and Western patients (Dong et al., 2000; Song et al., 2000). This suggests the possibility of a genetic and molecular difference influencing PC risk and incidence.

Studies have reported positive associations between types I and II diabetes mellitus and the risk of developing PC (Batabyal et al., 2014; Maisonneuve and Lowenfels, 2015). PC risk has been observed to decrease with the duration of diabetes, with oral diabetic medication and insulin use associated with reducing the PC risk. The relationship between diabetes and PC risk is of interest. Diabetes onset might be used as a marker for PC, and possibly help identify people vulnerable to developing PC. It has also been suggested that diabetes may be caused by precancerous conditions and undiagnosed PC, but studies into whether diabetes onset can be a marker of or predict the onset of PC are needed (Gullo et al., 1994). The effect of blood group antigens on cancer biology has been studied and related to various cancers, including PC, where blood group has been implicated as a PC risk factor. Historically, people with non-O blood, that is, A, B and AB, are at a higher risk of developing PC, and in particular, PDAC (Wolpin et al., 2009). The suggested reason behind this observation is the altered inflammatory state and glycosyltransferase activity

between the blood groups (Wolpin et al., 2009). This altered glycosyltransferase activity has been linked to carcinogenesis by affecting cell proliferation, invasion and metastasis (Hakomori, 1999).

Chronic pancreatitis is also associated with an increased risk of developing PC. Pancreatitis results from digestive enzymes being activated in the pancreas before being released into the small intestine, causing damage and inflammation attacking the pancreas (mainly protease enzymes). Chronic pancreatitis occurs after recurrent pancreatitis, resulting in destructive inflammation that leads to impaired and/or loss of pancreatic function. Chronic pancreatitis can have idiopathic and hereditary causes, but approximately 70% of call cases are attributed to alcohol abuse, another PC risk factor (Midha et al., 2016b; Whitcomb, 2004). The largest hereditary pancreatitis study has found people with hereditary pancreatitis to have a 60 times greater risk of developing PC (Howes et al., 2004; Lowenfels et al., 2000). Chronic pancreatitis has also been thought of as a possible consequence of PC, where tumour-related ductal obstruction leads to pancreatitis by hindering the proper release of digestive enzymes into the small intestine. The link between pancreatitis and PC has been established, but it takes more than 30 years for the inflammation to manifest as PC in some pancreatitis patients (Midha et al., 2016b).

Perhaps the most important non-modifiable risk factor related to PC development is genetic factors. It is estimated that more than 10% of PC patients have some genetic predisposition to PC. Germline mutations in genes related to cancer and PC development, have been identified in hereditary PC cases. These genes include mutated forms of *BRCA1*, *BRCA2*, *CDKN2A*, *STK11*, *ATM*, *PALB2*, *MLH1*, *MSH2*, *APC*, *MSH6*, *PRSS1* and *PMS2* (Solomon et al., 2012; Vincent et al., 2011). PC has also been linked to familial cancers, including hereditary breast and ovarian cancer, Peutz-Jeghers syndrome and hereditary non-polyposis colon cancer. The presence of germline mutations in the *BRCA2* gene is the chief contributor to hereditary PC. Studies have found these mutations in 15-17% of families with familial PC (Couch et al., 2007; Murphy et al., 2002). *PALB2* is considered a PC susceptibility gene, with germline mutations of this gene found in an estimated 3% of familial PC (Jones et al., 2009; Slater et al., 2010). *KRAS*, *SMAD4* and *p53* gene mutations are also associated with increased risk of developing various cancers, including PC (Klein, 2012).

1.1.3 *Screening, diagnosis, and management of pancreatic cancer*

Despite the various risk factors implicated in PC, the deciding factor of PC outcome is the stage of the tumour at diagnosis. At the time of diagnosis, only 20% of patients have surgically resectable tumours, with most cases being locally advanced or metastatic. This bodes terribly for survival (Vincent et al., 2011). Reasons for this include the non-specific symptoms of PC onset, and abundance of vasculature surrounding the pancreas, which aids in metastasis. Seeing that PC is diagnosed late after disease onset, effective and accessible screening and diagnosis modalities are required. The relative rarity of PC makes screening of low-risk, large groups uneconomical and inefficacious. It is recommended that people meeting the familial PC risk criteria undergo screening. But how and when this should happen remains to be determined (Unger et al., 2018). There is no recommended screening modality at present, with various imaging techniques and blood markers still being assessed as PC screening modalities (Grocock et al., 2009; Shin and Canto, 2012).

Diagnosing PC is challenging because early PC is generally clinically silent, and advanced disease symptoms are non-specific. This allows for the disease to go undiagnosed in its early stages and the non-specific advanced symptoms require differentiation from a broad spectrum of diseases (De La Cruz et al., 2014). These symptoms include, anorexia and weight-loss, abdominal pain, early satiety, nausea, jaundice, pale stools and dark urine. The non-specific symptoms and array of diseases that can be attributed to these symptoms mean that PC generally goes undiagnosed, making it mainly detected during autopsies (Avgerinos and Björnsson, 2001, Sens *et al.*, 2009). Given the relative rarity of PC, physicians do not come across PC cases regularly. It is therefore important that healthcare professionals be made aware of the relevant PC symptoms and act on it appropriately, given the expected increases in PC incidence.

Surgical resection of PC tumours remains the only effective treatment modality for PC, and its effectiveness is limited to early-stage PC, prior to tumour metastasis. The addition of adjuvant chemotherapy has been shown to improve survival rates post-surgery (Neoptolemos et al., 2017, 2010). The common chemotherapeutic regimen includes gemcitabine, capecitabine, and FOLFIRINOX. FOLFIRINOX is a combination drug, consisting of Leucovorin Calcium (**Fol**inic Acid), **F**luorouracil, **Irin**otecan Hydrochloride, and **Ox**aliplatin (Conroy et al., 2011). Gemcitabine is an analogue of deoxycytidine, which is converted into its active metabolites in the cell. These

metabolites inhibit ribonuclease reductase, an enzyme crucial to generating ribonucleotides needed in DNA synthesis and compete with cytosine ribonucleotides incorporated into DNA during DNA synthesis. This results in the premature stoppage of DNA synthesis and leads to the activation of apoptotic pathways resulting in cell death (Pereira and Corrêa, 2018). Capecitabine and FOLFIRINOX both contain 5-fluoroacil, which is converted into two metabolites. These metabolites inhibit the formation of a thymine ribonucleotide precursor, thereby impairing DNA synthesis leading to cell death (Conroy *et al.*, 2011; Pereira and Corrêa, 2018). Combinations of gemcitabine/capecitabine and gemcitabine/FOLFIRINOX have shown improved chemotherapeutic efficacy (Conroy et al., 2018). Current PC treatment strategies are limited and only improve disease outcome and survival minimally. This makes the exploration of new PC treatment avenues urgent. The risk of developing PC, especially in vulnerable groups, is best mitigated by controlling the modifiable risk factors relating to lifestyle, including vitamin D sufficiency.

1.2 Pancreatic cancer and pancreatic ductal adenocarcinoma biology

1.2.1 *Hallmarks of cancer*

Cancer development is a multi-step and multi-causal process, with two key cancer enabling processes- tumour-promoting inflammation and genome instability. Together, these two cancer enabling traits lead to what have become known as the "hallmarks of cancer" (Hanahan and Weinberg, 2011, 2000). These hallmarks provide a framework for organising and understanding the molecular and cellular biology involved in the development of normal cells to cancerous cells. These hallmarks are centred on a cancer cells' ability to selectively grow and proliferate, alter its responses to stress in favour of survival, alter cellular metabolism, modulate the immune system and tumour microenvironment (TME), inhibit and avoid cell death, induce angiogenesis and tumour vascularisation, and promote tumour invasion and metastasis. Holistically, these hallmarks serve the cancer cell a purpose of attempting to attain immortalisation, continuous proliferation, and migration away from the tumour origin. It has been observed that certain biological pathways, like pathways involving the RAS oncoproteins, can influence multiple cancer hallmarks. RAS signalling pathways have been implicated in cell growth and proliferation, angiogenesis promotion, immune system and apoptosis evasion, and altered cell metabolism (Pylayeva-Gupta *et al*., 2011). It is therefore plausible that a single signalling cascade can be implicated in and influence multiple cancer hallmarks.

Cancer cells possess the ability to continuously proliferate via dysregulated growth and proliferation pathways. Normal cells control the production, release, response to, and capabilities of growth and proliferation signals. This control ensures normal cell and tissue homeostasis. In cancer cells, control over these pathways is lost by aberrant signalling imparted by the improper regulation of growth and proliferation related ligands (e.g. growth factors; GFs) and receptors (e.g. growth factor receptors; GFRs) and intracellular signalling machinery (e.g. intracellular signal transducers) and signalling molecule regulators (e.g. proteases; negative feedback machinery) leading to sustained positive cell proliferation pathway signalling. This sustained proliferative signalling can be achieved in multiple ways. Cancer cells may trigger autocrine and/or paracrine signalling. The cancer cells can produce and secrete GFs and express the GFRs, as well as influence surrounding cells to produce GFs (Hanahan and Weinberg, 2011; Witsch et al., 2010).

This signalling can also be dysregulated by affecting the cell surface receptors of proliferation-stimulating ligands. Receptor expression can be regulated to favour proliferative signalling or can be mutated into oncoprotein forms of the normal receptor resulting in sustained proliferative signalling. This can be achieved by cell-surface receptor expression being up-regulated enabling the cancer cells to maximise the use of and response to limited GFs, and the mutated receptor not requiring its ligand to activate the signalling pathway, or by causing perpetual signalling by its inability to be 'switched-off'. Cancer cells can also influence the TME in a way that promotes the sequestering of GFs. It is also possible for the cancer cells to down-regulate receptors involved in growth-inhibiting pathways (Witsch *et al*., 2010). Even though proliferative signalling can be deregulated at the cell surface, cancer cells require that the cell cycle be deregulated to allow chronic proliferation (Malumbres and Barbacid, 2009).

Mutations in genes controlling various cell cycle processes have been found to be mutated in many cancers. The most commonly mutated cell cycle controlling genes are retinoblastoma protein (*RB*) and tumour protein 53 (*TP53*) (Dick and Rubin, 2013; Stracquadanio et al., 2016). RB protein is commonly inactive in a multitude of cancers, and like RAS, its protein family functions are involved in various cancer hallmarks (Dick and Rubin, 2013). *TP53* is the most commonly mutated cancer-associated gene, muted in more than 50% of all sequenced tumours (Stracquadanio et al., 2016). *TP53* gene products are involved in various cell growth and proliferation pathways. p53 protein detects and responds to cellular stresses, including nutrient insufficiency, hypoxia, excessive signalling and genome related stress. p53 can halt cell proliferation, and where certain repairs are necessary p53 can necessitate these repairs (e.g. DNA repair to progress through the cell cycle). If the damage is irreparable, p53 can either initiate terminal differentiation resulting in the cell being unable to divide further, or cell death via an apoptotic pathway (Kruiswijk et al., 2015).

The development and progression of cancer can be viewed as a non-stop 'up-regulation' of growth promoting and metastasis potentiating pathways (oncogene activation), and a permanent 'down-regulation' of growth inhibiting and controlled cell death pathways (TSG inactivation). But this is an oversimplified view. It has been observed that certain genes can function as tumour suppressors and tumour enhances at different stages of tumour development, as well as across different cancer types. The transforming growth factor β (TGF-β) ligand is normally an 'anti-growth' ligand, but

it has been implicated in tumour progression in later stage tumours by influencing the TME and the de-differentiation of cancer cells from their origin cell type (Pickup et al., 2013). The pleiotropic effects of TGF-β suggest that cancer cells may find ways to respond to 'anti-cancer' pressures and find ways to use and influence the TME in favour of tumour progression (Katsuno et al., 2013a; Pickup et al., 2013). It has also been observed that excessively high oncogene expression in tumours, like that of the RAS, RAF and MYC oncoproteins, can induce cell senescence and/or apoptosis, rather than continuous proliferation (Collado and Serrano, 2010; Evan and d'Adda di Fagagna, 2009; Lowe et al., 2004). Cells expressing lower than excessive but still elevated levels of these oncoproteins can avoid cell senescence and continuously proliferate (Collado and Serrano, 2010). The senesced cells remain completely viable. This cell senescence induction may be a defence mechanism protecting the cell against excessive signalling along the related pathways and against apoptosis. Excessive oncogenic signalling can lead to cell senescence, however, raised but less-than-excessive oncogenic signalling points to cancer's ability to strike a balance between maximally proliferating and avoiding anti-proliferative defences.

Senescence is a state of permanent cell cycle arrest and is normally induced when cells have exhausted their replicative potential and telomeres have reached critically short lengths. Senescence serves to protect the cell from genomic insult, where further cell division could result in chromosome breakage and fusion leading to genome instability and possibly neoplastic transforming mutations (Campisi, 2013). Most premalignant lesions present with short telomeres, and the barrier of cell senescence needs to be overcome for these lesions to become fully transformed neoplastic cells (Pérez-Mancera et al., 2014; Shay, 2016). This barrier is overcome by cancer cells up-regulating the telomerase enzyme, which is responsible for lengthening the telomeres, enabling subsequent cell proliferation.

Normal cells respond to stresses where possible and are controllably eliminated to maintain healthy tissue when they cannot respond appropriately. Cancer cells are exposed to various stresses-nutrient scarcity and hypoxia in the TME, DNA damage, and in some cases, anti-cancer treatments. Seeing that an unstable genome and continuous genetic insults drive tumour progression, it is reasonable that DNA repair mechanisms are impaired in cancer. However, excessive DNA damage leads to a halt in cell cycle and could result in cell death via apoptosis induction. Some familial cancers possess germline mutations in genes involved in DNA repair, and mutations involving

repair genes have been associated with cancer risk (Goode et al., 2002; O'Connor, 2015). However, the overexpression of certain DNA repair genes (e.g. RAD-51) has been observed in tumours, and this has been linked to increased resistance to treatment, since many chemotherapeutic agents target DNA repair mechanisms (Curtin, 2012; Srivastava and Raghavan, 2015). Cancer cells' response to DNA damage is multi-dimensional, but favours cell survival and tumour progression, and this can further be exploited as a therapeutic target.

In normal tissue, cells proliferating uncontrollably and with irreparable DNA damage undergo programmed cell death via apoptosis. This control mechanism is lost in cancer cells. Apoptosis can proceed via the extrinsic and/or intrinsic pathway, both resulting in the activation of downstream effector caspases. The extrinsic pathway involves external 'stress' ligand interaction with cell-surface receptors. In cancer, the intrinsic pathway is more relevant, as it involves the cell responding to internal stresses (e.g. DNA damage). Cancer cells can evade apoptosis through an array of processes. Commonly, inactivating mutations of the *TP53* gene can result in cancer cells being desensitised to apoptotic stimuli, although p53 independent apoptotic pathways do exist as well. Genetic and epigenetic factors can influence the increased and decreased expression of anti-apoptotic and pro-apoptotic gene products respectively. Contrarily, apoptosis has also been observed to continuously take place in tumours, and this has been seen as a possible mechanism by which tumours eliminate cell lineages less suitable to tumour development and select cells that are better for cancer progression to rather proliferate (Labi and Erlacher, 2015).

Cancer cells proliferate faster than normal cells and have an increased nutrient requirement. By altering their nutrient acquisition and metabolism, cancer cells gain an advantage over normal cells and this aids in tumour progression (Cairns and Mak, 2016). Nutrient acquisition and uptake, especially of glucose and amino acids like glutamine, are deregulated. Cancer cells also differentially utilise glycolysis and tricarboxylic acid cycle intermediates, and alter metabolite-TME interactions, as well as metabolite influenced gene regulation (Cairns and Mak, 2016; Pavlova and Thompson, 2016). Cancer cells have been observed to over-metabolise glucose, even in the presence of sufficient oxygen. This preferential anaerobic glycolysis of glucose produces lactate, and is known as the 'Warburg effect' (Warburg et al., 1927). The lactate produced can make the cancer cells seem oxygen and nutrient deficient, which further promotes nutrient and oxygen uptake into the cells from the TME. This manner of energy production (glycolysis) is

actually secondary to normal oxidative phosphorylation in cancer cells but provides a selective advantage to the cancer cells over normal cells, where both energy pathways are used to meet the elevated anabolic needs of cancer. Various oncogenic genes and pathways are involved in the upregulation of the glucose transporter proteins (GLUT), enabling the increased uptake of glucose (Szablewski, 2013). HIF, BRAF and KRAS oncoproteins have been observed to increase GLUT protein expression, and so has aberrant signalling along the growth promoting phosphatidylinositol 3-kinase–AKT pathway (PI3K/AKT), whilst MYC oncoprotein has been observed to increase the expression of glutamine synthesis (Altman et al., 2016; Hay, 2016; Pavlova and Thompson, 2016).

Other mechanisms by which cancer cells are able to proliferate and survive are via modulating the TME and immune system responses. The cancer stroma is composed of the basement membrane, extracellular matrix (ECM), immune cells, cancer associated fibroblasts (CAFs), cancer stem cells (CSCs) and the surrounding vasculature. Paracrine signalling between the cancer and stromal cells develops a cancer-progressive microenvironment. TME components can foster the development of many cancer hallmarks. CAFs, for example, have been implicated in providing tumour growth and proliferative advantages, by assisting in deregulating growth signalling pathways and cell cycle checkpoints, and assisting with tumour angiogenesis and invasion via paracrine signalling. (Bhowmick et al., 2004; Franco et al., 2010; Hill et al., 2005; Quail and Joyce, 2013). The stromal cells of the TME also contribute to tumour-enabling inflammation (Greten and Grivennikov, 2019).

Cancer is founded by cells containing the genetic mutations responsible for that cancer. These tumour cells are relatively homogeneous until much later in the tumour progression pathway, when distinct clonal subpopulations develop as a result of chromic proliferation and increasing genomic instability. As a consequence of this, and even though the cancer may develop from one single cell, tumours are histopathologically diverse. A single tumour may present with varied degrees of intra-tumour cell differentiation or de-differentiation, vascularity etc. Contributing to this tumour heterogeneity are a subclass of neoplastic cells called CSCs. These CSCs have an increased ability, compared to other tumour associated cell populations, to develop new tumours (Cho and Clarke, 2008; Lobo et al., 2007). It has been postulated that these CSCs may result from the neoplastic transformation of a normal tissue stem cell, or that partially differentiated/progenitor cells may undergo neoplastic transformation causing them to assume a more stem cell-like character

(Hanahan and Weinberg, 2011). These CSCs, like normal stem cells, can self-renew and seed the development of more differentiated cell types. The CSCs provide the tumour a self-renewal mechanism, and this has posed great challenges with regard to tumour regeneration post tumour surgical resection and/or chemo/radiation-therapy, whereby CSCs can respawn the tumour. CSCs are inherently plastic, and this characteristic can support tumour progression by allowing for the generation of functionally distinct tumour cell subpopulations. For example, an epithelial-turned-mesenchymal stem cell may take on the characteristics and roles of CAFs, since mesenchymal cells can be fibroblast like (Denu et al., 2016; Singh and Settleman, 2010). Observations like these are indicative of the possibility that a tumour could use its own cells, or rather its inherent CSCs, to produce stromal cells that promote a tumour progressive TME instead of relying solely on the host's stromal cells. In this way, cancer cell subpopulations can act as tumour-supporting 'stromal cells' to provide the tumour with an abetting microenvironment.

It is thought that our immune systems destroy cells that could be cancerous every day, however, not all cancer cells are detected and destroyed by immune cells (Afshar-Sterle et al., 2014). Cancer cells develop in the presence of immune surveillance of a functioning immune system by the process of 'cancer immuno-editing' (Dunn et al., 2002). The immune system can destroy as well as shape cancer via this cancer immune-editing process. The process involves an initial 'elimination' phase, whereby cancer cells are destroyed by immune responses. An 'equilibrium' phase then follows, where more 'immune resistant' immune cells are developed by the tumour, resulting in the development of cancer cell variants with reduced immunogenicity. This equilibrium phase can be prolonged and cancer cells can develop mutations to increase the tumour's resistance to immune pressures. The final phase of immune-editing is the 'escape' phase, where certain cancer cells escape immune surveillance. These tumour cell variants can evade immune detection and destruction via genetic mutations and epigenetic alterations, assisting uncontrolled proliferation and survival (Malmberg, 2004). Stromal cells have been observed to secrete immunosuppressive factors into the TME, promoting immune evasion (Jin et al., 2016). A tumours ability to modulate the immune system is a key role-player in tumour progression, and provides a therapeutic target for cancer

As is the case with normal tissue development, tumours require new vasculature to grow and metastasise (Folkman, 1971). In cancerous compared to normal tissue, angiogenesis is deregulated in favour of tumour growth and survival. Local hypoxia is the most common angiogenesis stimulator in cancer. The endothelial cells around the cancerous tissue possess an oxygen-sensing mechanism and can activate the hypoxia-inducible transcription factor family (HIF). These TFs regulate the expression of genes involved in angiogenesis, but also genes involved in cell survival and inflammation (Yang et al., 2013). Hypoxia is a common feature of solid tumours and HIF expression is elevated in many cancers (Hashimoto and Shibasaki, 2015). The hypoxia-induced angiogenesis provides the cancer opportunities to access more nutrients and oxygen, as well as a passage for the tumour to invade, migrate and metastasise.

The ability of cancer to invade surrounding and distal tissue and spawn secondary neoplasm is the defining feature of malignant cancer. Metastasis is a multistep process. Firstly, in order for cancer cells to migrate to and invade distal sites, they must invade through the ECM, including the basement membrane, and then access the tumour vasculature. These metastatic tumour cells must then survive circulatory transport, and then burrow through the vasculature and parenchyma at the distal organ/s. the cancer cells then need to survive in their new environment, and manipulate it to from an abetting TME, after which the metastases can proliferate and grow and colonise the new tissue/organ (Massagué and Obenauf, 2016; Steeg, 2006; Valastyan and Weinberg, 2011).

The combined and individual effects of the cancer hallmarks provide the developing tumour with growth permissive and anti-growth repressive assistance, enabling tumour progression and possible metastases. The hallmarks of cancer provide a framework for understanding the development and progression of PDAC.

1.2.2 Model of pancreatic neoplasia

The development and progression of PC is a multistep and multicausal process and is classically modelled and described by the morphological and molecular transformation of non-cancerous precursor PanIN lesions (lesions prior to in-situ disease) into invasive carcinoma (Hruban et al., 2000). These PanIN lesions are divided into low to high grade lesions, based on the degree of nuclear and cellular atypia. The lesion grades 1A and 1B (low grade), 2 (intermediate) and 3 (high grade) represent structurally abnormal cells with increased nuclear and cytological atypia characterized by enlarged nuclei, nuclear crowding, loss of polarity, pseudo-stratification (single layer cells with the cells nuclei positioned in a manner suggestive of stratified cells) and hyper-chromatism (Hruban et al., 2001). The PanIN stages progress from low to high grade lesions by the accumulated genetic changes and genomic insults that drive this histopathological progression, ultimately resulting in the progression to invasive PDAC. Certain genes have been observed to play important roles in the development of PDAC. The Kirsten rat sarcoma viral oncogene homologue (*kras*) oncogene has been found mutated in grade 1 PanIN lesions, as well as oncogenic micro ribonucleic acid (miRNA) overexpression and the activation of stromal cancer-associated factors (Ferro and Falasca, 2014; Xu et al., 2016; Yonemori et al., 2017). Intermediate grade 2 PanIN lesions present with overexpressed mucin family proteins and inactivating mutations of the genes involved in the P16/ cyclin-dependant kinase inhibitor 2A (*p16*/*CDKN2A*) pathway (Tinder et al., 2008; Patra, Bardeesy and Mizukami, 2017). Inactivating mutations in the cancer-associated tumour protein 53 (*TP53*), breast cancer 2 early onset (*BRCA2*) and SMAD family member 4 (*SMAD4*) genes are associated with late, stage 3 PanIN lesions (Golan et al., 2014; Weissmueller et al., 2014). The PanIN stages are characterized by distinct patterns of molecular processes, each characterized by genetic irregularities affecting specific genes and related molecular pathways.

1.2.3 Molecular genetics of pancreatic ductal adenocarcinoma

The molecular mechanisms of PC are complex with various mechanisms, including genetic and epigenetic changes, coming into play and affecting the tissue at different stages of disease progression. The lifecycle of a cell is controlled, at least in part, by proto-oncogenes and tumour suppressor genes. Proto-oncogenes encode proteins that are involved in the regulation of cell

growth, division, migration and apoptotic inhibition, while TSGs encode proteins that are involved in the regulation of cellular senescence, DNA repair and apoptotic activation. Oncogene activation and TSG suppression and inactivation coupled with epigenetic gene regulation promotes the development of PC, through well documented classical cancer-associated genes and signalling pathways. Whole genome sequencing has been used to explore the mutational landscape of the PC genome, and has revealed many structural variants of somatic chromosomes (Waddell et al., 2015). These mutations are involved in at least 12 unique signalling pathways that are found deregulated in cancers (Waddell et al., 2015) and are vital to PC development.

KRAS is a RAS GTPase family member and its oncogenic activation is considered an initiating event in PC development. This oncogene is activated by point mutations, described by Pylayeva-Gupta *et al*. (2011). The RAS family proteins function as switches controlling intracellular signalling cascades, and are involved in processes of apoptosis, cell proliferation and differentiation, and cell adhesion and migration. Dysregulated Ras signaling from mutated KRAS causes activation of downstream oncogenic signals, which down-regulate apoptotic processes and increases cell proliferation and metastatic potential (di Magliano and Logsdon, 2013; Pylayeva-Gupta et al., 2011). Oncogenic KRAS activation can also modulate the TME by activating pancreatic stellate (PSCs) and immune cells, fostering a tumour progressive environment (di Magliano and Logsdon, 2013). Activated oncogenic KRAS employs various effector pathways, including the rapidly accelerated fibrosarcoma (RAF) – mitogen-activated protein kinase (MAPK) pathway and the phosphatidylinositide 3-Kinase/AKT pathway (PI3K/AKT).

The RAS/RAF/MAPK signal transduction pathway transduces signals from the ECM to the cell nucleus, where it regulates the expression of certain genes involved in the processes of cell growth, proliferation and differentiation, and is therefore implicated in cell cycle regulation (Dhillon et al., 2007). This pathway is also involved in the processes of cell migration and is able to stimulate angiogenesis by directly regulating the expression of genes involved in blood vessel formation (Kranenburg et al., 2004). The PI3K/AKT pathway is involved in growth factor related signal transduction cascades, including insulin-like growth factor (IGF) responses. This pathway is involved in a myriad of processes, including promoting cellular metabolism, proliferation, survival and angiogenesis (Collins and Pasca di Magliano, 2013; Rodriguez-Viciana et al., 1996). c-MYC, a proto-oncogene which regulates multiple cellular functions, is also influenced by KRAS.

Oncogenic activation of c-MYC alone is insufficient for PC development, but the concurrent oncogenic activation of KRAS with c-MYC can strongly influence tumorigenesis (Hoffman and Liebermann, 2008). c-MYC regulates the expression of proteins involved in cell metabolism, cell cycle progression and stem cell likeness of the cancer cell (Miller et al., 2012).

The nuclear transcription factor κB (NFκB), a ubiquitous TF involved in immune and inflammatory responses, as well as other cell cycle and differentiation pathways, is also associated with mutated KRAS signaling in PDAC (Sclabas et al., 2003). Pro-inflammatory cytokines and GFs activate the NFκB pathway, which results in the regulation of genes involved in cancer-associated apoptosis and immune responses, amongst other processes (Ghosh et al., 1998; Hayden and Ghosh, 2004). Upregulated oncogenic NFκB signalling has been observed in multiple cancers, where it has been postulated as a contributor to cell survival (by deregulated apoptotic induction function), angiogenesis, an inflammatory TME and invasion (Orlowski and Baldwin, 2002). A part of PDAC resistance to chemotherapy may be attributed to the NFκB pathway, as it up-regulates the anti-apoptotic BCL-2 and BCL-XL proteins (Bharti and Aggarwal, 2002; Mayo and Baldwin, 2000). The oncogenic activation of a single gene like *KRAS* can have far-reaching tumorigenic effects on a cell by affecting multiple signalling cascades.

The *p53* TSG has been found mutated, generally by missense mutations affecting the protein's DNA-binding domain, in more than half of PDAC cases (Rozenblum et al., 1997; Stracquadanio et al., 2016). Given the proliferative controlling and tumour suppressive role of p53, it is generally found mutated in late stage 3 PanIN lesions which present with greater cellular dysplasia and possess characteristics of malignant progression (Maitra et al., 2003). *p53* inactivation requires loss of function mutations in both alleles, and this possibly results in its mutation being found in late stage PanIns because the cumulative genetic damage and telomere shortening triggers TP53 DNA damage checkpoints, that need to be overcome for tumour progression. As a consequence of the loss of p53 function, cells with possible pro-carcinogenic genetic and chromosomal aberrations will be able to survive and proliferate.

The tumour suppressor p16/CDKN2A protein is involved in cell cycle regulation. The protein regulates the progression of the cell cycle from G1 into S phase by binding cyclin-dependent kinases 4 and 6 (CDK4/6) , thereby terminating their interactions with cyclin D1 (Asghar et al.,

2015). p16 inactivation results in the unrestricted progression of the cell cycle through G1/S phase, resulting in deregulated and increased cell proliferation. p16 inactivation is generally observed in early-intermediate stage PanIN lesions (stage 1 B-2) and the frequency of its inactivation increases as the PanIN lesions progress into invasive cancer (Kanda et al., 2012).

The tumour suppressor SMAD4 protein is a transcriptional regulator that transduces extracellular TGFβ signaling to the nucleus. Its chief function involves the inhibition of cell proliferation by inducing cell cycle arrest during the G1 phase. Mutated or deleted SMAD4 has been observed in later stage PC, and this has been associated with PC tumour metastases and decreased survival rates (Blackford et al., 2009; Tascilar et al., 2001; Yamada et al., 2015).

In addition to the various contributions to PC progression made by oncogene activation and TSG inactivation and/or suppression, various growth factors and their cognate receptors are aberrantly expressed in PDAC. The expression of epidermal growth factor (EGF) and its receptor (EGFR) is upregulated in PDAC, in keeping with the deregulated autocrine signalling as a cancer hallmark (Barton et al., 1991). IGF expression is upregulated in PDAC tumour and stromal cells, with oncogenic activation of the IGF receptor (IGFR) displayed in the PDAC tumour cells (Bergmann et al., 1995). IGF signalling pathways are involved in cell metabolism, promotion of cell proliferation and survival, and the promotion of angiogenesis and tumour invasion (Ouban et al., 2003; Stoeltzing et al., 2003). The vascular endothelial growth factor (VEGF), which promotes endothelial cell survival and proliferation by binding its receptor (VEGF), is overexpressed in PDAC (Itakura et al., 1997). VEGF is a key mediator of angiogenesis and its overexpression in PDAC implicates it in promoting angiogenesis and fostering tumour invasion and metastases (Seo et al., 2000).

Cancer is a multifactorial disease, and a dysregulated epigenome is at its core. The epigenome comprises all the epigenetic signatures imprinted on the genome, without changing the genome sequence- it is a heritable change in phenotype with no change to the genotype. The epigenome is strongly influenced by the cell's environment. Epigenetic regulation is a form of gene expression regulation that takes place by covalently modifying DNA and/or its associated proteins (e.g. histones), by remodelling chromatin and by non-coding RNA (ncRNA) regulation. Whole PC genome sequencing conducted by Waddell *et al*. (2015) has revealed some oncogenic as well as tumour suppressive mutations in genes encoding epigenetic regulators. DNA methylation is the

most extensively studied form of epigenetic regulation, whereby selective DNA methylation influences the accessibility of the DNA to a range of transcription regulatory mechanisms. DNA methylating reactions are carried out by the DNA methyltransferase (DNMT) group of enzymes. DNMT1/3A/3B have been found to be overexpressed in PDAC compared to healthy pancreatic tissue, and DNMT family protein expression increases with progression from early PanIN lesions to invasive cancer (Gao et al., 2013).

Certain TSGs present with methylated gene promoters in PC, including the *BRCA1*, *APC* and *p16* tumour suppressors (Robertson, 2005). The APC tumour suppressor protein is involved in the processes of cell cycle and migration, and can influence gene expression by its associations with β-catenin and the Wnt signalling pathway. *APC* promoter methylation down-regulates gene expression, leading to a suppression of its tumour suppressor function (Hankey et al., 2018). BRCA1 protein is a part of the tumour suppressor, BRCA family, of proteins involved in cell cycle regulation and DNA repair (Gudmundsdottir and Ashworth, 2006). As with aberrant *APC* promoter methylation, aberrant methylation of the *BRCA1* gene promoter is oncogenic. The activation of oncogenes and silencing of TSGs can be attributed to epigenetic regulation. Oncogenes can be actively expressed through the loss of methylation patterns, while TSGs can be repressed through the gain of methylation patterns in TSG promoter regions. This dysregulated change in methylation patterns can result in cells acquiring the ability to continuously proliferate and evade apoptosis. Aberrant methylation patterns can cause mutation development and chromosomal instability - both are characteristics of cancer (Das and Singal, 2004). A plethora of ncRNAs that can regulate the expression of cancer-associated genes, are also being discovered in PC (for review see Tang *et al.*, 2014; Peng *et al.*, 2016).

Epigenetic gene regulation provides a molecular interface between the genome and the environment. Seeing that PC risk has been associated with many epigenome-influencing factors like lifestyle and vitamin D status, makes understanding epigenetic gene regulation in PC highly important for gaining insight into PC development and as a therapeutic target.

1.2.4 The immune landscape of pancreatic ductal adenocarcinoma

The PDAC TME consists of dense ECM and proliferating stromal (mainly fibroblastic) cells (Watanabe et al., 2003). The PDAC tumour also lacks vasculature, resulting in a generally hypoxic TME and reduced drug perfusion into the tumour (Erkan et al., 2016). The ECM serves as a nutrient source for PDAC tumours, but when stromal cells that secrete ECM components are depleted, the aggressiveness of the PDAC tumour is promoted, generally via immunosuppression (Kamphorst et al., 2015; Özdemir et al., 2014). Pancreatic stellate cells, the chief PDAC cancer associated fibroblasts, facilitate the formation of fibrous tissue in the PDAC tumour, as well as being involved in apoptotic inhibition of PDAC cells and metastasis initiation (Kleeff et al., 2016). PSCs also play crucial roles in immunosuppression in the PDAC TME, by secreting pro-inflammatory cytokines (e.g. IL-6), stimulating the growth and function of myeloid-derived suppressor cells (MDSCs) and sequestering $CD8^+$ T-cells, preventing these T-cells from entering into the PDAC tumour (Mace et al., 2013). $CD8^+$ T-cells are essential for anti-tumour immunity, and PSCs blocking $CD8^+$ T-cell entrance into PDAC tumours contributes to the immunosuppressant PDAC TME (Ene-Obong et al., 2013). MDSCs are a heterogeneous group of immature myeloid cells that can release reactive oxygen and nitrogen species into the TME and thereby inhibit T-cell proliferation and migration within the TME (Ugel et al., 2015). The PDAC TME is well populated by MDSCs, a hallmark of PC (Ene-Obong et al., 2013). MDSCs can also induce PDAC T-cell tolerance by expressing inhibitory ligands such as PD-L1 and CTLA-4. (Zhang et al., 2020). In tumour cells, MDSCs have been observed to promote PD-L1 expression in an EGFR/MAPK - dependent manner, which has prompted the suggestion that by reducing MDSCs through inhibiting MAPK/ERK signalling, $CD8^+$ T-cell intra-tumoural immune activity may be improved (Zhang et al., 2017). In mouse PDAC models, knock-down of MDSCs have been shown to improve $CD8^+$ T-cell mediated apoptosis, and arrest tumour growth. It has also been shown that by depleting MDSCs, $CD8^+$ T-cell immune response is improved in tumours (Ene-Obong et al., 2013).

Neutrophils are differentially associated with PDAC immunosuppression. Neutrophils are the most abundant circulating immune cells, forming an essential part of the innate immune system. Neutrophils with the CD71 surface marker have been observed to expand in the blood and tumours of cancer patients, and these neutrophils form part of the immune-infiltrate in multiple cancers,

including PDAC (Dinh et al., 2020; Ino et al., 2013). Intra-tumour neutrophils and raised interleukin-8 levels are associated with poor outcome with regards to immune checkpoint inhibitors and decreased survival rates in advanced cancer patients (Darvin et al., 2018). Immune checkpoint inhibitors are immuno-therapeutics that inhibit immune checkpoint proteins from binding their partner proteins. Immune checkpoint proteins function to attenuate the immune response and can inhibit T-cells from killing cancer cells. By intra-tumour neutrophils decreasing the efficacy of immune checkpoint inhibitors, cancer cells can evade immune response and killing (Darvin et al., 2018).

However, neutrophils have been observed to play a bi-facetted role in cancer. Some studies have proposed tumour-associated neutrophils to be either tumour suppressing or tumour promoting (Fridlender et al., 2009). The intra-tumour neutrophil phenotype seems to be highly dependent on TGF-β signalling in the tumour cells. Researchers have shown in a lung cancer model, that inhibiting TGF-β related signalling in tumour cells leads to the recruitment and activation of tumour suppressing neutrophils which can inhibit tumour development by killing cancer cells (Fridlender et al., 2009). Conversely, exposure to TGF-β signalling has been shown to transform intra-tumour neutrophils into tumour promoting neutrophils (Fridlender et al., 2009). These neutrophils possess immunosuppressive and tumour-promoting functions, and can promote angiogenesis and tumour metastasis (Schmielau and Finn, 2001; Shojaei *et al.*, 2007). The unique and plastic stroma of PDAC allows for the differential recruitment of lymphocytes. PDAC tumours generally possess lower quantitates of anti-tumour immune cells and higher quantities of immunosuppressive cells (Jaillon et al., 2020).

1.3 The epithelial to mesenchymal transition in pancreatic cancer

1.3.1 *Epithelial to mesenchymal transition of cancer*

The poor prognosis of PC is a result of the disease progressing rapidly and it being highly metastatic. The metastatic potential of PC is associated with the developmental epithelial-to-mesenchymal transition (EMT) programme (Rhim et al., 2012). The EMT programme can be simply defined as the phenotypic transition of a cell from an epithelial (E) state into a mesenchymal (M) state. Apical-basolateral polar E cells are organised into monolayers and exhibit cell-cell

adhesion. Anterio-posterior polar M cells are spindle shaped, and possess a strong propensity for migration. During the process of EMT, polarized E cells undergo various biochemical changes, resulting in them attaining the M phenotype. The E cells lose their E-type markers, such as E-cadherin and laminin, and gain M-type markers like N-cadherin and fibronectin (Kalluri and Weinberg, 2009). The EMT programme plays diverse and critical roles in embryo development, wound healing, and tissue regeneration. In cancer, the EMT programme is involved in metastatic pathways (Huber et al., 2005). In cancer-associated EMT, some E cells have been observed to retain their respective E-type characteristics whilst also acquiring M-type like traits (Thiery, 2002). However, the EMT is not terminal. These two cell types have been observed to exist on a continuum, where the cells can interconvert between E and M states (Soon et al., 2011). The EMT in tumour progression is governed by various signalling pathways, including soluble factor like GFs (fibroblast and hepatocyte GFs; TGF-β; Wnt signalling pathway) as well as ECM components; epigenetic regulation, and alternative splicing (Thiery, 2002). These signalling pathways generally induce EMT by regulating TFs involved in the EMT programme, and these TFs repress the *CDH1* gene that encodes E-cadherin. TGF-β signalling is a key EMT-inducing factor in PC (Ellenrieder et al., 2001). The binding of TGF-β to its receptors leads to downstream activation of SMAD nuclear TF members, which can regulate the expression of EMT-associated genes, which include EMT-associated TF genes (Heldin et al., 2012; Moustakas and Heldin, 2007). In PC with inactivated SMAD4, TGF-β can still induce EMT via pathways involving ERK/MAPK and PI3K signalling pathways (Derynck and Zhang, 2003). EMT TFs include epithelial suppressor TFs, like SNAIL and ZEB proteins, as well as mesenchymal inducing TFs like, Twist and PRRX proteins (Moustakas and Heldin, 2007; Wellner et al., 2009). ZEB and SNAIL serve the EMT by repressing the expression of E-type genes, like E-cadherin.

The Wnt/β-catenin signalling pathway can also induce EMT, by suppressing a protease involved in SNAIL degradation (Clevers, 2006). Oncogenic KRAS signalling activates the Wnt/β-catenin signalling pathway, which can induce EMT (Xu et al., 2015). This observation reinforces the far-reaching oncogenic potential of one (in this case, *KRAS*) oncogenic gene.

It appears that cells undergoing EMT can acquire stem cell-like features, which possibly implicates the EMT in CSC development, and may be a means by which EMT contributes to tumour plasticity and PDACs intrinsic resistance to chemotherapy (Polireddy and Chen, 2016).

1.3.2 *Subtypes of pancreatic ductal adenocarcinoma*

Eric Collisson *et al*. (2011) put forward three subtypes of PDAC, classical (epithelial-type), quasi-mesenchymal (QM), and exocrine-like (Collisson et al., 2011a). This was accomplished by the combined analysis of transcriptional profiles of primary PDAC samples obtained from multiple studies and human and mouse PDAC cell lines. The subtypes were defined based on subtype-specific gene expression, and defined gene signatures were assigned for each subtype. The classic (E) subtype presents with elevated expression of epithelial and adhesion-associated genes, the QM subtype presents with elevated mesenchyme-associated genes, and the exocrine like subtype presents with a relatively higher expression of cancer cell derived digestive enzyme genes (Collisson et al., 2011a). This sorting of PDAC into molecular subtypes has been the standard for PDAC characterisation. Subsequent research has shown the E and QM PDAC subtypes to interconvert between each other, consistent with the EMT programme in cancer (Wang et al., 2017).

1.4 Vitamin D/VDR as a transcription factor and regulator of gene expression

1.4.1 Physiologic role of vitamin D

Vitamin D is a group of fat-soluble hormones that are responsible for an array of biological processes. The most common precursor of biologically active vitamin D, cholecalciferol, is primarily synthesised in the skin via a UVB-dependent reaction involving the vitamin D precursor, 7-dehydrocholesterol. Some vitamin D can be obtained from the diet, mainly from fish, dairy, and vitamin D fortified foods, but this is insufficient and accounts for a very small percentage of circulating vitamin D (Bikle, 2014).

Cholecalciferol undergoes hydroxylation in the liver and kidney (mainly), forming the active form calcitriol or 1,25-dihydroxyvitamin D_3 (1,25-$(OH)_2D_3$ / 1,25-D_3), which has the greatest affinity for the vitamin D receptor (VDR). Circulating 1,25-D_3 plays important physiological roles in maintaining skeletal health (via calcium homeostasis), hormone secretion (regulates secretion of parathyroid hormone, insulin, renin), modulates immune function (regulates proliferation,

differentiation, and function of immune cells), and is also involved in cell proliferation and differentiation. Intracellular 1,25-D_3 level is controlled by the 1,25-D_3 metabolising enzymes, CYP27A1 (kidney, Fig 1.2) and CYP27B1 (liver, Fig 1.2) but chiefly by CYP24A1, a vitamin D hydroxylase, which is regulated by 1,25-D_3 itself (Anderson et al., 2003; Bikle, 2010; Nishimura et al., 1994). Circulating 25-hydroxyvitamin D_3 (25-D3) level is used to assess vitamin D sufficiency. There is no consensus about how much circulating vitamin D is optimal, as vitamin D requirement seems to vary between populations (Holick, 2007). Vitamin D deficiency can be defined as having a circulating 25-D_3 level below 20 ng/mL, and vitamin D sufficiency having a circulating 25-D_3 level above 30 ng/mL (Holick, 2007). It is estimated that about one billion people across the developed and developing world are vitamin D deficient (Naeem, 2010).

1.4.2 Vitamin D as a regulator of gene expression

Vitamin D exerts its various effects via its receptor, VDR. VDR is comprised of an N-terminal DNA binding domain (via two zinc fingers), a C-terminal ligand (vitamin D) binding domain, and a 'hinge region' that connects the N- and C- terminal domains (Haussler et al., 2011; Pike and Meyer, 2010). VDR is a nuclear steroid-hormone receptor, and acts as a TF when bound to its ligand. VDR generally complexes with the retinoid X receptor (RXR), forming a heterodimer, regulating the expression of vitamin D target genes (Christakos et al., 2003). The vitamin D target genes possess certain DNA sequences known as vitamin D response elements (VDREs), which the VDR/RXR heterodimer interacts with (DeLuca, 2004). VDREs can be located upstream of the transcription start site (TSS) and/or be intronic (DeLuca, 2004). VDRE sequences can vary, but the most common VDRE sequence, also the one with the greatest VDR affinity, is a motif called DR3 (Carlberg et al., 1993). The transcription of vitamin D target genes can require the recruitment of co-regulators, which can be activating or suppressing (McKenna et al., 1999). These co-regulators are differentially expressed across cell types and tissues, providing a degree of vitamin tissue specificity with regards to its genomic actions (Bikle, 2010; Oda et al., 2003). Some VDR co-regulators include enzymes that alter chromatin accessibility, like histone acetyltransferases and deacetylases, as well as methyltransferases and demethylases which are also associated with the epigenetic effects of vitamin D (Fetahu et al., 2014). VDR-regulated genes and binding sites vary across cell types, and the binding sites are generally associated with other TFs, as well as

presenting with distinct epigenetic signatures on the histones H3 and H4 (Carlberg et al., 2012; Ernst et al., 2011).

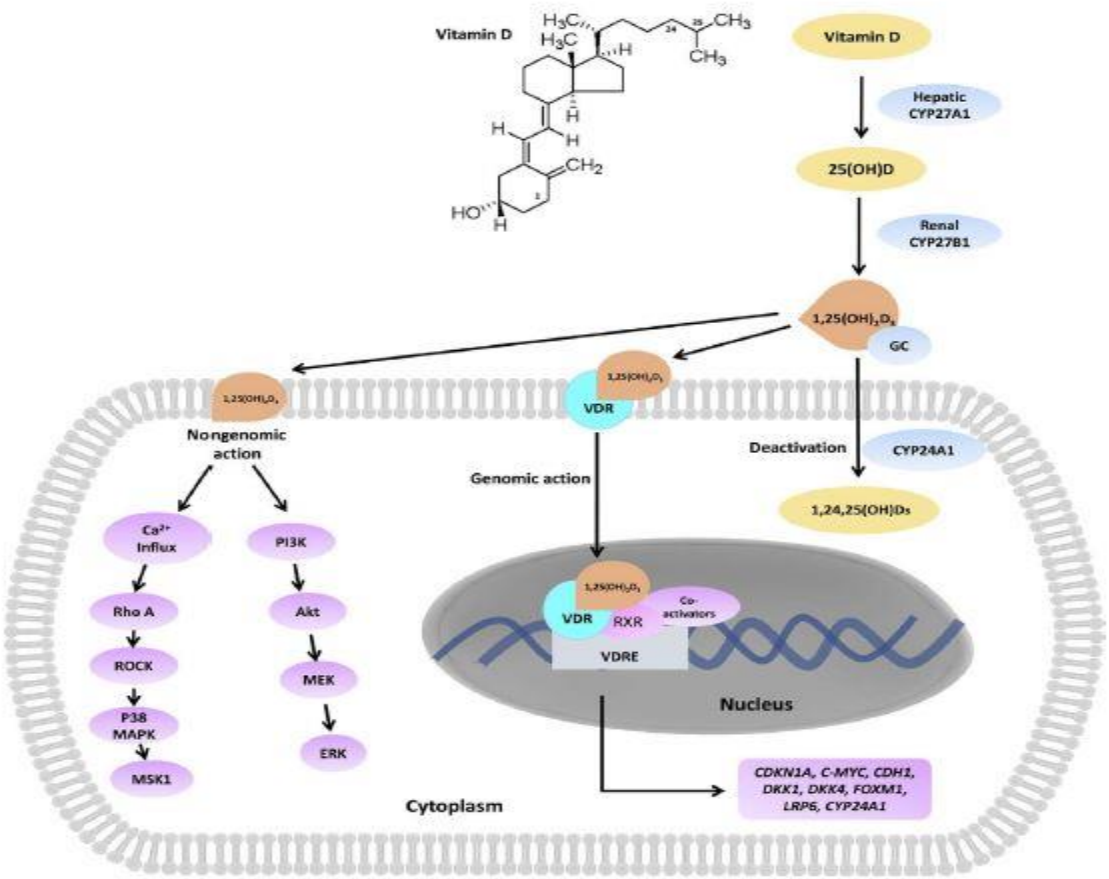

Figure 1.2 Vitamin D metabolism and signalling. Biologically active 1,25-dihydroxyvitamin D_3 exerts its genomic effects by binding the vitamin D receptor (VDR), which translocates into the nucleus and acts as a regulator of gene expression, chiefly as a transcription factor, in conjunction with the retinoid X receptor (RXR) and other transcription machinery. The liganded VDR/RXR heterodimer targets genes possessing vitamin D response elements (VDREs). The expression of these genes, like *CYP24A1*, is regulated by the heterodimer. 1,25-dihydroxyvitamin D_3 exerts a non-genomic effect by inducing the rapid increase in cytosolic calcium ion concentration [Ca^{2+}], which can activate downstream signaling pathways like the PI3K/Akt/MAPK pathway [adapted from Wu et al., 2019].

1.4.3 Vitamin D and pancreatic cancer

Many clinical and experimental observations have found vitamin D to influence the tumorigenic process, from the beginning to tumour metastasis (Giammanco et al., 2015). The important vitamin

D-cancer relationship was conceived from epidemiological studies that associated cancer incidence and mortality with sun exposure and season of cancer diagnosis (Giovannucci, 2005). These epidemiological observations pointed to an inverse relationship between cancer incidence and sun exposure, with the protective sun exposure linked to vitamin D production. Growing research has shown vitamin D to be both protective and therapeutic against cancer. The mechanisms by which vitamin D exerts its protective and therapeutic functions include (observed in vitro and in vivo across much research) pro-apoptotic, pro-differentiation, immune modulatory, anti-inflammatory and anti-angiogenic –relating mechanisms (Deeb et al., 2007). Liganded VDR, as a TF, has been observed to regulate the expression of critical cellular pathways, including cell growth, cell cycle, cell differentiation, apoptosis and cell adhesion – all critical cancer-associated pathways. Vitamin D regulates the expression of *p21*, *p53*, and *p27* TSGs, whose products are involved in DNA repair and cell cycle control (Bragdon, 2008; Huang et al., 2004). Vitamin D can also upregulate *BRCA1* and *BRCA2* TSGs, both involved in DNA repair (Campbell et al., 2000). Vitamin D has been associated with apoptosis through its effect on the *TP53* TSG (Maruyama et al., 2006). Vitamin D can also resist the transition from G_1 to S phase of the cell cycle by binding and inhibiting cyclin D, which inhibits the CDKs needed for transcribing the genes necessary for the G_1 - S phase transition (Bragdon, 2008). Vitamin D has been observed to increase E-cadherin expression (this is also an E-type gene), and alter the cellular location of β-catenin, which altered the expression of the oncogenic MYC protein and increased cell adhesion associated with decreased metastatic potential (Pendás-Franco et al., 2007). Vitamin D has exhibited anti-angiogenic effects by decreasing VEGF levels, implicating it in decreased angiogenesis and invasive potential (Bajbouj et al., 2020). Just as normal vitamin D/VDR function is tissue specific, so is its effect on different cancers, where its growth controlling capabilities vary amongst malignancies (Campbell et al., 2010).

There is experimental evidence for vitamin D affecting various cancer-associated pathways, as well as having anti-tumoural effects (including in vitro and in vivo effects on PC). However, little is known on the molecular effects of vitamin D on PC, and the research shows contrasting results. The effects of vitamin D on cancer seem to be different between cancers, but maybe more importantly, between stages of cancer progression. Some research shows vitamin D to protect against PC (Liu et al., 2018). Studies have found vitamin D metabolising enzymes to be up-regulated in PC cells, possibly implicating vitamin D as a protective factor by its regulation of cell

cycle progression and cell differentiation (Schwartz et al., 2004). Vitamin D treatment has shown synergistic effects with chemotherapy and radiotherapy. Notably, Porter *et al.* (2019) showed vitamin D to differentially modulate the E and QM PDAC subtypes. PDAC exhibits a great degree of tumour plasticity and resistance to chemotherapy, both attributed to the ability of epithelial and mesenchymal cells to exist on a continuum, via the cancer EMT programme. This correlates with vitamin D differentially influencing different stages of cancer, as the cancer EMT programme can be viewed as a tumour progressive step. Given the effect vitamin D has on the expression of cancer-associated genes, as well as the epigenome, it is thus essential to attain insight into the effects of vitamin D on the E and QM PDAC subtypes. Transcriptomic analysis of gene expression using RNA-sequencing may hold significant benefit in understanding the molecular mechanisms of the PDAC response to vitamin D.

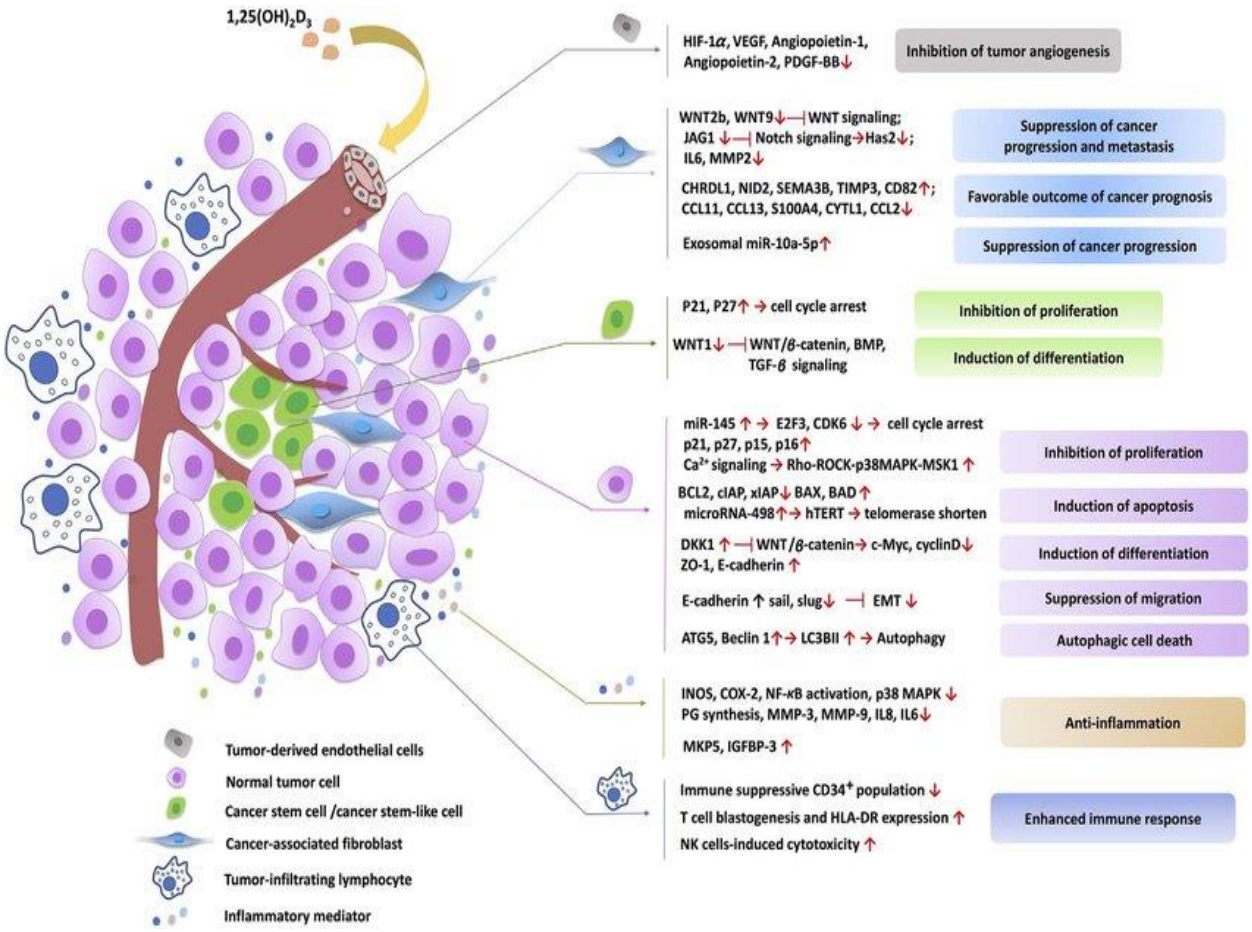

Figure 1.3 Anti-cancer mechanisms of vitamin D within the tumour microenvironment (TME). Biologically active 1,25-dihydroxyvitamin D_3 exerts various anti-cancer effects in the TME, including inhibiting tumour angiogenesis, cell growth and proliferation, and migration, and promoting the processes of cell differentiation and apoptosis. Vitamin D can decrease tumour-promoting inflammation and enhance immune responses against cancer cells in the TME. Vitamin D exerts these anti-tumoural effects on the cancer cells, tumour vasculature, cancer-associated fibroblasts and the immune cells present in the TME [adapted from Wu et al., 2019].

1.5 RNA-Sequencing and transcriptomics

The development of high-throughput technologies has facilitated the use of genomics, epigenomics, transcriptomics, proteomics and metabolomics for profiling disease, and enabled elucidation of the molecular mechanisms associated with disease.

Profiling of the transcriptome was performed in this research. The transcriptome is all the RNA transcripts present in the cell at a given point and is representative of the gene expression of the cell at that point (Wang, Gerstein and Snyder, 2009). Insight into gene expression across conditions and disease states can be gained by analysing the transcriptome. The transcriptome, however, does present high complexity, where alternate and differential splicing events can generate gene isoforms, and just the vast variation that is encountered in transcript abundance.

Transcriptomics is still one of the most widely used tools to gain insight into gene expression across conditions and disease states. The transcriptome, however, does present high complexity, where alternate and differential splicing events can generate gene isoforms, and just the vast variation that is encountered in transcript abundance.

The most widely used transcriptomic techniques are the microarray and RNA sequencing technology (RNA-Seq). Briefly, we describe the RNA-sequencing technique employed by Illumina sequencers, specifically, the NextSeq 500 sequencer that was used to sequence the cDNA of this study. RNA-Seq technology works on the basis of sequencing the complete set cDNA, reverse transcribed from the transcripts of the transcriptome. The cDNA is sorted into 'libraries'. This sequencing platform works by fluorophore detection. The libraries first go through bridge amplification, which generates clonal clusters of the library molecules. This amplification happens directly on the surface of the sequencing flow cell. The nucleotides used during sequencing on this platform are uniquely labelled. Guanine nucleotides are unlabelled. Cytosine nucleotides are labelled with a red fluorophore, adenine nucleotides with a green and red fluorophore, and thymine with a green fluorophore. The nucleotides are pushed through the flow cell lanes and anneal to the library clusters one at a time, after which the excess nucleotides are washed away. Fluorophore emissions from each cluster are imaged, and on this sequencing platform, only green and red images are taken. Each nucleotide presents a different colour emission (or no emission for guanine nucleotides). The resulting emissions data is converted into a nucleotide sequence by software.

The fluorophore is then cleaved via an enzymatic reaction, allowing for the next round of nucleotide annealing to take place.

1.6 Aims and objectives

Given the effect vitamin D has on the expression of cancer-associated genes, as well as the epigenome, we aimed to attain insight into the effects of vitamin D on the E and QM PDAC subtypes, by analysing the gene expression profile of resected patient PDAC samples in response to in vivo 10 nM 1,25-$(OH)_2D_3$ supplementation, as well as the differential response to vitamin D between the E and QM PDAC subtypes. The aim of this study was thus to identify differentially expressed genes between human pancreatic ductal adenocarcinoma (PDAC) cells in response to vitamin D supplementation. To achieve this aim, the following objectives were set:

1. Determine transcript-level abundances from RNA-Seq data obtained from human PDAC cell lines and summarise to gene-level counts.
2. Identify differentially expressed genes in human PDAC cells in a.) response to 10 nM 1,25-$(OH)_2D_3$ supplementation and b.) E vs QM PDAC subtypes.
3. Identify the biological processes associated with the differentially expressed genes.

Chapter 2: Methodology

2.1 Description of the data set

The RNA-Seq data used in this study was obtained from the research conducted by Porter *et al*. (2019) and was downloaded from the European Nucleotide Archive (ENA) as 72 paired-end FASTQ files, resulting in 36 paired-end sequencing files. The data was derived from 6 PDAC patients and consisted of three technical replicates from both conditions (10 nM1,25$(OH)_2D_3$ treated or control; 6 patients X 2 conditions X 3 technical replicates = 36 paired-end sequencing files); https://www.ebi.ac.uk/ena/browser/view/PRJNA592159).

2.1.1 *Cell culture and treatments*

In their study, Porter *et al*. (2019) generated cell lines from metastatic ascites fluid of PDAC patients (n = 6) at the Massachusetts General Hospital (MSG) in accordance with the relevant discarded tissue protocols as set out by the MSG. All samples were de-identified prior to being used in any studies.

The cell lines were grown as tumorspheres under non-adherent conditions in 3D media (Invitrogen/Life Technologies) appropriate for spheroid development at 37 ^{0}C, 5% CO_2 and 90%-95% humidity (Fig 2.1). The media contained serum-free RPMI, 20 ng/mL epidermal growth factor, 20 ng/mL fibroblast growth factor, 20 µL/mL B27 cell supplement (Invitrogen/Life Technologies), and 1% penicillin-streptomycin (Gibco/Life Technologies). 200 000 cells per well were transferred to the wells of an ultra-low attachment culture dish with the 3D media to allow tumour spheroid formation. The cells were treated with 10 nM 1,25$(OH)_2D_3$ or dimethyl sulfoxide (DMSO) vehicle control on day zero, and re-supplemented 72 hours later. Dose-response studies have found 10 nM 1,25$(OH)_2D_3$ supplementation to increase VDR expression and activity and increase the expression of vitamin D/VDR target genes, while not negatively impacting *in vitro* cell viability (Liu et al., 2009, 2006). The tumorspheres were harvested on day five.

2.1.2 *RNA extraction and sequencing*

RNA was extracted using the Qiagen miRNEasy Mini Kit, which enabled purification of total RNA (Fig. 2.1). This kit employs phenol/guanidine-based lysis of samples with silica membrane-based purification of total RNA. The lysis reagent is a monophasic solution of phenol and guanidine thiocyanate, which enables lysis of tissues, inhibition of RNases, and removal of most of the proteins and cellular DNA from the lysate by organic extraction. An on-column DNAse treatment was also used to ensure no contaminant DNA was present.

The Illumina Smarter Stranded Total RNA-Seq kit v20 was used to generate cDNA sequencing libraries from total RNA (Fig 2.1). Pooled libraries were sequenced using the Illumina NextSeq 500 sequencer. No details regarding sequencing dates, lanes or batches were disclosed by the authors. The researchers carried out preliminary quality control (QC) on the raw Illumina reads prior to uploading the data. This included trimming of read ends to remove Ns, which are a result of the inability of the Illumina software to make a base-call for that base. Ns are usually found in reads near the beginning and end of the sequencing files as these reads originate from the edge of the flow cells where imaging is more difficult. Trimmed reads with less than 40 bases were discarded, along with bases with a Phred score of less than 20. Samples were then classified either as an epithelial type PDAC (n = 3) or a quasi-mesenchymal type PDAC (n = 3) based on transcriptional profiling of the patient samples. This was achieved by comparing the transcriptional profiles of the patient PDAC samples to published gene sets (Collisson et al., 2011b), which detail gene signatures associated with PDAC subtypes. Patient PDAC samples associated with increased expression of a specific PDAC subtype gene-set were classified as the appropriate PDAC tumour subtype.

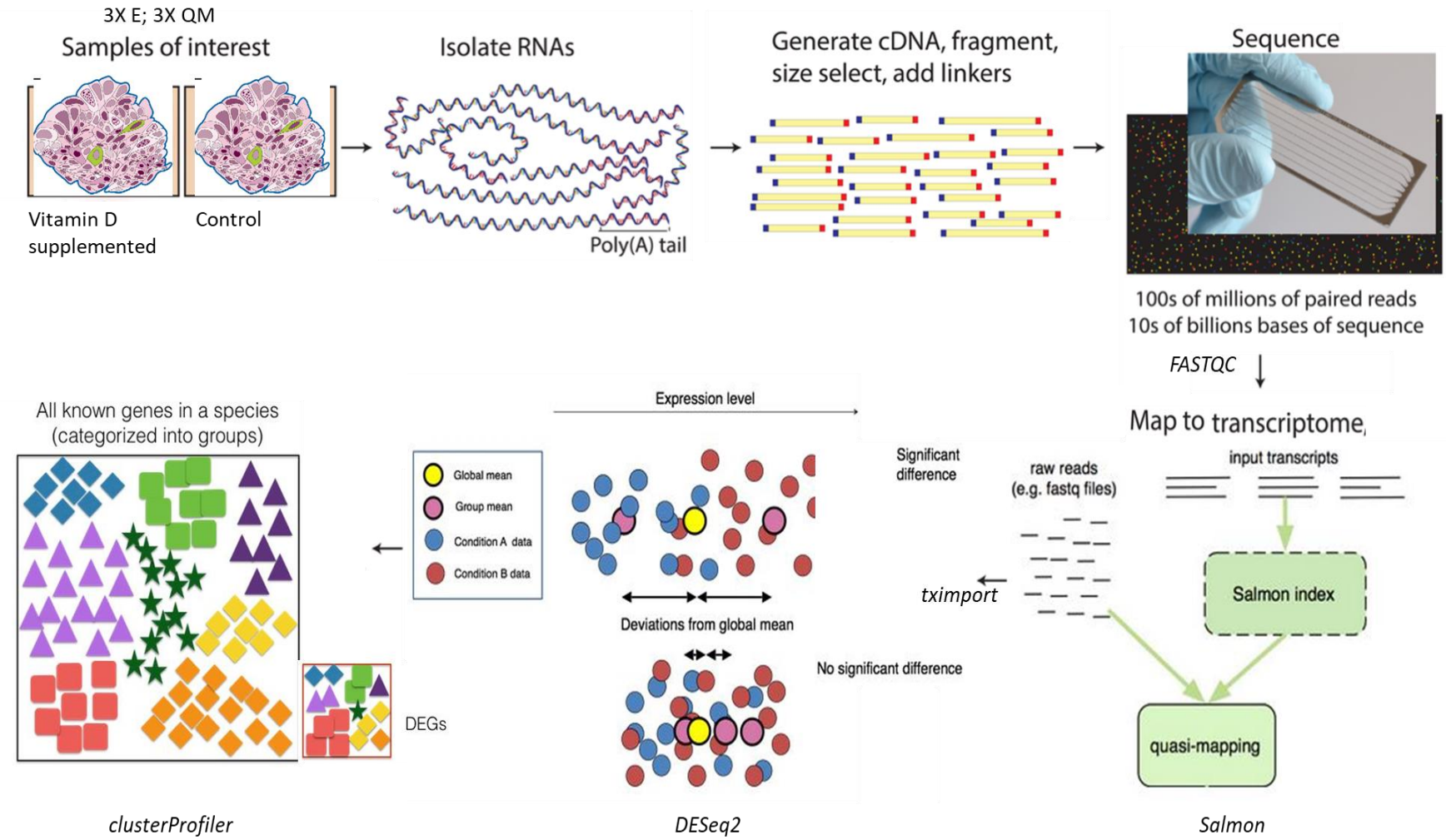

Fig 2.1 General workflow of transcriptomic analysis. Patient derived pancreatic ductal adenocarcinoma (PDAC) cells were cultured as tumorspheres, supplemented with or without 10 nM $1,25(OH)_2D_3$. Total RNA was extracted from the PDAC cells and cDNA libraries were generated from reverse transcribing the RNA. The cDNA libraries were sequenced using the Illumina NextSeq 500 sequencer. The sequencing data was then subjected to preliminary quality control, where after the RNA sequence reads were mapped against a reference transcriptome, providing a transcript abundance estimate, which was then summarised to the gene level. The gene-level summaries were then used for differential gene expression (DGE) analysis and the DGE results were subsequently used for gene ontology and pathway analyses [adapted from Khetani, 2018; Mistry, 2019] .

2.2 RNA-Seq analysis methodology

The workflow diagram (Fig. 2.2) describes the methodology used in this study, and shows the general RNA-Seq analysis steps taken to generate a set of differentially expressed genes. Firstly, the quality of the sequencing files was assessed using FASTQC and MULTIQC (Andrews , 2010; Ewels *et al.*, 2016). The RNA-Seq reads were then mapped to a reference transcriptome and transcript abundance estimates were obtained using Salmon v 1.5.0 (Patro et al., 2017). These transcript abundances were then imported into the R statistical environment (R core team, 2022), where it was subsequently summarised to the gene-level using tximport v1.22.0 (Soneson *et al*, 2016). The gene-level estimates were then used for differential gene expression analysis using DESeq2 v1.34.0 (Love *et al*, 2014). Batch effect correction was applied using sva v3.42.0 (Leek, 2014). Differential gene expression analysis was then performed and the differentially expressed genes were used for gene ontology and pathway analysis to gain biological insight into the differentially expressed genes using clusterProfiler v4.2.2 (Yu et al., 2012).

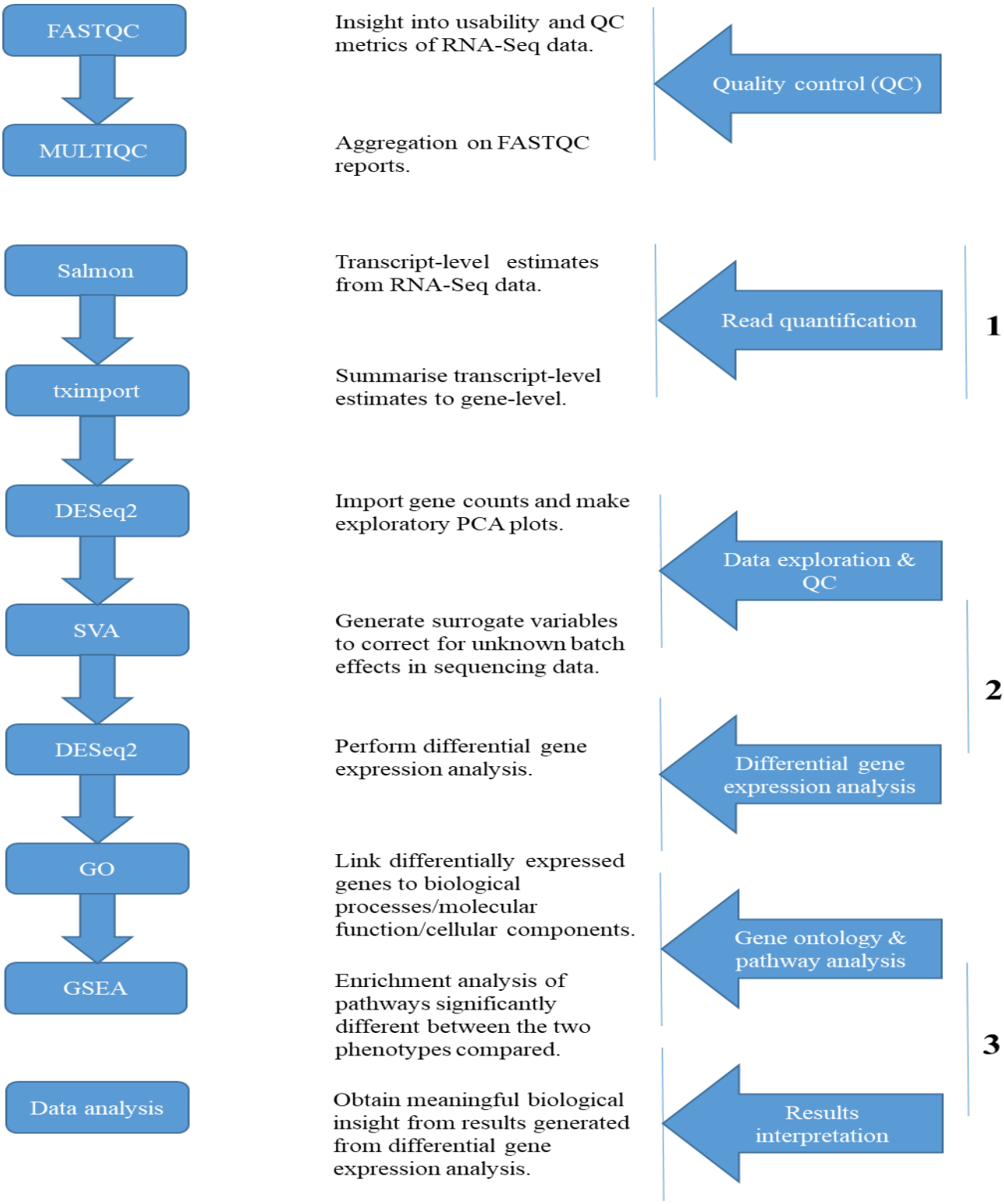

Figure 2.2 Flow chart of general RNA-Seq data analysis steps taken during this research. The appropriate bioinformatics tools were selected and the above steps were followed sequentially, leading to the generation of a list of differentially expressed genes for further analysis. The numbers 1-3 correspond to the steps taken to achieve the objectives 1-3, respectively. QC - quality control; SVA – surrogate variable analysis; GO – gene ontology; GSEA – gene set enrichment analysis.

2.2.1 *Quality control of RNA sequencing data from FASTQ files*

The quality of the downloaded RNA-Seq data was assessed prior to any data analysis. This was done to ensure that only data of appropriate quality would be used for downstream analyses. The FastQC (Andrews, 2010) quality control tool was used to assess the quality and usability of the RNA-Seq data. FastQC is a quality control (QC) tool used to assess the basic QC metrics of raw next generation sequencing data. RNA-Seq data sequence read files were imported as FASTQ files from the ENA into FastQC using the Galaxy bioinformatics platform (https://usegalaxy.org/). The *Galaxy* platform provided a user-friendly interface only requiring the user to specify the files to run through FastQC. FastQC generated plots and summary statistics detailing, amongst other metrics, the quality score of each base in the sequence (where a higher score indicates a lower probability that the base was called incorrectly), sequence duplication levels, adaptor content, and the number of sequence reads per file. FastQC looks at the Phred quality score, calculated by comparing read signals to the probability of accurate base-reading. Phred scores are related to base-calling error probabilities in a logarithmic manner ($Q = -10 \log10 P$), such that scores of 50, 40 and 30 indicate base call accuracies of 99.999%, 99.99% and 99.9% respectively.

MultiQC (Ewels *et al.*, 2016; https://usegalaxy.org/) was then used to aggregate the individually generated FastQC reports to allow for ease of reporting and simultaneous visualisation and comparison of the QC metrics of all FASTQ files. The individually generated FastQC reports were specified and grouped together and MultiQC, was used to aggregate and output QC reports and plots of all FASTQ files (E- and QM-type PDAC samples together).

2.2.2 *Read mapping and quantification of gene expression*

Alignment of sequencing reads from the FASTQ files and quantification of gene expression is required to perform transcriptional profiling. This step maps sequence reads against a reference genome or transcriptome to give a measure of how many times a given transcript occurs in the given data set, and hence a measure of gene expression. There were two possible approaches to attain gene expression quantification- use a traditional alignment approach like that provided by Tophat2 (Kim et al., 2013) or Bowtie (Langmead et al., 2009), or through a more recent pseudo-

alignment (alignment-independent) approach like that provided by Salmon (Patro et al., 2017) or kallisto (Bray et al., 2016).

Traditional alignment-dependant approaches work by aligning genomic (Bowtie) or transcriptomic (Tophat2) reads against a reference genome. This provides a possible genomic co-ordinate from which a specific read may originate. Most recently, pseudo-alignment approaches have been developed. Pseudo-alignment/mapping approaches differ from alignment approaches in that the mapping approach asks only where a read comes from, whereas alignment approaches query where the read comes from with a base-base correspondence. Pseudo-alignment/mapping approaches determine for each read what transcript it is compatible with, rather than to what transcript does it align. This creates a set of transcripts that each read is compatible with. Here transcript abundance is quantified by k-mers and k-mer counts. A k-mer is a substring of a biological sequence, in this case, a substring of the RNA-Seq reads. Approaches to quantification like kallisto and Salmon have improved on earlier approaches like Sailfish (Patro et al., 2014) that required that reads be 'shredded' into the k-mers. Pseudo-alignments hence define a relationship between a read and a set of compatible transcripts, based on quasi-mapping the k-mers to paths in a transcript De Bruijn graph in kallisto.

For this study, a pseudo-alignment (mapping-based) approach using Salmon was selected (Fig. 2.2). This approach allows for faster quantification of gene expression, is less computationally extensive and presents with a similar accuracy when compared with traditional alignment approaches (Patro et al., 2017). Salmon couples quasi-mapping with a two-phase inference procedure. Salmon makes this inference by making use of a realistic and expressive model of RNA-Seq data, which accounts for the biases and experimental attributes observed in RNA-Seq data (Patro et al., 2017).

The Salmon quasi-mapping procedure works by estimating where a read best maps to the transcriptome via identifying where informative sequences present in the given read map to on the transcriptome, rather than via a base-by-base alignment. The Salmon reference index is generated and this provides an easily and rapidly searchable format of the transcriptome, allowing for the rapid matching of positions in the transcriptome from which a read could have originated. Essentially, the index creates a 'signature' for each transcript of the transcriptome of length k (k-mers; default k = 31). The index comprises a suffix array (SA, sorted array of suffixes of a

sequence) of the transcriptome and a hash table that maps each transcript of the transcriptome to its location in the suffix array (Fig. 2.2; Patro *et al.*, 2017). A quality index is of utmost importance as it determines if a read will be mapped and quantified. If the RNA-Seq data contains reads from transcripts not present in the reference transcriptome, these reads will not be mapped and quantified. This is also why no trimming of reads is necessary (e.g. adaptor sequences) as k-mers of these reads will not be in the reference transcriptome and hence, will not be present in the Salmon index.

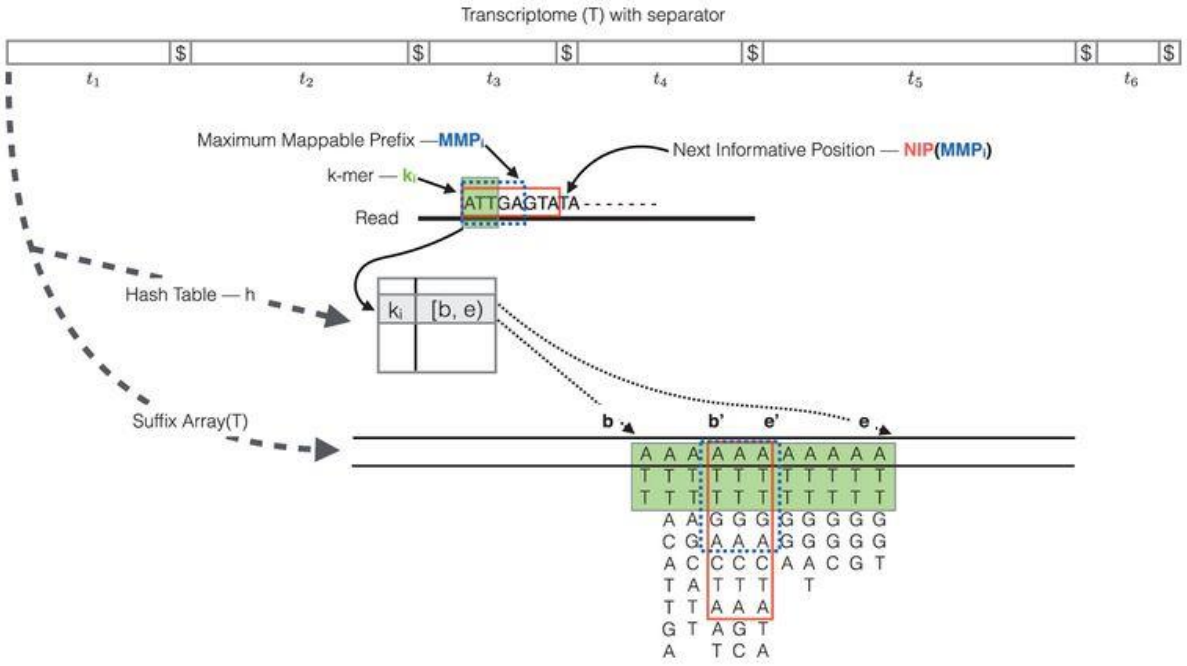

Figure 2.3 Diagrammatic representation of how Salmon quantification works. The transcriptome (shown are transcripts *t*1-*t*6) is converted into a separated string (T), upon which the suffix array (SA[T]) and hash table (h) are constructed. The mapping operation begins with a k-mer (shown $k = 3$; normally k=31) mapping to an interval [*b*,*e*) in SA[T]. Given this interval and the read, the maximum mappable prefix (MMP_i) and the next informative position (NIP) are calculated. The search for the next hashable k-mer begins *k* (shown $k = 3$; normally k=31) bases away before the NIP [adapted from Srivastava *et al.*, 2016].

Briefly, the Salmon read mapping is performed by scanning the read from left to right until a k-mer appearing in the hash table is identified. This k-mer is then queried in the hash table and all suffixes containing that k-mer are retrieved (Patro et al., 2017; Srivastava et al., 2016). The maximal matching prefix (MMP) is then pinned down by Salmon detecting the longest read sequence that exactly matches with the reference suffixes. Salmon then detects the next informative position (NIP) by moving over the length one k-mer. Salmon repeats this process for the length of the read and then generates mappings by determining the set of transcripts that appear

in all of the MMPs for that read. The orientation and location of the transcript set are output for each read. The transcript abundance is then estimated by modelling sample-specific parameters and biases present in RNA-Seq data. Unaccounted biases can lead to unacceptable false-positive rates in differential gene expression analysis (Patro et al., 2017).

The FASTQ files were downloaded from the ENA and Salmon v1.5.0 (Patro et al., 2017) was used to quantify the three technical replicates per patient sample together into one single transcript quantification output file. This ensured that technical replicates were collapsed properly before DGE analysis. Salmon generated an index from the target transcriptome (in this case, Gencode v38). This index is a structure that the tool uses to quasi-map the RNA-Seq reads during quantification. One index need only be constructed once per transcriptome, and it can then be reused to quantify many experiments. The *index* command of Salmon was used to build the index, the author recommended parameters for correcting for GC bias common in RNA-Seq data and the *validate mappings* option was checked, and a k-mer length of 31 was selected. The Salmon quantification step was run as per author's recommendations (https://combine-lab.github.io/salmon/getting_started/). Quantification files and Salmon log files detailing the run details of the quantification were saved.

tximport v1.22.0 (Soneson *et al*., 2016) was then used to summarise the transcript level counts to gene-level estimates. tximport matches given transcripts to a gene of origin and generates a matrix of gene counts. This approach corrects for potential changes in gene length across samples (e.g., from differential isoform usage) to avoid discarding those fragments that can align to multiple genes with homologous sequence, thus increasing sensitivity. A transcripts-to-gene (tx2gene) file was required for this step and was generated using Bioconductor packages in R using the Gencode human release 38 comprehensive gene annotation (https://www.gencodegenes.org/human/). The gene-level summaries were then used in DESeq2 for DGE analysis.

2.2.3 *Differential gene expression analysis*

To identify genes differentially expressed (DE) in response to 10 nM $1,25(OH)_2D_3$ supplementation in the E and QM PDAC subtypes, DESeq2 v1.34.0 (Love *et al*., 2014) was employed. DESeq2 DE analysis involves multiple steps. Briefly, DESeq2 models raw counts by using normalisation factors (size factors) to account for differences in library depth. DESeq2 then estimates the gene-wise dispersions and shrinks these estimates to generate estimates of dispersion to model the counts accurately. DESeq2 then fits a negative binomial model to the data and performs hypothesis testing using the Wald test.

The internal normalisation step of DESeq2 involves calculating a geometric mean for each gene across all samples. The gene counts are then divided by this mean, for all samples. The median of these ratios (gene count/geometric mean) of a sample then forms the 'size factor' for that sample. These steps correct for sequencing depth and RNA composition bias. Sequencing depth refers to the total number of reads obtained from a high-throughput sequencing run. Samples may have differing sequencing depths, and it may seem that in one sample a gene appears to have doubled in expression compared to another sample, but it is actually a consequence of that sample having double the sequencing depth. The normalisation step corrects for different sequencing depths so that gene counts are not skewed in a way that incorrectly impacts the DGE analysis. RNA composition bias can occur when there are a few highly differentially expressed genes between experimental conditions, differences in the number of genes expressed between samples, or the presence of contamination. RNA composition must be accounted for to ensure accurate comparison of gene expression between samples, and particularly when performing DGE analysis (Anders and Huber, 2010).

DESeq2 requires biological replicates to estimate within-group variance (dispersion) reliably, by employing shrinkage estimation for dispersions and fold changes. Each gene is assigned an estimated dispersion value through a model fit procedure. A generalized linear model is then fit for each gene by DESeq2 employing a negative binomial distribution, followed by the Wald test for significance testing. This is done because RNA-Seq count data generally presents with over-dispersion where the variance is greater than the mean, and modelling the counts must account for this over-dispersion (Love et al., 2014). Count outliers are detected and the genes removed from

analysis, using Cooks' distance. Also, genes possessing a mean normalised count below a threshold (determined by a DESeq2 optimisation process) are removed to improve the detection power for differentially expressed genes.

The null hypothesis upon which DESeq2 operates stipulates that most genes are not differentially expressed between test groups. DESeq2 employs statistical tests to determine if based on the observed data, the null hypothesis is true. The Wald test is used for hypothesis testing between the experimental groups (in our case 10 nM $1,25(OH)_2D_3$ supplementation versus control). The Wald test statistic is calculated, along with the probability that the test statistic is at least as extreme as the observed value, were selected at random. This probability gives the p-value of the test. A small p-value allows us to reject the null hypothesis (i.e. that a gene is not DE).

The DESeq2 analysis output from comparing gene expression between experimental conditions includes (for each gene): an average of the normalised counts taken over all the samples, a log2 fold change between the experimental conditions for that gene, the Walt test statistic, the Wald test p-value, and a Benjamini-Hochberg adjusted p-value for false discovery correction.

A count matrix of integer values representing the counts of a gene produced from tximport was used to create the DESeq data set (dds) using the DESeq2 package. The genes with zero counts were removed and the data was normalised. The data normalisation was performed using functions for normalisation from the DESeq2 package. Principal component analysis (PCA) was performed to visualise variation within and between the human PDAC cell samples and conditions. This data exploratory step served as an important QC measure to check on whether the samples differed from each other based on treatment condition and PDAC cell type. Results obtained from this step showed indistinct clustering by condition and PDAC subtype, which prompted the sva batch effect correction step. The sva v3.42.0 package (Leek, 2014) contains functions for removing batch effects and unwanted variation in high-throughput experiments. The *svaseq* function of the sva package was used for this sequencing data. The function first identifies latent factors that need to be estimated and then generates a set of surrogate variables (SV) in matrix form where the columns correspond to the estimated SV. The estimated SVs were tested so as not to over-fit the data. The SV matrix was then included in the design model of DESeq2. The *deseq* function for differential gene expression (DGE) analysis was used and results for significantly expressed genes were extracted. A gene was considered to be significantly differentially expressed when it had a p-value

of less than 0.05 ($p < 0.05$), and was considered up or down regulated when it showed a log2 fold change (LFC) of more/less than 1. The LFC is the effect size estimate that shows how much the gene's expression seems to have changed between the compared samples. This value is reported on a logarithmic scale to base 2: for example, a log2 fold change of 1 means that the gene's expression is increased by a multiplicative factor of $2^1 = 2$. A results table including only differentially expressed genes (DEGs) was constructed and the *ensembl* and *entrez* gene identifiers were matched to the corresponding gene symbol. The results table was filtered to remove any gene without a gene symbol. Volcano plots representing the DEGs with p-adj < 0.10 and a Venn diagram comparing the DEGs ($p < 0.05$) between the E and QM subtypes were generated. The DGE analysis results were extracted to be used in further analyses. The lists of DEGs were used for gene ontology and pathway analysis to gain biological insight from the DEGs lists, and the DEGs list was compared to known and characterised cancer-associated gene lists to look at the effect $1,25(OH)_2D_3$ supplementation had on oncogenes, tumour suppressor and fusion genes.

2.2.4 *Gene ontology and pathway analysis*

The output of the DGE analysis yielded a list of genes differentially expressed in response to vitamin D supplementation. To gain biological insight from the list of differentially expressed DEGs, functional analysis was conducted using over-representation and functional class scoring approaches. These analyses were conducted to determine if biological pathways, functions and interactions were enriched within the list of DEGs and to identify genes involved in these pathways.

Functional enrichment tools perform over-representation analysis by querying databases containing information regarding gene functions and interactions. The gene ontology (GO) project database, maintained by the gene ontology consortium, was used in this study (Ashburner et al., 2000); (Gene Ontology Consortium, 2021). This database categorises genes into gene sets based on pathway involvement, shared functions etc. These GO terms (categories) are organised into three ontologies- biological process (BP), molecular function (MF) and cellular component (CC). BP refers to the biological role that the gene or its product is involved in (e.g. transcription). MF refers to the biochemical activity of the gene product (e.g. ligand), and CC refers to the cellular

location of the gene product (e.g. nucleus). The BP ontology was used as it encompasses the biological functions of the genes at large. A single gene may be part of multiple GO terms as its product may be involved in multiple processes.

clusterProfiler v4.2.2 (Yu et al., 2012) was used to perform over-representation analysis (ORA) on BP GO terms associated with the list of DEGs. clusterProfiler performs statistical enrichment analysis using hypergeometric testing. In statistics and probability, the hypergeometric distribution is a discrete probability distribution used to determine the probability of obtaining a certain number of successes without replacement from a specific sample size. With regards to ORA in our case, the hypergeometric distribution describes the probability of a number of genes (from the list of DEGs) being associated with a certain category (GO term). This was done for all genes from the list of DEGs from the population of genes expressed by these human PDAC cells. This hypergeometric test provides a p-value for each category tested.

clusterProfiler required the list of DEGs and a background set of genes to compare the list to (all the genes expressed in the PDAC samples). The list of DEGs were split into up- (log2 fold change > 0) and down-regulated (log2 fold change < 0) lists containing only the log2 fold changes and the *entrez* gene identifier. The entire expression profile was used as the background gene list. The up- and down-regulated DEG subsets were then analysed using the *enrichGO* function of the clusterProfiler package for having gene sets enriched in the respective lists. The output of the function returned the enriched GO categories, after false discovery rate correction. This output was saved and used to generate bar plots of the top 30 enriched GO terms, as well as category netplots (cnet) for the top four enriched GO terms. The bar plots were generated to show the number of genes associated with the GO terms and the p-adjusted values for these terms. The category netplots were generated to show the relationships between the genes associated with the top four most significant GO terms and the fold changes of the genes associated with these terms. This was done to identify genes that are important to several of the most affected biological processes. The *enrichGO* output was then rerun for the entire list of DEGs (up- and down-regulated). This output was then merged with the list of DEGs. This was done to construct a Venn diagram, comparing the DEGs between the E and QM PDAC subtypes, using the *GOVenn* function of the GOplot v1.0.2 package (Walter *et al*., 2015). The GOplot package provided a means of combining gene expression and functional analysis data.

Functional class scoring via gene set enrichment analysis (GSEA) was then performed using clusterProfiler and the Pathview v1.34.0 package (Luo and Brouwer, 2013). The Pathview package provided a tool for pathway-based data integration and visualisation. This was conducted to determine whether gene sets for particular biological pathways were enriched among positive or negative fold changes using the gene-level statistics or log2 fold changes for all genes from the DGE analysis results.

Functional class scoring operates on the hypothesis that while large changes in individual genes can have significant effects on pathways, weaker but coordinated changes in sets of functionally related genes may also result in significant effects. Therefore, instead of setting a threshold to identify significant genes, functional class scoring considers all genes in the analysis. This method provided a means for testing coordinated differential expression over gene sets, instead of changes of individual genes.

The *gseKEGG* function of clusterProfiler was used to generate gene set enrichment analysis of KEGG gene sets. KEGG (Kyoto Encyclopaedia of Genes and Genomes) (Kanehisa and Goto, 2000) is a collection of databases of genomes and biological processes. KEGG pathway maps represent experimental knowledge on metabolism and functions of the cell. These pathways contain a network of molecular interactions and reactions, linking genes and gene products in the pathway. The KEGG enrichment output was used to generate KEGG pathway plots using the Pathview package.

Chapter 3: Results

3.1 Quality control

3.1.1 *Quality control of raw sequence data using FastQC revealed good quality RNA-Seq reads*

To identify any possible sequencing files with poor quality reads prior to any further analysis, the data used in this study was run through FASTQC and MULTIQC using the Galaxy bioinformatics platform (Andrews , 2010; Ewels *et al.*, 2016). All 72 FASTQ files (36 paired-end sequencing files) used in this study passed the quality control thresholds (Fig. 3.1). One set of sequencing files from an E-type PDAC patient had a raised level of sequence duplication, but this did not make the sample unusable, and was corrected for in the DESeq2 normalisation process without the need for deduplication.

3.1.2 Quantification of transcript and gene level abundance estimates

To obtain transcript and gene-level quantification from the RNA-Seq data following quality control of the raw sequencing data, the g-zipped FASTQ files underwent the process of quantification using Salmon v1.5.0 (Patro et al., 2017). In total, 227 533 480 and 62 429 272 reads from the six control and six $1,25(OH)_2D_3$ treated samples (collapsed) were mapped against 236 186 transcripts, respectively. On average, 49.78% of the E-type PDAC sample reads (Table 2.1) and 50.64% of the QM-type PDAC sample reads (Table 2.1) were pseudo-mapped to the reference transcriptome. The tximport v1.22.0 package was then used to summarise the transcript counts to the gene level (Soneson *et al*, 2016). The transcript quantification estimates from the epithelial type PDAC samples were summarised to 54 052 genes by tximport, and the transcript quantification estimates from the quasi-mesenchymal type PDAC samples were summarised to 53 033 genes. The percentage of reads pseudo-mapped to the reference transcriptome by Salmon was fairly consistent with minimal variations- all mapping rates fell in the range of 46%-56% with a mean mapping rate of 50.21%.

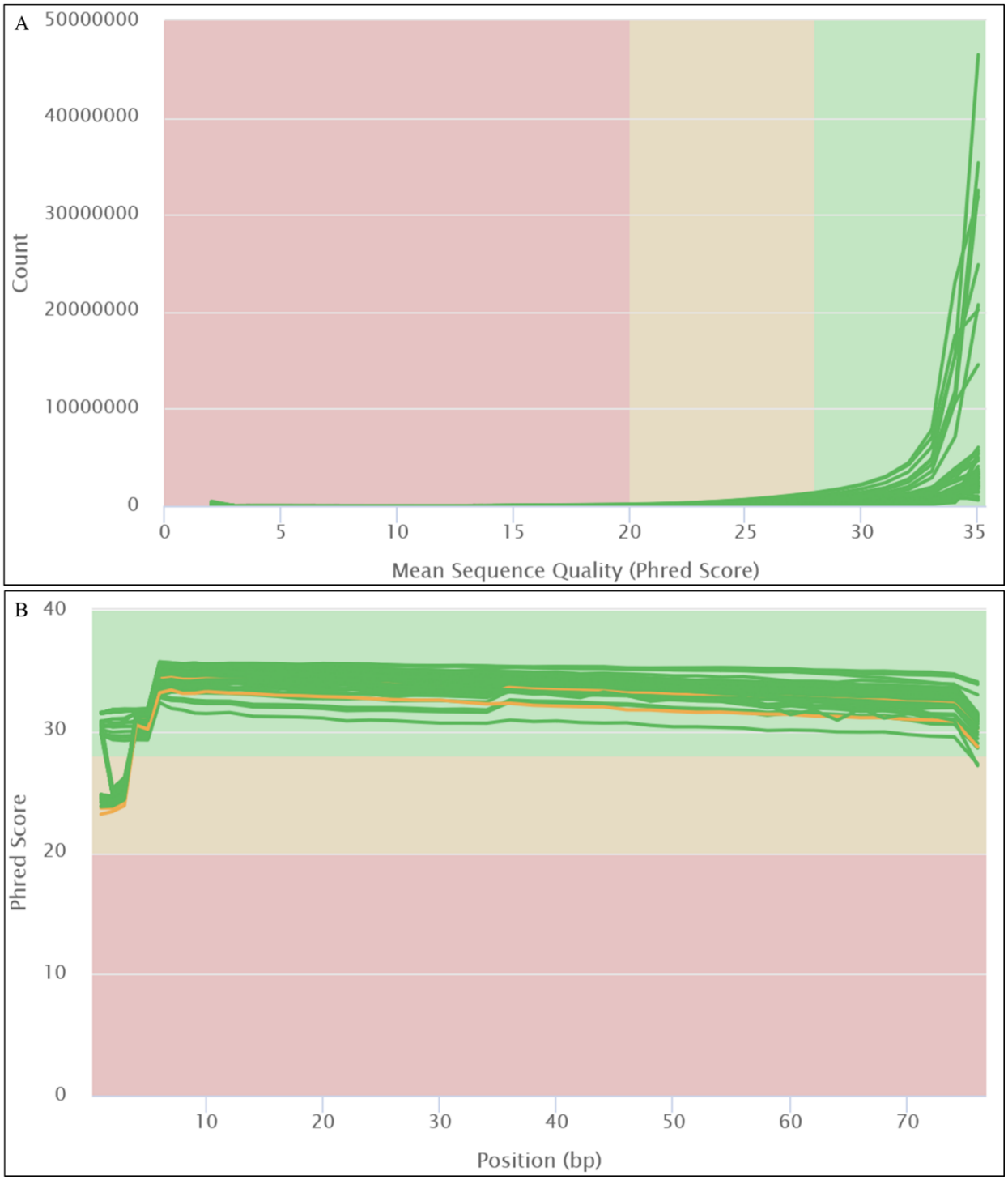

Figure 3.1 *MULTIQC* aggregation of *FASTQC* plots shows high quality RNA sequencing reads. The representative graphs show the quality of the RNA-Seq reads, measured as "mean sequence quality" (Phred score, A) and "per base sequence quality" (position in sequence read, B). The RNA-Seq reads were derived from epithelial (n = 3) and quasi-mesenchymal (n = 3) pancreatic ductal adenocarcinoma tumorspheres cultured with or without *in vitro* 10 nM $1,25(OH)_2D_3$ supplementation. Colour divisions represent the quality of base calls: green – good; yellow – reasonable; red – poor.

Table 2.1 Salmon mapping rates show acceptable RNA sequence read mapping to a reference transcriptome.

	E-type mapping rate (%)	QM-type mapping rate (%)
Control-1	54.5551	55.4551
Control-2	48.4292	49.4529
Control-3	49.3419	47.4919
$1,25(OH)_2D_3$-1	46.9323	49.6232
$1,25(OH)_2D_3$-2	47.8628	48.2886
$1,25(OH)_2D_3$-3	51.5396	53.5496

3.1.3 *Principal component analysis revealed batch effect biases*

To observe the similarities and differences between the RNA-Seq samples and the possible presence of batch effects, the principal component analysis (PCA) function of the DESeq2 package was used to generate PCA plots. PCA plots were first generated using the rlog normalised counts of the pre-collapsed technical replicates. This was done to establish if the samples clustered by condition regardless of sample origin (different patients presenting with the same PDAC subtype) but no apparent clustering was observed by sample. PCA plots were then generated using the collapsed replicates (Fig 3.2) comparing conditions ($1,25(OH)_2D_3$ treated vs DMSO vehicle control) per PDAC subtype as this comparison is what drove the question of this study. No apparent clustering by condition was observed in the E-type samples. Some measure of clustering by condition was observed in a pair of control and a pair of treated samples of the QM-subtype, but no strong clustering by condition was observed. Taken together, these observations indicate the presence of batch effects. The sva v3.42.0 package was used to correct for the possible batch effects and supported the separation of samples from different batches (Fig 3.3; Leek, 2014). Four surrogate variables (SV) were estimated for each PDAC subtype. The four SV were tested in the DGE analysis so as not to over-fit the data. The first three and two SV were included in the E and QM PDAC subtypes DGE analysis design, respectively. Including these surrogate variables improved the DGE analysis.

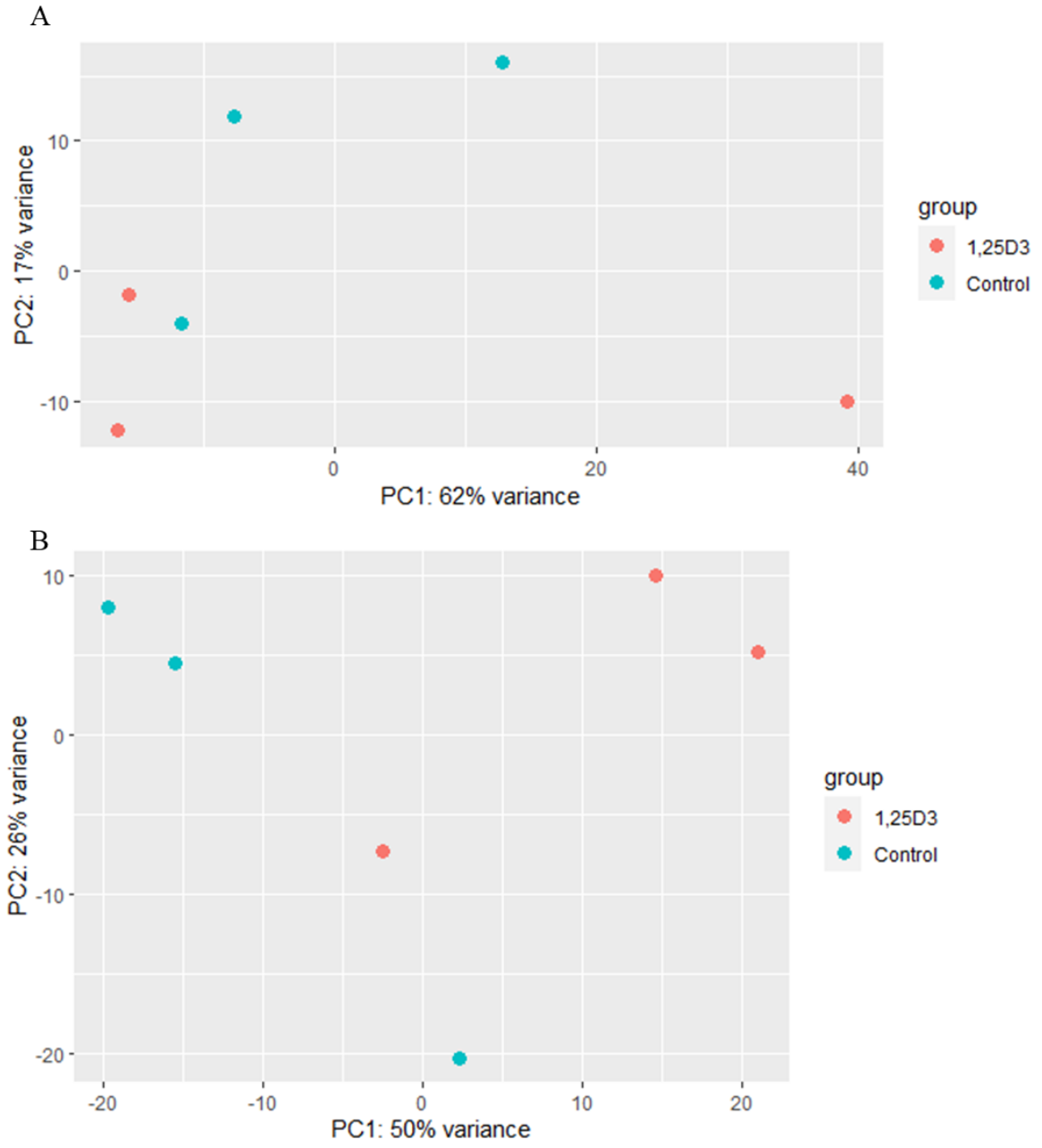

Figure 3.2 Principal component analysis (PCA) with *DESeq2* showed no apparent clustering by condition. The PCA plots represent the RNA expression profiles of the epithelial (A; n = 3) and quasi-mesenchymal (B; n = 3) pancreatic ductal adenocarcinoma tumorspheres cultured with (red) or without (blue; control) *in vitro* 10 nM $1,25(OH)_2D_3$ supplementation.

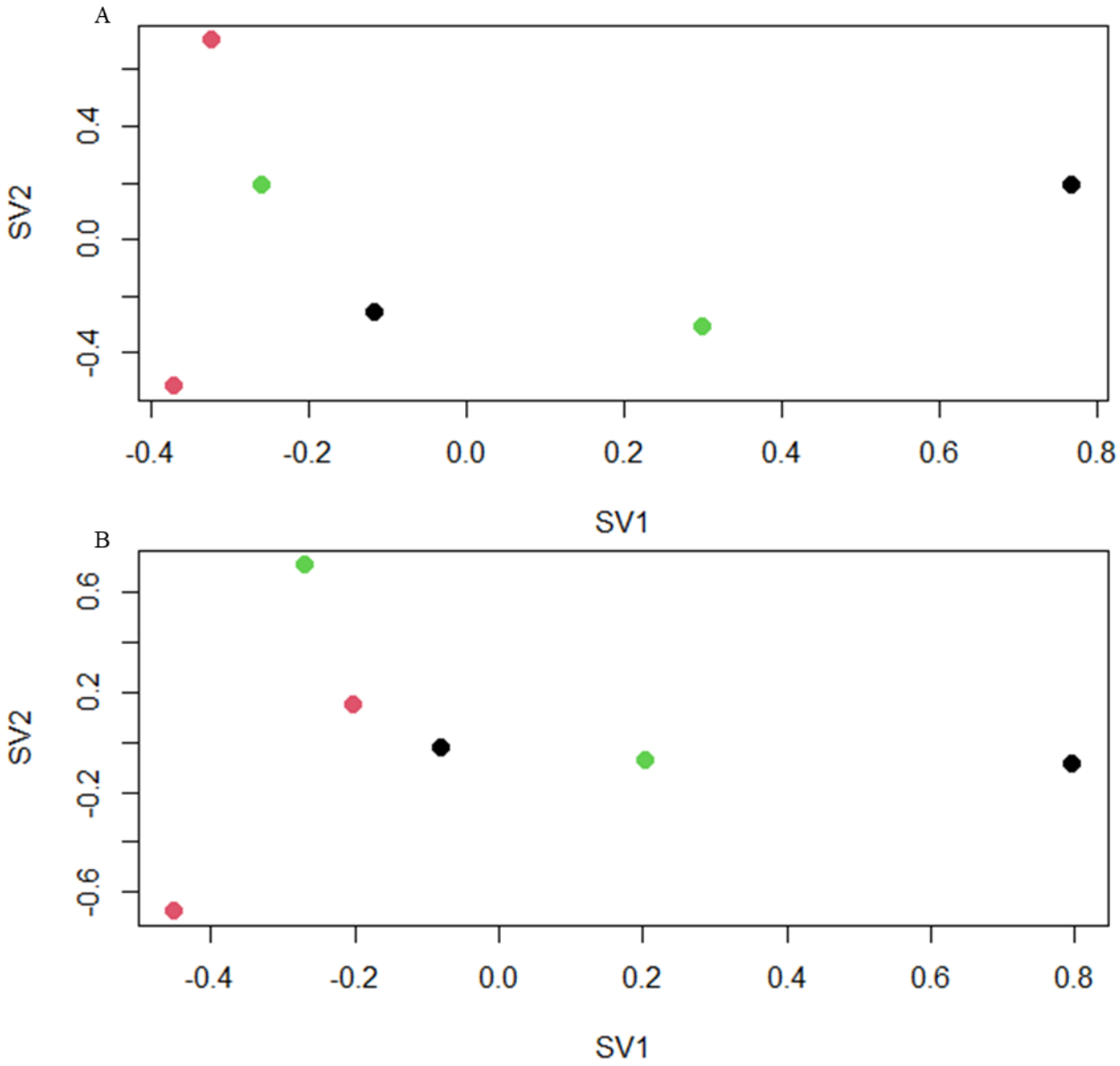

Figure 3.3 Surrogate variables 1 (SV1) and 2 (SV2) plotted across samples shows samples separation by condition. The surrogate variable analysis (*SVA*) batch effect correction yielded three and two estimated surrogate variables for the epithelial (A) and quasi-mesenchymal (B) respectively. The SV1-SV2 plot shows separation of samples (dots of the same colour) by condition ($1,25(OH)_2D_3$ supplemented vs control) from different batches. The black, red and green dots represent samples from the three epithelial and three quasi-mesenchymal patient samples, respectively.

3.2 Differential Gene Expression Analysis

3.2.1 *DESeq2 quality control*

To identify genes differentially expressed between 1,25(OH)2D3-treated and control PDAC samples, DESeq2 v1.34.0 was used to perform DGE analysis (Love *et al*, 2014). The quality of the DGE analysis output was assessed by generating quality control plots using DESeq2 functions. The mean estimate dispersion plots (Fig. S1) show that the DESeq2 algorithm had effectively shrunk gene estimates to reduce variance between the samples. The data was scattered around the curve with the dispersion decreasing with increasing mean expression levels, indicating that the data is a good fit for the DESeq2 DGE model. The mean-average log ratio plot (Fig. S2) revealed that most DEGs are found within the mean normalised counts range of 100-1000 with no DEGs found from weakly expressed genes.

3.2.2 *Identification of differentially expressed genes*

To identify differentially expressed genes in both epithelial and quasi-mesenchymal PDAC subtypes, the *DESeq* and *results* functions of the DESeq2 package were used. The estimated surrogate variables were included in the design of the *DESeq* model. DGE analysis yielded 1 991 and 1 744 DEGs (p-value < 0.05) in the E and QM subtypes respectively. Of these DEGS, 933 (E) and 390 (QM) passed the stringent Benjamini-Hochberg false discovery rate (FDR) correction p-adjusted value of < 0.10 (padj < 0.10; Figs. 3.4 and 3.5). Genes presenting with a p-value < 0.05 were considered DE. Out of all the DEGs, 42 genes were commonly up-regulated, 23 commonly down-regulated, and 270 genes contra-regulated between the PDAC subtypes. 1 111 and 705 genes were uniquely differentially expressed in the E and QM PDAC subtypes respectively (Fig. 3.6). Interestingly, the vitamin D metabolising enzyme, *CYP24A1*, was significantly up-regulated in response to $1,25(OH)_2D_3$ supplementation in the E PDAC subtype, but not in the QM subtype. Notably, certain oncogenes and tumour suppressor genes (TSGs) had opposite expression profiles in response to $1,25(OH)_2D_3$ supplementation. For example, the *MYC* and *JUN* oncogenes were up-regulated in the QM subtype and down regulated in the E subtype, while the tumour suppressor gene *FOXP1* was up-regulated in the E subtype and down regulated in the QM subtype in response

to $1,25(OH)_2D_3$ supplementation (Table S3). $1,25(OH)_2D_3$ supplementation down-regulated the expression of oncogenes *TGFB2* in the E PDAC subtype and mucin family genes in the QM subtype, but also down-regulated the expression of the tumour suppressor gene, *TSPYL5* (Fig. 3.5). In total, 117 and 82 cancer related genes were differentially expressed in the E and QM PDAC subtypes in response to $1,25(OH)_2D_3$ supplementation respectively (Table 3.2 and 3.3).

Figure 3.4 1,25(OH)$_2$D$_3$ supplementation resulted in 933 differentially expressed genes (DEGs) in the epithelial pancreatic ductal adenocarcinoma (PDAC) subtype. The volcano plot shows the DEGs with a $\log_2$ fold-change and $-\log_{10}$ adjusted p-value (padj < 0.10) when comparing 1,25(OH)$_2$D$_3$ treated vs control samples (n = 3; green = 2-fold up-regulated; blue = 2-fold down-regulated). The vitamin D metabolising enzyme, *CYP24A1*, was significantly up-regulated while the expression of the oncogene TGFB2 was down-regulated in response to 1,25(OH)$_2$D$_3$ supplementation, respectively.

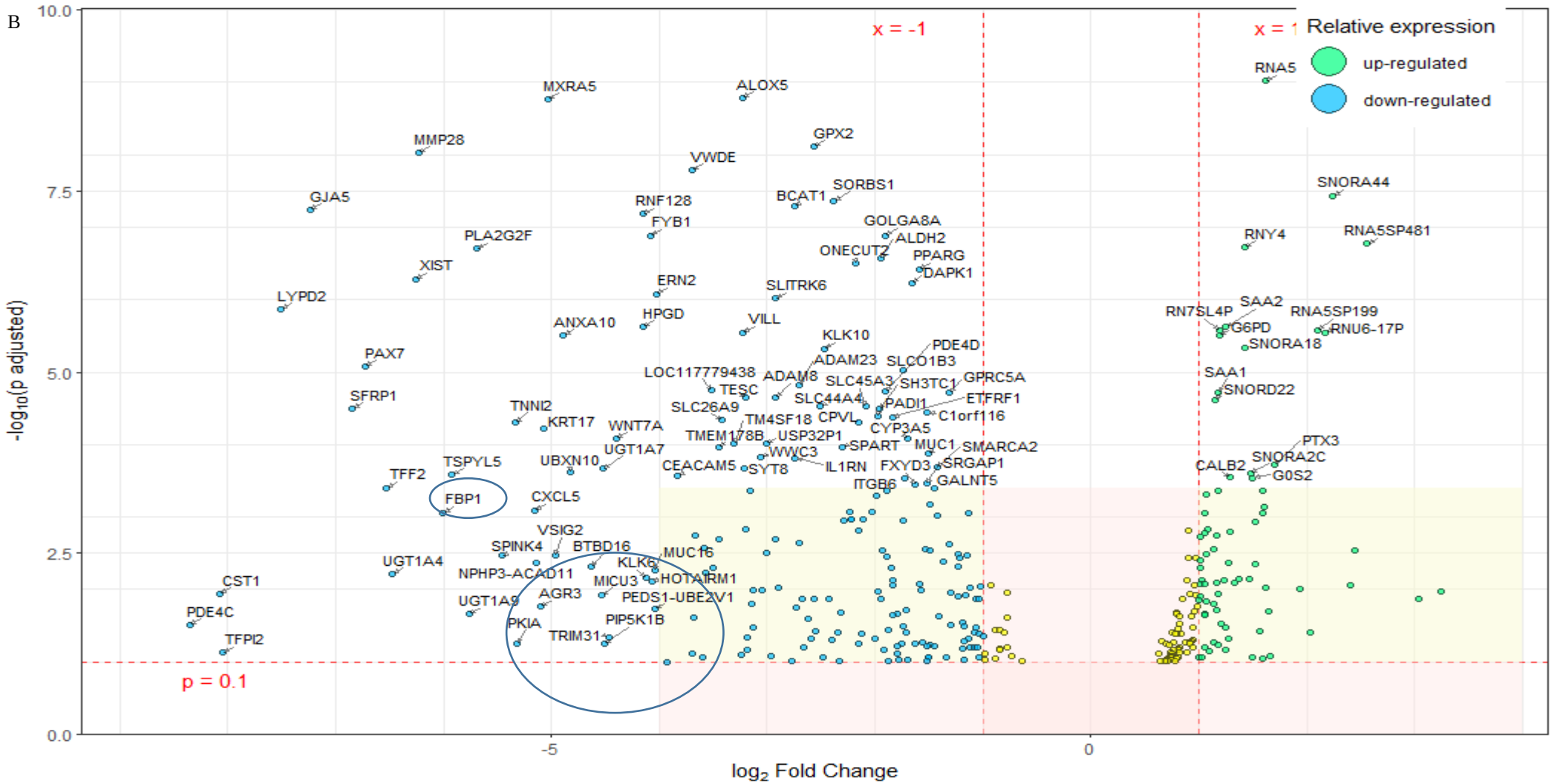

Figure 3.5 1,25(OH)2D3 supplementation resulted in 390 differentially expressed genes (DEGs) in the quasi-mesenchymal pancreatic ductal adenocarcinoma (PDAC) subtype. The volcano plot shows the DEGs with a log2 fold-change and –log10 adjusted p-value (padj < 0.10) when comparing 1,25(OH)2D3 treated vs control samples (n = 3; green = 2-fold up-regulated; blue = 2-fold down-regulated). Expression of mucin family genes and the tumour suppressor gene, *TSPYL5*, were down-regulated in response to $1,25(OH)_2D_3$ supplementation.

Table 3.2 $1,25(OH)_2D_3$ supplementation resulted in differential expression of cancer associated genes in the epithelial pancreatic ductal adenocarcinoma subtype.

Gene ID	Gene name	log2FC	p-value	Cancer hallmark	Tissue type[a]	Role in Cancer
CNOT3	CCR4-NOT transcription complex subunit 3	-0.922	$1.17E^{-09}$	Yes	L	TSG
HIP1	huntingtin interacting protein 1	-1.303	$1.03E^{-06}$	Yes	L, E	oncogene, fusion
LCP1	lymphocyte cytosolic protein 1 (L-plastin)	-0.924	$2.54E^{-06}$	No	L	fusion
MYC	v-myc myelocytomatosis viral oncogene homolog (avian)	-0.758	$1.24E^{-05}$	Yes	L, E	oncogene, fusion
PPARG	peroxisome proliferative activated receptor, gamma	0.763	$1.68E^{-05}$	Yes	E	TSG, fusion
U2AF1	U2 small nuclear RNA auxiliary factor 1	-0.711	$3.48E^{-05}$	No	L	oncogene
NIN	ninein (GSK3B interacting protein)	-0.707	$4.27E^{-05}$	No	L	fusion
ID3	inhibitor of DNA binding 3, HLH protein	-1.713	$4.33E^{-05}$	No	L	TSG
HSP90AB1	heat shock protein 90kDa alpha (cytosolic), class B member 1	-0.481	0.000051	No	L	fusion
CALR	calreticulin	-0.483	0.000103	Yes	L	oncogene
CCND2	cyclin D2	-3.189	0.000103	Yes	L	oncogene, fusion
DEK	DEK oncogene (DNA binding)	-0.531	0.000117	No	L	oncogene, fusion
FLNA	filamin A	-0.499	0.000117	No	E	
ERBB2	v-erb-b2 erythroblastic leukemia viral oncogene homolog 2	0.601	0.000153	Yes	E	oncogene, fusion
MB21D2	Mab-21 domain containing 2	-1.627	0.000191	No	E	
EGFR	epidermal growth factor receptor	-0.578	0.000194	Yes	E, O	oncogene
HNRNPA2B1	heterogeneous nuclear ribonucleoprotein A2/B1	-0.446	0.000221	Yes	E	oncogene, fusion
LASP1	LIM and SH3 protein 1	-0.455	0.000332	No	L	fusion
NFIB	nuclear factor I/B	-0.665	0.000339	No	E	fusion
ASXL1	additional sex combs like 1	-0.709	0.000345	Yes	L	TSG

[a]E - epithelial; L- leukaemia/lymphoma; M – mesenchymal; O – other.

Table 3.3 1,25(OH)$_2$D$_3$ supplementation resulted in differential expression of cancer associated genes in the quasi-mesenchymal pancreatic ductal adenocarcinoma subtype.

Gene ID	Gene name	log2FC	p-value	Cancer hallmark	Tissue type[a]	Role in Cancer
KRAS	v-Ki-ras2 Kirsten rat sarcoma 2 viral oncogene homolog	-2.365	2.31E^{-19}	Yes	L, E, M, O	oncogene
ALDH2	aldehyde dehydrogenase 2 family (mitochondrial)	-1.952	4.99E^{-10}	No	M	fusion
PPARG	peroxisome proliferative activated receptor, gamma	-1.594	7.49E^{-10}	Yes	E	TSG, fusion
PAX7	paired box gene 7	-6.730	2.36E^{-08}	Yes	M	fusion
SLC45A3	solute carrier family 45, member 3	-2.088	1.01E^{-07}	Yes	E	fusion
MUC1	mucin 1, transmembrane	-1.507	5.79E^{-07}	No	L	fusion
EPAS1	endothelial PAS domain protein 1	1.069	2.61E^{-06}	Yes	E, M	oncogene, TSG
MUC16	mucin 16, cell surface associated	-4.040	4.51E^{-05}	No	E	oncogene
KDM5A	lysine (K)-specific demethylase 5A, JARID1A	-0.933	8.21E^{-05}	No	L	oncogene, fusion
IDH2	isocitrate dehydrogenase 2 (NADP+), mitochondrial	0.967	0.000122	Yes	O	oncogene
CCND2	cyclin D2	-3.678	0.000296	Yes	L	oncogene, fusion
MECOM	MDS1 and EVI1 complex locus	-1.179	0.000396	No	L	oncogene, fusion
LCP1	lymphocyte cytosolic protein 1 (L-plastin)	0.952	0.000414	No	L	fusion
ID3	inhibitor of DNA binding 3, HLH protein	1.246	0.000417	No	L	TSG
KNL1	cancer susceptibility candidate 5	-0.840	0.000457	Yes	L	TSG, fusion
U2AF1	U2 small nuclear RNA auxiliary factor 1	0.769	0.000783	No	L	oncogene
PIM1	pim-1 oncogene	-1.346	0.001485	Yes	L	oncogene, fusion
FGFR2	fibroblast growth factor receptor 2	-1.703	0.001709	Yes	E	oncogene, fusion
FOXP1	forkhead box P1	-0.848	0.002051	No	L	oncogene, fusion
TOP1	topoisomerase (DNA) I	0.603	0.002172	No	L	fusion

[a]E - epithelial; L- leukaemia/lymphoma; M – mesenchymal; O – other.

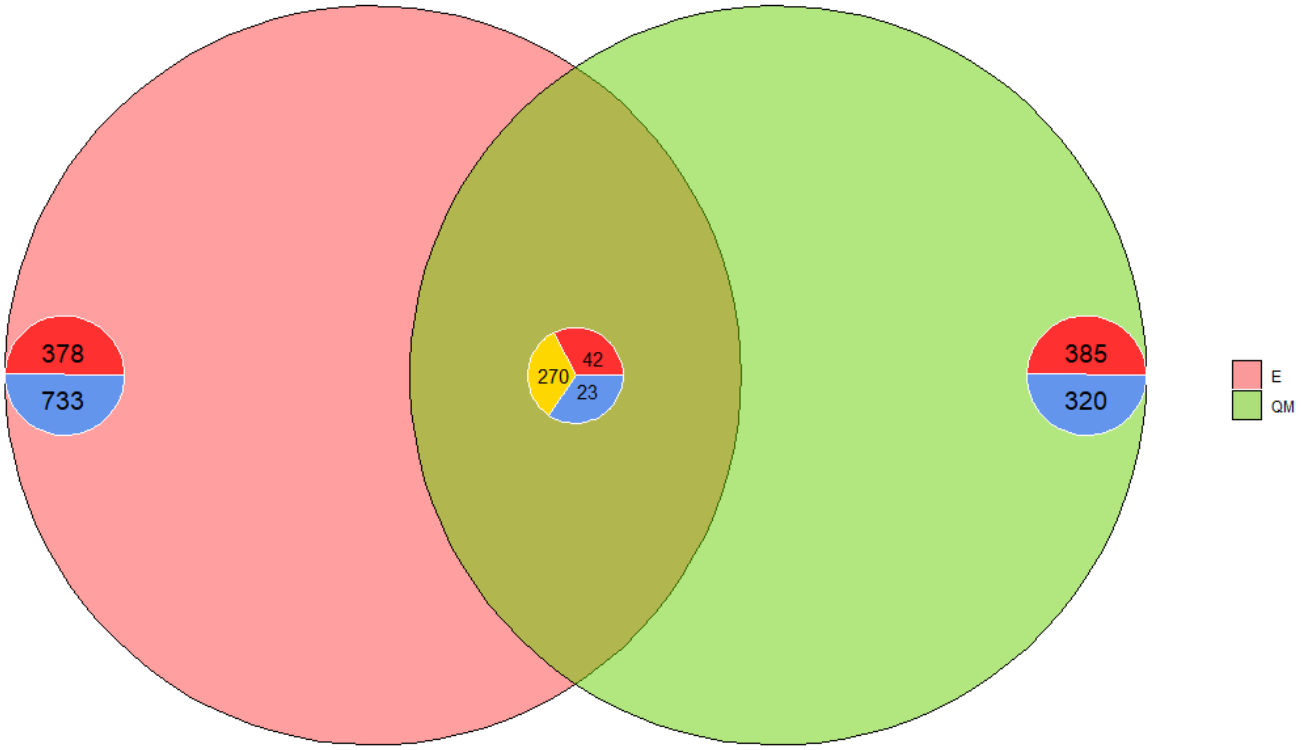

Figure 3.6 Comparison of differentially expressed genes (DEGs) between the epithelial and quasi-mesenchymal pancreatic ductal adenocarcinoma subtypes in response to 1,25(OH)$_2$D$_3$ supplementation revealed 270 contra-regulated DEGs. DEGs from E and QM PDAC subtypes were compared- 42 (red) and 23 (blue) genes were commonly up- and down-regulated in both E (pink) and QM (green) PDAC subtypes, respectively, in response to 1,25(OH)$_2$D$_3$ supplementation. 270 DEGs had opposite expressions between the E and QM PDAC subtypes (yellow) in response to 1,25(OH)$_2$D$_3$ supplementation. E = epithelial; QM = quasi-mesenchymal.

3.3 Gene ontology term enrichment and pathway analysis

3.3.1 *Gene ontology terms and functional enrichment*

To gain biological insight into the list of DEGs, functional analysis using an over-representation analysis (ORA) approach was conducted. clusterProfiler v4.2.2 was used to perform ORA on gene ontology (GO) terms associated with the list of DEGs (Yu et al., 2012). These analyses were conducted to determine if biological pathways, functions and interactions were enriched from the list of DEGs and to identify genes involved in these pathways. Biological processes (BP) related to normal cellular energy production were enriched in the E subtype from the up-regulated DEGs (Fig 3.7 A). BP related to cellular responses to hypoxia were enriched in the QM subtype from the up-regulated DEGs (Fig 3.7 B). Notably, both E and QM subtypes presented with BP terms relating to immune responses, enriched from their respective DEGs up-regulated in response to $1,25(OH)_2D_3$ supplementation. BP related to the cell cycle and mitosis were enriched from the down-regulated DEGs in the E subtype (Fig 3.8 A), while BP relating to integrin-mediated cell adhesion, normal pancreas and epithelial cell development were enriched from the down-regulated DEGs in the QM subtype (Fig 3.8 B).

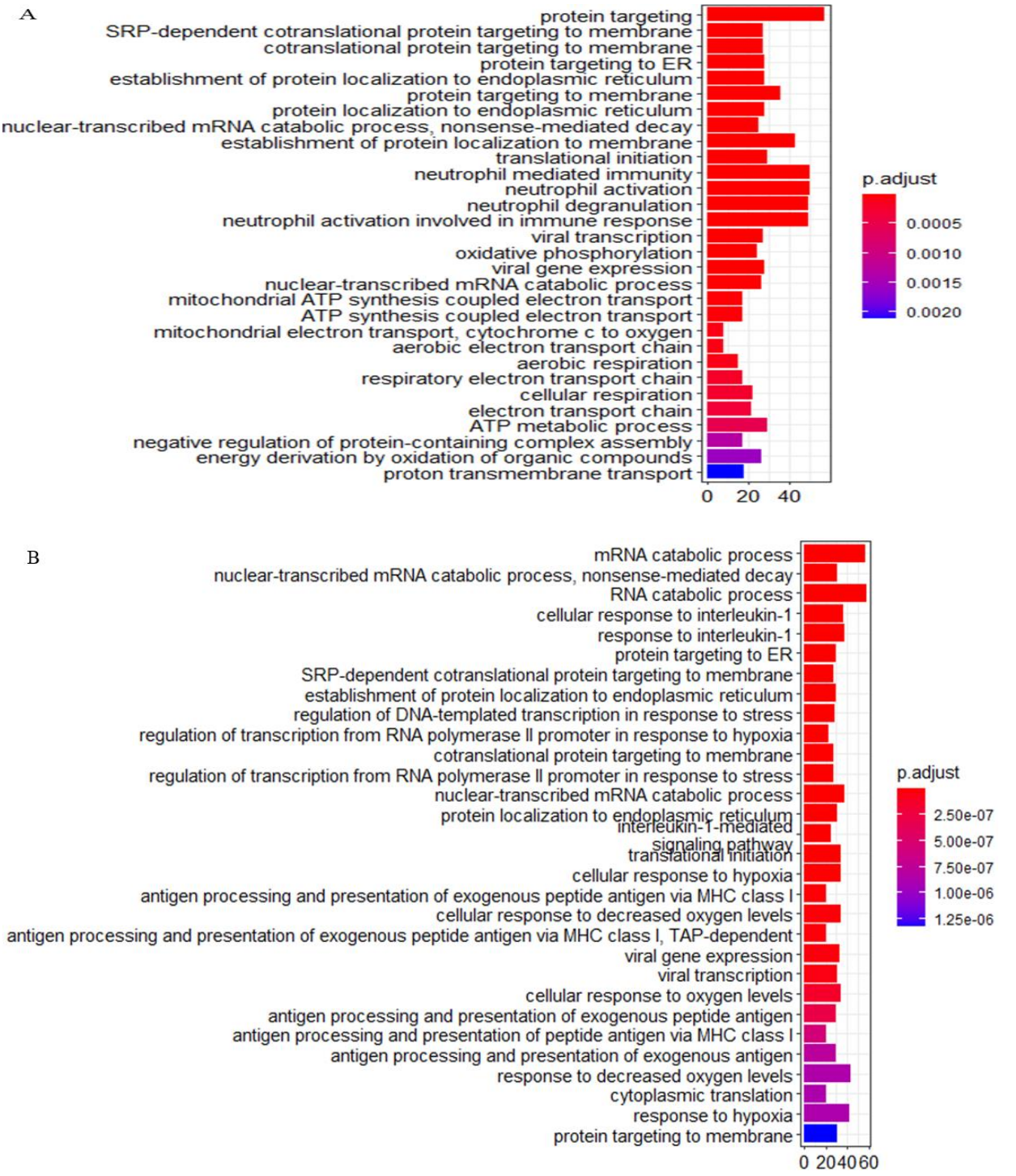

Figure 3.7 Biological processes related to cellular respiration and immune responses were enriched in the E PDAC subtype, while processes related to cellular response to hypoxia and immune responses were enriched in the QM subtype in response to 1,25(OH)$_2$D$_3$ supplementation. Gene ontology (GO) bar plot of the top 30 GO terms related to biological processes (BP) enriched from the up-regulated differentially expressed genes (DEGs) when comparing 1,25(OH)$_2$D$_3$ treated vs control samples in the epithelial (A, n = 3) and quasi-mesenchymal (B, n = 3) pancreatic ductal adenocarcinoma (PDAC)) subtypes. Bars are coloured by adjusted p-value (padj) where blue is higher and red is a lower padj. Bar size is a measure of the number of genes from the list of up-regulated DEGs present in the given GO term. E = epithelial, QM = quasi-mesenchymal.

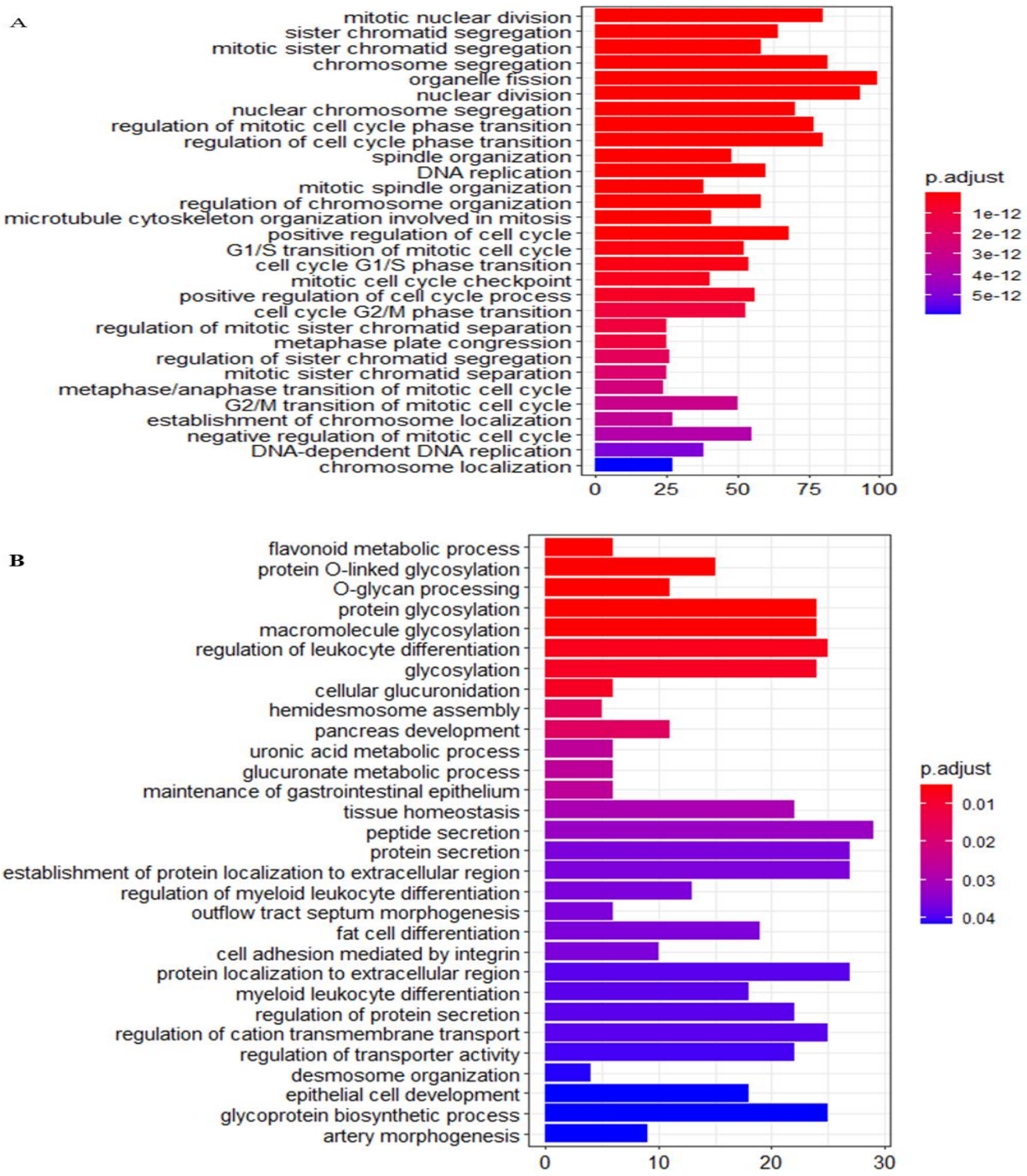

Figure 3.8 Biological processes related to cell cycle and mitosis were enriched in the E subtype while processes related to epithelial cell and pancreas development, and integrin mediated cell adhesion were enriched in the QM subtype in response to 1,25(OH)$_2$D$_3$ supplementation. Gene ontology (GO) bar plot of the top 30 GO terms related to biological processes (BP) enriched from the down-regulated differentially expressed genes (DEGs) when comparing 1,25(OH)$_2$D$_3$ treated vs control samples in the epithelial (A, n = 3) and quasi-mesenchymal (B, n = 3) pancreatic ductal adenocarcinoma (PDAC)) subtypes. Bars are coloured by adjusted p-value (padj) where blue is higher and red is a lower padj. Bar size is a measure of the number of genes from the list of up-regulated DEGs present in the given GO term. E = epithelial, QM = quasi-mesenchymal.

3.3.2 *Kyoto encyclopaedia of genes and genomes (KEGG) pathways*

Gene set enrichment analysis (GSEA) using clusterProfiler was conducted using a functional class scoring (FCS) approach to test for coordinated differential expression over gene sets. The GSEA results were visualised as Kyoto Encyclopaedia of Genes and Genomes (KEGG) pathways using the Pathview v1.34.0 package (Luo and Brouwer, 2013). Nine and twenty-five KEGG pathways were found to have coordinated DE over gene sets in the E and QM PDAC subtypes respectively, in response to 10 nM $1,25(OH)_2D_3$ supplementation. Two pathways presenting with co-ordinated differential gene expression from both E and QM PDAC subtypes were of interest, respectively. In the E PDAC subtype, the calcium signalling pathway had many of its constituents down-regulated (Fig 3.9). The calcium signalling pathway and its constituents are involved in cellular processes related to cell proliferation. In the QM PDAC subtype, an antigen presentation and processing pathway presented with co-ordinated differential expression in response to $1,25(OH)_2D_3$ supplementation (Fig 3.10). Genes related to initiating and assisting in immune responses were up-regulated in this pathway.

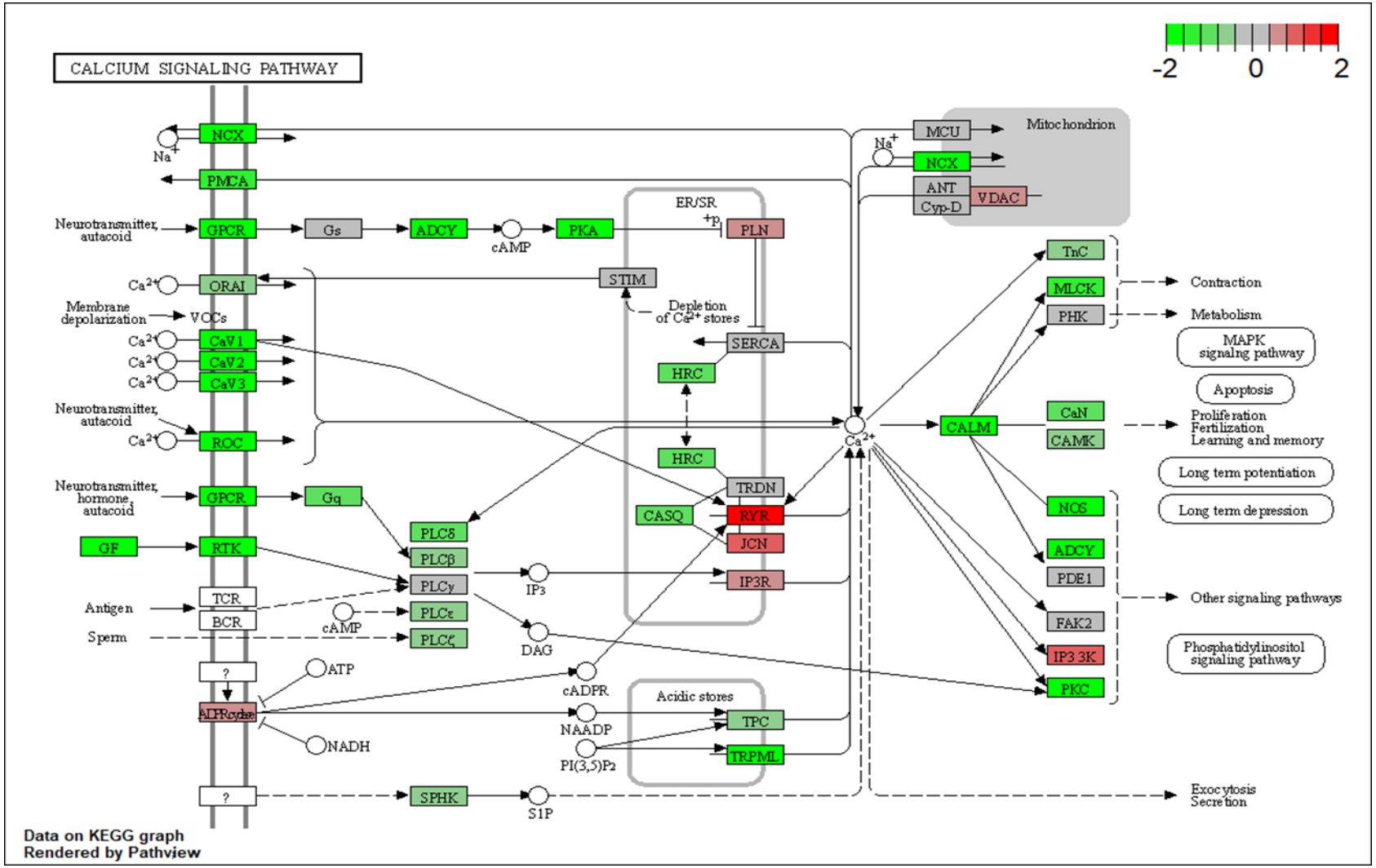

Figure 3.9 KEGG calcium signalling pathway linked to cell proliferation with general down-regulation of pathway constituents. This pathway has coordinated differential expression over gene sets in the epithelial pancreatic ductal adenocarcinoma subtype in response to 10 nM $1,25(OH)_2D_3$ supplementation. Green – down-regulated; red – up-regulated. Straight line arrows indicate molecular interaction or relation; broken line arrows indicate indirect link, circles represent chemical compounds.

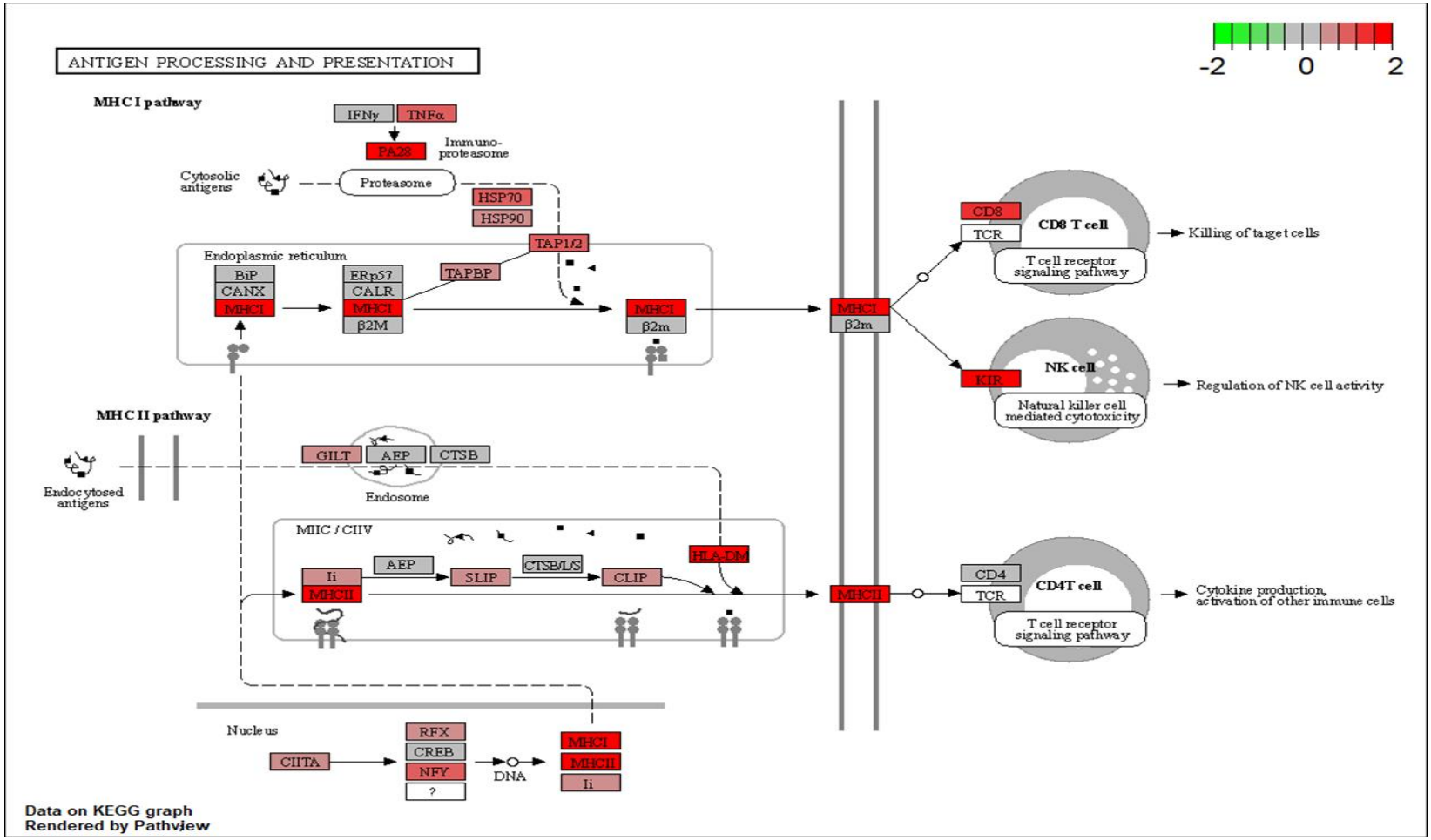

Figure 3.10 KEGG antigen processing and presentation signalling pathway linked to initiating and assisting in immune responses with general up-regulation of pathway constituents. This pathway has coordinated differential expression over gene sets in the quasi-mesenchymal pancreatic ductal adenocarcinoma subtype in response to 10 nM $1,25(OH)_2D_3$ supplementation. Green – down-regulated; red – up-regulated. Straight line arrows indicate molecular interaction or relation; broken line arrows indicate indirect link, circles represent chemical compounds.

Chapter 4: Discussion

Pancreatic cancer, and in particular, pancreatic ductal adenocarcinoma is an extremely dangerous malignancy with poor disease prognosis (McGuigan et al., 2018). Current clinical treatments are insufficiently effective, necessitating the research of alternate preventative and therapeutic options (Quiñonero et al., 2019). Various epidemiological studies have associated vitamin D deficiency with an increased cancer incidence (Liu et al., 2018). $1,25(OH)_2D_3$ has been touted as a potential preventative, as well as a therapeutic option for cancer, and has been shown to increase the efficacy of various chemotherapeutic drugs *in vitro* and *in vivo* (Ma *et al*., 2010). However, the effects of $1,25(OH)_2D_3$ on the outcome of PDAC remains to be ascertained. $1,25(OH)_2D_3$ has been shown to differentially modulate the epithelial and mesenchymal subtypes present in PDAC. The plasticity of the PDAC tumour is, in part, attributed to the epithelial-to-mesenchymal transition of the tumour cells, and this plasticity is linked to the inherent chemoresistance of PDAC. Thus, insight into the effect of $1,25(OH)_2D_3$ on these PDAC subtypes is required, as well as the mechanisms and key role-players involved in the differential response to $1,25(OH)_2D_3$ observed between these two PDAC subtypes.

The parent study, wherefrom our RNA-Seq data was generated, analysed the differences in gene expression in the E and QM PDAC subtypes in response to $1,25(OH)_2D_3$ supplementation, as well as the effect of the chemotherapeutic agent, FOLFIRINOX, on gene expression (Porter et al., 2019). The study also observed, amongst other observations, the migratory capacity and metastatic potential of the PDAC subtypes in murine models in response to $1,25(OH)_2D_3$ supplementation (Porter et al., 2019). Some of our findings were similar to what these researchers found, however, our study was unique in that we analysed the genes differentially expressed in common in the E and QM PDAC subtypes in response to $1,25(OH)_2D_3$ supplementation. Our study aimed to find genes differentially expressed in response to $1,25(OH)_2D_3$ supplementation, and elucidate whether these DEGs are associated with the differential response to $1,25(OH)_2D_3$ observed between the PDAC subtypes, and if these genes are associated with the EMT and plasticity of the PDAC tumour. Understanding the fluidity of the PDAC subtypes will aid in developing effective treatment regimens against these different subpopulations.

For this, we compared and analysed the transcriptional profiles of human PDAC cells cultured from the resected tumours of PDAC patients (E: n = 3; QM n = 3) supplemented with or without 10 nM $1,25(OH)_2D_3$. We identified genes differentially expressed in each PDAC subtype, as well as biological processes enriched from these differentially expressed genes in response to 10 nM $1,25(OH)_2D_3$ supplementation. We then compared the genes commonly differentially expressed in response to $1,25(OH)_2D_3$ between the PDAC subtypes, to gain insight into possible differences in vitamin D responsiveness between the PDAC subtypes, and analyse the cancer-associated genes that were contra-regulated between the PDAC subtypes, in response to $1,25(OH)_2D_3$ supplementation. In total, DGE analysis yielded 1 991 and 1 744 DEGs (Wald Test p-value < 0.05) in the E and QM subtypes respectively. Comparing the DEGs of the PDAC subtypes revealed 335 commonly DEGs, of which 270 were contra-regulated, indicating a differential response to $1,25(OH)_2D_3$ between the subtypes.

4.1 Effective quality control revealed acceptable data quality

Quality control was carried out on the raw RNA-Seq read FASTQ files using FASTQC, and effectively checked the quality of the data. None of the 72 paired-end FASTQ files were flagged for poor quality, enabling the use of all the available data for this study.

The Salmon mapping rates were consistent across samples, indicative of unbiased and successful transcript abundance estimation. The mean mapping rate of 50.21% is consistent with acceptable read mapping from human-derived RNA-Seq data. There are various reasons for the observed mapping rates falling in this range, even though the reads were of high quality. It is possible that this occurred as a result of the majority of the reads being around 74 base pairs (bp) to 76 bp long, which is not especially high (Patro *et al.*, 2017). The default Salmon k-mer length of 31 is optimised for 75 bp and higher (Patro et al., 2017). The majority of our reads just fall into the optimised size range. A more plausible explanation for the observed Salmon mapping rates is the possibility that a considerable number of reads came from outside the annotated transcriptome, and hence were not mapped against the transcriptome. Since we analysed the transcriptome of primary human cells derived from PDAC patients, it is possible that a proportion of the transcripts present in the cells are not annotated (yet), and Salmon can only quantify what it knows about in

terms of annotated transcripts (Patro et al., 2017). Novel genes, gene isoforms, and intron retention events cannot be identified by Salmon, as these annotations might not be in the transcriptome. We note that an average of 10 000 000 reads were discarded due to low mapping scores, per sample, which suggests that those reads were not a good match for the underlying annotated transcripts. Considering that the human transcriptome is well annotated, the most probable cause of the observed mapping rates is poor initial RNA quality/degraded RNA, which is a feature of patient-derived RNA samples. Nevertheless, the Salmon mapping rates were acceptable to proceed with DGE analysis.

Principal component analysis revealed indistinct clustering by condition in both PDAC subtypes, necessitating the batch effect correction step which was carried out using the sva package. The batch effect correction improved the DGE analysis output. The quality of the DGE analysis was confirmed by generating mean estimate dispersion plots and mean-average log ratio plots which showed that DESeq2 had effectively reduced intra-sample variance and that the data was a good fit for the DESeq2 model. Moreover, the results confirmed that most DEGs were found in the same mean normalised range with no DEGs coming from weakly expressed genes. We considered a gene to be DE when it presented with a p-value of less than 0.05 ($p < 0.05$) as determined by the Wald test employed by DESeq2 (Love *et al*., 2014). This was chosen ahead of the more stringent Benjamini-Hochberg false discovery corrected adjusted p-value of less than 0.1 ($padj < 0.1$) because of the low number of DEGs obtained from the DGE analysis, but was deemed adequate for the purposes of our study.

4.2 1,25(OH)$_2$D$_3$ supplementation resulted in differential gene expression in human epithelial and quasi-mesenchymal pancreatic ductal adenocarcinoma subtypes

4.2.1 *CYP24A1 was up-regulated in the epithelial pancreatic ductal adenocarcinoma subtype only*

Aberrant gene expression is integral to the development and progression of cancer (Suzuki et al., 2014). The dysregulation of genes involved in the biological processes of cell growth and proliferation, stress responses in favour of survival, cellular metabolism, immune system and tumour microenvironment modulation, inhibition and avoidance of cell death, angiogenesis and

tumour vascularisation, tumour invasion and metastasis, and a dysregulated epigenome all contribute to cancer progression, beginning with an unstable genome and tumour-promoting inflammation (Hanahan and Weinberg, 2011, 2000). $1,25(OH)_2D_3$/VDR is a transcription factor and powerful regulator of gene expression (Carlberg and Campbell, 2013). The effect of $1,25(OH)_2D_3$ as an gene expression regulator has been most prominently observed in immune cells, which appear to be the most responsive of cell types to $1,25(OH)_2D_3$ (Dimitrov et al., 2021; Pike et al., 2016). The effects of $1,25(OH)_2D_3$ across cell types is being continuously built upon, including cancerous cells.

Interestingly, we note that the $1,25(OH)_2D_3$ metabolising enzyme, *CYP24A1*, was significantly up-regulated in the E-subtype in response to $1,25(OH)_2D_3$ supplementation, but not in the QM-subtype. *CYP24A1* regulates intracellular $1,25(OH)_2D_3$ concentration by catabolising it, and its expression is regulated by $1,25(OH)_2D_3$/VDR via a feedback loop (Bikle, 2014). *CYP24A1* is a target of $1,25(OH)_2D_3$/VDR and its expression is used as a marker for VDR expression and activity (Bikle, 2014). *CYP24A1* has been observed to be amplified and overexpressed in cancer cells, and numerous studies have found $1,25(OH)_2D_3$'s anti-tumoural activity to be associated with decreased *CYP24A1* levels (Deeb et al., 2007; Hu and Zhang, 2018; Zhalehjoo et al., 2017). This points to dysregulated $1,25(OH)_2D_3$ metabolism and signalling in cancer-associated/tumourigenic pathways, and that altered $1,25(OH)_2D_3$ metabolism by *CYP24A1* in cancerous cells may impair its anti-tumoural functions. This is further exemplified by the anti-tumoural effects of $1,25(OH)_2D_3$ being amplified in response to *CYP24A1* inhibition in cancer cells (Kósa et al., 2013; Muindi et al., 2010). The observed increase of $1,25(OH)_2D_3$'s anti-tumoural effect by *CYP24A1* inhibition is most likely due to increased $1,25(OH)_2D_3$ exposure, as its catabolism is reduced by *CYP24A1* inhibition, but the exact causes remain to be fully elucidated (Muindi et al., 2010). The up-regulation of *CYP24A1* in only the E subtype indicates a differential response to $1,25(OH)_2D_3$ between these subtypes, which may partially explain the overall differential response between the two cell types. We note this differential response in the number and type of DEGs from each subtype - more genes were DE in the E subtype compared to the QM subtype.

4.3 $1,25(OH)_2D_3$ supplementation resulted in differential expression of cancer associated genes in the epithelial and quasi-mesenchymal pancreatic ductal adenocarcinoma subtypes.

4.3.1 *Cell growth and proliferation promoting related genes were down-regulated in the epithelial pancreatic ductal adenocarcinoma subtype in response to 1,25(OH)$_2$D$_3$ supplementation*

The expression of some cancer-related genes (genes involved in cancer-associated pathways/cancer hallmarks) presented with mixed expression in each PDAC subtype. In both PDAC subtypes, RAS family oncogenes were down-regulated in response to 1,25(OH)$_2$D$_3$ supplementation- the *NRAS* and *KRAS* oncogenes were down-regulated in the E and QM subtypes, respectively. *RAS* family mutations (generally amplifications, especially in *KRAS*) are considered PC initiators, and are found mutated and overexpressed in early PC development (Ferro and Falasca, 2014; Pylayeva-Gupta et al., 2011). RAS family proteins relay upstream signals to downstream effectors. Common *RAS* family downstream effector pathways are the MAPK and PI3K pathways. 1,25(OH)$_2$D$_3$ down-regulating *RAS* family genes can have wide-spread effects on cancer-associated pathways, since *RAS* gene products (RAS GTPases) are involved in the regulation (generally activation via phosphorylating effector proteins) of genes and pathways involved in cell growth and proliferation, apoptosis evasion and cell survival, as well as the loss of cell adhesion and promoting cell migration (di Magliano and Logsdon, 2013; Pylayeva-Gupta et al., 2011). *RAS* family oncogenes can influence these biological processes by regulating pathways like the MAPK and PI3K/AKT pathways, both well characterised pathways that are tumourigenic when dysregulated. In the context of RAS-MAPK signalling, activated RAS proteins recruit cytosolic rapidly accelerated fibrosarcoma (RAF) family proteins, which are activated through various interactions including RAS and can the activate MAPK family proteins, as well as extracellular signal-related kinase (ERK) family proteins (Erijman and Shifman, 2016). Activation of these downstream effectors can then lead to the promotion of tumourigenic pathways. However, the mitogen activated protein kinases 1 and 12 genes (*MAPK1* and *MAPK12*) were slightly up-regulated in the QM subtype, even though *KRAS* was down-regulated. This may be the result of RAS-independent MAPK activation, where *RAF* mutations result in active RAF family proteins leading to dysregulated RAF signalling and hence, activation of MAPK pathways (Wan et al., 2004).

4.3.2 *1,25(OH)$_2$D$_3$ may augment the JAK/STAT pathway in pancreatic ductal adenocarcinoma*

The Janus kinase 1 (*JAK1*) gene was up-regulated in both PDAC subtypes in response to 1,25(OH)$_2$D$_3$ supplementation. *JAK1* encodes a tyrosine protein kinase, whose major functions are to initiate responses to various cytokines through interacting with cytokine receptors (CRs; e.g. interleukin family receptors; Gadina *et al.*, 2001). In the E subtype, 1,25(OH)$_2$D$_3$ supplementation resulted in co-ordinated down-regulation of multiple cytokines and interleukins, but in-depth analysis of the DE of these cytokines is out of the scope of this study. Cytokines that bind class I or class II CRs employ the JAK-STAT signalling pathway to exert their effects on cells. Activated JAK proteins will activate and dimerise signal transducers and activators of transcription (STATs) proteins, which then relay the cytokine signal by moving to the nucleus, binding DNA and activating the transcription of target genes (Darnell, 1997). The JAK/STAT pathway can inhibit apoptosis and promote cell proliferation and malignant transformation in the pancreas. The presence of reactive oxidative species in the pancreas can activate the JAK/STAT pathway, as well as induce the production and secretion of inflammatory cytokines like IL-1β and IL-6 and tumour necrosis factor-α (TNF-α). We note an up-regulation of JAK1, even though vitamin D has been associated with controlling ROS mainly through regulating the expression of the klotho gene *KL*, a TSG (Yu and Kim, 2012). However, *KL* is found severely down-regulated in many solid tumours, including PDAC (Zhou et al., 2017). Downstream of JAK1 activation, we also note the up-regulation of matrix metalloproteinases (*MMP*) 7 and 14 in the E subtype, but down-regulation of *MMP* 19 and 28 in the QM subtype. MMPs mainly function in the extracellular space, degrading cell-surface and matrix proteins. MMPs are involved in promoting local inflammation and tumour cell migration and metastasis by breaking through the basement membrane and allowing tumour cells to migrate (Slapak et al., 2020). Another downstream effector of JAK1 inflammation induction, are the cyclooxygenase (COX) proteins, which promote inflammation and have been associated with pancreatitis, a PC risk factor (Hill et al., 2012). In the E subtype, *COX2/5B/6A/6B1/7A2/7B* were up-regulated in response to 1,25(OH)$_2$D$_3$ supplementation, with *COX6B1*/*7A2*/*8A* up-regulated in the QM subtype. *COX2* is a major pro-inflammatory role-player in the JAK/STAT pathway (Hill et al., 2012). Interestingly, the expression of *IL-1β* was contra-regulated between the subtypes, with *IL-1β* being up-regulated in the QM subtype only, along with *IL-1α*. This is further exemplified by the over-representation analysis on up-regulated genes

showing enrichment of GO terms relating to interleukin 1 response. Taken together, the up-regulation of *JAK1* and its downstream effectors indicate that $1,25(OH)_2D_3$ may augment JAK/STAT signalling in a pro-inflammatory and pro-tumorigenic manner.

4.3.3 *$1,25(OH)_2D_3$ differentially regulates oncogenic MYC and its downstream effectors in epithelial and quasi-mesenchymal pancreatic ductal adenocarcinoma subtypes*

In the E subtype, $1,25(OH)_2D_3$ supplementation resulted in general down-regulation of cell-cycle associated genes, as evidenced by enriched gene ontology biological processes from the down-regulated DEGs being related to cell cycle functions. BPs relating to DNA replication, progression through the cell cycle phases, mitotic machinery and mitotic nuclear division were enriched from the down-regulated DEGs. The chief anti-tumoural functions of $1,25(OH)_2D_3$ include resisting proliferation via cell cycle arrest between the G_0 and G_1 phases, inducing differentiation, inducing apoptosis, inhibiting tumour angiogenesis and modulating various signalling pathways in cancerous cells (Deeb et al., 2007; Feldman et al., 2014). We note the anti-proliferative effects of $1,25(OH)_2D_3$ supplementation seen in the E subtype. The *MYC* oncogene was down-regulated in the E subtype in response to $1,25(OH)_2D_3$ supplementation, but up-regulated in the QM subtype. MYC is aberrantly active in PDAC, and is a master regulator of various processes, including increased DNA replication associated with tumour growth, cell growth and proliferation and inhibition of cell senescence (Gabay et al., 2014; Hessmann et al., 2016). The expression, and by extension, activity of *MYC*, is regulated by its transcriptional repressor, MXD1. $1,25(OH)_2D_3$ has be shown to suppress the expression of genes regulated by MYC, by positively regulating the expression of *MXD1* (Salehi-Tabar *et al.*, 2012). In the E subtype, we note the up-regulation of *MXD1* in response to $1,25(OH)_2D_3$ supplementation. Taken together, the results of our over-representation analysis on down-regulated cell-cycle pathway constituent genes and DGE analysis on *MYC* and its transcriptional repressor *MXD1* indicate that $1,25(OH)_2D_3$ may decrease cell cycle and proliferative capacity in the E subtype and provide a molecular basis for the anti-tumorigenic effect of vitamin D.

Conversely, MYC expression was up-regulated in the QM subtype in response to $1,25(OH)_2D_3$ supplementation. There was no enrichment of cell-cycle pathways from down-regulated genes in

the QM subtype. However, biological processes relating to cellular responses to hypoxia were enriched from the up-regulated DEGs in the QM subtype. MYC oncoproteins play crucial roles in activating tumour angiogenesis (Baudino et al., 2002). The hypoxia inducible factor alpha subunit gene (*HIF1A*) was found up-regulated in the QM subtype in response to $1,25(OH)_2D_3$ supplementation. *HIF1A* encodes the alpha/α subunit of the HIF, which is a TF that controls the cellular response to hypoxia. The dysregulation and over-expression of HIF in cancer positively regulates tumour angiogenesis, as well as the cancerous processes of cell survival and tumour cell invasion (Yang et al., 2013). PDAC tumours lack vasculature are generally hypoxic, and this has been positively associated with PDAC aggressiveness and chemoresistance (Tao et al., 2021). *HIF1A* expression is not only regulated by hypoxia, but also by activated oncogenes (Yuen and Díaz, 2014). MYC has been shown to positively regulate the expression and activity of HIF1α post-transcriptionally (Chen et al., 2013; Doe et al., 2012; Weili et al., 2019). The overexpression of MYC has also been shown to stabilise HIF1α and promote its non-physiologic cellular build-up (Doe et al., 2012). Together, oncogenic MYC and HIF function to promote tumour angiogenesis, metastasis and chemoresistance and have also been implicated in altered cellular metabolism- the Warburg effect. Collaboration between MYC and HIF has been seen to increase the cell's metabolic requirements, through increased glucose uptake and its subsequent conversion to lactate (Dang, 2007). Normal mitochondrial respiration can also be down-regulated by HIF, through its induction of pyruvate dehydrogenase kinase (Dang, 2007). The MYC-HIF interaction may account for a part of the observed Warburg effect in cancers and attenuation of mitochondrial respiration. Notably, GO terms relating to biological processes involving normal energy production/aerobic respiration/oxidative phosphorylation were enriched from the up-regulated DEGs in the E subtype only. The lactate dehydrogenase A (*LDHA*) gene was found down-regulated in the E subtype in response to $1,25(OH)_2D_3$ supplementation. Aberrant up-regulation of LDHA is implicated in cancer progression. Over-expression of LDHA is involved in altered cell metabolism, or the Warburg effect in cancer cells, and its aberrant expression is governed, in part, by MYC-HIF interactions (Koukourakis et al., 2003). In PC, the MYC-LDHA interaction has been observed to promote tumour progression (He et al., 2015). The activation of a single oncogene or repression of a TSG can have far-reaching and profound effects on cancer-associated processes and pathways in a cell. We see that just from the differential expression of *MYC* in the E and QM PDAC subtypes in response to $1,25(OH)_2D_3$ supplementation, various processes relating to

oncogenic *MYC* are influenced (positively and negatively), and again point to differential vitamin D/VDR signalling between these PDAC subtypes.

4.3.4 *1,25(OH)$_2$D$_3$ supplementation down-regulated cell cycle associated cyclins in epithelial and quasi-mesenchymal pancreatic ductal adenocarcinoma subtypes*

Cyclin D2 (*CCND2*) was strongly down-regulated in both PDAC subtypes, along with *CCND1* in the E subtype, in response to 1,25(OH)$_2$D$_3$ supplementation. Cyclins D1 and D2 are crucial cell cycle regulators, controlling the progression through G_1 to S phase of the cell cycle in complex with the cyclin-dependant kinases (CDK) 4 and 6. *CDK6* was down-regulated in the QM subtype, in response to 1,25(OH)$_2$D$_3$ supplementation. The CCND1/2-CDK4/6 complex promotes progression through the cell cycle by phosphorylating and inactivating the RB protein (Kato et al., 1993; Lundberg and Weinberg, 1998). Cyclin–CDK complexes co-ordinate the completion of DNA replication, which subsequently allows for cell cycle progression leading to cell proliferation (Malumbres and Barbacid, 2009). Cyclins D1/2 are aberrantly expressed (generally over-expressed) in multiple human cancers (Deshpande et al., 2005; Musgrove et al., 2011). Cyclin D1 has also been shown to modulate transcription by regulating the expression of various TFs and histone deacetylase 3 (HDAC3; Coqueret, 2002). HDAC3 is an enzyme involved in histone modification, and can alter chromatin accessibility and hence influence the transcription of genes found in those parts of the genome. Targeting cyclins D1/2/3 via silencing has shown to promote cell cycle arrest at the G_1 phase and reduce cell growth and metastasis in various cancer cells in vivo (He *et al.*, 2018; Yu *et al.*, 2018; Ding *et al.*, 2019). The cell cycle arrest effect of 1,25(OH)$_2$D$_3$ is thought to be mediated by it upregulating the cyclin dependant kinase inhibitor 1 (*p21*), which inhibits CKD4/6 and hence supresses cyclin D1/2 activity (Bhoora and Punchoo, 2020; Jensen et al., 2001). However, we note that *p21* was not up-regulated in either subtype in response to 1,25(OH)$_2$D$_3$ supplementation, even though *CCND1* and *CCND2* were down-regulated.

4.3.5 *1,25(OH)$_2$D$_3$ supplementation resulted in co-ordinated general down-regulation of calcium signalling pathway constituent genes in the epithelial pancreatic ductal adenocarcinoma subtype*

In the E subtype, $1,25(OH)_2D_3$ supplementation resulted in co-ordinated differential expression, encompassing a general down-regulation of calcium signalling pathway genes. Calcium signalling is relayed via Ca^{2+} channels, pumps and exchangers, and where its presence or absence influences effectors of a pathway (Bong and Monteith, 2018). Calcium signalling is ubiquitous and plays crucial roles in normal cell signalling. When dysregulated, calcium signalling pathways can influence the cancer associated processes of cell proliferation and invasiveness, as well as influence the EMT of cancer cells. Calcium signalling positively influences the expression of early cell proliferation-associated genes, like *MYC*, *FOS* family, and *JUN*, all of which were down-regulated in the E subtype in response to $1,25(OH)_2D_3$ supplementation (Roderick and Cook, 2008; Shapovalov et al., 2016). The *FOS* family and *JUN* are genes encoding TFs, whose expression is transiently induced by extracellular mitogenenic stimuli. These TFs are involved in regulating the expression of genes involved in cell growth and proliferation (van Dam and Castellazzi, 2001). *FOS*/*B*/*L1* along with *JUN* were down-regulated in the E subtype in response to $1,25(OH)_2D_3$ supplementation, with *FOSB* being up-regulated in the QM subtype. Calcium signalling pathways are also involved in cancer cell migration and invasive pathways (Prevarskaya et al., 2011). Calcium signalling is also involved in regulating apoptosis, as evidenced by the inhibition of a sarcoplasmic and endoplasmic reticulum adenosine triphosphatase (SERCA; ATPase) to promote apoptosis in multiple cell lines as well as in clinical trials in cancer patients (Mahalingam et al., 2016). SERCA is a calcium ATPase protein pump, necessary for cell viability by pumping Ca^{2+} ions from the cell cytosol into the lumen of the sarcoplasmic reticulum (Tadini-Buoninsegni et al., 2018). The loss of *PTEN*, a TSG, is a cancer hallmark observed in multiple cancers, and its loss is linked to aggressive cancer phenotypes and promoting an immunosuppressive TME (Vidotto et al., 2020). Ca^{2+}- dependent apoptotic pathways have been observed down-regulated by the loss of PTEN (Kuchay et al., 2017). We note an up-regulation of *PTEN* in the E subtype in response to $1,25(OH)_2D_3$ supplementation. In the E subtype, we observed changes in known and characterised oncogenes and TSGs and related pathways that are sensitive to calcium signalling, highlighting the relevance of calcium signalling in cancer.

4.4 $1,25(OH)_2D_3$ supplementation resulted in differential expression of immune-related genes in human epithelial and quasi-mesenchymal pancreatic ductal adenocarcinoma subtypes.

4.4.1 *Biological processes relating to positive regulation of T-cell mediated immunity were enriched from up-regulated genes in the quasi-mesenchymal pancreatic ductal adenocarcinoma subtype in response to $1,25(OH)_2D_3$ supplementation.*

$1,25(OH)_2D_3$ supplementation resulted in co-ordinated general up-regulation of antigen processing and presentation genes in the quasi-mesenchymal pancreatic ductal adenocarcinoma subtype. We note the up-regulation of major histocompatibility complex class I and II (MHCI/II) encoding genes - human leukocyte antigen A, B, C, and E genes (*HLA-A/B/C/E/DRB1*). These MHCs encoded by these HLA genes present peptide fragments on the cell surface, allowing for the peptide to be recognised by the appropriate T-cells (Hennecke and Wiley, 2001). In the context of cancer, the MHCs can present peptides marking a cell as cancerous, and can thus target T-cells to cancer cells for immune-mediated destruction (Garrido et al., 2016; Garrido and Aptsiauri, 2019). Low or absent MHC class I and II expression has been associated with higher grade malignancies and metastatic potential in various human cancers, but not much is known about MHC class I and II expression in human PDAC (Scupoli et al., 1996). Here we note that $1,25(OH)_2D_3$ supplementation has increased *HLA* genes encoding MHCs, which points to the possibility that these PDAC cells may increase cell-surface MHC I/II expression and presentation of peptides marking the PDAC cells as cancerous. This might then lead to the recruitment of CD8 T-cells to kill PDAC tumour cells, and influence CD4 T-cells to activate and recruit other immune cells for killing PDAC tumour cells. In the TME, CD8 T-cell immune function is inhibited by PD-L1 secreted from MDSCs (Zhang et al., 2017). HLA class II gene products also bind the killer Ig-like receptor (KIR) family of receptors on natural killer (NK) cells. NK cells serve as the main effector cells toward cancer in innate immunity in the TME, but the specific roles of NK cells remains controversial and depends largely on the type of cancer (Hinshaw and Shevde, 2019). Consistent with CD8 T cells, NK cells are also inhibited by elevated PD-L1 expression in the TME (Concha-Benavente *et al.*, 2018) The possibility of $1,25(OH)_2D_3$ supplementation regulating genes related to immune cell recruitment for killing PDAC tumour cells requires experimental validation.

Research has shown vitamin D/VDR to increase the immune response of $CD8^+$ T cells, as well as decrease the immunosuppressive ability of MDSCs, which has been a key challenge with regards to checkpoint immunotherapy in PC (Fleet et al., 2020; Karkeni et al., 2019). However, other studies have found vitamin D analogues to reduce T-cell-mediated immunity in PDAC cell culture models, while simultaneously reducing the tumour supportive activity of human pancreatic CAFs (Gorchs et al., 2020). The biological effects of vitamin D can differ between different cell types and stromal components, and can possibly differentially influence immune responses in the PDAC tumour.

4.4.2 *Biological processes relating to neutrophil mediated immunity were enriched from up-regulated genes in the epithelial pancreatic ductal adenocarcinoma subtype in response to 1,25(OH)2D3 supplementation.*

We note the differential expression of immune-related genes in both PDAC subtypes in response to $1,25(OH)_2D_3$ supplementation. From the up-regulated DEGs in the E subtype, biological processes relating to neutrophil-mediated immunity were enriched. *HLA-A*/*B* were up-regulated in the E-subtype in response to $1,25(OH)_2D_3$ supplementation as well. Neutrophil-mediated immune responses were not enriched from the DEGs from the QM subtype. This may be, in part at least, the result of differential *TGF-β* gene expression between the subtypes in response to $1,25(OH)_2D_3$ supplementation. *TGF-β 1* and *2* expression was down-regulated in the E subtype, whereas *TGF-β2* was up-regulated in the QM subtype in response to $1,25(OH)_2D_3$ supplementation. The exposure of intra-tumoural neutrophils to TGF-β signalling greatly impacts the tumour immune-role of the neutrophils (Fridlender et al., 2009). The down-regulation of TGF-β signalling in these E subtype cells could serve to promote pathways that lead to the transformation of intra-tumour neutrophils into tumour-suppressor neutrophils and hence promote neutrophil-mediated immune responses against the cancerous cells. This hypothesis would require experimental validation. We note the differential effect of $1,25(OH)_2D_3$ on the different subtypes of PDAC. The unique and plastic stroma of PDAC may allow for the differential recruitment of lymphocytes.

4.5 The epithelial-to-mesenchymal transition and the differential response to 1,25(OH)$_2$D$_3$ on the gene expression profiles of human epithelial and quasi-mesenchymal pancreatic ductal adenocarcinoma cells

4.5.1 *Differential TGFB expression may drive the EMT in human PDAC cells*

Comparing the DEGs of the E and QM subtypes revealed 335 genes DE in common, of which 270 were contra-regulated between the subtypes. Approximately 81% of the commonly DEGs had exhibited inverse expression patterns between the E and QM subtypes, in response to 1,25(OH)$_2$D$_3$ supplementation. This is a large proportion and indicates a differential response to 1,25(OH)$_2$D$_3$ between these PDAC subtypes. We noted that the gene encoding the vitamin D metabolising enzyme, *CYP24A1*, was only up-regulated in the E subtype, in response to 1,25(OH)$_2$D$_3$ supplementation. The TF, VDR, is reportedly expressed in both PDAC subtypes, so it is unlikely that the differential response to 1,25(OH)$_2$D$_3$ supplementation observed between the PDAC subtypes is a result of differential VDR expression (Hummel et al., 2014). The observed differential response might be, in part, due to the EMT in PDAC. The EMT is a developmental programme, whereby epithelial cells begin expressing mesenchymal-like genes and undergo a change in phenotype. The down-regulation of E-cadherin, encoded by the *CDH1* gene is a common feature of the EMT, whereas mesenchymal-like markers like N-cadherin (*CDH2*), vimentin (*VIM*) and fibronectin (*FN1*) are up-regulated during the EMT (Lee et al., 2006; Thiery et al., 2009). Our DGE analysis revealed the up-regulation of the epithelial marker, *CDH1*, in the QM subtype in response to 1,25(OH)$_2$D$_3$ supplementation. We also note the down-regulation of VIM but up-regulation of FN1 in the E subtype in response to 1,25(OH)$_2$D$_3$ supplementation. The EMT is regulated mainly by a group of TFs, consisting of 'mesenchymal promoters' and 'epithelial repressors'. In the E subtype, our DGE analysis revealed the down-regulation of the epithelial repressor gene, *SNAI2*, called Slug, which encodes the Snail 2 TF. Snail 2 represses *CDH1* expression, and is also involved in apoptosis inhibition (Ganesan, Mallets and Gomez-Cambronero, 2016).

TGF-β signalling is arguably the primary driver of the EMT. TGF-β signalling has been shown to increase the expression of the EMT TFs, including Snail 1 and 2, whereas TGF-β silencing by knock-down of its downstream pathway constituents has been shown to decrease the expression

of EMT TFs (Dangi-Garimella et al., 2012; Hotz et al., 2007). Even though TGF-β signalling promotes the EMT, its role in cancer development depends on the stage of cancer. In early tumours, TGF-β signalling has been shown to be tumour suppressive, whereas in late stage tumours, it has been shown to be tumour-promoting (Derynck and Zhang, 2003; Katsuno et al., 2013b; Shen et al., 2017; Shi and Massagué, 2003). The *TGFB2* gene, which encodes the TGF-β2 protein, was down-regulated in the E subtype but up-regulated in the QM subtype in response to $1,25(OH)_2D_3$ supplementation. *TGFB1* was also down-regulated in the E subtype. The differential expression of *TGFB* genes is indicative of the differing states of these PDAC cells with regards to the EMT.

TNF-α compelled NF-κB signalling has been shown to stabilise Snail protein, and increase the activity of these TFs (Wu et al., 2009). In this way, inflammatory signalling via NF-κB can increase EMT and cancer cell invasion (Wu et al., 2009). TGF-β-induced EMT has also been shown to be dependent on NF-κB signalling (Maier et al., 2010). However, we note the up-regulation of *NFKBIA*, a gene that encodes the alpha subunit of the NF-κB inhibitor, in the QM subtype in response to $1,25(OH)_2D_3$ supplementation, as well as the up-regulation of tumour necrosis factor alpha induced protein 3 (*TNFAIP3*) genes in both PDAC subtypes, along with up-regulated *TNFAIP2* in the QM subtype. *TNFAIP* expression is rapidly induced by TNF-α and has been shown to inhibit NF-κB protein activation (Das et al., 2018). Taken together, the DE of these genes point to attenuated NF-κB signalling by $1,25(OH)_2D_3$ up-regulating NF-κB inhibitors.

Claudin (*CLDN*) genes encode proteins that are crucial for tight junction formation and function. Claudin 1 expression is positively associated with E type markers. *CLDN1* was down-regulated in the E subtype and up-regulated in the QM subtype in response to $1,25(OH)_2D_3$ supplementation. This is interesting because $1,25(OH)_2D_3$ has been observed to up-regulate *CLDN1* in epithelial cells (Kong et al., 2008; Zhao et al., 2012). $1,25(OH)_2D_3$ supplementation also resulted in the upregulation of *FLNA* in the QM subtype, but down-regulation in the E subtype. *FLNA* encodes the epithelial-associated filamin A protein (Larriba et al., 2016; Pálmer et al., 2003). $1,25(OH)_2D_3$ supplementation also resulted in up-regulation of integrin subunit β 4/5/6 (*ITGB4/5/6)* in the E subtype and down-regulation in the QM subtype. We observe the mixed effects of $1,25(OH)_2D_3$ supplementation on promoting epithelial and mesenchymal markers in the PDAC subtypes.

4.5.2 *Biological processes relating to integrin mediated cell adhesion, normal pancreas and epithelial cell development were enriched from the down-regulated differentially expressed genes in the quasi-mesenchymal pancreatic ductal adenocarcinoma subtype in response to* $1,25(OH)_2D_3$ *supplementation.*

Integrin-mediated cell adhesion genes were down-regulated in the QM subtype, indicating the possibility of loss of cell adhesion by integrin in this subtype and metastasis promotion in response to $1,25(OH)_2D_3$ supplementation. Gene ontology terms for epithelial cell development were also enriched from the genes down-regulated in the QM subtype- indicating the general lack of epithelial markers in these cells, in response to $1,25(OH)_2D_3$ supplementation. $1,25(OH)_2D_3$ has also been implicated in promoting differentiation, and this is one of its anti-tumour functions. However, we observe the enrichment of normal pancreas development (and by extension, normal pancreatic cell differentiation to form functional cells and pancreatic tissue) terms from the genes down-regulated in the QM subtype- further exemplifying the differential response to $1,25(OH)_2D_3$ supplementation between epithelial and mesenchymal cells.

Research has shown $1,25(OH)_2D_3$ to inhibit the expression of EMT TFs, and Snail 1 and 2 TFs to inhibit *VDR* gene expression and hence inhibit the molecular action of $1,25(OH)_2D_3$. By binding certain regions of the *VDR* gene promoter, Snail 1 and 2 have been shown to repress *VDR* expression, while also reducing the half-life of *VDR* RNA in colon cancer cells (Larriba et al., 2009; Pálmer et al., 2004). In breast cancer cells, TNF-α induced *VDR* repression resulted in TGF-β-induced EMT (Larriba et al., 2016; Zhang et al., 2014). Conversely, $1,25(OH)_2D_3$ supplementation was shown to protect against TNF-α-induced VDR loss, as well as suppress TGF-β mediated increases of breast cancer cell migration (Larriba et al., 2016; Zhang et al., 2014).

PDAC cell fate and phenotype, like any other cells, can be regulated by extra-cellular signals, like $1,25(OH)_2D_3$. The EMT related TFs and $1,25(OH)_2D_3$ seem to differentially regulate the epithelial cell phenotype, with $1,25(OH)_2D_3$ promoting the E phenotype and the EMT TFs promoting the acquisition of the M phenotype. A negative feedback loop exists between EMT TFs and VDR, which can attenuate the cellular effect of $1,25(OH)_2D_3$, and this may lead to a cancer cell acquiring the phenotype (E/M) dictated by extracellular cues (TGF-β-induced EMT versus $1,25(OH)_2D_3$ promoting the E phenotype). The VDR-EMT TF negative feedback loop may first amplify the existing signal and later stabilise cell fate. For example, the generation of PDAC metastases is

highly related to EMT induction, but the formation of new tumours from metastases at distal sites requires the mesenchymal to epithelial transition (MET), which would require VDR to be up-regulated and EMT TFs to be down-regulated during this process. This balance between VDR and the EMT TFs may explain some part of the reversibility of the EMT, as well as how E and QM PDAC cells can exist on a continuum and interconvert between each subtype (Porter et al., 2019).

4.6 Study limitations and challenges

The RNA-Seq data used in this study was generated by Porter *et al.*, (2019). The researchers generated the PDAC cells from the resected tumours of PDAC patients, and the tumours were classified as epithelial-like or quasi-mesenchymal-like based on the PDAC gene signatures published by Collisson *et al.*, (2011). Various limitations were present at the onset of this research project, as we had not generated the sequencing data ourselves. The authors of the parent study did not disclose much regarding certain QC measures (like RNA quality- related to our obtained mapping rates), and information regarding the sequencing procedure (dates, times, lanes, batches etc.) – this is where we encountered probably the biggest limitation, batch effects. The presence of batch effects presented a challenge with regards to analysing the RNA expression profiles appropriately, but was overcome by undertaking the appropriate corrective measures.

The six PDAC tumour samples obtained from the patients provide a small sample size, and this provides challenges for maximising the use of the cells as well as possibly losing some diversity and variation as a result of analysing few samples. We considered each patient's samples (one control and one $1,25(OH)_2D_3$ supplemented) as a biological replicate, by collapsing the three technical replicates. The authors originally compared the RNA expression profiles of the technical replicates, which they considered biological replicates. In this way, we are confident that the observed transcriptional differences are due to the response to $1,25(OH)_2D_3$ supplementation, and that some biological variability is obtained by comparing the patients samples together. RNA sequencing is an expensive technique, but comparing the RNA expression profiles of the patient samples to VDR positive and negative commercially available cell lines would have added another dimension to deciphering the effects of $1,25(OH)_2D_3$ on PC cells expressing VDR. Nonetheless,

the fact that this sequencing data was not obtained from immortalized cell lines provides a clear representation of what is happening at the transcriptomic level in human PDAC cells.

An experimental detail that we would change is the use of ethanol instead of DMSO as a $1,25(OH)_2D_3$ vehicle and control. The amount of ethanol used as a vehicle and control when supplementing with 10 nM $1,25(OH)_2D_3$ is much safer for cells and will probably more truly reflect the effect of the $1,25(OH)_2D_3$ supplementation. $1,25(OH)_2D_3$ readily dissolves in ethanol, and previous work performed in our laboratory has shown ethanol to be safe for cultured cells. DMSO is more cytotoxic than ethanol (Nguyen et al., 2020). $1,25(OH)_2D_3$ is also more soluble in ethanol than it is in DMSO (Almarri et al., 2017) and a lot less ethanol would be required to deliver the appropriate dose of $1,25(OH)_2D_3$ to the culture media.

4.7 Conclusions and future works

Our DGE analysis has revealed differential expression of multiple oncogenes, tumour suppressor genes, as well as epithelial/mesenchymal associated genes. Broadly, $1,25(OH)_2D_3$ supplementation resulted in DGE in favour of growth pathway inhibition and cell cycle arrest, immune response activation and augmentation of the epithelial phenotype in the E subtype cells. Notably, *TGFB1/2* genes were down-regulated in the E subtype after $1,25(OH)_2D_3$ supplementation, but *TGFB2* was up-regulated in the QM subtype. TGF-β-induced EMT may explain the difference in response to $1,25(OH)_2D_3$ supplementation observed between the cell types. Since *CY24A1* was only up-regulated in the E subtype, it is plausible to speculate that VDR activity was higher in the E subtype cells, as evidenced by the greater response to $1,25(OH)_2D_3$ in the E subtype cells compared to the QM subtype cells (more DEGs in E subtype; augmentation of the epithelial phenotype). In the QM subtype cells, $1,25(OH)_2D_3$ supplementation resulted in varied DE of cancer promoting and suppressing genes, as well as varied expression of epithelial and mesenchymal marker genes. Transcriptome profiling of human PDAC cells, in response to $1,25(OH)_2D_3$ supplementation as well as in conjunction with the common PDAC chemotherapeutic drugs (e.g. FOLFIRONOX) can shed more light onto the anti-PDAC tumoural activity of $1,25(OH)_2D_3$ supplementation.

In our study, a vast amount of data and subsequent results were generated, and some of these *in silico* generated results can be taken to the laboratory for validation. For example, various long non-coding RNAs have been associated with the EMT programme in PDAC recently (Ma et al., 2021; Takahashi et al., 2021; Zhang et al., 2021). Our DGE analysis revealed the differential expression of multiple non-coding and regulatory RNAs that can further be explored as targets involved in PDAC EMT. The strong chemoresistance of the PDAC tumour lies in its plasticity, whereby the tumour cells can interconvert between epithelial and mesenchymal-like states, as well as influence the PDAC tumour micro-environment. $1,25(OH)_2D_3$ remains an attractive researchable PC preventative and therapeutic, and vitamin D sufficiency has been associated with decreased PC risk, increased genome stability and a healthy epigenome. However, in an unstable tumour like PDAC, the effects of $1,25(OH)_2D_3$ supplementation may not always be desirable. $1,25(OH)_2D_3$ supplementation may possibly augment the mesenchymal phenotype in QM subtype cells, supported by the findings of Porter *et al.*, (2019). These researchers found $1,25(OH)_2D_3$ supplementation to promote epithelial type markers and decrease metastatic potential in the E subtype, but reinforce mesenchymal type markers in the QM subtype and promote metastasis and PDAC tumour aggression. Whether this observed difference in promoting epithelial versus mesenchymal markers and difference in tumour aggression is due to the effect of $1,25(OH)_2D_3$ on the existing and present phenotype of the PDAC cells, or whether this difference is related to *VDR* repression remains unclear. Nonetheless, *VDR* repression is a hallmark of the EMT. VDR is commonly down-regulated in many advanced stage cancers, and the EMT programme relates to disease progression and advancement (Carlberg and Muñoz, 2022). Perhaps the PDAC EMT is a consequence of VDR first being down-regulated in PDAC tumour cells, leading to the expression of EMT TFs. Cumulative genetic insult resulting in an unstable genome, or hyper-methylation of the *VDR* gene promoter can lead to VDR loss or down-regulated expression. But whether this is a possible driver for PDAC EMT remains to be determined. We can conclude that the differential response to $1,25(OH)_2D_3$ between the human epithelial and quasi-mesenchymal PDAC cells is in part the result of differential signalling involving TGF-β-induced EMT, which has been shown to alter the *VDR* and EMT-related transcription factor expression.

Bibliography

Afshar-Sterle, S., Zotos, D., Bernard, N.J., Scherger, A.K., Rödling, L., Alsop, A.E., Walker, J., Masson, F., Belz, G.T., Corcoran, L.M., O'Reilly, L.A., Strasser, A., Smyth, M.J., Johnstone, R., Tarlinton, D.M., Nutt, S.L., Kallies, A., 2014. Fas ligand–mediated immune surveillance by T cells is essential for the control of spontaneous B cell lymphomas. Nat. Med. 20, 283–290. https://doi.org/10.1038/nm.3442

Almarri, F., Haq, N., Alanazi, F.K., Mohsin, K., Alsarra, I.A., Aleanizy, F.S., Shakeel, F., 2017. Solubility and thermodynamic function of vitamin D3 in different mono solvents. J. Mol. Liq. 229, 477–481. https://doi.org/10.1016/j.molliq.2016.12.105

Altman, B.J., Stine, Z.E., Dang, C.V., 2016. From Krebs to clinic: glutamine metabolism to cancer therapy. Nat. Rev. Cancer 16, 619–634. https://doi.org/10.1038/nrc.2016.71

Anders, S., Huber, W., 2010. Differential expression analysis for sequence count data. Genome Biol. 11, R106. https://doi.org/10.1186/gb-2010-11-10-r106

Anderson, P., May, B., Morris, H., 2003. Vitamin D Metabolism: New Concepts and Clinical Implications. Clin. Biochem. Rev. 24, 13–26.

Asghar, U., Witkiewicz, A.K., Turner, N.C., Knudsen, E.S., 2015. The history and future of targeting cyclin-dependent kinases in cancer therapy. Nat. Rev. Drug Discov. 14, 130–146. https://doi.org/10.1038/nrd4504

Avgerinos, D.V., Björnsson, J., 2001. Malignant neoplasms: discordance between clinical diagnoses and autopsy findings in 3,118 cases. APMIS Acta Pathol. Microbiol. Immunol. Scand. 109, 774–780. https://doi.org/10.1034/j.1600-0463.2001.d01-145.x

Bajbouj, K., Shafarin, J., Sawan, A., Shehada, A., Elkhalifa, W.E., 2020. Abstract 5030: Vitamin D exhibits therapeutic anti-tumor and anti-angiogenic potential by reducing VEGF levels and altering TIMP/MMP system in breast cancer. Cancer Res. 80, 5030. https://doi.org/10.1158/1538-7445.AM2020-5030

Barton, C.M., Hall, P.A., Hughes, C.M., Gullick, W.J., Lemoine, N.R., 1991. Transforming growth factor alpha and epidermal growth factor in human pancreatic cancer. J. Pathol. 163, 111–116. https://doi.org/10.1002/path.1711630206

Batabyal, P., Vander Hoorn, S., Christophi, C., Nikfarjam, M., 2014. Association of diabetes mellitus and pancreatic adenocarcinoma: a meta-analysis of 88 studies. Ann. Surg. Oncol. 21, 2453–2462. https://doi.org/10.1245/s10434-014-3625-6

Baudino, T.A., McKay, C., Pendeville-Samain, H., Nilsson, J.A., Maclean, K.H., White, E.L., Davis, A.C., Ihle, J.N., Cleveland, J.L., 2002. c-Myc is essential for vasculogenesis and angiogenesis during development and tumor progression. Genes Dev. 16, 2530–2543. https://doi.org/10.1101/gad.1024602

Bergmann, U., Funatomi, H., Yokoyama, M., Beger, H.G., Korc, M., 1995. Insulin-like growth factor I overexpression in human pancreatic cancer: evidence for autocrine and paracrine roles. Cancer Res. 55, 2007–2011.

Berrington de Gonzalez, A., Sweetland, S., Spencer, E., 2003. A meta-analysis of obesity and the risk of pancreatic cancer. Br. J. Cancer 89, 519–523. https://doi.org/10.1038/sj.bjc.6601140

Bharti, A.C., Aggarwal, B.B., 2002. Nuclear factor-kappa B and cancer: its role in prevention and therapy. Biochem. Pharmacol. 64, 883–888. https://doi.org/10.1016/s0006-2952(02)01154-1

Bhoora, S., Punchoo, R., 2020. Policing Cancer: Vitamin D Arrests the Cell Cycle. Int. J. Mol. Sci. 21, 9296. https://doi.org/10.3390/ijms21239296

Bhowmick, N.A., Neilson, E.G., Moses, H.L., 2004. Stromal fibroblasts in cancer initiation and progression. Nature 432, 332–337. https://doi.org/10.1038/nature03096

Bikle, D.D., 2014. Vitamin D Metabolism, Mechanism of Action, and Clinical Applications. Chem. Biol. 21, 319–329. https://doi.org/10.1016/j.chembiol.2013.12.016

Bikle, D.D., 2010. VITAMIN D: Newly Discovered Actions Require Reconsideration of Physiologic Requirements. Trends Endocrinol. Metab. TEM 21, 375–384. https://doi.org/10.1016/j.tem.2010.01.003

Blackford, A., Serrano, O.K., Wolfgang, C.L., Parmigiani, G., Jones, S., Zhang, X., Parsons, D.W., Lin, J.C.-H., Leary, R.J., Eshleman, J.R., Goggins, M., Jaffee, E.M., Iacobuzio-Donahue, C.A., Maitra, A., Cameron, J.L., Olino, K., Schulick, R., Winter, J., Herman, J.M., Laheru, D., Klein, A.P., Vogelstein, B., Kinzler, K.W., Velculescu, V.E., Hruban, R.H., 2009. SMAD4 gene mutations are associated with poor prognosis in pancreatic cancer. Clin. Cancer Res. Off. J. Am. Assoc. Cancer Res. 15, 4674–4679. https://doi.org/10.1158/1078-0432.CCR-09-0227

Bong, A.H.L., Monteith, G.R., 2018. Calcium signaling and the therapeutic targeting of cancer cells. Biochim. Biophys. Acta BBA - Mol. Cell Res., Calcium signaling in health, disease and therapy 1865, 1786–1794. https://doi.org/10.1016/j.bbamcr.2018.05.015

Bosch de Basea, M., Porta, M., Alguacil, J., Puigdomènech, E., Gasull, M., Garrido, J.A., López, T., PANKRAS II Study Group, 2011. Relationships between occupational history and serum concentrations of organochlorine compounds in exocrine pancreatic cancer. Occup. Environ. Med. 68, 332–338. https://doi.org/10.1136/oem.2009.054197

Bosetti, C., Bertuccio, P., Negri, E., La Vecchia, C., Zeegers, M.P., Boffetta, P., 2012. Pancreatic cancer: overview of descriptive epidemiology. Mol. Carcinog. 51, 3–13. https://doi.org/10.1002/mc.20785

Bragdon, B., 2008. Molecular basis of the potential of vitamin D to prevent cancer. Curr. Med. Res. Opin.

Bray, F., Ferlay, J., Soerjomataram, I., Siegel, R.L., Torre, L.A., Jemal, A., 2018. Global cancer statistics 2018: GLOBOCAN estimates of incidence and mortality worldwide for 36 cancers in 185 countries. CA. Cancer J. Clin. 68, 394–424. https://doi.org/10.3322/caac.21492

Bray, N.L., Pimentel, H., Melsted, P., Pachter, L., 2016. Near-optimal probabilistic RNA-seq quantification. Nat. Biotechnol. 34, 525–527. https://doi.org/10.1038/nbt.3519

Cairns, R.A., Mak, T.W., 2016. The current state of cancer metabolism. Nat. Rev. Cancer 16, 613–614. https://doi.org/10.1038/nrc.2016.100

Calle, E.E., Rodriguez, C., Walker-Thurmond, K., Thun, M.J., 2003. Overweight, obesity, and mortality from cancer in a prospectively studied cohort of U.S. adults. N. Engl. J. Med. 348, 1625–1638. https://doi.org/10.1056/NEJMoa021423

Campbell, F.C., Xu, H., El-Tanani, M., Crowe, P., Bingham, V., 2010. The yin and yang of vitamin D receptor (VDR) signaling in neoplastic progression: operational networks and tissue-specific growth control. Biochem. Pharmacol. 79, 1–9. https://doi.org/10.1016/j.bcp.2009.09.005

Campbell, M.J., Gombart, A.F., Kwok, S.H., Park, S., Koeffler, H.P., 2000. The anti-proliferative effects of 1alpha,25(OH)2D3 on breast and prostate cancer cells are associated with induction of BRCA1 gene expression. Oncogene 19, 5091–5097. https://doi.org/10.1038/sj.onc.1203888

Campisi, J., 2013. Aging, cellular senescence, and cancer. Annu. Rev. Physiol. 75, 685–705. https://doi.org/10.1146/annurev-physiol-030212-183653

Cancer Statistics Review, 1975-2015 - Previous Version - SEER Cancer Statistics Review [WWW Document], n.d. . SEER. URL https://seer.cancer.gov/archive/csr/1975_2015/index.html (accessed 2.6.22).

Carlberg, C., Bendik, I., Wyss, A., Meier, E., Sturzenbecker, L.J., Grippo, J.F., Hunziker, W., 1993. Two nuclear signalling pathways for vitamin D. Nature 361, 657–660. https://doi.org/10.1038/361657a0

Carlberg, C., Campbell, M.J., 2013. Vitamin D receptor signaling mechanisms: integrated actions of a well-defined transcription factor. Steroids 78, 127–136. https://doi.org/10.1016/j.steroids.2012.10.019

Carlberg, C., Muñoz, A., 2022. An update on vitamin D signaling and cancer. Semin. Cancer Biol., New biological and immunological approaches to cancer therapy: basic and clinical aspects 79, 217–230. https://doi.org/10.1016/j.semcancer.2020.05.018

Carlberg, C., Seuter, S., Heikkinen, S., 2012. The first genome-wide view of vitamin D receptor locations and their mechanistic implications. Anticancer Res. 32, 271–282.

Chen, C., Cai, S., Wang, G., Cao, X., Yang, X., Luo, X., Feng, Y., Hu, J., 2013. c-Myc enhances colon cancer cell-mediated angiogenesis through the regulation of HIF-1α. Biochem. Biophys. Res. Commun. 430, 505–511. https://doi.org/10.1016/j.bbrc.2012.12.006

Cho, R.W., Clarke, M.F., 2008. Recent advances in cancer stem cells. Curr. Opin. Genet. Dev. 18, 48–53. https://doi.org/10.1016/j.gde.2008.01.017

Christakos, S., Dhawan, P., Liu, Y., Peng, X., Porta, A., 2003. New insights into the mechanisms of vitamin D action. J. Cell. Biochem. 88, 695–705. https://doi.org/10.1002/jcb.10423

Clevers, H., 2006. Wnt/beta-catenin signaling in development and disease. Cell 127, 469–480. https://doi.org/10.1016/j.cell.2006.10.018

Collado, M., Serrano, M., 2010. Senescence in tumours: evidence from mice and humans. Nat. Rev. Cancer 10, 51–57. https://doi.org/10.1038/nrc2772

Collins, M.A., Pasca di Magliano, M., 2013. Kras as a key oncogene and therapeutic target in pancreatic cancer. Front. Physiol. 4, 407. https://doi.org/10.3389/fphys.2013.00407

Collisson, E.A., Sadanandam, A., Olson, P., Gibb, W.J., Truitt, M., Gu, S., Cooc, J., Weinkle, J., Kim, G.E., Jakkula, L., Feiler, H.S., Ko, A.H., Olshen, A.B., Danenberg, K.L., Tempero, M.A., Spellman, P.T., Hanahan, D., Gray, J.W., 2011a. Subtypes of Pancreatic Ductal Adenocarcinoma and Their Differing Responses to Therapy. Nat. Med. 17, 500–503. https://doi.org/10.1038/nm.2344

Collisson, E.A., Sadanandam, A., Olson, P., Gibb, W.J., Truitt, M., Gu, S., Cooc, J., Weinkle, J., Kim, G.E., Jakkula, L., Feiler, H.S., Ko, A.H., Olshen, A.B., Danenberg, K.L., Tempero, M.A., Spellman, P.T., Hanahan, D., Gray, J.W., 2011b. Subtypes of pancreatic ductal adenocarcinoma and their differing responses to therapy. Nat. Med. 17, 500–503. https://doi.org/10.1038/nm.2344

Concha-Benavente, F., Kansy, B., Moskovitz, J., Moy, J., Chandran, U., Ferris, R.L., 2018. PD-L1 Mediates Dysfunction in Activated PD-1+ NK Cells in Head and Neck Cancer Patients. Cancer Immunol. Res. 6, 1548–1560. https://doi.org/10.1158/2326-6066.CIR-18-0062

Conroy, T., Desseigne, F., Ychou, M., Bouché, O., Guimbaud, R., Bécouarn, Y., Adenis, A., Raoul, J.-L., Gourgou-Bourgade, S., de la Fouchardière, C., Bennouna, J., Bachet, J.-B., Khemissa-Akouz, F., Péré-Vergé, D., Delbaldo, C., Assenat, E., Chauffert, B., Michel, P., Montoto-Grillot, C., Ducreux, M., Groupe Tumeurs Digestives of Unicancer, PRODIGE Intergroup, 2011. FOLFIRINOX versus gemcitabine for metastatic pancreatic cancer. N. Engl. J. Med. 364, 1817–1825. https://doi.org/10.1056/NEJMoa1011923

Conroy, T., Hammel, P., Hebbar, M., Ben Abdelghani, M., Wei, A.C., Raoul, J.-L., Chone, L., Francois, E., Artru, P., Biagi, J.J., Lecomte, T., Assenat, E., Faroux, R., Ychou, M., Volet, J., Sauvanet, A., Jouffroy-Zeller, C., Rat, P., Castan, F., Bachet, J.-B., 2018. Unicancer GI PRODIGE 24/CCTG PA.6 trial: A multicenter international randomized phase III trial of adjuvant mFOLFIRINOX versus gemcitabine (gem) in patients with resected pancreatic ductal adenocarcinomas. J. Clin. Oncol. 36, LBA4001–LBA4001. https://doi.org/10.1200/JCO.2018.36.18_suppl.LBA4001

Coqueret, O., 2002. Linking cyclins to transcriptional control. Gene 299, 35–55. https://doi.org/10.1016/s0378-1119(02)01055-7

Couch, F.J., Johnson, M.R., Rabe, K.G., Brune, K., de Andrade, M., Goggins, M., Rothenmund, H., Gallinger, S., Klein, A., Petersen, G.M., Hruban, R.H., 2007. The prevalence of BRCA2 mutations

in familial pancreatic cancer. Cancer Epidemiol. Biomark. Prev. Publ. Am. Assoc. Cancer Res. Cosponsored Am. Soc. Prev. Oncol. 16, 342–346. https://doi.org/10.1158/1055-9965.EPI-06-0783
Curtin, N.J., 2012. DNA repair dysregulation from cancer driver to therapeutic target. Nat. Rev. Cancer 12, 801–817. https://doi.org/10.1038/nrc3399
Dang, C.V., 2007. The interplay between MYC and HIF in the Warburg effect. Ernst Schering Found. Symp. Proc. 35–53. https://doi.org/10.1007/2789_2008_088
Dangi-Garimella, S., Krantz, S.B., Shields, M.A., Grippo, P.J., Munshi, H.G., 2012. Epithelial-mesenchymal transition and pancreatic cancer progression, in: Grippo, P.J., Munshi, H.G. (Eds.), Pancreatic Cancer and Tumor Microenvironment. Transworld Research Network, Trivandrum (India).
Darnell, J.E., 1997. STATs and gene regulation. Science 277, 1630–1635. https://doi.org/10.1126/science.277.5332.1630
Darvin, P., Toor, S.M., Sasidharan Nair, V., Elkord, E., 2018. Immune checkpoint inhibitors: recent progress and potential biomarkers. Exp. Mol. Med. 50, 1–11. https://doi.org/10.1038/s12276-018-0191-1
Das, T., Chen, Z., Hendriks, R.W., Kool, M., 2018. A20/Tumor Necrosis Factor α-Induced Protein 3 in Immune Cells Controls Development of Autoinflammation and Autoimmunity: Lessons from Mouse Models. Front. Immunol. 9.
De La Cruz, M.S.D., Young, A.P., Ruffin, M.T., 2014. Diagnosis and management of pancreatic cancer. Am. Fam. Physician 89, 626–632.
Deeb, K.K., Trump, D.L., Johnson, C.S., 2007. Vitamin D signalling pathways in cancer: potential for anticancer therapeutics. Nat. Rev. Cancer 7, 684–700. https://doi.org/10.1038/nrc2196
DeLuca, H.F., 2004. Overview of general physiologic features and functions of vitamin D. Am. J. Clin. Nutr. 80, 1689S–96S. https://doi.org/10.1093/ajcn/80.6.1689S
Denu, R.A., Nemcek, S., Bloom, D.D., Goodrich, A.D., Kim, J., Mosher, D.F., Hematti, P., 2016. Fibroblasts and Mesenchymal Stromal/Stem Cells are Phenotypically Indistinguishable. Acta Haematol. 136, 85–97. https://doi.org/10.1159/000445096
Derynck, R., Zhang, Y.E., 2003. Smad-dependent and Smad-independent pathways in TGF-beta family signalling. Nature 425, 577–584. https://doi.org/10.1038/nature02006
Deshpande, A., Sicinski, P., Hinds, P.W., 2005. Cyclins and cdks in development and cancer: a perspective. Oncogene 24, 2909–2915. https://doi.org/10.1038/sj.onc.1208618
Dhillon, A.S., Hagan, S., Rath, O., Kolch, W., 2007. MAP kinase signalling pathways in cancer. Oncogene 26, 3279–3290. https://doi.org/10.1038/sj.onc.1210421
di Magliano, M.P., Logsdon, C.D., 2013. Roles for KRAS in pancreatic tumor development and progression. Gastroenterology 144, 1220–1229. https://doi.org/10.1053/j.gastro.2013.01.071
Dick, F.A., Rubin, S.M., 2013. Molecular mechanisms underlying RB protein function. Nat. Rev. Mol. Cell Biol. 14, 297–306. https://doi.org/10.1038/nrm3567
Dimitrov, V., Barbier, C., Ismailova, A., Wang, Y., Dmowski, K., Salehi-Tabar, R., Memari, B., Groulx-Boivin, E., White, J.H., 2021. Vitamin D-regulated Gene Expression Profiles: Species-specificity and Cell-specific Effects on Metabolism and Immunity. Endocrinology 162, bqaa218. https://doi.org/10.1210/endocr/bqaa218
Ding, Z., Li, R., Zhang, Q., Wang, Y., Jiang, Y., Meng, Q., Xi, Q., Wu, G., 2019. Prognostic role of cyclin D2/D3 in multiple human malignant neoplasms: A systematic review and meta-analysis. Cancer Med. 8, 2717–2729. https://doi.org/10.1002/cam4.2152
Dinh, H.Q., Eggert, T., Meyer, M.A., Zhu, Y.P., Olingy, C.E., Llewellyn, R., Wu, R., Hedrick, C.C., 2020. Coexpression of CD71 and CD117 Identifies an Early Unipotent Neutrophil Progenitor Population in Human Bone Marrow. Immunity 53, 319-334.e6. https://doi.org/10.1016/j.immuni.2020.07.017

Doe, M.R., Ascano, J.M., Kaur, M., Cole, M.D., 2012. Myc posttranscriptionally induces HIF1 protein and target gene expression in normal and cancer cells. Cancer Res. 72, 949–957. https://doi.org/10.1158/0008-5472.CAN-11-2371

Dong, M., Nio, Y., Tamura, K., Song, M.M., Guo, K.J., Guo, R.X., Dong, Y.T., 2000. Ki-ras point mutation and p53 expression in human pancreatic cancer: a comparative study among Chinese, Japanese, and Western patients. Cancer Epidemiol. Biomark. Prev. Publ. Am. Assoc. Cancer Res. Cosponsored Am. Soc. Prev. Oncol. 9, 279–284.

Dunn, G.P., Bruce, A.T., Ikeda, H., Old, L.J., Schreiber, R.D., 2002. Cancer immunoediting: from immunosurveillance to tumor escape. Nat. Immunol. 3, 991–998. https://doi.org/10.1038/ni1102-991

Ellenrieder, V., Hendler, S.F., Boeck, W., Seufferlein, T., Menke, A., Ruhland, C., Adler, G., Gress, T.M., 2001. Transforming growth factor beta1 treatment leads to an epithelial-mesenchymal transdifferentiation of pancreatic cancer cells requiring extracellular signal-regulated kinase 2 activation. Cancer Res. 61, 4222–4228.

Ene-Obong, A., Clear, A.J., Watt, J., Wang, J., Fatah, R., Riches, J.C., Marshall, J.F., Chin-Aleong, J., Chelala, C., Gribben, J.G., Ramsay, A.G., Kocher, H.M., 2013. Activated pancreatic stellate cells sequester CD8+ T cells to reduce their infiltration of the juxtatumoral compartment of pancreatic ductal adenocarcinoma. Gastroenterology 145, 1121–1132. https://doi.org/10.1053/j.gastro.2013.07.025

Erijman, A., Shifman, J.M., 2016. RAS/Effector Interactions from Structural and Biophysical Perspective. Mini Rev. Med. Chem. 16, 370–375. https://doi.org/10.2174/1389557515666151001141838

Erkan, M., Kurtoglu, M., Kleeff, J., 2016. The role of hypoxia in pancreatic cancer: a potential therapeutic target? Expert Rev. Gastroenterol. Hepatol. 10, 301–316. https://doi.org/10.1586/17474124.2016.1117386

Ernst, J., Kheradpour, P., Mikkelsen, T.S., Shoresh, N., Ward, L.D., Epstein, C.B., Zhang, X., Wang, L., Issner, R., Coyne, M., Ku, M., Durham, T., Kellis, M., Bernstein, B.E., 2011. Mapping and analysis of chromatin state dynamics in nine human cell types. Nature 473, 43–49. https://doi.org/10.1038/nature09906

Evan, G.I., d'Adda di Fagagna, F., 2009. Cellular senescence: hot or what? Curr. Opin. Genet. Dev. 19, 25–31. https://doi.org/10.1016/j.gde.2008.11.009

Ewels, P., Magnusson, M., Lundin, S., Käller, M., 2016. MultiQC: summarize analysis results for multiple tools and samples in a single report. Bioinformatics 32, 3047–3048. https://doi.org/10.1093/bioinformatics/btw354

Ezzati, M., Henley, S.J., Lopez, A.D., Thun, M.J., 2005. Role of smoking in global and regional cancer epidemiology: current patterns and data needs. Int. J. Cancer 116, 963–971. https://doi.org/10.1002/ijc.21100

Feldman, D., Krishnan, A.V., Swami, S., Giovannucci, E., Feldman, B.J., 2014. The role of vitamin D in reducing cancer risk and progression. Nat. Rev. Cancer 14, 342–357. https://doi.org/10.1038/nrc3691

Ferro, R., Falasca, M., 2014. Emerging role of the KRAS-PDK1 axis in pancreatic cancer. World J. Gastroenterol. WJG 20, 10752–10757. https://doi.org/10.3748/wjg.v20.i31.10752

Fetahu, I.S., Höbaus, J., Kállay, E., 2014. Vitamin D and the epigenome. Front. Physiol. 5, 164. https://doi.org/10.3389/fphys.2014.00164

Fleet, J.C., Burcham, G.N., Calvert, R.D., Elzey, B.D., Ratliff, T.L., 2020. 1α, 25 Dihydroxyvitamin D (1,25(OH)2D) inhibits the T cell suppressive function of myeloid derived suppressor cells (MDSC). J. Steroid Biochem. Mol. Biol. 198, 105557. https://doi.org/10.1016/j.jsbmb.2019.105557

Folkman, J., 1971. Tumor angiogenesis: therapeutic implications. N. Engl. J. Med. 285, 1182–1186. https://doi.org/10.1056/NEJM197111182852108

Franco, O.E., Shaw, A.K., Strand, D.W., Hayward, S.W., 2010. Cancer associated fibroblasts in cancer pathogenesis. Semin. Cell Dev. Biol. 21, 33–39. https://doi.org/10.1016/j.semcdb.2009.10.010

Fridlender, Z.G., Sun, J., Kim, S., Kapoor, V., Cheng, G., Ling, L., Worthen, G.S., Albelda, S.M., 2009. Polarization of tumor-associated neutrophil phenotype by TGF-beta: "N1" versus "N2" TAN. Cancer Cell 16, 183–194. https://doi.org/10.1016/j.ccr.2009.06.017

Gabay, M., Li, Y., Felsher, D.W., 2014. MYC activation is a hallmark of cancer initiation and maintenance. Cold Spring Harb. Perspect. Med. 4, a014241. https://doi.org/10.1101/cshperspect.a014241

Gadina, M., Hilton, D., Johnston, J.A., Morinobu, A., Lighvani, A., Zhou, Y.-J., Visconti, R., O'Shea, J.J., 2001. Signaling by Type I and II cytokine receptors: ten years after. Curr. Opin. Immunol. 13, 363–373. https://doi.org/10.1016/S0952-7915(00)00228-4

Ganesan, R., Mallets, E., Gomez-Cambronero, J., 2016. The transcription factors Slug (SNAI2) and Snail (SNAI1) regulate phospholipase D (PLD) promoter in opposite ways towards cancer cell invasion. Mol. Oncol. 10, 663–676. https://doi.org/10.1016/j.molonc.2015.12.006

Gao, J., Wang, L., Xu, J., Zheng, J., Man, X., Wu, H., Jin, J., Wang, K., Xiao, H., Li, S., Li, Z., 2013. Aberrant DNA methyltransferase expression in pancreatic ductal adenocarcinoma development and progression. J. Exp. Clin. Cancer Res. 32, 86. https://doi.org/10.1186/1756-9966-32-86

Garrido, F., Aptsiauri, N., 2019. Cancer immune escape: MHC expression in primary tumours versus metastases. Immunology 158, 255–266. https://doi.org/10.1111/imm.13114

Garrido, F., Aptsiauri, N., Doorduijn, E.M., Garcia Lora, A.M., van Hall, T., 2016. The urgent need to recover MHC class I in cancers for effective immunotherapy. Curr. Opin. Immunol. 39, 44–51. https://doi.org/10.1016/j.coi.2015.12.007

Genkinger, J.M., Spiegelman, D., Anderson, K.E., Bergkvist, L., Bernstein, L., van den Brandt, P.A., English, D.R., Freudenheim, J.L., Fuchs, C.S., Giles, G.G., Giovannucci, E., Hankinson, S.E., Horn-Ross, P.L., Leitzmann, M., Männistö, S., Marshall, J.R., McCullough, M.L., Miller, A.B., Reding, D.J., Robien, K., Rohan, T.E., Schatzkin, A., Stevens, V.L., Stolzenberg-Solomon, R.Z., Verhage, B.A.J., Wolk, A., Ziegler, R.G., Smith-Warner, S.A., 2009. Alcohol intake and pancreatic cancer risk: a pooled analysis of fourteen cohort studies. Cancer Epidemiol. Biomark. Prev. Publ. Am. Assoc. Cancer Res. Cosponsored Am. Soc. Prev. Oncol. 18, 765–776. https://doi.org/10.1158/1055-9965.EPI-08-0880

Ghosh, S., May, M.J., Kopp, E.B., 1998. NF-kappa B and Rel proteins: evolutionarily conserved mediators of immune responses. Annu. Rev. Immunol. 16, 225–260. https://doi.org/10.1146/annurev.immunol.16.1.225

Giammanco, M., Di Majo, D., La Guardia, M., Aiello, S., Crescimannno, M., Flandina, C., Tumminello, F.M., Leto, G., 2015. Vitamin D in cancer chemoprevention. Pharm. Biol. 53, 1399–1434. https://doi.org/10.3109/13880209.2014.988274

Giovannucci, E., 2005. The epidemiology of vitamin D and cancer incidence and mortality: a review (United States). Cancer Causes Control CCC 16, 83–95. https://doi.org/10.1007/s10552-004-1661-4

Goode, E.L., Ulrich, C.M., Potter, J.D., 2002. Polymorphisms in DNA repair genes and associations with cancer risk. Cancer Epidemiol. Biomark. Prev. Publ. Am. Assoc. Cancer Res. Cosponsored Am. Soc. Prev. Oncol. 11, 1513–1530.

Gorchs, L., Ahmed, S., Mayer, C., Knauf, A., Fernández Moro, C., Svensson, M., Heuchel, R., Rangelova, E., Bergman, P., Kaipe, H., 2020. The vitamin D analogue calcipotriol promotes an anti-tumorigenic phenotype of human pancreatic CAFs but reduces T cell mediated immunity. Sci. Rep. 10, 17444. https://doi.org/10.1038/s41598-020-74368-3

Greten, F.R., Grivennikov, S.I., 2019. Inflammation and Cancer: Triggers, Mechanisms, and Consequences. Immunity 51, 27–41. https://doi.org/10.1016/j.immuni.2019.06.025

Grocock, C., Harcus, M., Neoptolemos, J., 2009. Screening of High-Risk Families for Pancreatic Cancer. Pancreatology 9, 215–222. https://doi.org/10.1159/000210262
Gudmundsdottir, K., Ashworth, A., 2006. The roles of BRCA1 and BRCA2 and associated proteins in the maintenance of genomic stability. Oncogene 25, 5864–5874. https://doi.org/10.1038/sj.onc.1209874
Gullo, L., Pezzilli, R., Morselli-Labate, A.M., Italian Pancreatic Cancer Study Group, 1994. Diabetes and the risk of pancreatic cancer. N. Engl. J. Med. 331, 81–84. https://doi.org/10.1056/NEJM199407143310203
Hakomori, S., 1999. Antigen structure and genetic basis of histo-blood groups A, B and O: their changes associated with human cancer. Biochim. Biophys. Acta 1473, 247–266. https://doi.org/10.1016/s0304-4165(99)00183-x
Hanahan, D., Weinberg, R.A., 2011. Hallmarks of Cancer: The Next Generation. Cell 144, 646–674. https://doi.org/10.1016/j.cell.2011.02.013
Hanahan, D., Weinberg, R.A., 2000. The hallmarks of cancer. Cell 100, 57–70. https://doi.org/10.1016/s0092-8674(00)81683-9
Hankey, W., Frankel, W.L., Groden, J., 2018. Functions of the APC tumor suppressor protein dependent and independent of canonical WNT signaling: Implications for therapeutic targeting. Cancer Metastasis Rev. 37, 159–172. https://doi.org/10.1007/s10555-017-9725-6
Hartwig, A., Krüger, I., Beyersmann, D., 1994. Mechanisms in nickel genotoxicity: the significance of interactions with DNA repair. Toxicol. Lett. 72, 353–358. https://doi.org/10.1016/0378-4274(94)90048-5
Hashimoto, T., Shibasaki, F., 2015. Hypoxia-inducible factor as an angiogenic master switch. Front. Pediatr. 3, 33. https://doi.org/10.3389/fped.2015.00033
Haussler, M.R., Jurutka, P.W., Mizwicki, M., Norman, A.W., 2011. Vitamin D receptor (VDR)-mediated actions of 1α,25(OH)$_2$vitamin D$_3$: genomic and non-genomic mechanisms. Best Pract. Res. Clin. Endocrinol. Metab. 25, 543–559. https://doi.org/10.1016/j.beem.2011.05.010
Hay, N., 2016. Reprogramming glucose metabolism in cancer: can it be exploited for cancer therapy? Nat. Rev. Cancer 16, 635–649. https://doi.org/10.1038/nrc.2016.77
Hayden, M.S., Ghosh, S., 2004. Signaling to NF-kappaB. Genes Dev. 18, 2195–2224. https://doi.org/10.1101/gad.1228704
He, T.-L., Zhang, Y.-J., Jiang, H., Li, X., Zhu, H., Zheng, K.-L., 2015. The c-Myc–LDHA axis positively regulates aerobic glycolysis and promotes tumor progression in pancreatic cancer. Med. Oncol. Northwood Lond. Engl. 32, 187. https://doi.org/10.1007/s12032-015-0633-8
He, X., Chen, S.-Y., Yang, Z., Zhang, J., Wang, W., Liu, M.-Y., Niu, Y., Wei, X.-M., Li, H.-M., Hu, W.-N., Sun, G.-G., 2018. miR-4317 suppresses non-small cell lung cancer (NSCLC) by targeting fibroblast growth factor 9 (FGF9) and cyclin D2 (CCND2). J. Exp. Clin. Cancer Res. CR 37, 230. https://doi.org/10.1186/s13046-018-0882-4
Heldin, C.-H., Vanlandewijck, M., Moustakas, A., 2012. Regulation of EMT by TGFβ in cancer. FEBS Lett. 586, 1959–1970. https://doi.org/10.1016/j.febslet.2012.02.037
Hennecke, J., Wiley, D.C., 2001. T Cell Receptor–MHC Interactions up Close. Cell 104, 1–4. https://doi.org/10.1016/S0092-8674(01)00185-4
Hessmann, E., Schneider, G., Ellenrieder, V., Siveke, J.T., 2016. MYC in pancreatic cancer: novel mechanistic insights and their translation into therapeutic strategies. Oncogene 35, 1609–1618. https://doi.org/10.1038/onc.2015.216
Hidalgo, M., Cascinu, S., Kleeff, J., Labianca, R., Löhr, J.-M., Neoptolemos, J., Real, F.X., Van Laethem, J.-L., Heinemann, V., 2015. Addressing the challenges of pancreatic cancer: Future directions for improving outcomes. Pancreatology 15, 8–18. https://doi.org/10.1016/j.pan.2014.10.001

Hill, R., Li, Y., Tran, L.M., Dry, S., Calvopina, J.H., Garcia, A., Kim, C., Wang, Y., Donahue, T.R., Herschman, H.R., Wu, H., 2012. Cell intrinsic role of COX-2 in pancreatic cancer development. Mol. Cancer Ther. 11, 2127–2137. https://doi.org/10.1158/1535-7163.MCT-12-0342

Hill, R., Song, Y., Cardiff, R.D., Van Dyke, T., 2005. Selective evolution of stromal mesenchyme with p53 loss in response to epithelial tumorigenesis. Cell 123, 1001–1011. https://doi.org/10.1016/j.cell.2005.09.030

Hinshaw, D.C., Shevde, L.A., 2019. The Tumor Microenvironment Innately Modulates Cancer Progression. Cancer Res. 79, 4557–4566. https://doi.org/10.1158/0008-5472.CAN-18-3962

Hoffman, B., Liebermann, D.A., 2008. Apoptotic signaling by c-MYC. Oncogene 27, 6462–6472. https://doi.org/10.1038/onc.2008.312

Holick, M.F., 2007. Vitamin D deficiency. N. Engl. J. Med. 357, 266–281. https://doi.org/10.1056/NEJMra070553

Hotz, B., Arndt, M., Dullat, S., Bhargava, S., Buhr, H.-J., Hotz, H.G., 2007. Epithelial to mesenchymal transition: expression of the regulators snail, slug, and twist in pancreatic cancer. Clin. Cancer Res. Off. J. Am. Assoc. Cancer Res. 13, 4769–4776. https://doi.org/10.1158/1078-0432.CCR-06-2926

Howes, N., Lerch, M.M., Greenhalf, W., Stocken, D.D., Ellis, I., Simon, P., Truninger, K., Ammann, R., Cavallini, G., Charnley, R.M., Uomo, G., Delhaye, M., Spicak, J., Drumm, B., Jansen, J., Mountford, R., Whitcomb, D.C., Neoptolemos, J.P., European Registry of Hereditary Pancreatitis and Pancreatic Cancer (EUROPAC), 2004. Clinical and genetic characteristics of hereditary pancreatitis in Europe. Clin. Gastroenterol. Hepatol. Off. Clin. Pract. J. Am. Gastroenterol. Assoc. 2, 252–261. https://doi.org/10.1016/s1542-3565(04)00013-8

Hu, N., Zhang, H., 2018. CYP24A1 depletion facilitates the antitumor effect of vitamin D3 on thyroid cancer cells. Exp. Ther. Med. 16, 2821–2830. https://doi.org/10.3892/etm.2018.6536

Huang, Y.-C., Chen, J.-Y., Hung, W.-C., 2004. Vitamin D3 receptor/Sp1 complex is required for the induction of p27Kip1 expression by vitamin D3. Oncogene 23, 4856–4861. https://doi.org/10.1038/sj.onc.1207621

Huber, M.A., Kraut, N., Beug, H., 2005. Molecular requirements for epithelial-mesenchymal transition during tumor progression. Curr. Opin. Cell Biol. 17, 548–558. https://doi.org/10.1016/j.ceb.2005.08.001

Hummel, D., Aggarwal, A., Borka, K., Bajna, E., Kállay, E., Horváth, H.C., 2014. The vitamin D system is deregulated in pancreatic diseases. J. Steroid Biochem. Mol. Biol. 144, 402–409. https://doi.org/10.1016/j.jsbmb.2014.07.011

Ino, Y., Yamazaki-Itoh, R., Shimada, K., Iwasaki, M., Kosuge, T., Kanai, Y., Hiraoka, N., 2013. Immune cell infiltration as an indicator of the immune microenvironment of pancreatic cancer. Br. J. Cancer 108, 914–923. https://doi.org/10.1038/bjc.2013.32

Itakura, J., Ishiwata, T., Friess, H., Fujii, H., Matsumoto, Y., Büchler, M.W., Korc, M., 1997. Enhanced expression of vascular endothelial growth factor in human pancreatic cancer correlates with local disease progression. Clin. Cancer Res. Off. J. Am. Assoc. Cancer Res. 3, 1309–1316.

Jaillon, S., Ponzetta, A., Di Mitri, D., Santoni, A., Bonecchi, R., Mantovani, A., 2020. Neutrophil diversity and plasticity in tumour progression and therapy. Nat. Rev. Cancer 20, 485–503. https://doi.org/10.1038/s41568-020-0281-y

Jensen, S.S., Madsen, M.W., Lukas, J., Binderup, L., Bartek, J., 2001. Inhibitory effects of 1alpha,25-dihydroxyvitamin D(3) on the G(1)-S phase-controlling machinery. Mol. Endocrinol. Baltim. Md 15, 1370–1380. https://doi.org/10.1210/mend.15.8.0673

Jin, P., Zhao, Y., Liu, H., Chen, J., Ren, J., Jin, J., Bedognetti, D., Liu, S., Wang, E., Marincola, F., Stroncek, D., 2016. Interferon-γ and Tumor Necrosis Factor-α Polarize Bone Marrow Stromal Cells Uniformly to a Th1 Phenotype. Sci. Rep. 6, 26345. https://doi.org/10.1038/srep26345

Jones, S., Hruban, R.H., Kamiyama, M., Borges, M., Zhang, X., Parsons, D.W., Lin, J.C.-H., Palmisano, E., Brune, K., Jaffee, E.M., Iacobuzio-Donahue, C.A., Maitra, A., Parmigiani, G., Kern, S.E., Velculescu, V.E., Kinzler, K.W., Vogelstein, B., Eshleman, J.R., Goggins, M., Klein, A.P., 2009. Exomic sequencing identifies PALB2 as a pancreatic cancer susceptibility gene. Science 324, 217. https://doi.org/10.1126/science.1171202

Kalluri, R., Weinberg, R.A., 2009. The basics of epithelial-mesenchymal transition. J. Clin. Invest. 119, 1420–1428. https://doi.org/10.1172/JCI39104

Kamphorst, J.J., Nofal, M., Commisso, C., Hackett, S.R., Lu, W., Grabocka, E., Vander Heiden, M.G., Miller, G., Drebin, J.A., Bar-Sagi, D., Thompson, C.B., Rabinowitz, J.D., 2015. Human pancreatic cancer tumors are nutrient poor and tumor cells actively scavenge extracellular protein. Cancer Res. 75, 544–553. https://doi.org/10.1158/0008-5472.CAN-14-2211

Kanda, M., Matthaei, H., Wu, J., Hong, S.-M., Yu, J., Borges, M., Hruban, R.H., Maitra, A., Kinzler, K., Vogelstein, B., Goggins, M., 2012. Presence of somatic mutations in most early-stage pancreatic intraepithelial neoplasia. Gastroenterology 142, 730-733.e9. https://doi.org/10.1053/j.gastro.2011.12.042

Karkeni, E., Morin, S.O., Bou Tayeh, B., Goubard, A., Josselin, E., Castellano, R., Fauriat, C., Guittard, G., Olive, D., Nunès, J.A., 2019. Vitamin D Controls Tumor Growth and CD8+ T Cell Infiltration in Breast Cancer. Front. Immunol. 10, 1307. https://doi.org/10.3389/fimmu.2019.01307

Kato, J., Matsushime, H., Hiebert, S.W., Ewen, M.E., Sherr, C.J., 1993. Direct binding of cyclin D to the retinoblastoma gene product (pRb) and pRb phosphorylation by the cyclin D-dependent kinase CDK4. Genes Dev. 7, 331–342. https://doi.org/10.1101/gad.7.3.331

Katsuno, Y., Lamouille, S., Derynck, R., 2013a. TGF-β signaling and epithelial-mesenchymal transition in cancer progression. Curr. Opin. Oncol. 25, 76–84. https://doi.org/10.1097/CCO.0b013e32835b6371

Katsuno, Y., Lamouille, S., Derynck, R., 2013b. TGF-β signaling and epithelial-mesenchymal transition in cancer progression. Curr. Opin. Oncol. 25, 76–84. https://doi.org/10.1097/CCO.0b013e32835b6371

Khetani, M.P., Radhika, 2018. Functional Analysis for RNA-seq [WWW Document]. Introd. DGE - Arch. URL https://hbctraining.github.io/DGE_workshop_salmon/lessons/functional_analysis_2019.html (accessed 6.6.22).

Kim, D., Pertea, G., Trapnell, C., Pimentel, H., Kelley, R., Salzberg, S.L., 2013. TopHat2: accurate alignment of transcriptomes in the presence of insertions, deletions and gene fusions. Genome Biol. 14, R36. https://doi.org/10.1186/gb-2013-14-4-r36

Kleeff, J., Korc, M., Apte, M., La Vecchia, C., Johnson, C.D., Biankin, A.V., Neale, R.E., Tempero, M., Tuveson, D.A., Hruban, R.H., Neoptolemos, J.P., 2016. Pancreatic cancer. Nat. Rev. Dis. Primer 2, 1–22. https://doi.org/10.1038/nrdp.2016.22

Klein, A.P., 2012. Genetic susceptibility to pancreatic cancer. Mol. Carcinog. 51, 14–24. https://doi.org/10.1002/mc.20855

Kong, J., Zhang, Z., Musch, M., Ning, G., Sun, J., Hart, J., Bissonnette, M., Li, Y., 2008. Novel role of the vitamin D receptor in maintaining the integrity of the intestinal mucosal barrier. Am. J. Physiol. Gastrointest. Liver Physiol. 294, G208-16. https://doi.org/10.1152/ajpgi.00398.2007

Kósa, J.P., Horváth, P., Wölfling, J., Kovács, D., Balla, B., Mátyus, P., Horváth, E., Speer, G., Takács, I., Nagy, Z., Horváth, H., Lakatos, P., 2013. CYP24A1 inhibition facilitates the anti-tumor effect of vitamin D3 on colorectal cancer cells. World J. Gastroenterol. WJG 19, 2621–2628. https://doi.org/10.3748/wjg.v19.i17.2621

Koukourakis, M.I., Giatromanolaki, A., Sivridis, E., Bougioukas, G., Didilis, V., Gatter, K.C., Harris, A.L., 2003. Lactate dehydrogenase-5 (LDH-5) overexpression in non-small-cell lung cancer tissues is

linked to tumour hypoxia, angiogenic factor production and poor prognosis. Br. J. Cancer 89, 877–885. https://doi.org/10.1038/sj.bjc.6601205
Kranenburg, O., Gebbink, M.F.B.G., Voest, E.E., 2004. Stimulation of angiogenesis by Ras proteins. Biochim. Biophys. Acta 1654, 23–37. https://doi.org/10.1016/j.bbcan.2003.09.004
Kruiswijk, F., Labuschagne, C.F., Vousden, K.H., 2015. p53 in survival, death and metabolic health: a lifeguard with a licence to kill. Nat. Rev. Mol. Cell Biol. 16, 393–405. https://doi.org/10.1038/nrm4007
Kuchay, S., Giorgi, C., Simoneschi, D., Pagan, julia, Missiroli, S., Saraf, A., Florens, L., Washburn, M.P., Collazo-Lorduy, A., Castillo-Martin, M., Cordon-Cardo, C., Sebti, S.M., Pinton, P., Pagano, M., 2017. PTEN counteracts FBXL2 to promote IP3R3– and Ca2+–mediated apoptosis limiting tumour growth. Nature 546, 554–558. https://doi.org/10.1038/nature22965
Kuzmickiene, I., Everatt, R., Virviciute, D., Tamosiunas, A., Radisauskas, R., Reklaitiene, R., Milinaviciene, E., 2013. Smoking and other risk factors for pancreatic cancer: a cohort study in men in Lithuania. Cancer Epidemiol. 37, 133–139. https://doi.org/10.1016/j.canep.2012.10.001
Labi, V., Erlacher, M., 2015. How cell death shapes cancer. Cell Death Dis. 6, e1675. https://doi.org/10.1038/cddis.2015.20
Laconi, E., Marongiu, F., DeGregori, J., 2020. Cancer as a disease of old age: changing mutational and microenvironmental landscapes. Br. J. Cancer 122, 943–952. https://doi.org/10.1038/s41416-019-0721-1
Langmead, B., Trapnell, C., Pop, M., Salzberg, S.L., 2009. Ultrafast and memory-efficient alignment of short DNA sequences to the human genome. Genome Biol. 10, R25. https://doi.org/10.1186/gb-2009-10-3-r25
Larriba, M.J., García de Herreros, A., Muñoz, A., 2016. Vitamin D and the Epithelial to Mesenchymal Transition. Stem Cells Int. 2016, 6213872. https://doi.org/10.1155/2016/6213872
Larriba, M.J., Martín-Villar, E., García, J.M., Pereira, F., Peña, C., de Herreros, A.G., Bonilla, F., Muñoz, A., 2009. Snail2 cooperates with Snail1 in the repression of vitamin D receptor in colon cancer. Carcinogenesis 30, 1459–1468. https://doi.org/10.1093/carcin/bgp140
Lee, J.M., Dedhar, S., Kalluri, R., Thompson, E.W., 2006. The epithelial-mesenchymal transition: new insights in signaling, development, and disease. J. Cell Biol. 172, 973–981. https://doi.org/10.1083/jcb.200601018
Leek, J.T., 2014. svaseq: removing batch effects and other unwanted noise from sequencing data. Nucleic Acids Res. 42, e161–e161. https://doi.org/10.1093/nar/gku864
Levi, F., Lucchini, F., Negri, E., La Vecchia, C., 2003. Pancreatic cancer mortality in Europe: the leveling of an epidemic. Pancreas 27, 139–142. https://doi.org/10.1097/00006676-200308000-00006
Li, D., Morris, J.S., Liu, J., Hassan, M.M., Day, R.S., Bondy, M.L., Abbruzzese, J.L., 2009. Body mass index and risk, age of onset, and survival in patients with pancreatic cancer. JAMA 301, 2553–2562. https://doi.org/10.1001/jama.2009.886
Liu, P.T., Schenk, M., Walker, V.P., Dempsey, P.W., Kanchanapoomi, M., Wheelwright, M., Vazirnia, A., Zhang, X., Steinmeyer, A., Zügel, U., Hollis, B.W., Cheng, G., Modlin, R.L., 2009. Convergence of IL-1beta and VDR activation pathways in human TLR2/1-induced antimicrobial responses. PloS One 4, e5810. https://doi.org/10.1371/journal.pone.0005810
Liu, P.T., Stenger, S., Li, H., Wenzel, L., Tan, B.H., Krutzik, S.R., Ochoa, M.T., Schauber, J., Wu, K., Meinken, C., Kamen, D.L., Wagner, M., Bals, R., Steinmeyer, A., Zügel, U., Gallo, R.L., Eisenberg, D., Hewison, M., Hollis, B.W., Adams, J.S., Bloom, B.R., Modlin, R.L., 2006. Toll-like receptor triggering of a vitamin D-mediated human antimicrobial response. Science 311, 1770–1773. https://doi.org/10.1126/science.1123933

Liu, Y., Wang, X., Sun, X., Lu, S., Liu, S., 2018. Vitamin intake and pancreatic cancer risk reduction: A meta-analysis of observational studies. Medicine (Baltimore) 97, e0114. https://doi.org/10.1097/MD.0000000000010114

Lobo, N.A., Shimono, Y., Qian, D., Clarke, M.F., 2007. The biology of cancer stem cells. Annu. Rev. Cell Dev. Biol. 23, 675–699. https://doi.org/10.1146/annurev.cellbio.22.010305.104154

Love, M.I., Huber, W., Anders, S., 2014. Moderated estimation of fold change and dispersion for RNA-seq data with DESeq2. Genome Biol. 15, 550. https://doi.org/10.1186/s13059-014-0550-8

Lowe, S.W., Cepero, E., Evan, G., 2004. Intrinsic tumour suppression. Nature 432, 307–315. https://doi.org/10.1038/nature03098

Lowenfels, A.B., Maisonneuve, P., Whitcomb, D.C., 2000. Risk factors for cancer in hereditary pancreatitis. International Hereditary Pancreatitis Study Group. Med. Clin. North Am. 84, 565–573. https://doi.org/10.1016/s0025-7125(05)70240-6

Luckett, B.G., Su, L.J., Rood, J.C., Fontham, E.T.H., 2012. Cadmium exposure and pancreatic cancer in south Louisiana. J. Environ. Public Health 2012, 180186. https://doi.org/10.1155/2012/180186

Lundberg, A.S., Weinberg, R.A., 1998. Functional inactivation of the retinoblastoma protein requires sequential modification by at least two distinct cyclin-cdk complexes. Mol. Cell. Biol. 18, 753–761. https://doi.org/10.1128/MCB.18.2.753

Ma, G., Li, G., Gou, A., Xiao, Z., Xu, Y., Song, S., Guo, K., Liu, Z., 2021. Long non-coding RNA ELFN1-AS1 in the pathogenesis of pancreatic cancer. Ann. Transl. Med. 9, 877. https://doi.org/10.21037/atm-21-2376

Ma, Y., Trump, D.L., Johnson, C.S., 2010. Vitamin D in combination cancer treatment. J. Cancer 1, 101–107.

Mace, T.A., Bloomston, M., Lesinski, G.B., 2013. Pancreatic cancer-associated stellate cells: A viable target for reducing immunosuppression in the tumor microenvironment. Oncoimmunology 2, e24891. https://doi.org/10.4161/onci.24891

Mahalingam, D., Wilding, G., Denmeade, S., Sarantopoulas, J., Cosgrove, D., Cetnar, J., Azad, N., Bruce, J., Kurman, M., Allgood, V.E., Carducci, M., 2016. Mipsagargin, a novel thapsigargin-based PSMA-activated prodrug: results of a first-in-man phase I clinical trial in patients with refractory, advanced or metastatic solid tumours. Br. J. Cancer 114, 986–994. https://doi.org/10.1038/bjc.2016.72

Maier, H.J., Schmidt-Strassburger, U., Huber, M.A., Wiedemann, E.M., Beug, H., Wirth, T., 2010. NF-kappaB promotes epithelial-mesenchymal transition, migration and invasion of pancreatic carcinoma cells. Cancer Lett. 295, 214–228. https://doi.org/10.1016/j.canlet.2010.03.003

Maisonneuve, P., Lowenfels, A.B., 2015. Risk factors for pancreatic cancer: a summary review of meta-analytical studies. Int. J. Epidemiol. 44, 186–198. https://doi.org/10.1093/ije/dyu240

Maitra, A., Adsay, N.V., Argani, P., Iacobuzio-Donahue, C., De Marzo, A., Cameron, J.L., Yeo, C.J., Hruban, R.H., 2003. Multicomponent analysis of the pancreatic adenocarcinoma progression model using a pancreatic intraepithelial neoplasia tissue microarray. Mod. Pathol. Off. J. U. S. Can. Acad. Pathol. Inc 16, 902–912. https://doi.org/10.1097/01.MP.0000086072.56290.FB

Malmberg, K.-J., 2004. Effective immunotherapy against cancer: a question of overcoming immune suppression and immune escape? Cancer Immunol. Immunother. CII 53, 879–892. https://doi.org/10.1007/s00262-004-0577-x

Malumbres, M., Barbacid, M., 2009. Cell cycle, CDKs and cancer: a changing paradigm. Nat. Rev. Cancer 9, 153–166. https://doi.org/10.1038/nrc2602

Malvezzi, M., Carioli, G., Bertuccio, P., Rosso, T., Boffetta, P., Levi, F., La Vecchia, C., Negri, E., 2016. European cancer mortality predictions for the year 2016 with focus on leukaemias. Ann. Oncol. Off. J. Eur. Soc. Med. Oncol. 27, 725–731. https://doi.org/10.1093/annonc/mdw022

Maruyama, R., Aoki, F., Toyota, M., Sasaki, Y., Akashi, H., Mita, H., Suzuki, H., Akino, K., Ohe-Toyota, M., Maruyama, Y., Tatsumi, H., Imai, K., Shinomura, Y., Tokino, T., 2006. Comparative Genome Analysis Identifies the Vitamin D Receptor Gene as a Direct Target of p53-Mediated Transcriptional Activation. Cancer Res. 66, 4574–4583. https://doi.org/10.1158/0008-5472.CAN-05-2562

Massagué, J., Obenauf, A.C., 2016. Metastatic colonization by circulating tumour cells. Nature 529, 298–306. https://doi.org/10.1038/nature17038

Mathers, C.D., Fat, D.M., Inoue, M., Rao, C., Lopez, A.D., 2005. Counting the dead and what they died from: an assessment of the global status of cause of death data. Bull. World Health Organ. 83, 171–177. https://doi.org//S0042-96862005000300009

Mayo, M.W., Baldwin, A.S., 2000. The transcription factor NF-kappaB: control of oncogenesis and cancer therapy resistance. Biochim. Biophys. Acta 1470, M55-62. https://doi.org/10.1016/s0304-419x(00)00002-0

McGuigan, A., Kelly, P., Turkington, R.C., Jones, C., Coleman, H.G., McCain, R.S., 2018. Pancreatic cancer: A review of clinical diagnosis, epidemiology, treatment and outcomes. World J. Gastroenterol. 24, 4846–4861. https://doi.org/10.3748/wjg.v24.i43.4846

McKenna, N.J., Lanz, R.B., O'Malley, B.W., 1999. Nuclear receptor coregulators: cellular and molecular biology. Endocr. Rev. 20, 321–344. https://doi.org/10.1210/edrv.20.3.0366

Michaud, D.S., Skinner, H.G., Wu, K., Hu, F., Giovannucci, E., Willett, W.C., Colditz, G.A., Fuchs, C.S., 2005. Dietary patterns and pancreatic cancer risk in men and women. J. Natl. Cancer Inst. 97, 518–524. https://doi.org/10.1093/jnci/dji094

Michaud, D.S., Vrieling, A., Jiao, L., Mendelsohn, J.B., Steplowski, E., Lynch, S.M., Wactawski-Wende, J., Arslan, A.A., Bueno-de-Mesquita, H.B., Fuchs, C.S., Gross, M., Helzlsouer, K., Jacobs, E.J., LaCroix, A., Petersen, G., Zheng, W., Allen, N., Ammundadottir, L., Bergmann, M.M., Boffetta, P., Buring, J.E., Canzian, F., Chanock, S.J., Clavel-Chapelon, F., Clipp, S., Freiberg, M.S., Gaziano, J.M., Giovannucci, E.L., Hankinson, S., Hartge, P., Hoover, R.N., Hubbell, F.A., Hunter, D.J., Hutchinson, A., Jacobs, K., Kooperberg, C., Kraft, P., Manjer, J., Navarro, C., Peeters, P.H.M., Shu, X.-O., Stevens, V., Thomas, G., Tjønneland, A., Tobias, G.S., Trichopoulos, D., Tumino, R., Vineis, P., Virtamo, J., Wallace, R., Wolpin, B.M., Yu, K., Zeleniuch-Jacquotte, A., Stolzenberg-Solomon, R.Z., 2010. Alcohol intake and pancreatic cancer: a pooled analysis from the pancreatic cancer cohort consortium (PanScan). Cancer Causes Control CCC 21, 1213–1225. https://doi.org/10.1007/s10552-010-9548-z

Midha, S., Chawla, S., Garg, P.K., 2016a. Modifiable and non-modifiable risk factors for pancreatic cancer: A review. Cancer Lett. 381, 269–277. https://doi.org/10.1016/j.canlet.2016.07.022

Midha, S., Sreenivas, V., Kabra, M., Chattopadhyay, T.K., Joshi, Y.K., Garg, P.K., 2016b. Genetically Determined Chronic Pancreatitis but not Alcoholic Pancreatitis Is a Strong Risk Factor for Pancreatic Cancer. Pancreas 45, 1478–1484. https://doi.org/10.1097/MPA.0000000000000684

Miller, D.M., Thomas, S.D., Islam, A., Muench, D., Sedoris, K., 2012. c-Myc and cancer metabolism. Clin. Cancer Res. Off. J. Am. Assoc. Cancer Res. 18, 5546–5553. https://doi.org/10.1158/1078-0432.CCR-12-0977

Mistry, M.P. and M., 2019. Quantification of transcript abundance using Salmon [WWW Document]. Introd. RNA-Seq Using High-Perform. Comput. - Arch. URL https://hbctraining.github.io/Intro-to-rnaseq-hpc-salmon/lessons/04_quasi_alignment_salmon.html (accessed 2.22.22).

Mizuno, S., Nakai, Y., Isayama, H., Kawahata, S., Saito, T., Takagi, K., Watanabe, T., Uchino, R., Hamada, T., Miyabayashi, K., Kogure, H., Sasaki, T., Yamamoto, N., Sasahira, N., Hirano, K., Tsujino, T., Ijichi, H., Tateishi, K., Tada, M., Koike, K., 2014. Smoking, family history of cancer, and diabetes mellitus are associated with the age of onset of pancreatic cancer in Japanese patients. Pancreas 43, 1014–1017. https://doi.org/10.1097/MPA.0000000000000158

Moustakas, A., Heldin, C.-H., 2007. Signaling networks guiding epithelial-mesenchymal transitions during embryogenesis and cancer progression. Cancer Sci. 98, 1512–1520. https://doi.org/10.1111/j.1349-7006.2007.00550.x

Muindi, J.R., Yu, W.-D., Ma, Y., Engler, K.L., Kong, R.-X., Trump, D.L., Johnson, C.S., 2010. CYP24A1 Inhibition Enhances the Antitumor Activity of Calcitriol. Endocrinology 151, 4301–4312. https://doi.org/10.1210/en.2009-1156

Murphy, K.M., Brune, K.A., Griffin, C., Sollenberger, J.E., Petersen, G.M., Bansal, R., Hruban, R.H., Kern, S.E., 2002. Evaluation of candidate genes MAP2K4, MADH4, ACVR1B, and BRCA2 in familial pancreatic cancer: deleterious BRCA2 mutations in 17%. Cancer Res. 62, 3789–3793.

Musgrove, E.A., Caldon, C.E., Barraclough, J., Stone, A., Sutherland, R.L., 2011. Cyclin D as a therapeutic target in cancer. Nat. Rev. Cancer 11, 558–572. https://doi.org/10.1038/nrc3090

Naeem, Z., 2010. Vitamin D Deficiency- An Ignored Epidemic. Int. J. Health Sci. 4, V–VI.

Neoptolemos, J.P., Palmer, D.H., Ghaneh, P., Psarelli, E.E., Valle, J.W., Halloran, C.M., Faluyi, O., O'Reilly, D.A., Cunningham, D., Wadsley, J., Darby, S., Meyer, T., Gillmore, R., Anthoney, A., Lind, P., Glimelius, B., Falk, S., Izbicki, J.R., Middleton, G.W., Cummins, S., Ross, P.J., Wasan, H., McDonald, A., Crosby, T., Ma, Y.T., Patel, K., Sherriff, D., Soomal, R., Borg, D., Sothi, S., Hammel, P., Hackert, T., Jackson, R., Büchler, M.W., European Study Group for Pancreatic Cancer, 2017. Comparison of adjuvant gemcitabine and capecitabine with gemcitabine monotherapy in patients with resected pancreatic cancer (ESPAC-4): a multicentre, open-label, randomised, phase 3 trial. Lancet Lond. Engl. 389, 1011–1024. https://doi.org/10.1016/S0140-6736(16)32409-6

Neoptolemos, J.P., Stocken, D.D., Bassi, C., Ghaneh, P., Cunningham, D., Goldstein, D., Padbury, R., Moore, M.J., Gallinger, S., Mariette, C., Wente, M.N., Izbicki, J.R., Friess, H., Lerch, M.M., Dervenis, C., Oláh, A., Butturini, G., Doi, R., Lind, P.A., Smith, D., Valle, J.W., Palmer, D.H., Buckels, J.A., Thompson, J., McKay, C.J., Rawcliffe, C.L., Büchler, M.W., European Study Group for Pancreatic Cancer, 2010. Adjuvant chemotherapy with fluorouracil plus folinic acid vs gemcitabine following pancreatic cancer resection: a randomized controlled trial. JAMA 304, 1073–1081. https://doi.org/10.1001/jama.2010.1275

Nguyen, S.T., Nguyen, H.T.-L., Truong, K.D., 2020. Comparative cytotoxic effects of methanol, ethanol and DMSO on human cancer cell lines. Biomed. Res. Ther. 7, 3855–3859. https://doi.org/10.15419/bmrat.v7i7.614

Nishimura, A., Shinki, T., Jin, C.H., Ohyama, Y., Noshiro, M., Okuda, K., Suda, T., 1994. Regulation of messenger ribonucleic acid expression of 1 alpha,25-dihydroxyvitamin D3-24-hydroxylase in rat osteoblasts. Endocrinology 134, 1794–1799. https://doi.org/10.1210/endo.134.4.8137744

Oberstein, P.E., Olive, K.P., 2013. Pancreatic cancer: why is it so hard to treat? Ther. Adv. Gastroenterol. 6, 321–337. https://doi.org/10.1177/1756283X13478680

O'Connor, M.J., 2015. Targeting the DNA Damage Response in Cancer. Mol. Cell 60, 547–560. https://doi.org/10.1016/j.molcel.2015.10.040

Oda, Y., Sihlbom, C., Chalkley, R.J., Huang, L., Rachez, C., Chang, C.-P.B., Burlingame, A.L., Freedman, L.P., Bikle, D.D., 2003. Two distinct coactivators, DRIP/mediator and SRC/p160, are differentially involved in vitamin D receptor transactivation during keratinocyte differentiation. Mol. Endocrinol. Baltim. Md 17, 2329–2339. https://doi.org/10.1210/me.2003-0063

Ojajärvi, I.A., Partanen, T.J., Ahlbom, A., Boffetta, P., Hakulinen, T., Jourenkova, N., Kauppinen, T.P., Kogevinas, M., Porta, M., Vainio, H.U., Weiderpass, E., Wesseling, C.H., 2000. Occupational exposures and pancreatic cancer: a meta-analysis. Occup. Environ. Med. 57, 316–324. https://doi.org/10.1136/oem.57.5.316

Orlowski, R.Z., Baldwin, A.S., 2002. NF-kappaB as a therapeutic target in cancer. Trends Mol. Med. 8, 385–389. https://doi.org/10.1016/s1471-4914(02)02375-4

Ouban, A., Muraca, P., Yeatman, T., Coppola, D., 2003. Expression and distribution of insulin-like growth factor-1 receptor in human carcinomas. Hum. Pathol. 34, 803–808. https://doi.org/10.1016/s0046-8177(03)00291-0

Özdemir, B.C., Pentcheva-Hoang, T., Carstens, J.L., Zheng, X., Wu, C.-C., Simpson, T.R., Laklai, H., Sugimoto, H., Kahlert, C., Novitskiy, S.V., De Jesus-Acosta, A., Sharma, P., Heidari, P., Mahmood, U., Chin, L., Moses, H.L., Weaver, V.M., Maitra, A., Allison, J.P., LeBleu, V.S., Kalluri, R., 2014. Depletion of carcinoma-associated fibroblasts and fibrosis induces immunosuppression and accelerates pancreas cancer with reduced survival. Cancer Cell 25, 719–734. https://doi.org/10.1016/j.ccr.2014.04.005

Pálmer, H.G., Larriba, M.J., García, J.M., Ordóñez-Morán, P., Peña, C., Peiró, S., Puig, I., Rodríguez, R., de la Fuente, R., Bernad, A., Pollán, M., Bonilla, F., Gamallo, C., de Herreros, A.G., Muñoz, A., 2004. The transcription factor SNAIL represses vitamin D receptor expression and responsiveness in human colon cancer. Nat. Med. 10, 917–919. https://doi.org/10.1038/nm1095

Pálmer, H.G., Sánchez-Carbayo, M., Ordóñez-Morán, P., Larriba, M.J., Cordón-Cardó, C., Muñoz, A., 2003. Genetic signatures of differentiation induced by 1alpha,25-dihydroxyvitamin D3 in human colon cancer cells. Cancer Res. 63, 7799–7806.

Patro, R., Duggal, G., Love, M.I., Irizarry, R.A., Kingsford, C., 2017. Salmon provides fast and bias-aware quantification of transcript expression. Nat. Methods 14, 417–419. https://doi.org/10.1038/nmeth.4197

Patro, R., Mount, S.M., Kingsford, C., 2014. Sailfish enables alignment-free isoform quantification from RNA-seq reads using lightweight algorithms. Nat. Biotechnol. 32, 462. https://doi.org/10.1038/nbt.2862

Pavlova, N.N., Thompson, C.B., 2016. The Emerging Hallmarks of Cancer Metabolism. Cell Metab. 23, 27–47. https://doi.org/10.1016/j.cmet.2015.12.006

Pendás-Franco, N., González-Sancho, J.M., Suárez, Y., Aguilera, O., Steinmeyer, A., Gamallo, C., Berciano, M.T., Lafarga, M., Muñoz, A., 2007. Vitamin D regulates the phenotype of human breast cancer cells. Differ. Res. Biol. Divers. 75, 193–207. https://doi.org/10.1111/j.1432-0436.2006.00131.x

Peng, J.-F., Zhuang, Y.-Y., Huang, F.-T., Zhang, S.-N., 2016. Noncoding RNAs and pancreatic cancer. World J. Gastroenterol. 22, 801–814. https://doi.org/10.3748/wjg.v22.i2.801

Pereira, N.P., Corrêa, J.R., 2018. Pancreatic cancer: treatment approaches and trends. J. Cancer Metastasis Treat. 4, 30. https://doi.org/10.20517/2394-4722.2018.13

Pérez-Mancera, P.A., Young, A.R.J., Narita, M., 2014. Inside and out: the activities of senescence in cancer. Nat. Rev. Cancer 14, 547–558. https://doi.org/10.1038/nrc3773

Pernick, N.L., Sarkar, F.H., Philip, P.A., Arlauskas, P., Shields, A.F., Vaitkevicius, V.K., Dugan, M.C., Adsay, N.V., 2003. Clinicopathologic analysis of pancreatic adenocarcinoma in African Americans and Caucasians. Pancreas 26, 28–32. https://doi.org/10.1097/00006676-200301000-00006

Pickup, M., Novitskiy, S., Moses, H.L., 2013. The roles of TGFβ in the tumour microenvironment. Nat. Rev. Cancer 13, 788–799. https://doi.org/10.1038/nrc3603

Pike, J.W., Meyer, M.B., 2010. The Vitamin D Receptor: New Paradigms for the Regulation of Gene Expression by 1,25-Dihydroxyvitamin D3. Endocrinol. Metab. Clin. North Am. 39, 255–269. https://doi.org/10.1016/j.ecl.2010.02.007

Pike, J.W., Meyer, M.B., Benkusky, N.A., Lee, S.M., St. John, H., Carlson, A., Onal, M., Shamsuzzaman, S., 2016. Genomic Determinants of Vitamin D-Regulated Gene Expression. Vitam. Horm. 100, 21–44. https://doi.org/10.1016/bs.vh.2015.10.011

Polireddy, K., Chen, Q., 2016. Cancer of the Pancreas: Molecular Pathways and Current Advancement in Treatment. J. Cancer 7, 1497–1514. https://doi.org/10.7150/jca.14922

Porter, R.L., Magnus, N.K.C., Thapar, V., Morris, R., Szabolcs, A., Neyaz, A., Kulkarni, A.S., Tai, E., Chougule, A., Hillis, A., Golczer, G., Guo, H., Yamada, T., Kurokawa, T., Yashaswini, C., Ligorio, M.,

Vo, K.D., Nieman, L., Liss, A.S., Deshpande, V., Lawrence, M.S., Maheswaran, S., Castillo, C.F.-D., Hong, T.S., Ryan, D.P., O'Dwyer, P.J., Drebin, J.A., Ferrone, C.R., Haber, D.A., Ting, D.T., 2019. Epithelial to mesenchymal plasticity and differential response to therapies in pancreatic ductal adenocarcinoma. Proc. Natl. Acad. Sci. 116, 26835–26845. https://doi.org/10.1073/pnas.1914915116

Pourshams, A., Sepanlou, S.G., Ikuta, K.S., Bisignano, C., Safiri, S., Roshandel, G., Sharif, M., Khatibian, M., Fitzmaurice, C., Nixon, M.R., Abbasi, N., Afarideh, M., Ahmadian, E., Akinyemiju, T., Alahdab, F., Alam, T., Alipour, V., Allen, C.A., Anber, N.H., Ansari-Moghaddam, A., Arabloo, J., Badawi, A., Bagherzadeh, M., Belayneh, Y.M., Biadgo, B., Bijani, A., Biondi, A., Bjørge, T., Borzì, A.M., Bosetti, C., Briko, A.N., Briko, N.I., Carreras, G., Carvalho, F., Choi, J.-Y.J., Chu, D.-T., Dang, A.K., Daryani, A., Davitoiu, D.V., Demoz, G.T., Desai, R., Dey, S., Do, H.T., Do, H.P., Eftekhari, A., Esteghamati, A., Farzadfar, F., Fernandes, E., Filip, I., Fischer, F., Foroutan, M., Gad, M.M., Gallus, S., Geta, B., Gorini, G., Hafezi-Nejad, N., Harvey, J.D., Hasankhani, M., Hasanzadeh, A., Hassanipour, S., Hay, S.I., Hidru, H.D., Hoang, C.L., Hostiuc, S., Househ, M., Ilesanmi, O.S., Ilic, M.D., Irvani, S.S.N., Balalami, N.J., James, S.L., Joukar, F., Kasaeian, A., Kassa, T.D., Kengne, A.P., Khalilov, R., Khan, E.A., Khater, A., Shadmani, F.K., Kocarnik, J.M., Komaki, H., Koyanagi, A., Kumar, V., Vecchia, C.L., Lopukhov, P.D., Manafi, F., Manafi, N., Manda, A.-L., Mansour-Ghanaei, F., Mehta, D., Mehta, V., Meier, T., Meles, H.G., Mengistu, G., Miazgowski, T., Mohamadnejad, M., Mohammadian-Hafshejani, A., Mohammadoo-Khorasani, M., Mohammed, S., Mohebi, F., Mokdad, A.H., Monasta, L., Moossavi, M., Moradzadeh, R., Naik, G., Negoi, I., Nguyen, C.T., Nguyen, L.H., Nguyen, T.H., Olagunju, A.T., Olagunju, T.O., Pennini, A., Rabiee, M., Rabiee, N., Radfar, A., Rahimi, M., Rath, G.K., Rawaf, D.L., Rawaf, S., Reiner, R.C., Rezaei, N., Rezapour, A., Saad, A.M., Saadatagah, S., Sahebkar, A., Salimzadeh, H., Samy, A.M., Sanabria, J., Sarveazad, A., Sawhney, M., Sekerija, M., Shabalkin, P., Shaikh, M.A., Sharma, R., Sheikhbahaei, S., Shirkoohi, R., Malleshappa, S.K.S., Sisay, M., Soreide, K., Soshnikov, S., Sotoudehmanesh, R., Starodubov, V.I., Subart, M.L., Tabarés-Seisdedos, R., Tadesse, D.B.B., Traini, E., Tran, B.X., Tran, K.B., Ullah, I., Vacante, M., Vahedian-Azimi, A., Varavikova, E., Westerman, R., Wondafrash, D.D.Z., Xu, R., Yonemoto, N., Zadnik, V., Zhang, Z.-J., Malekzadeh, R., Naghavi, M., 2019. The global, regional, and national burden of pancreatic cancer and its attributable risk factors in 195 countries and territories, 1990–2017: a systematic analysis for the Global Burden of Disease Study 2017. Lancet Gastroenterol. Hepatol. 4, 934–947. https://doi.org/10.1016/S2468-1253(19)30347-4

Prevarskaya, N., Skryma, R., Shuba, Y., 2011. Calcium in tumour metastasis: new roles for known actors. Nat. Rev. Cancer 11, 609–618. https://doi.org/10.1038/nrc3105

Pylayeva-Gupta, Y., Grabocka, E., Bar-Sagi, D., 2011. RAS oncogenes: weaving a tumorigenic web. Nat. Rev. Cancer 11, 761–774. https://doi.org/10.1038/nrc3106

Quail, D.F., Joyce, J.A., 2013. Microenvironmental regulation of tumor progression and metastasis. Nat. Med. 19, 1423–1437. https://doi.org/10.1038/nm.3394

Quiñonero, F., Mesas, C., Doello, K., Cabeza, L., Perazzoli, G., Jimenez-Luna, C., Rama, A.R., Melguizo, C., Prados, J., 2019. The challenge of drug resistance in pancreatic ductal adenocarcinoma: a current overview. Cancer Biol. Med. 16, 688–699. https://doi.org/10.20892/j.issn.2095-3941.2019.0252

Rahman, F., Cotterchio, M., Cleary, S.P., Gallinger, S., 2015. Association between alcohol consumption and pancreatic cancer risk: a case-control study. PloS One 10, e0124489. https://doi.org/10.1371/journal.pone.0124489

Reichard, J.F., Puga, A., 2010. Effects of arsenic exposure on DNA methylation and epigenetic gene regulation. Epigenomics 2, 87–104. https://doi.org/10.2217/epi.09.45

Rhim, A.D., Mirek, E.T., Aiello, N.M., Maitra, A., Bailey, J.M., McAllister, F., Reichert, M., Beatty, G.L., Rustgi, A.K., Vonderheide, R.H., Leach, S.D., Stanger, B.Z., 2012. EMT and dissemination precede pancreatic tumor formation. Cell 148, 349–361. https://doi.org/10.1016/j.cell.2011.11.025

Robertson, K.D., 2005. DNA methylation and human disease. Nat. Rev. Genet. 6, 597–610. https://doi.org/10.1038/nrg1655

Roderick, H.L., Cook, S.J., 2008. Ca2+ signalling checkpoints in cancer: remodelling Ca2+ for cancer cell proliferation and survival. Nat. Rev. Cancer 8, 361–375. https://doi.org/10.1038/nrc2374

Rodriguez-Viciana, P., Warne, P.H., Vanhaesebroeck, B., Waterfield, M.D., Downward, J., 1996. Activation of phosphoinositide 3-kinase by interaction with Ras and by point mutation. EMBO J. 15, 2442–2451.

Rozenblum, E., Schutte, M., Goggins, M., Hahn, S.A., Panzer, S., Zahurak, M., Goodman, S.N., Sohn, T.A., Hruban, R.H., Yeo, C.J., Kern, S.E., 1997. Tumor-suppressive pathways in pancreatic carcinoma. Cancer Res. 57, 1731–1734.

Salehi-Tabar, R., Nguyen-Yamamoto, L., Tavera-Mendoza, L.E., Quail, T., Dimitrov, V., An, B.-S., Glass, L., Goltzman, D., White, J.H., 2012. Vitamin D receptor as a master regulator of the c-MYC/MXD1 network. Proc. Natl. Acad. Sci. U. S. A. 109, 18827–18832. https://doi.org/10.1073/pnas.1210037109

Schmielau, J., Finn, O.J., 2001. Activated granulocytes and granulocyte-derived hydrogen peroxide are the underlying mechanism of suppression of t-cell function in advanced cancer patients. Cancer Res. 61, 4756–4760.

Schwartz, G.G., Eads, D., Rao, A., Cramer, S.D., Willingham, M.C., Chen, T.C., Jamieson, D.P., Wang, L., Burnstein, K.L., Holick, M.F., Koumenis, C., 2004. Pancreatic cancer cells express 25-hydroxyvitamin D-1 alpha-hydroxylase and their proliferation is inhibited by the prohormone 25-hydroxyvitamin D3. Carcinogenesis 25, 1015–1026. https://doi.org/10.1093/carcin/bgh086

Sclabas, G.M., Fujioka, S., Schmidt, C., Evans, D.B., Chiao, P.J., 2003. NF-kappaB in pancreatic cancer. Int. J. Gastrointest. Cancer 33, 15–26. https://doi.org/10.1385/IJGC:33:1:15

Scupoli, M.T., Sartoris, S., Tosi, G., Ennas, M.G., Nicolis, M., Cestari, T., Zamboni, G., Martignoni, G., Lemoine, N.R., Scarpa, A., Accolla, R.S., 1996. Expression of MHC class I and class II antigens in pancreatic adenocarcinomas. Tissue Antigens 48, 301–311. https://doi.org/10.1111/j.1399-0039.1996.tb02649.x

Sens, M.A., Zhou, X., Weiland, T., Cooley, A.M., 2009. Unexpected neoplasia in autopsies: potential implications for tissue and organ safety. Arch. Pathol. Lab. Med. 133, 1923–1931. https://doi.org/10.1043/1543-2165-133.12.1923

Seo, Y., Baba, H., Fukuda, T., Takashima, M., Sugimachi, K., 2000. High expression of vascular endothelial growth factor is associated with liver metastasis and a poor prognosis for patients with ductal pancreatic adenocarcinoma. Cancer 88, 2239–2245. https://doi.org/10.1002/(sici)1097-0142(20000515)88:10<2239::aid-cncr6>3.0.co;2-v

Shapovalov, G., Ritaine, A., Skryma, R., Prevarskaya, N., 2016. Role of TRP ion channels in cancer and tumorigenesis. Semin. Immunopathol. 38, 357–369. https://doi.org/10.1007/s00281-015-0525-1

Shay, J.W., 2016. Role of Telomeres and Telomerase in Aging and Cancer. Cancer Discov. 6, 584–593. https://doi.org/10.1158/2159-8290.CD-16-0062

Shen, W., Tao, G., Zhang, Y., Cai, B., Sun, J., Tian, Z., 2017. TGF-β in pancreatic cancer initiation and progression: two sides of the same coin. Cell Biosci. 7, 39. https://doi.org/10.1186/s13578-017-0168-0

Shi, Y., Massagué, J., 2003. Mechanisms of TGF-beta signaling from cell membrane to the nucleus. Cell 113, 685–700. https://doi.org/10.1016/s0092-8674(03)00432-x

Shin, E.J., Canto, M.I., 2012. Pancreatic cancer screening. Gastroenterol. Clin. North Am. 41, 143–157. https://doi.org/10.1016/j.gtc.2011.12.001

Shojaei, F., Wu, X., Zhong, C., Yu, L., Liang, X.-H., Yao, J., Blanchard, D., Bais, C., Peale, F.V., van Bruggen, N., Ho, C., Ross, J., Tan, M., Carano, R.A.D., Meng, Y.G., Ferrara, N., 2007. Bv8 regulates myeloid-cell-dependent tumour angiogenesis. Nature 450, 825–831. https://doi.org/10.1038/nature06348

Silverman, D.T., Hoover, R.N., Brown, L.M., Swanson, G.M., Schiffman, M., Greenberg, R.S., Hayes, R.B., Lillemoe, K.D., Schoenberg, J.B., Schwartz, A.G., Liff, J., Pottern, L.M., Fraumeni, J.F., 2003. Why do Black Americans have a higher risk of pancreatic cancer than White Americans. Epidemiol. Camb. Mass 14, 45–54. https://doi.org/10.1097/00001648-200301000-00013

Singh, A., Settleman, J., 2010. EMT, cancer stem cells and drug resistance: an emerging axis of evil in the war on cancer. Oncogene 29, 4741–4751. https://doi.org/10.1038/onc.2010.215

Slapak, E.J., Duitman, J., Tekin, C., Bijlsma, M.F., Spek, C.A., 2020. Matrix Metalloproteases in Pancreatic Ductal Adenocarcinoma: Key Drivers of Disease Progression? Biology 9, 80. https://doi.org/10.3390/biology9040080

Slater, E.P., Langer, P., Niemczyk, E., Strauch, K., Butler, J., Habbe, N., Neoptolemos, J.P., Greenhalf, W., Bartsch, D.K., 2010. PALB2 mutations in European familial pancreatic cancer families. Clin. Genet. 78, 490–494. https://doi.org/10.1111/j.1399-0004.2010.01425.x

Solomon, S., Das, S., Brand, R., Whitcomb, D.C., 2012. Inherited pancreatic cancer syndromes. Cancer J. Sudbury Mass 18, 485–491. https://doi.org/10.1097/PPO.0b013e318278c4a6

Soneson, C., Love, M.I., Robinson, M.D., 2016. Differential analyses for RNA-seq: transcript-level estimates improve gene-level inferences. F1000Research 4, 1521. https://doi.org/10.12688/f1000research.7563.2

Song, M.M., Nio, Y., Dong, M., Tamura, K., Furuse, K., Tian, Y.L., He, S.G., Shen, K., 2000. Comparison of K-ras point mutations at codon 12 and p21 expression in pancreatic cancer between Japanese and Chinese patients. J. Surg. Oncol. 75, 176–185. https://doi.org/10.1002/1096-9098(200011)75:3<176::aid-jso5>3.0.co;2-w

Soon, L., Tachtsidis, A., Fok, S., Williams, E., Newgreen, D., Thompson, E., 2011. The continuum of epithelial mesenchymal transition - implication of hybrid states for migration and survival in development and cancer. Cancer Metastasis Biol. Basis Ther. 117–130.

Srivastava, A., Sarkar, H., Gupta, N., Patro, R., 2016. RapMap: a rapid, sensitive and accurate tool for mapping RNA-seq reads to transcriptomes. Bioinformatics 32, i192–i200. https://doi.org/10.1093/bioinformatics/btw277

Srivastava, M., Raghavan, S.C., 2015. DNA double-strand break repair inhibitors as cancer therapeutics. Chem. Biol. 22, 17–29. https://doi.org/10.1016/j.chembiol.2014.11.013

Steeg, P.S., 2006. Tumor metastasis: mechanistic insights and clinical challenges. Nat. Med. 12, 895–904. https://doi.org/10.1038/nm1469

Stoeltzing, O., Liu, W., Reinmuth, N., Fan, F., Parikh, A.A., Bucana, C.D., Evans, D.B., Semenza, G.L., Ellis, L.M., 2003. Regulation of Hypoxia-Inducible Factor-1α, Vascular Endothelial Growth Factor, and Angiogenesis by an Insulin-Like Growth Factor-I Receptor Autocrine Loop in Human Pancreatic Cancer. Am. J. Pathol. 163, 1001–1011.

Stolzenberg-Solomon, R.Z., Cross, A.J., Silverman, D.T., Schairer, C., Thompson, F.E., Kipnis, V., Subar, A.F., Hollenbeck, A., Schatzkin, A., Sinha, R., 2007. Meat and meat-mutagen intake and pancreatic cancer risk in the NIH-AARP cohort. Cancer Epidemiol. Biomark. Prev. Publ. Am. Assoc. Cancer Res. Cosponsored Am. Soc. Prev. Oncol. 16, 2664–2675. https://doi.org/10.1158/1055-9965.EPI-07-0378

Stracquadanio, G., Wang, X., Wallace, M.D., Grawenda, A.M., Zhang, P., Hewitt, J., Zeron-Medina, J., Castro-Giner, F., Tomlinson, I.P., Goding, C.R., Cygan, K.J., Fairbrother, W.G., Thomas, L.F., Sætrom, P., Gemignani, F., Landi, S., Schuster-Böckler, B., Bell, D.A., Bond, G.L., 2016. The

importance of p53 pathway genetics in inherited and somatic cancer genomes. Nat. Rev. Cancer 16, 251–265. https://doi.org/10.1038/nrc.2016.15
Suzuki, A., Makinoshima, H., Wakaguri, H., Esumi, H., Sugano, S., Kohno, T., Tsuchihara, K., Suzuki, Y., 2014. Aberrant transcriptional regulations in cancers: genome, transcriptome and epigenome analysis of lung adenocarcinoma cell lines. Nucleic Acids Res. 42, 13557–13572. https://doi.org/10.1093/nar/gku885
Szablewski, L., 2013. Expression of glucose transporters in cancers. Biochim. Biophys. Acta 1835, 164–169. https://doi.org/10.1016/j.bbcan.2012.12.004
Tadini-Buoninsegni, F., Smeazzetto, S., Gualdani, R., Moncelli, M.R., 2018. Drug Interactions With the Ca2+-ATPase From Sarco(Endo)Plasmic Reticulum (SERCA). Front. Mol. Biosci. 5.
Takahashi, K., Taniue, K., Ono, Y., Fujiya, M., Mizukami, Y., Okumura, T., 2021. Long Non-Coding RNAs in Epithelial-Mesenchymal Transition of Pancreatic Cancer. Front. Mol. Biosci. 8.
Tang, Y.-T., Xu, X.-H., Yang, X.-D., Hao, J., Cao, H., Zhu, W., Zhang, S.-Y., Cao, J.-P., 2014. Role of non-coding RNAs in pancreatic cancer: The bane of the microworld. World J. Gastroenterol. WJG 20, 9405–9417. https://doi.org/10.3748/wjg.v20.i28.9405
Tao, J., Yang, G., Zhou, W., Qiu, J., Chen, G., Luo, W., Zhao, F., You, L., Zheng, L., Zhang, T., Zhao, Y., 2021. Targeting hypoxic tumor microenvironment in pancreatic cancer. J. Hematol. Oncol.J Hematol Oncol 14, 14. https://doi.org/10.1186/s13045-020-01030-w
Tascilar, M., Skinner, H.G., Rosty, C., Sohn, T., Wilentz, R.E., Offerhaus, G.J., Adsay, V., Abrams, R.A., Cameron, J.L., Kern, S.E., Yeo, C.J., Hruban, R.H., Goggins, M., 2001. The SMAD4 protein and prognosis of pancreatic ductal adenocarcinoma. Clin. Cancer Res. Off. J. Am. Assoc. Cancer Res. 7, 4115–4121.
Thiery, J.P., 2002. Epithelial-mesenchymal transitions in tumour progression. Nat. Rev. Cancer 2, 442–454. https://doi.org/10.1038/nrc822
Thiery, J.P., Acloque, H., Huang, R.Y.J., Nieto, M.A., 2009. Epithelial-mesenchymal transitions in development and disease. Cell 139, 871–890. https://doi.org/10.1016/j.cell.2009.11.007
Ugel, S., De Sanctis, F., Mandruzzato, S., Bronte, V., 2015. Tumor-induced myeloid deviation: when myeloid-derived suppressor cells meet tumor-associated macrophages. J. Clin. Invest. 125, 3365–3376. https://doi.org/10.1172/JCI80006
Unger, K., Mehta, K.Y., Kaur, P., Wang, Y., Menon, S.S., Jain, S.K., Moonjelly, R.A., Suman, S., Datta, K., Singh, R., Fogel, P., Cheema, A.K., 2018. Metabolomics based predictive classifier for early detection of pancreatic ductal adenocarcinoma. Oncotarget 9, 23078–23090. https://doi.org/10.18632/oncotarget.25212
Valastyan, S., Weinberg, R.A., 2011. Tumor metastasis: molecular insights and evolving paradigms. Cell 147, 275–292. https://doi.org/10.1016/j.cell.2011.09.024
van Dam, H., Castellazzi, M., 2001. Distinct roles of Jun : Fos and Jun : ATF dimers in oncogenesis. Oncogene 20, 2453–2464. https://doi.org/10.1038/sj.onc.1204239
Vidotto, T., Melo, C.M., Castelli, E., Koti, M., dos Reis, R.B., Squire, J.A., 2020. Emerging role of PTEN loss in evasion of the immune response to tumours. Br. J. Cancer 122, 1732–1743. https://doi.org/10.1038/s41416-020-0834-6
Vincent, A., Herman, J., Schulick, R., Hruban, R.H., Goggins, M., 2011. Pancreatic cancer. Lancet Lond. Engl. 378, 607–620. https://doi.org/10.1016/S0140-6736(10)62307-0
Waddell, Nicola, Pajic, M., Patch, A.-M., Chang, D.K., Kassahn, K.S., Bailey, P., Johns, A.L., Miller, D., Nones, K., Quek, K., Quinn, M.C.J., Robertson, A.J., Fadlullah, M.Z.H., Bruxner, T.J.C., Christ, A.N., Harliwong, I., Idrisoglu, S., Manning, S., Nourse, C., Nourbakhsh, E., Wani, S., Wilson, P.J., Markham, E., Cloonan, N., Anderson, M.J., Fink, J.L., Holmes, O., Kazakoff, S.H., Leonard, C., Newell, F., Poudel, B., Song, S., Taylor, D., Waddell, Nick, Wood, S., Xu, Q., Wu, J., Pinese, M., Cowley, M.J., Lee, H.C., Jones, M.D., Nagrial, A.M., Humphris, J., Chantrill, L.A., Chin, V.,

Steinmann, A.M., Mawson, A., Humphrey, E.S., Colvin, E.K., Chou, A., Scarlett, C.J., Pinho, A.V., Giry-Laterriere, M., Rooman, I., Samra, J.S., Kench, J.G., Pettitt, J.A., Merrett, N.D., Toon, C., Epari, K., Nguyen, N.Q., Barbour, A., Zeps, N., Jamieson, N.B., Graham, J.S., Niclou, S.P., Bjerkvig, R., Grützmann, R., Aust, D., Hruban, R.H., Maitra, A., Iacobuzio-Donahue, C.A., Wolfgang, C.L., Morgan, R.A., Lawlor, R.T., Corbo, V., Bassi, C., Falconi, M., Zamboni, G., Tortora, G., Tempero, M.A., Gill, A.J., Eshleman, J.R., Pilarsky, C., Scarpa, A., Musgrove, E.A., Pearson, J.V., Biankin, A.V., Grimmond, S.M., 2015. Whole genomes redefine the mutational landscape of pancreatic cancer. Nature 518, 495–501. https://doi.org/10.1038/nature14169

Wan, P.T.C., Garnett, M.J., Roe, S.M., Lee, S., Niculescu-Duvaz, D., Good, V.M., Jones, C.M., Marshall, C.J., Springer, C.J., Barford, D., Marais, R., Cancer Genome Project, 2004. Mechanism of activation of the RAF-ERK signaling pathway by oncogenic mutations of B-RAF. Cell 116, 855–867. https://doi.org/10.1016/s0092-8674(04)00215-6

Wang, S., Huang, S., Sun, Y.L., 2017. Epithelial-Mesenchymal Transition in Pancreatic Cancer: A Review. BioMed Res. Int. 2017, 2646148. https://doi.org/10.1155/2017/2646148

Wang, Y.-T., Gou, Y.-W., Jin, W.-W., Xiao, M., Fang, H.-Y., 2016. Association between alcohol intake and the risk of pancreatic cancer: a dose-response meta-analysis of cohort studies. BMC Cancer 16, 212. https://doi.org/10.1186/s12885-016-2241-1

Warburg, O., Wind, F., Negelein, E., 1927. THE METABOLISM OF TUMORS IN THE BODY. J. Gen. Physiol. 8, 519–530. https://doi.org/10.1085/jgp.8.6.519

Watanabe, I., Hasebe, T., Sasaki, S., Konishi, M., Inoue, K., Nakagohri, T., Oda, T., Mukai, K., Kinoshita, T., 2003. Advanced pancreatic ductal cancer: fibrotic focus and beta-catenin expression correlate with outcome. Pancreas 26, 326–333. https://doi.org/10.1097/00006676-200305000-00003

Weili, Z., Zhikun, L., Jianmin, W., Qingbao, T., 2019. Knockdown of USP28 enhances the radiosensitivity of esophageal cancer cells via the c-Myc/hypoxia-inducible factor-1 alpha pathway. J. Cell. Biochem. 120, 201–212. https://doi.org/10.1002/jcb.27305

Wellner, U., Schubert, J., Burk, U.C., Schmalhofer, O., Zhu, F., Sonntag, A., Waldvogel, B., Vannier, C., Darling, D., zur Hausen, A., Brunton, V.G., Morton, J., Sansom, O., Schüler, J., Stemmler, M.P., Herzberger, C., Hopt, U., Keck, T., Brabletz, S., Brabletz, T., 2009. The EMT-activator ZEB1 promotes tumorigenicity by repressing stemness-inhibiting microRNAs. Nat. Cell Biol. 11, 1487–1495. https://doi.org/10.1038/ncb1998

Whitcomb, D.C., 2004. Inflammation and Cancer V. Chronic pancreatitis and pancreatic cancer. Am. J. Physiol. Gastrointest. Liver Physiol. 287, G315-319. https://doi.org/10.1152/ajpgi.00115.2004

Witsch, E., Sela, M., Yarden, Y., 2010. Roles for growth factors in cancer progression. Physiol. Bethesda Md 25, 85–101. https://doi.org/10.1152/physiol.00045.2009

Wolpin, B.M., Chan, A.T., Hartge, P., Chanock, S.J., Kraft, P., Hunter, D.J., Giovannucci, E.L., Fuchs, C.S., 2009. ABO blood group and the risk of pancreatic cancer. J. Natl. Cancer Inst. 101, 424–431. https://doi.org/10.1093/jnci/djp020

Wu, X., Hu, W., Lu, L., Zhao, Y., Zhou, Y., Xiao, Z., Zhang, L., Zhang, H., Li, X., Li, W., Wang, S., Cho, C.H., Shen, J., Li, M., 2019. Repurposing vitamin D for treatment of human malignancies via targeting tumor microenvironment. Acta Pharm. Sin. B 9, 203–219. https://doi.org/10.1016/j.apsb.2018.09.002

Wu, Y., Deng, J., Rychahou, P.G., Qiu, S., Evers, B.M., Zhou, B.P., 2009. Stabilization of snail by NF-kappaB is required for inflammation-induced cell migration and invasion. Cancer Cell 15, 416–428. https://doi.org/10.1016/j.ccr.2009.03.016

Xu, W., Wang, Z., Zhang, W., Qian, K., Li, H., Kong, D., Li, Y., Tang, Y., 2015. Mutated K-ras activates CDK8 to stimulate the epithelial-to-mesenchymal transition in pancreatic cancer in part via the Wnt/β-catenin signaling pathway. Cancer Lett. 356, 613–627. https://doi.org/10.1016/j.canlet.2014.10.008

Yamada, S., Fujii, T., Shimoyama, Y., Kanda, M., Nakayama, G., Sugimoto, H., Koike, M., Nomoto, S., Fujiwara, M., Nakao, A., Kodera, Y., 2015. SMAD4 expression predicts local spread and treatment failure in resected pancreatic cancer. Pancreas 44, 660–664. https://doi.org/10.1097/MPA.0000000000000315

Yang, Y., Sun, M., Wang, L., Jiao, B., 2013. HIFs, angiogenesis, and cancer. J. Cell. Biochem. 114, 967–974. https://doi.org/10.1002/jcb.24438

Yu, G., Wang, L.-G., Han, Y., He, Q.-Y., 2012. clusterProfiler: an R Package for Comparing Biological Themes Among Gene Clusters. OMICS J. Integr. Biol. 16, 284–287. https://doi.org/10.1089/omi.2011.0118

Yu, J.H., Kim, H., 2012. Role of Janus Kinase/Signal Transducers and Activators of Transcription in the Pathogenesis of Pancreatitis and Pancreatic Cancer. Gut Liver 6, 417–422. https://doi.org/10.5009/gnl.2012.6.4.417

Yu, X., Zhang, Y., Cavazos, D., Ma, X., Zhao, Z., Du, L., Pertsemlidis, A., 2018. miR-195 targets cyclin D3 and survivin to modulate the tumorigenesis of non-small cell lung cancer. Cell Death Dis. 9, 193. https://doi.org/10.1038/s41419-017-0219-9

Yuen, A., Díaz, B., 2014. The impact of hypoxia in pancreatic cancer invasion and metastasis. Hypoxia 2, 91–106. https://doi.org/10.2147/HP.S52636

Zhalehjoo, N., Shakiba, Y., Panjehpour, M., 2017. Gene expression profiles of CYP24A1 and CYP27B1 in malignant and normal breast tissues. Mol. Med. Rep. 15, 467–473. https://doi.org/10.3892/mmr.2016.5992

Zhang, X., Li, F., Zhou, Y., Mao, F., Lin, Y., Shen, S., Li, Y., Zhang, S., Sun, Q., 2021. Long noncoding RNA AFAP1-AS1 promotes tumor progression and invasion by regulating the miR-2110/Sp1 axis in triple-negative breast cancer. Cell Death Dis. 12, 1–11. https://doi.org/10.1038/s41419-021-03917-z

Zhang, Y., Guo, Q., Zhang, Z., Bai, N., Liu, Z., Xiong, M., Wei, Y., Xiang, R., Tan, X., 2014. VDR Status Arbitrates the Prometastatic Effects of Tumor-Associated Macrophages. Mol. Cancer Res. 12, 1181–1191. https://doi.org/10.1158/1541-7786.MCR-14-0036

Zhang, Y., Lazarus, J., Steele, N.G., Yan, W., Lee, H.-J., Nwosu, Z.C., Halbrook, C.J., Menjivar, R.E., Kemp, S.B., Sirihorachai, V.R., Velez-Delgado, A., Donahue, K., Carpenter, E.S., Brown, K.L., Irizarry-Negron, V., Nevison, A.C., Vinta, A., Anderson, M.A., Crawford, H.C., Lyssiotis, C.A., Frankel, T.L., Bednar, F., Pasca di Magliano, M., 2020. Regulatory T-cell Depletion Alters the Tumor Microenvironment and Accelerates Pancreatic Carcinogenesis. Cancer Discov. 10, 422–439. https://doi.org/10.1158/2159-8290.CD-19-0958

Zhang, Y., Velez-Delgado, A., Mathew, E., Li, D., Mendez, F.M., Flannagan, K., Rhim, A.D., Simeone, D.M., Beatty, G.L., Pasca di Magliano, M., 2017. Myeloid cells are required for PD-1/PD-L1 checkpoint activation and the establishment of an immunosuppressive environment in pancreatic cancer. Gut 66, 124–136. https://doi.org/10.1136/gutjnl-2016-312078

Zhao, H., Zhang, H., Wu, H., Li, H., Liu, L., Guo, J., Li, C., Shih, D.Q., Zhang, X., 2012. Protective role of 1,25(OH)2 vitamin D3 in the mucosal injury and epithelial barrier disruption in DSS-induced acute colitis in mice. BMC Gastroenterol. 12, 57. https://doi.org/10.1186/1471-230X-12-57

Zhou, X., Fang, X., Jiang, Y., Geng, L., Li, X., Li, Y., Lu, K., Li, P., Lv, X., Wang, X., 2017. Klotho, an anti-aging gene, acts as a tumor suppressor and inhibitor of IGF-1R signaling in diffuse large B cell lymphoma. J. Hematol. Oncol.J Hematol Oncol 10, 37. https://doi.org/10.1186/s13045-017-0391-5

Supplementary results

DESeq2 quality control

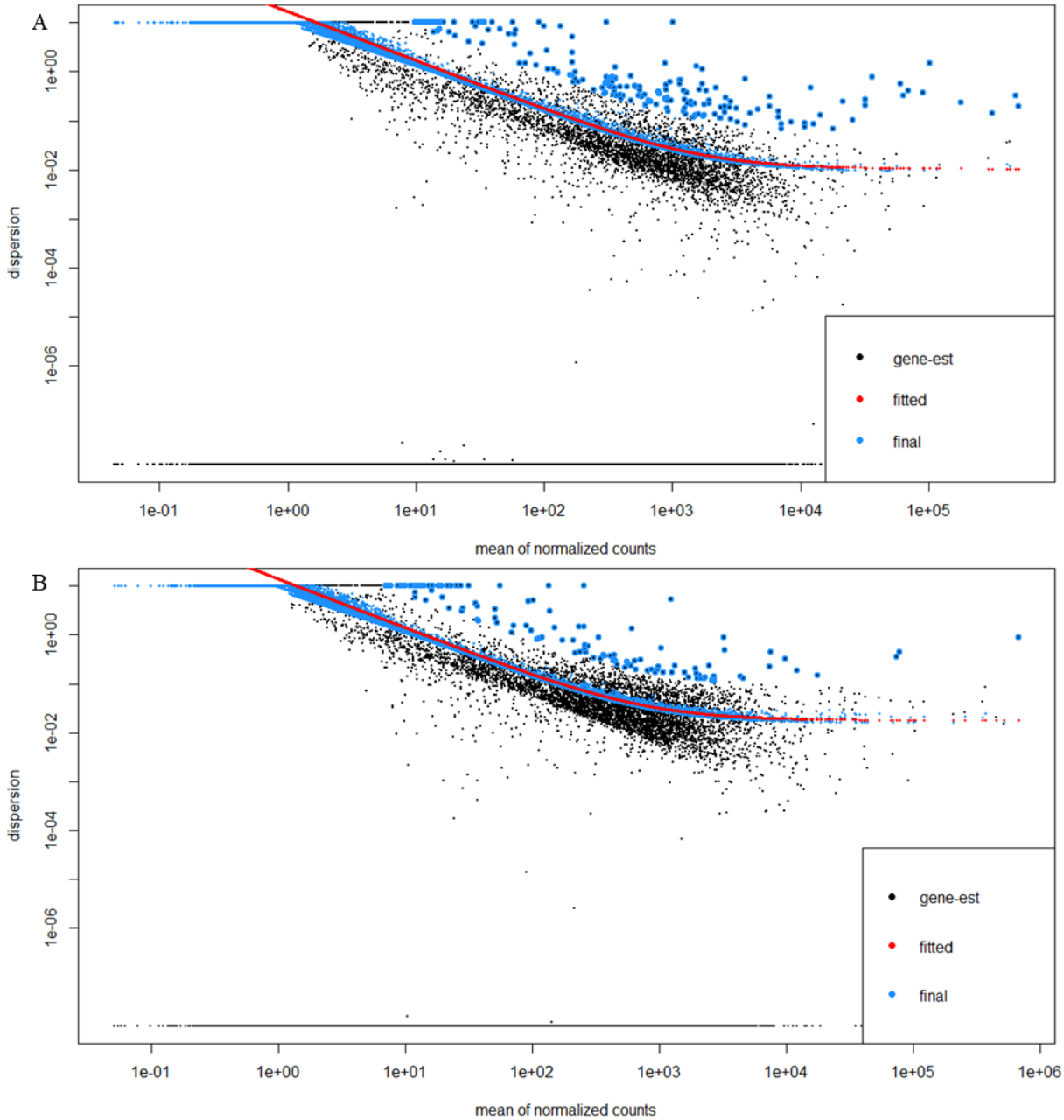

Figure S1 Mean estimate dispersion plots show that the *DESeq2* algorithm had effectively shrunk gene estimates to reduce variance between the samples. The red line in is a curve fitted to the dispersion estimate of each gene and each black dot is a gene with an associated mean expression level and maximum likelihood estimation of the dispersion with the final estimates (blue) shrunk from the gene-wise estimates towards the fitted estimates. A - epithelial; B - quasi-mesenchymal. Black dots - initial maximum likelihood gene-wise dispersion estimates; blue dots – estimates after shrinkage estimation; red line - curve fitted to the dispersion estimate of each gene.

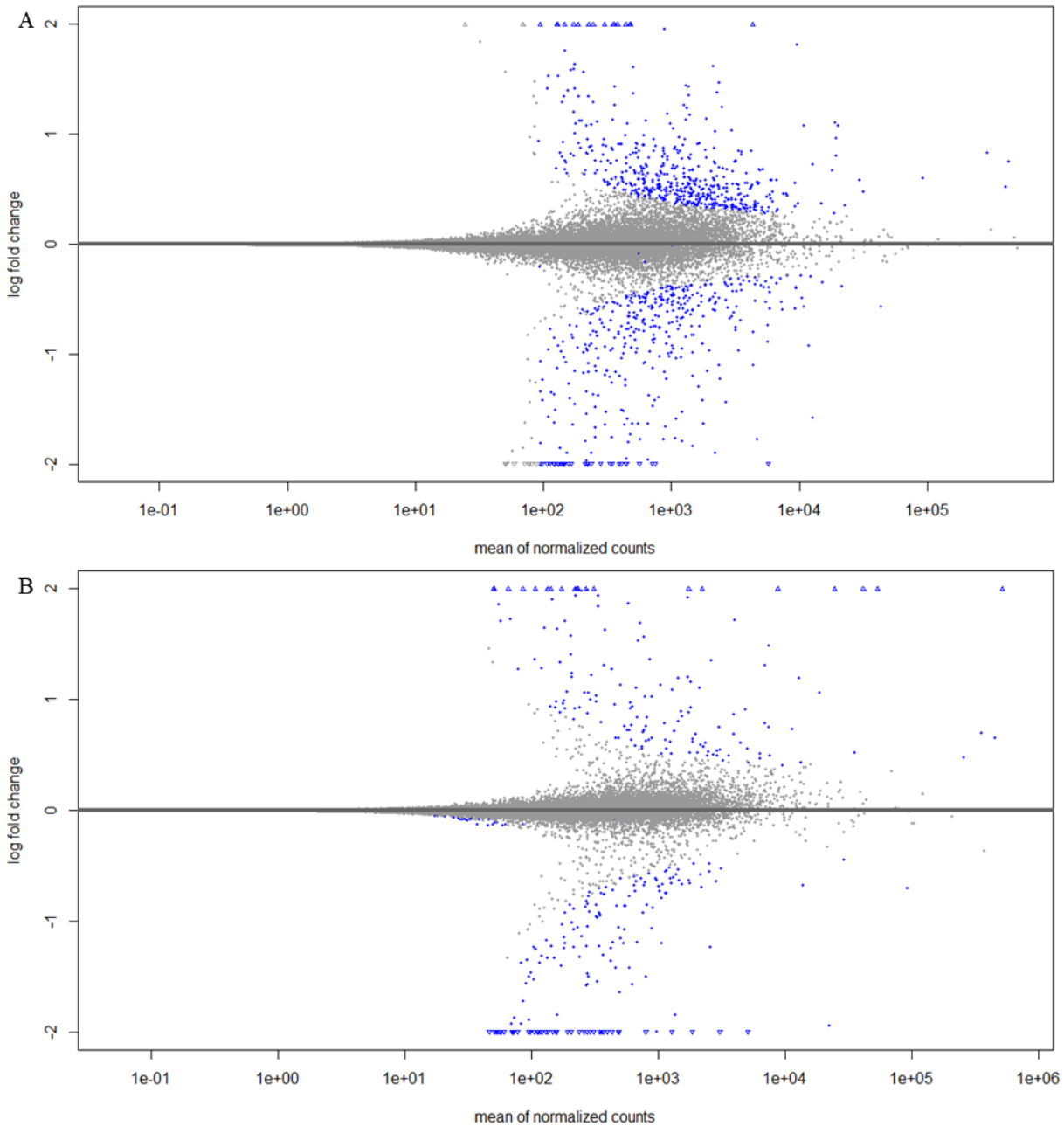

Figure S2 M (log ratio) A (mean average) plots show shrunken log_2-fold changes shrinkage towards zero with a relatively symmetrical distribution of up and down regulated genes. Each grey dot represents a gene and the blue dots represent differentially expressed genes. The MA plots generated from the shrunken log_2 fold changes show shrinkage towards zero with a somewhat symmetrical distribution of up and down regulated genes. A - epithelial; B - quasi-mesenchymal.

Table S1 1,25(OH)$_2$D$_3$ supplementation resulted in differential expression of cancer associated genes in the epithelial pancreatic ductal adenocarcinoma subtype.

Gene ID	Gene name	log2FC	p-value	Cancer hallmark	Tissue type	Role in Cancer
CNOT3	CCR4-NOT transcription complex subunit 3	-0.9221057	1.17E-09	Yes	L	TSG
HIP1	huntingtin interacting protein 1	-1.3027814	1.03E-06	Yes	L, E	oncogene, fusion
LCP1	lymphocyte cytosolic protein 1 (L-plastin)	-0.9236318	2.54E-06	No	L	fusion
MYC	v-myc myelocytomatosis viral oncogene homolog (avian)	-0.75783	0.0000124	Yes	L, E	oncogene, fusion
PPARG	peroxisome proliferative activated receptor, gamma	0.7631229	0.0000168	Yes	E	TSG, fusion
U2AF1	U2 small nuclear RNA auxiliary factor 1	-0.7105637	0.0000348	No	L	oncogene
NIN	ninein (GSK3B interacting protein)	-0.7068634	0.0000427	No	L	fusion
ID3	inhibitor of DNA binding 3, HLH protein	-1.7131597	0.0000433	No	L	TSG
HSP90AB1	heat shock protein 90kDa alpha (cytosolic), class B member 1	-0.4810745	0.000051	No	L	fusion
CALR	calreticulin	-0.4825433	0.0001028	Yes	L	oncogene
CCND2	cyclin D2	-3.1892427	0.0001033	Yes	L	oncogene, fusion
DEK	DEK oncogene (DNA binding)	-0.5310527	0.0001168	No	L	oncogene, fusion
FLNA	filamin A	-0.4985908	0.000117	No	E	
ERBB2	v-erb-b2 erythroblastic	0.6006217	0.0001526	Yes	E	oncogene, fusion

	leukemia viral oncogene homolog 2, neuro/glioblastoma derived oncogene homolog (avian)					
MB21D2	Mab-21 domain containing 2	-1.6269441	0.0001906	No	E	
EGFR	epidermal growth factor receptor (erythroblastic leukemia viral (v-erb-b) oncogene homolog, avian)	-0.5775576	0.0001945	Yes	E, O	oncogene
HNRNPA2B1	heterogeneous nuclear ribonucleoprotein A2/B1	-0.4464838	0.0002208	Yes	E	oncogene, fusion
LASP1	LIM and SH3 protein 1	-0.4554593	0.0003324	No	L	fusion
NFIB	nuclear factor I/B	-0.6652877	0.0003393	No	E	fusion
ASXL1	additional sex combs like 1	-0.7094533	0.0003454	Yes	L	TSG
MUC4	mucin 4, cell surface associated	-1.2826534	0.0003693	No	E	oncogene
LPP	LIM domain containing preferred translocation partner in lipoma	0.523952	0.0004147	No	L, M	oncogene, fusion
PPP2R1A	protein phosphatase 2, regulatory subunit A, alpha	-0.5127116	0.0007417	No	E	TSG
CHD2	chromodomain helicase DNA binding protein 2	0.4510061	0.0007733	No	E, L	TSG
NF2	neurofibromatosis type 2 gene	-0.6842147	0.0009153	Yes	O	TSG

BRCA1	familial breast/ovarian cancer gene 1	-0.6149945	0.0010101	Yes	E	TSG
NBEA	neurobeachin	0.6833071	0.0010742	No	E, L	
GATA2	GATA binding protein 2	-1.0634062	0.0011105	Yes	L	oncogene
B2M	beta-2-microglobulin	0.4261715	0.0011108	Yes	E, L	TSG
BRCA2	familial breast/ovarian cancer gene 2	-0.7574445	0.0011157	Yes	L, E	TSG
MSH2	mutS homolog 2 (E. coli)	-0.6939872	0.0011771	No	E	TSG
FANCA	Fanconi anemia, complementation group A	-0.9989445	0.0013285	No	L	TSG
QKI	QKI, KH domain containing, RNA binding	-0.6369612	0.0016148	Yes	E, O	oncogene, TSG
IDH1	isocitrate dehydrogenase 1 (NADP+), soluble	0.4629087	0.0016831	Yes	O	oncogene
ERCC5	excision repair cross-complementing rodent repair deficiency, complementation group 5 (xeroderma pigmentosum, complementation group G (Cockayne syndrome))	0.5742584	0.0017536	Yes	E	TSG
EPAS1	endothelial PAS domain protein 1	-0.5078237	0.0019078	Yes	E, M	oncogene, TSG
ETV6	ets variant gene 6 (TEL oncogene)	0.5998543	0.0020815	Yes	L, E, M	TSG, fusion

MYH9	myosin, heavy polypeptide 9, non-muscle	-0.3694142	0.002412	No	L	TSG, fusion
TOP1	topoisomerase (DNA) I	-0.4279128	0.0024509	No	L	fusion
CCND1	cyclin D1	-0.3977576	0.0031955	Yes	L, E	oncogene, fusion
FAT4	FAT atypical cadherin 4	-1.2385238	0.0032401	Yes	E, L	TSG
KNSTRN	kinetochore localized astrin/SPAG5 binding protein	-0.6560568	0.0037703	No	E	oncogene
SYK	spleen tyrosine kinase	0.8819448	0.0039608	No	L	oncogene, fusion
BCLAF1	BCL2 associated transcription factor 1	-0.4235576	0.0039982	No	E	
SMC1A	structural maintenance of chromosomes 1A	-0.4130712	0.0040358	No	L	TSG
MAML2	mastermind-like 2 (Drosophila)	-0.6734739	0.0044438	No	E	oncogene, fusion
DCTN1	dynactin 1	-0.4261771	0.0047988	No	M	fusion
HSP90AA1	heat shock protein 90kDa alpha (cytosolic), class A member 1	-0.3258647	0.0048943	No	L	fusion
SFPQ	splicing factor proline/glutamine rich(polypyrimidine tract binding protein associated)	-0.3651201	0.0049017	Yes	E	TSG, fusion
ERBB3	erb-b2 receptor tyrosine kinase 3	0.4729542	0.004908	Yes	E	oncogene
FANCD2	Fanconi anemia, complementation group D2	-0.661882	0.0052626	Yes	L	TSG
CTCF	CCCTC-binding factor	-0.5280407	0.0059954	Yes	E	TSG

MECOM	MDS1 and EVI1 complex locus	0.5644628	0.0060643	No	L	oncogene, fusion
KDM6A	lysine (K)-specific demethylase 6A, UTX	-0.5663144	0.0063978	Yes	E, L	oncogene, TSG
EZH2	enhancer of zeste homolog 2	-0.6657357	0.0064257	Yes	L	oncogene, TSG
RUNX1	runt-related transcription factor 1 (AML1)	-0.5196532	0.0064585	No	L	oncogene, TSG, fusion
RPL5	ribososomal protein L5	0.3379838	0.0068208	No	L	TSG
BCL9	B-cell CLL/lymphoma 9	0.7602328	0.0071584	Yes	L	oncogene, fusion
EXT1	multiple exostoses type 1 gene	-0.5476553	0.0073044	No	M	TSG, fusion
AFF4	AF4/FMR2 family, member 4	0.3908665	0.0074809	Yes	L	oncogene, fusion
ELF3	E74 like ETS transcription factor 3	0.4156479	0.0075853	No	E	TSG
NDRG1	N-myc downstream regulated 1	0.5614468	0.0078003	Yes	E	TSG, fusion
FKBP9	FK506 binding protein 9	0.5863586	0.009528	No		
FEN1	flap structure-specific endonuclease 1	-0.5228825	0.0106204	No	E	TSG
MSH6	mutS homolog 6 (E. coli)	-0.4140228	0.0114814	No	E	TSG
RALGDS	ral guanine nucleotide dissociation stimulator	0.7298836	0.0116077	No	L	fusion
PER1	period homolog 1 (Drosophila)	-0.8386596	0.011784	Yes	L	TSG, fusion
RFWD3	ring finger and WD repeat domain 3	-0.5171033	0.0128181	No	E	TSG

PTPN11	protein tyrosine phosphatase, non-receptor type 11	-0.3664747	0.0129737	Yes	L	oncogene
POLE	polymerase (DNA directed), epsilon, catalytic subunit	-0.4732002	0.0130226	No	E	TSG
NCOR2	nuclear receptor corepressor 2	0.3553683	0.0130828	Yes	E	TSG
JAK1	Janus kinase 1	0.4387993	0.0131053	Yes	L	oncogene, TSG
TNFAIP3	tumor necrosis factor, alpha-induced protein 3	0.6577731	0.013256	Yes	L	TSG
SMAD3	SMAD family member 3	0.3838647	0.0140094	Yes	E	TSG
SET	SET translocation	-0.3146552	0.0144126	No	L	oncogene, fusion
CDK12	cyclin-dependent kinase 12	-0.368618	0.0149042	Yes	E	TSG
FOXP1	forkhead box P1	0.5981526	0.0154602	No	L	oncogene, fusion
AKT3	v-akt murine thymoma viral oncogene homolog 3	-0.5017175	0.0160467	No	O	oncogene
LATS2	large tumor suppressor kinase 2	-0.6290997	0.0165147	Yes	E	TSG
KLF6	Kruppel-like factor 6	-0.4027033	0.0172243	No	E, O	TSG
APOBEC3B	apolipoprotein B mRNA editing enzyme catalytic subunit 3B	-0.757296	0.017916	Yes	E	oncogene, TSG
NPM1	nucleophosmin (nucleolar phosphoprotein B23, numatrin)	-0.2910632	0.0190833	Yes	L	oncogene, fusion
KDM5C	lysine (K)-specific demethylase 5C (JARID1C)	0.4213768	0.0192354	Yes	E	TSG
POLQ	DNA polymerase theta	-0.4945216	0.0192874	No	E	oncogene, TSG

CHD4	chromodomain helicase DNA binding protein 4	-0.3102313	0.0199954	Yes	E	oncogene
KDM5A	lysine (K)-specific demethylase 5A, JARID1A	0.3343963	0.0211498	No	L	oncogene, fusion
KAT7	lysine acetyltransferase 7	-0.5006541	0.022378	No	E	oncogene
ABL2	c-abl oncogene 2, non-receptor tyrosine kinase	-0.5180962	0.0227183	No	L	oncogene, fusion
BUB1B	BUB1 budding uninhibited by benzimidazoles 1 homolog beta (yeast)	-0.5083303	0.0227246	Yes	M	TSG
HLA-A	major histocompatibility complex, class I, A	0.3017203	0.0229665	No	E	fusion
ARHGEF12	RHO guanine nucleotide exchange factor (GEF) 12 (LARG)	0.3161979	0.0233246	No	L	TSG, fusion
EZR	ezrin	-0.2951879	0.023631	Yes	E	fusion
CDX2	caudal type homeo box transcription factor 2	1.1213459	0.0242048	No	L	TSG, fusion
PSIP1	PC4 and SFRS1 interacting protein 1 (LEDGF)	-0.4584894	0.0244565	Yes	L	oncogene, fusion
ERC1	ELKS/RAB6-interacting/CAST family member 1	0.3582399	0.0259337	Yes	E	fusion
ELF4	E74-like factor 4 (ets domain transcription factor)	0.5560146	0.0309779	Yes	L	oncogene, TSG, fusion
EWSR1	Ewing sarcoma breakpoint region 1 (EWS)	-0.3188633	0.0332794	Yes	L, M, E	oncogene, fusion

TPM4	tropomyosin 4	0.3000689	0.0346705	No	L	fusion
PTEN	phosphatase and tensin homolog gene	0.3683249	0.0351437	Yes	L, E, M, O	TSG
ARHGAP35	Rho GTPase activating protein 35	-0.3137374	0.0352556	No	E	TSG
NOTCH2	Notch homolog 2	-0.3112959	0.0365055	Yes	L, E	oncogene, TSG
JUN	jun oncogene	-0.3359185	0.0370083	No	M	oncogene
SMAD4	SMAD family member 4	-0.6291254	0.0373557	Yes	E	TSG
ATR	ATR serine/threonine kinase	0.3757762	0.0374532	Yes	E, L	TSG
ETNK1	ethanolamine kinase 1	0.3968055	0.0376559	Yes	L	TSG
SUZ12	suppressor of zeste 12 homolog (Drosophila)	-0.3524414	0.0398559	Yes	M	oncogene, TSG, fusion
BTG1	B-cell translocation gene 1, anti-proliferative	0.433955	0.0407337	No	L	TSG, fusion
TFPT	TCF3 (E2A) fusion partner (in childhood leukaemia)	-0.5547306	0.0408133	No	L	fusion
STRN	striatin, calmodulin binding protein	-0.3442219	0.0410623	No	E	fusion
STAG2	stromal antigen 2	-0.3646009	0.0410761	Yes	E, L, M, O	TSG
TMSB4X	Thymosin Beta 4 X-Linked	-0.2786239	0.0412439	No	L	oncogene
SRSF2	serine/arginine-rich splicing factor 2	-0.3489456	0.0425966	No	L	oncogene
DROSHA	drosha ribonuclease III	0.3667465	0.0443477	Yes	E, O	TSG
NRAS	neuroblastoma RAS viral (v-ras) oncogene homolog	-0.4489884	0.0454846	Yes	L, E	oncogene

FANCG	Fanconi anemia, complementation group G	-0.7001043	0.0459059	No	L	TSG
MTOR	mechanistic target of rapamycin	-0.3508266	0.0466358	Yes	E	oncogene
KMT2D	lysine (K)-specific methyltransferase 2D	-0.2856964	0.0492025	Yes	O, E	oncogene, TSG

Table S2 1,25(OH)$_2$D$_3$ supplementation resulted in differential expression of cancer associated genes in the quasi-mesenchymal pancreatic ductal adenocarcinoma subtype.

Gene ID	Gene name	log2FC	p-value	Cancer hallmark	Tissue type	Role in Cancer
KRAS	v-Ki-ras2 Kirsten rat sarcoma 2 viral oncogene homolog	-2.3652694	2.31E-19	Yes	L, E, M, O	oncogene
ALDH2	aldehyde dehydrogenase 2 family (mitochondrial)	-1.9519138	4.99E-10	No	M	fusion
PPARG	peroxisome proliferative activated receptor, gamma	-1.5938705	7.49E-10	Yes	E	TSG, fusion
PAX7	paired box gene 7	-6.7299742	2.36E-08	Yes	M	fusion
SLC45A3	solute carrier family 45, member 3	-2.0883556	1.01E-07	Yes	E	fusion
MUC1	mucin 1, transmembrane	-1.5067062	5.79E-07	No	L	fusion
EPAS1	endothelial PAS domain protein 1	1.0689932	2.61E-06	Yes	E, M	oncogene, TSG
MUC16	mucin 16, cell surface associated	-4.0402977	0.0000451	No	E	oncogene
KDM5A	lysine (K)-specific demethylase 5A, JARID1A	-0.9326501	0.0000821	No	L	oncogene, fusion
IDH2	isocitrate dehydrogenase 2	0.9674232	0.0001225	Yes	O	oncogene

	(NADP+), mitochondrial					
CCND2	cyclin D2	-3.6780318	0.0002962	Yes	L	oncogene, fusion
MECOM	MDS1 and EVI1 complex locus	-1.178768	0.0003961	No	L	oncogene, fusion
LCP1	lymphocyte cytosolic protein 1 (L-plastin)	0.9515432	0.000414	No	L	fusion
ID3	inhibitor of DNA binding 3, HLH protein	1.2455948	0.000417	No	L	TSG
KNL1	cancer susceptibility candidate 5	-0.839735	0.000457	Yes	L	TSG, fusion
U2AF1	U2 small nuclear RNA auxiliary factor 1	0.7694612	0.0007832	No	L	oncogene
PIM1	pim-1 oncogene	-1.3459909	0.001485	Yes	L	oncogene, fusion
FGFR2	fibroblast growth factor receptor 2	-1.703081	0.0017087	Yes	E	oncogene, fusion
FOXP1	forkhead box P1	-0.8475863	0.002051	No	L	oncogene, fusion
TOP1	topoisomerase (DNA) I	0.6027933	0.0021715	No	L	fusion
RNF43	ring finger protein 43	-0.9132452	0.0024658	Yes	E	TSG
HLA-A	major histocompatibility complex, class I, A	0.6086984	0.0024861	No	E	fusion
MYC	v-myc myelocytomatosis viral oncogene homolog (avian)	0.6607257	0.0028119	Yes	L, E	oncogene, fusion
ERC1	ELKS/RAB6-interacting/CAST family member 1	-0.7252779	0.0030892	Yes	E	fusion
CD274	CD274 molecule	0.9317039	0.0032668	No	L	TSG, fusion
LASP1	LIM and SH3 protein 1	0.6135108	0.0037028	No	L	fusion
GATA3	GATA binding protein 3	-1.3091804	0.0038608	Yes	E	oncogene, TSG

CD74	CD74 molecule, major histocompatibility complex, class II invariant chain	0.6106687	0.0040006	No	E	oncogene, fusion
HIF1A	hypoxia inducible factor 1 alpha subunit	0.6694128	0.0040679	Yes	E, O	oncogene
IKBKB	inhibitor of kappa light polypeptide gene enhancer in B-cells, kinase beta	-0.778169	0.0041525	Yes	L	oncogene
CNTRL	centriolin	-0.8543903	0.0041915	No	L	fusion
RPL5	ribososomal protein L5	0.57136	0.0045796	No	L	TSG
CARD11	caspase recruitment domain family, member 11	-1.0232856	0.0047077	Yes	L	oncogene
CDK6	cyclin-dependent kinase 6	-0.8510447	0.0054284	Yes	L	oncogene, fusion
CREB3L1	cAMP responsive element binding protein 3-like 1	-1.6349496	0.0055777	Yes	M	TSG, fusion
DROSHA	drosha ribonuclease III	-0.6210918	0.0061456	Yes	E, O	TSG
DNAJB1	DnaJ heat shock protein family (Hsp40) member B1	0.5824773	0.0067859	No	E	fusion
NONO	non-POU domain containing, octamer-binding	0.5735133	0.0068401	Yes	E	fusion
CDH1	cadherin 1, type 1, E-cadherin (epithelial) (ECAD)	0.5527186	0.0079708	Yes	E	TSG
FLNA	filamin A	0.6593261	0.0084027	No	E	
NBEA	neurobeachin	-0.9145895	0.0089382	No	E, L	
ITK	IL2-inducible T-cell kinase	-1.6778836	0.0120104	No	L	fusion
IL7R	interleukin 7 receptor	-1.3635947	0.0124287	Yes	L	oncogene

SIX1	SIX homeobox 1	-1.5164793	0.0127524	Yes	O	oncogene
SIRPA	signal regulatory protein alpha	0.6706984	0.013064	No	E	TSG
TNFAIP3	tumor necrosis factor, alpha-induced protein 3	0.7571868	0.0139828	Yes	L	TSG
MRTFA	megakaryoblastic leukemia (translocation) 1	-0.6887128	0.0144196	No	L	oncogene, TSG, fusion
DAXX	death-domain associated protein	0.5794881	0.0156901	Yes	E	oncogene, TSG
TFPT	TCF3 (E2A) fusion partner (in childhood leukaemia)	0.7441416	0.0156948	No	L	fusion
HIP1	huntingtin interacting protein 1	0.6569998	0.0163529	Yes	L, E	oncogene, fusion
BCLAF1	BCL2 associated transcription factor 1	0.4965726	0.0189241	No	E	
TNC	tenascin C	0.8262729	0.0199871	No	E	oncogene
DCTN1	dynactin 1	0.4779033	0.0205592	No	M	fusion
LRIG3	leucine-rich repeats and immunoglobulin-like domains 3	-0.871392	0.0221659	No	E	TSG, fusion
PRKACA	protein kinase cAMP-activated catalytic subunit alpha	0.546695	0.02241	Yes	E	oncogene
PBX1	pre-B-cell leukemia transcription factor 1	-0.7153282	0.0239365	Yes	L, M	oncogene, fusion
PTPRB	protein tyrosine phosphatase, receptor type, B	-0.8311781	0.0245061	Yes	E	TSG
MAX	Myc associated factor X	0.655028	0.0255086	No	E, O	TSG
ERBB3	erb-b2 receptor tyrosine kinase 3	-0.5548606	0.0259597	Yes	E	oncogene
AKT1	v-akt murine thymoma viral oncogene homolog 1	0.5005172	0.0260065	Yes	E	oncogene

CREBBP	CREB binding protein (CBP)	0.4628644	0.027033	Yes	L	oncogene, TSG, fusion
MAP2K2	mitogen-activated protein kinase kinase 2	0.4862831	0.0272743	Yes	E	oncogene
BAP1	BRCA1 associated protein-1 (ubiquitin carboxy-terminal hydrolase)	0.5227739	0.0273872	Yes	E	TSG
RNF43	ring finger protein 43	-2.7028917	0.029231	Yes	E	TSG
ATR	ATR serine/threonine kinase	-0.5204303	0.0292311	Yes	E, L	TSG
ABL1	v-abl Abelson murine leukemia viral oncogene homolog 1	0.5285526	0.0293856	Yes	L	oncogene, fusion
FAT1	FAT atypical cadherin 1	-0.4687564	0.031833	Yes	E, L	TSG
CNOT3	CCR4-NOT transcription complex subunit 3	0.6149023	0.0318737	Yes	L	TSG
TMSB4X	Thymosin Beta 4 X-Linked	0.4888342	0.0323794	No	L	oncogene
PCBP1	poly(rC) binding protein 1	0.4533654	0.0346104	No	E	
JAK1	Janus kinase 1	0.4682284	0.0348941	Yes	L	oncogene, TSG
CBFB	core-binding factor, beta subunit	0.543961	0.0362478	Yes	L	TSG, fusion
ATIC	5-aminoimidazole-4-carboxamide ribonucleotide formyltransferase/IMP cyclohydrolase	0.4847132	0.0362976	Yes	L	fusion
MLLT10	myeloid/lymphoid or mixed-lineage leukemia; translocated to, 10 (AF10)	-0.557262	0.0369505	Yes	L	oncogene, fusion
NDRG1	N-myc downstream regulated 1	-0.6992908	0.0380779	Yes	E	TSG, fusion

BRD3	bromodomain containing 3	0.5323797	0.0405336	No	E	oncogene, fusion
HMGA1	high mobility group AT-hook 1	0.4046077	0.0412916	No	E, M	oncogene, fusion
MAPK1	mitogen-activated protein kinase 1	0.46243	0.0452414	Yes	E, L	oncogene
HOXA13	homeo box A13	-2.1676509	0.0461799	No	L	oncogene, fusion
XPC	xeroderma pigmentosum, complementation group C	-0.501448	0.0465978	No	E	TSG
CTNNB1	catenin (cadherin-associated protein), beta 1	0.4030137	0.049118	Yes	E, M, O	oncogene, fusion
SDC4	syndecan 4	0.4655132	0.0499887	No	E	fusion

Table S3 Differentially expressed genes common between the epithelial and quasi-mesenchymal pancreatic ductal adenocarcinoma subtypes in response to $1,25(OH)_2D_3$ supplementation. 270 genes were contra-regulated, 42 commonly up-regulated, and 23 commonly down-regulated in the epithelial and quasi-mesenchymal pancreatic ductal adenocarcinoma subtypes in response to $1,25(OH)_2D_3$ supplementation

Gene ID	log2FC-E	log2FC-QM	Trend	Gene ID	log2FC-E	log2FC-QM	Trend
ABHD2	0.842374	-0.54725	Change	*PDPR*	-0.94874	0.624845	Change
ABHD4	0.587361	-0.53171	Change	*PEG10*	-3.78431	0.504142	Change
ADAM23	1.301201	-2.69714	Change	*PER3*	0.522388	-0.83722	Change
ADARB1	-0.91937	0.755634	Change	*PHAX*	-0.69199	0.552981	Change
ADCY5	0.955481	-3.93497	Change	*PHLDB2*	-1.33735	0.935521	Change
ADIPOR2	0.362253	-0.56707	Change	*PIM3*	-0.55601	0.5685	Change
ADRB2	-0.96736	0.837372	Change	*PLAU*	-0.48047	0.800041	Change
AHCY	-0.38495	0.474764	Change	*PLEK2*	0.855786	-0.92242	Change
AIF1L	-0.49524	0.605832	Change	*PLEKHA5*	0.305063	-0.73015	Change
ALCAM	-0.62905	0.662656	Change	*PLK2*	-0.72038	0.606546	Change
ALDH1L2	-1.84099	0.992015	Change	*PMEPA1*	1.044822	-3.28795	Change
ALDH3A1	1.701848	-1.36873	Change	*POF1B*	0.890912	-1.97564	Change
ALOX5	0.894907	-3.22857	Change	*PPARG*	0.763123	-1.59387	Change
AMOTL2	-0.76928	0.518118	Change	*PPL*	-0.49203	0.545257	Change
ANP32E	-0.43032	0.5195	Change	*PPP1R15A*	-0.4699	0.582178	Change
ANXA4	0.933553	-0.53593	Change	*PPP1R1B*	1.270452	-3.98658	Change
AOC1	0.969134	-2.33357	Change	*PPP1R26*	-0.6402	0.543243	Change
ARFGEF3	0.64318	-0.80864	Change	*PPP4R1*	-0.62813	0.596182	Change
ARHGEF17	-0.7168	0.538647	Change	*PPP6R1*	-0.28661	0.480602	Change
ATR	0.375776	-0.52043	Change	*PRKCA*	0.396377	-0.69636	Change
ATXN2L	-0.36508	0.479094	Change	*PRPF31*	-0.82271	0.623094	Change
AXL	-2.49577	0.728353	Change	*PRSS3*	1.215419	-2.70618	Change
BASP1	-1.60413	0.601123	Change	*PRXL2A*	0.538692	-0.8837	Change
BCLAF1	-0.42356	0.496573	Change	*PSD3*	0.517686	-0.59728	Change
BRD7	-0.58491	0.472536	Change	*PSMC5*	-0.40267	0.482656	Change
BTBD11	-1.50136	0.838027	Change	*PSMD7*	-0.37832	0.526782	Change
CABIN1	-0.53028	0.506732	Change	*PSME1*	-0.50188	0.851995	Change
CACNA1C	1.203509	-2.05104	Change	*PTPRM*	-0.4717	0.60615	Change
CALD1	-1.24931	0.869757	Change	*PTX3*	-2.20437	1.697151	Change
CALU	-0.48239	0.537799	Change	*PVR*	-0.67869	0.539677	Change
CAPN5	0.729274	-0.98522	Change	*RAB11FIP3*	-0.94544	0.738335	Change
CARD9	-1.31073	0.947074	Change	*RAB12*	-0.72415	0.646998	Change
CARHSP1	-0.6031	0.636364	Change	*RAB31*	-0.55103	0.824096	Change
CAVIN1	-0.55795	0.737151	Change	*RALBP1*	-1.01223	0.827962	Change
CAVIN2	-2.58526	0.818686	Change	*RANBP17*	0.749629	-1.9518	Change

CCN1	-2.32956	1.059631	Change	*RCC1*	-0.76417	0.630695	Change
CCN2	-2.60859	1.00147	Change	*RGPD6*	0.588456	-0.67617	Change
CCT5	-0.65642	0.477404	Change	*RGS2*	0.852271	-1.19794	Change
CCT7	-0.50546	0.473199	Change	*RIOK3*	0.536164	-0.72398	Change
CDC25B	-0.42421	0.526323	Change	*RIPOR1*	-0.49173	0.594241	Change
CEACAM6	1.431222	-2.08381	Change	*RNF40*	-0.42888	0.482918	Change
CEMIP2	0.328195	-0.77972	Change	*RNU5B-1*	-0.63677	0.614698	Change
CHFR	0.981334	-1.98397	Change	*RNU5E-1*	-1.02204	0.923379	Change
CHMP1B	-0.71098	0.725189	Change	*RPS6KA5*	-1.08544	0.645479	Change
CITED2	-1.23738	0.715704	Change	*RRP1B*	-0.66137	0.559976	Change
CLDN1	-1.0952	0.589929	Change	*RSL1D1*	-0.36473	0.623172	Change
CNN3	-1.33062	0.58511	Change	*RTN4RL1*	-1.99274	0.911483	Change
CNOT3	-0.92211	0.614902	Change	*SAMD4A*	-1.62472	0.620792	Change
COL17A1	0.848154	-2.21836	Change	*SDR16C5*	1.084994	-1.50351	Change
CPSF2	-0.50533	0.551223	Change	*SERP1*	0.353689	-0.59847	Change
CRAT	1.054345	-1.57814	Change	*SGK2*	0.989197	-1.84904	Change
CRIM1	-1.46038	0.481136	Change	*SHMT2*	-0.43365	0.499156	Change
CTNNAL1	-1.12748	0.487857	Change	*SIGMAR1*	-0.47917	0.532603	Change
CTPS1	-0.87991	0.569875	Change	*SIK1B*	-1.12675	0.935079	Change
CYP4F12	0.99127	-2.40415	Change	*SKIL*	0.411988	-0.72847	Change
DBN1	-0.41736	0.576823	Change	*SLC35F6*	-0.50995	0.525148	Change
DCTN1	-0.42618	0.477903	Change	*SLC38A2*	-0.59367	0.521748	Change
DDX21	-0.30371	0.417432	Change	*SLC39A4*	0.980715	-1.27139	Change
DEF8	-0.89616	0.724061	Change	*SLC7A5*	-0.71345	0.815322	Change
DGKA	0.757183	-0.85703	Change	*SOCS3*	-0.99334	0.827112	Change
DHRS9	1.113796	-1.84162	Change	*SOX7*	-1.23553	0.865202	Change
DHX38	-0.57197	0.544464	Change	*SPATA13*	0.587852	-0.72066	Change
DLC1	-1.98937	0.789855	Change	*SREBF1*	0.674278	-0.63988	Change
DNAJA1	-0.59266	0.605377	Change	*SREBF2*	0.590439	-0.45903	Change
DROSHA	0.366746	-0.62109	Change	*STING1*	-1.04393	0.629888	Change
DUSP5	-0.74868	0.695221	Change	*STK17B*	-1.10101	0.527836	Change
EEF1A2	-0.63049	0.741248	Change	*STMN1*	-0.45887	0.587225	Change
EIF4A3	-0.45561	0.545128	Change	*STMN3*	-1.42823	1.01394	Change
EIF4G1	-0.42416	0.398503	Change	*SYT7*	-1.44063	0.802867	Change
ELFN2	0.856857	-1.79495	Change	*TACSTD2*	-0.51217	0.778329	Change
ENG	-1.16101	0.69199	Change	*TBC1D4*	-0.74863	1.018989	Change
EPAS1	-0.50782	1.068993	Change	*TBK1*	0.746061	-0.69597	Change
EPHB2	-0.69655	0.92252	Change	*TFDP2*	0.489414	-0.58529	Change
EPHB3	-1.09804	0.636235	Change	*TFPT*	-0.55473	0.744142	Change
EPN1	-0.66942	0.694627	Change	*TGFB2*	-1.72371	0.920308	Change
EPS8	0.297764	-0.84388	Change	*TLN1*	-0.50338	0.397739	Change

ERBB3	0.472954	-0.55486	Change	*TMBIM1*	0.707518	-0.8088	Change
ERC1	0.35824	-0.72528	Change	*TMSB4X*	-0.27862	0.488834	Change
ETF1	-0.33929	0.498304	Change	*TNIK*	0.527224	-1.23227	Change
FARP1	0.521006	-0.54519	Change	*TNNT1*	-0.98912	0.649821	Change
FBLIM1	0.838637	-0.73017	Change	*TOP1*	-0.42791	0.602793	Change
FBP1	1.064264	-6.00225	Change	*TOPORS*	-0.77576	0.567227	Change
FERMT2	-1.42713	0.607277	Change	*TRIM28*	-0.61938	0.704205	Change
FHL1	-1.85358	0.863275	Change	*TRIM29*	0.555155	-3.16312	Change
FLNA	-0.49859	0.659326	Change	*TUBB*	-0.63705	0.408607	Change
FNTA	0.6015	-0.72589	Change	*TUBB3*	-0.82072	0.680008	Change
FOSB	-1.60621	0.781005	Change	*TUBG1*	-0.65662	0.577659	Change
FOXP1	0.598153	-0.84759	Change	*TUFM*	-0.50474	0.538614	Change
FRMD3	-2.15901	0.836947	Change	*TWSG1*	-1.08365	0.582178	Change
G3BP1	-0.55446	0.597064	Change	*TYMS*	-1.78239	0.60806	Change
GAPDH	-0.27569	0.513493	Change	*U2AF1*	-0.71056	0.769461	Change
GBP1	-0.72147	0.746947	Change	*UBE2G2*	-0.68864	0.516692	Change
GPX2	1.048657	-2.57067	Change	*UBE2S*	-1.33234	0.67559	Change
GSN	0.796499	-0.69751	Change	*UGT1A1*	0.995754	-3.15338	Change
GSTM3	0.986975	-1.89557	Change	*USP14*	-1.01147	0.6946	Change
HBEGF	-0.76046	0.654461	Change	*VAPA*	-0.52009	0.652016	Change
HCLS1	-1.01306	0.745341	Change	*VASN*	-0.95881	0.799553	Change
HEG1	-2.26902	0.720542	Change	*WWC1*	-0.42187	0.516405	Change
HGSNAT	0.772849	-1.13368	Change	*ZBTB7C*	1.35455	-3.01015	Change
HIP1	-1.30278	0.657	Change	*ZDHHC2*	0.917964	-1.18666	Change
HNRNPA0	-0.62066	0.534649	Change	*ZDHHC20*	0.63385	-1.07006	Change
HPGD	0.741294	-4.15256	Change	*ZNF598*	-0.55696	0.62829	Change
HRNR	-0.90942	0.779286	Change	*ABCG2*	-1.02728	-1.02342	DOWN
HSPA4	-0.5414	0.567478	Change	*CCND2*	-3.18924	-3.67803	DOWN
HSPBP1	-0.57104	0.760532	Change	*DDIAS*	-0.92387	-0.875	DOWN
ICAM1	-0.76387	0.957214	Change	*DST*	-0.32284	-0.51893	DOWN
ID1	-0.95399	0.512991	Change	*ECT2*	-0.31851	-0.41726	DOWN
ID3	-1.71316	1.245595	Change	*EFEMP1*	-1.63269	-1.83652	DOWN
IFIT2	-0.53893	0.446234	Change	*FGF19*	-5.21437	-4.85892	DOWN
IL1B	-1.66843	0.95319	Change	*FOS*	-0.43094	-0.6191	DOWN
IMPA2	-1.1492	0.734956	Change	*IGFBP5*	-1.52904	-1.86696	DOWN
IMPDH2	-0.38705	0.458949	Change	*ITGBL1*	-0.80505	-1.83075	DOWN
INSR	0.677305	-2.15232	Change	*KRT17*	-1.64138	-5.07769	DOWN
IRF1	-0.68509	0.852348	Change	*MSLN*	-4.29791	-2.9286	DOWN
ISG15	-0.52322	0.560837	Change	*NSG1*	-1.55008	-1.35654	DOWN
ITGB4	0.52232	-0.63717	Change	*OLFM4*	-4.39705	-8.48667	DOWN
ITGB5	0.558858	-0.58066	Change	*ONECUT2*	-1.77325	-2.17733	DOWN

ITGB6	0.906219	-1.72702	Change	*PLAC8*	-1.56164	-0.72262	DOWN
KCNQ1	1.02586	-1.12581	Change	*RSAD2*	-0.84622	-0.85131	DOWN
KDM5A	0.334396	-0.93265	Change	*SRGAP1*	-0.49017	-1.52476	DOWN
KIF13B	0.443381	-1.2219	Change	*TFF2*	-1.76188	-6.52885	DOWN
KIRREL1	-1.33174	0.606208	Change	*TFPI2*	-0.80026	-8.04685	DOWN
KLF10	-0.96891	0.531589	Change	*TIMP3*	-2.35903	-0.78364	DOWN
KLHL5	-0.80681	0.522553	Change	*TM4SF4*	-2.63433	-5.49494	DOWN
LASP1	-0.45546	0.613511	Change	*TMEM47*	-0.92537	-1.89686	DOWN
LCP1	-0.92363	0.951543	Change	*ATP5F1D*	0.614354	0.632257	UP
LIMK1	-0.55203	0.525358	Change	*CAPNS1*	1.017129	0.977146	UP
LPIN2	-0.67927	0.857622	Change	*CLMN*	0.858267	0.693705	UP
LRP3	1.27656	-2.69695	Change	*CSTB*	0.389134	0.551019	UP
LXN	1.530345	-0.96611	Change	*CXCL8*	1.105356	1.23942	UP
LYZ	0.897947	-1.71184	Change	*DCXR*	0.806425	0.651094	UP
MAN1A1	-0.70056	0.475037	Change	*DHCR24*	0.703595	0.462835	UP
MAP1LC3B	-0.47872	0.643824	Change	*EIF5AL1*	1.643024	1.168101	UP
MATR3	-0.33616	0.719781	Change	*ENY2*	0.580738	0.508893	UP
MCFD2	-0.66126	0.602492	Change	*FTH1*	0.31211	0.716595	UP
MECOM	0.564463	-1.17877	Change	*FUCA1*	0.609181	0.579966	UP
MMRN2	-0.80374	0.642512	Change	*GPX1*	0.522919	0.740951	UP
MT1E	-1.91172	0.889779	Change	*HLA-A*	0.30172	0.608698	UP
MT2A	-1.74698	1.077865	Change	*HLA-B*	0.415659	0.612749	UP
MTHFD1	-0.73138	0.495136	Change	*IL4R*	0.558872	0.660539	UP
MTHFD2	-0.52636	0.604465	Change	*JAK1*	0.438799	0.468228	UP
MTSS2	-0.87022	0.621805	Change	*MCTS1*	1.058901	0.678443	UP
MUC20	1.314126	-0.74876	Change	*NAA38*	0.667108	0.744964	UP
MYADM	-0.67889	0.503462	Change	*NIBAN1*	0.887431	0.610536	UP
MYC	-0.75783	0.660726	Change	*PDE2A*	1.311505	0.804277	UP
MYH14	0.777807	-2.89566	Change	*RAB8A*	0.501589	0.587152	UP
MYL12A	-0.60744	0.753233	Change	*RNU4-1*	0.816486	0.524185	UP
MYL12B	-0.53671	0.73919	Change	*RNU4-2*	0.8737	0.689975	UP
MYO10	-0.40211	0.49135	Change	*RPL32*	0.472305	0.459959	UP
MYO6	0.314887	-0.70481	Change	*RPL38*	0.350116	0.511862	UP
NABP1	-0.78807	0.494544	Change	*RPL5*	0.337984	0.57136	UP
NAPG	-0.45764	0.66259	Change	*RPS27*	1.036029	0.485642	UP
NCL	-0.56699	0.397212	Change	*RPS29*	1.513876	1.030792	UP
NCOA7	-0.70973	0.540215	Change	*SERF2*	0.568995	0.738774	UP
NDRG1	0.561447	-0.69929	Change	*SERPINB1*	1.210238	0.707255	UP
NFATC3	-0.4885	0.500514	Change	*SHISA5*	0.726078	0.560441	UP
NNT	0.45318	-0.6862	Change	*SLC22A18*	0.932057	0.641707	UP
NOP56	-0.33811	0.518614	Change	*SLPI*	1.44782	0.837283	UP

NRARP	-0.91647	0.89752	Change	*SNRPD2*	0.430322	0.540886	UP
NRCAM	1.275922	-2.32585	Change	*SOD2*	0.410162	0.754375	UP
NRP2	0.940814	-1.48924	Change	*SRP14*	0.738525	0.586877	UP
NUAK2	-1.09614	0.941256	Change	*STK24*	0.535436	0.417022	UP
NUDT21	-0.41582	0.523211	Change	*TIMP1*	0.723143	0.677572	UP
NXN	-1.5357	0.634681	Change	*TMC6*	0.34001	0.511445	UP
P4HB	-0.34122	0.403277	Change	*TNFAIP3*	0.657773	0.757187	UP
PARD3	-0.37518	0.581729	Change	*UBB*	0.280384	0.446186	UP
PDAP1	-0.35975	0.521113	Change	*UBC*	0.294388	0.430941	UP
PDP1	-0.50853	0.593567	Change				

Table S4 Complete list of genes differentially expressed in response to 1,25(OH)$_2$D$_3$ supplementation in the epithelial pancreatic ductal adenocarcinoma subtype.

Gene ID	log2FC	p-value	Gene ID	log2FC	p-value	Gene ID	log2FC	p-value
THBS1	-2.4711	1.03E-51	*KIF20B*	-0.5014	0.006896	*TMEM123*	0.45666	0.001399
MTND1P23	4.17712	1.40E-39	*MAP4*	-0.4285	0.006916	*BRD7*	-0.5849	0.001421
CAV1	-3.6249	1.02E-34	*CRNDE*	1.48105	0.006954	*ABHD12B*	-1.7576	0.001444
CCN1	-2.3296	2.74E-34	*ZNF598*	-0.557	0.006964	*COL4A2*	-0.9586	0.001455
F3	-1.9519	1.82E-26	*STMN1*	-0.4589	0.006972	*DCXR*	0.80643	0.001466
BHLHE41	1.68915	4.27E-26	*FOS*	-0.4309	0.007012	*PUM3*	-0.5716	0.001505
TYMS	-1.7824	1.01E-24	*EPHB3*	-1.098	0.007029	*ELOVL6*	-0.6935	0.001508
NDC80	-1.7825	1.71E-23	*POF1B*	0.89091	0.00704	*HSPG2*	-0.4567	0.001519
CEACAM6	1.43122	6.67E-23	*GSK3B*	0.46199	0.007044	*TK1*	-0.7334	0.001523
H19	-2.292	1.02E-22	*KLHL9*	-1.9879	0.00705	*SHISA5*	0.72608	0.001524
ESRG	-1.4973	2.63E-22	*SNORA73A*	0.73111	0.007068	*NEDD9*	-0.9067	0.00153
AXL	-2.4958	1.59E-21	*BTBD11*	-1.5014	0.007079	*PADI1*	0.8647	0.001552
TOP2A	-1.205	6.16E-21	*AFAP1-AS1*	-0.5875	0.007105	*ADAM23*	1.3012	0.001556
CRIM1	-1.4604	1.59E-18	*JUP*	0.40066	0.007106	*CHP1*	0.55349	0.00156
CCN2	-2.6086	4.95E-18	*TRAM2*	-0.7502	0.007139	*EREG*	-0.5288	0.00156
TIMP3	-2.359	1.00E-17	*BCL9*	0.76023	0.007158	*SPINT2*	0.43076	0.001566
MT2A	-1.747	1.26E-17	*ANKH*	0.80209	0.007169	*DAZAP2*	0.57858	0.001574

LINC00324	-2.0478	2.48E-17	*SNORD26*	2.2092	0.007184	*FADS1*	-0.5028	0.001593
TGFBI	-2.1204	5.99E-17	*TUBB3*	-0.8207	0.007187	*YPEL2*	1.13141	0.001611
CLU	1.5418	8.00E-16	*GOLPH3L*	0.71364	0.007187	*QKI*	-0.637	0.001615
IGFBP3	1.25165	5.24E-15	*LYAR*	-0.7033	0.007194	*PPP1R15A*	-0.4699	0.001634
SLPI	1.44782	7.26E-15	*PSD3*	0.51769	0.007201	*KRT16*	1.53601	0.001647
RPS29	1.51388	1.15E-14	*EXT1*	-0.5477	0.007304	*BSCL2*	1.2269	0.001652
LINC02582	-1.6718	1.26E-14	*SHCBP1*	-0.8791	0.007315	*HNRNPU*	-0.3973	0.001678
LOC105369760	2.30091	1.67E-14	*MTDH*	0.39178	0.007318	*IDH1*	0.46291	0.001683
RALBP1	-1.0122	1.86E-14	*CENPBD1P1*	0.70801	0.007352	*DNA2*	-1.2262	0.001684
LRRK1	-1.0345	2.78E-14	*CLIC5*	-0.9212	0.007458	*ZC3H8*	0.88476	0.001694
TGM2	-1.1561	2.79E-14	*AFF4*	0.39087	0.007481	*SUPT16H*	-0.4366	0.001697
UBE2S	-1.3323	3.03E-14	*SNORD28*	1.7321	0.007559	*ADGRG6*	-0.5666	0.001716
COTL1	-1.0214	9.90E-14	*ELF3*	0.41565	0.007585	*ERCC5*	0.57426	0.001754
TNFSF18	-4.9911	2.27E-13	*NOB1*	-0.5396	0.007591	*CEP78*	-0.7259	0.001754
CALB1	-1.923	5.08E-13	*LRP10*	0.40477	0.00764	*NBL1*	0.72705	0.001758
CAVIN2	-2.5853	5.65E-13	*CENPK*	-0.7872	0.007681	*AGPAT2*	0.75485	0.00176
MTCL1	-1.4313	7.02E-13	*FBP1*	1.06426	0.00769	*HES1*	-0.5222	0.001774
RPS27	1.03603	9.43E-13	*ALS2CL*	0.63353	0.007717	*EXO1*	-1.0484	0.001776
PCNT	-1.1305	9.56E-13	*N4BP3*	1.09918	0.007725	*GLB1L2*	0.85494	0.001795
MUC20	1.31413	1.91E-12	*CDC23*	-0.704	0.007784	*ABCC1*	-0.5748	0.001804
FOSB	-1.6062	2.66E-12	*GPR158*	-1.652	0.007794	*MARVELD1*	-1.0505	0.001844
ZNF114	-2.3383	2.94E-12	*TNFRSF6B*	-1.9901	0.007799	*PRSS23*	-0.9139	0.001874
LMNB1	-1.1919	3.20E-12	*NDRG1*	0.56145	0.0078	*PCNA*	-0.5894	0.001888
CAPNS1	1.01713	5.61E-12	*ZNF600*	1.14978	0.007805	*CSE1L*	-0.5004	0.001888
CLSPN	-1.299	6.04E-12	*ITM2C*	0.51885	0.007827	*LINC02331*	-2.3716	0.001896
PLAC8	-1.5616	8.29E-12	*MAML3*	0.9147	0.007853	*EPAS1*	-0.5078	0.001908
USP14	-1.0115	9.18E-12	*EPHB6*	-1.0648	0.007905	*TPM2*	-0.8583	0.001913

PSAP	0.8848	9.85E-12	*F2RL1*	-0.6147	0.00793	*TNIK*	0.52722	0.00192
MKI67	-0.8593	1.34E-11	*FTSJ3*	-0.4567	0.007985	*UBE2E3*	0.74453	0.001931
RPL37P6	4.52981	1.62E-11	*ALDH1B1*	-0.6287	0.007991	*CIP2A*	-0.691	0.001932
F2R	-1.9012	1.88E-11	*DAAM1*	-0.5932	0.007997	*ARFGEF3*	0.64318	0.001964
SNORD13	2.592	2.33E-11	*ZDHHC2*	0.91796	0.008112	*NDUFA12*	0.72904	0.001975
TPX2	-1.0504	3.32E-11	*STXBP6*	-1.1457	0.008116	*ZNF714*	-1.0165	0.001979
RHOBTB3	-1.1471	3.33E-11	*JADE1*	-0.7215	0.008148	*VIM*	-1.5088	0.001991
S100A11	1.02433	3.36E-11	*UHRF1BP1*	-0.5364	0.008159	*TBC1D4*	-0.7486	0.001998
SNHG1	1.24943	8.00E-11	*ZBTB7C*	1.35455	0.008184	*RPL35A*	0.49758	0.002001
ERRFI1	-1.1545	8.20E-11	*RNF40*	-0.4289	0.008204	*CXCL8*	1.10536	0.002006
ANKRD1	-3.7991	9.56E-11	*CEP250*	-0.491	0.008222	*NUP205*	-0.5549	0.00203
FAM102A	1.19296	1.25E-10	*CCP110*	-0.6676	0.008267	*COX7A2*	0.72615	0.002042
MIR663AHG	0.74077	1.33E-10	*DMTN*	1.07901	0.008279	*RAB31*	-0.551	0.002058
SULT1C2	1.60952	1.49E-10	*CASP4*	0.50417	0.008295	*ETV6*	0.59985	0.002081
ENC1	-1.145	2.31E-10	*MON2*	0.48804	0.008308	*HSD17B4*	0.57832	0.002087
CYP24A1	3.25109	2.38E-10	*ARHGEF17*	-0.7168	0.00839	*STMN3*	-1.4282	0.002119
KLF13	1.27325	2.62E-10	*MTR*	-0.5516	0.008468	*MAD2L1*	-0.7859	0.002127
RPS25	0.95794	2.81E-10	*LYZ*	0.89795	0.008562	*NOLC1*	-0.4526	0.00213
NET1	0.99226	3.35E-10	*ADGRG1*	0.50126	0.008583	*KIF18B*	-0.7481	0.002132
PPP1R1B	1.27045	3.61E-10	*KIAA0586*	-0.677	0.008638	*SDCBP2*	1.05977	0.002152
HMMR	-1.4083	6.02E-10	*ASF1B*	-0.963	0.008667	*ITGBL1*	-0.8051	0.002157
OGFRL1	-1.2783	6.87E-10	*RNU5A-8P*	-1.3518	0.008725	*ALOX5*	0.89491	0.002186
CYP3A5	1.01641	7.28E-10	*SHKBP1*	0.59117	0.008727	*DHX38*	-0.572	0.002188
S100A6	0.79087	1.01E-09	*CDC25C*	-1.0994	0.008748	*HRNR*	-0.9094	0.002202
CNOT3	-0.9221	1.17E-09	*AURKB*	-0.743	0.008765	*ICAM1*	-0.7639	0.002202
COL12A1	-2.6168	1.22E-09	*PITRM1*	0.57562	0.008818	*CIB1*	0.7707	0.002215
AGR2	1.31677	1.39E-09	*RNA5SP298*	-1.0718	0.008845	*CACNG4*	-1.7531	0.002232

UHRF1	-1.2588	1.63E-09	*RIF1*	-0.3868	0.008884	*CBX1*	-0.5411	0.002264
CNN3	-1.3306	1.76E-09	*DSG2*	0.44434	0.008887	*UTP20*	-0.5615	0.002265
SERPINB1	1.21024	2.15E-09	*SLC25A6*	0.498	0.008892	*FBXL16*	-1.6104	0.002268
UGT1A10	1.07869	2.69E-09	*PSEN1*	0.43005	0.008892	*ZWINT*	-0.7214	0.002282
SNORD10	1.02156	2.79E-09	*XPOT*	0.37876	0.008894	*HCFC1*	-0.473	0.002282
PMEPA1	1.04482	3.57E-09	*SNORD1C*	1.83131	0.008921	*SATB1*	0.87383	0.002296
LRRC61	-1.7144	3.80E-09	*P4HB*	-0.3412	0.008937	*IRF1*	-0.6851	0.002304
CTNNAL1	-1.1275	4.03E-09	*CDC42EP3*	-0.5482	0.008951	*SNORD11*	2.23874	0.002339
SERPINE1	-2.5124	4.35E-09	*HNRNPAB*	-0.4047	0.008964	*VASN*	-0.9588	0.002341
HMGB2	-0.9651	4.73E-09	*TTF2*	-0.6596	0.009048	*SNORA31B*	1.18978	0.002344
ARHGEF28	1.04378	5.09E-09	*XRCC2*	-0.8229	0.009048	*ATP5MC2*	0.7358	0.002348
LXN	1.53035	5.87E-09	*BEX3*	-0.6255	0.009138	*TSEN34*	-0.5996	0.002357
FRAS1	-1.3446	6.18E-09	*CCDC144A*	0.57885	0.009143	*SERPINH1*	-0.5745	0.002373
THOC1	-1.0583	7.30E-09	*HNRNPDL*	-0.3923	0.009151	*RPL39*	0.49011	0.002396
ZBED9	-1.5579	8.23E-09	*ZNF808*	1.01918	0.009169	*MYH9*	-0.3694	0.002412
KIF20A	-1.3024	9.41E-09	*SRSF6*	-0.4005	0.009194	*EPB41L4A*	0.87911	0.002429
TUBA1B	-0.7096	1.61E-08	*TPI1*	-0.3643	0.009221	*TOP1*	-0.4279	0.002451
CPD	0.80667	1.69E-08	*CCAR1*	-0.4186	0.009237	*TMEM59*	0.54304	0.002484
TGFB2	-1.7237	1.71E-08	*DSN1*	-0.8797	0.009278	*ONECUT2*	-1.7733	0.002488
CDC6	-1.0374	2.03E-08	*SLC5A3*	-0.4726	0.009394	*SAT2*	1.07757	0.002488
PHLDB2	-1.3374	2.25E-08	*IGFL2-AS1*	-0.6978	0.009402	*NPHP3-ACAD11*	-3.6418	0.002499
RRM2	-0.8955	2.50E-08	*H2AZ1*	-0.4736	0.009406	*KDM1A*	-0.4634	0.002503
P3H2	-1.7956	2.52E-08	*GSE1*	-0.4722	0.009496	*DAD1*	0.54242	0.002506
CALD1	-1.2493	2.57E-08	*FKBP9*	0.58636	0.009528	*GIT1*	0.61133	0.002529
MGC32805	-2.7202	2.64E-08	*CREG2*	0.82002	0.009558	*CFAP20*	-0.9657	0.002533
SELENOW	1.038	2.73E-08	*ERGIC1*	0.44171	0.009562	*INPP4B*	0.51583	0.002537
RNU4-2	0.8737	2.76E-08	*HSPBP1*	-0.571	0.00961	*KIF24*	-1.0144	0.002565

SNORD8	1.26756	2.84E-08	*PLAU*	-0.4805	0.009642	*SKAP2*	0.58003	0.002567
AJUBA	-1.5745	2.86E-08	*LTBP1*	-0.9068	0.009706	*KPNB1*	-0.3936	0.002568
MX1	-0.9952	2.90E-08	*SPECC1L*	-0.5068	0.009734	*LARS1*	-0.4767	0.00257
DLC1	-1.9894	3.43E-08	*HASPIN*	-0.9867	0.009773	*PROM2*	0.60406	0.00259
AKR1C2	1.07951	4.19E-08	*BARX2*	-1.1509	0.00978	*EXOSC3*	-0.747	0.002613
ALDH1L2	-1.841	4.60E-08	*NKAPD1*	0.63165	0.009781	*DYNC1LI2*	-0.486	0.00263
RPL37	0.78045	4.64E-08	*SLC39A4*	0.98072	0.009927	*IL1B*	-1.6684	0.002645
PRKDC	-0.7093	5.56E-08	*KHSRP*	-0.4043	0.009948	*SASH1*	-0.7653	0.002651
RAB11FIP1	0.89121	5.68E-08	*PPAT*	-0.7083	0.009983	*SNX18*	-0.898	0.002659
AHNAK2	0.99312	6.79E-08	*H1-2*	-0.3858	0.010012	*PLEKHB1*	1.07123	0.00267
RPLP1	0.68372	7.59E-08	*ZNF580*	-0.9496	0.010015	*SESTD1*	0.72952	0.002683
SNORD97	0.97879	8.26E-08	*TOMM7*	0.65695	0.010024	*DHRS9*	1.1138	0.002709
RPL41	0.74161	8.57E-08	*PAK1*	0.55603	0.010028	*CYP1B1*	-0.9081	0.002744
IFI44L	-1.2989	8.83E-08	*ULK2*	1.12774	0.010039	*CAD*	-0.5891	0.002746
CENPF	-0.7288	8.88E-08	*MRPL52*	0.67859	0.010042	*NEDD4L*	-0.5751	0.002753
KIF23	-1.0204	1.11E-07	*GCSH*	-0.6754	0.01008	*TTK*	-0.7564	0.002766
EMP1	-0.7904	1.20E-07	*NOL11*	-0.4481	0.010081	*DGKA*	0.75718	0.002806
TSKU	1.11704	1.25E-07	*DNAJB11*	-0.4001	0.010094	*CDCA5*	-0.7208	0.002822
SH3PXD2A	-1.7889	1.31E-07	*PRXL2A*	0.53869	0.010182	*ANTXR1*	-0.7592	0.002827
MYBL1	-1.895	1.75E-07	*KDM5B*	0.43415	0.010239	*PLEK2*	0.85579	0.002858
CITED2	-1.2374	1.81E-07	*TEAD1*	-0.4504	0.010299	*ITM2B*	0.52963	0.002874
HEG1	-2.269	1.96E-07	*KLHL24*	0.59188	0.010347	*PRR14L*	-0.5316	0.002875
CENPN	-1.5295	2.13E-07	*SCARNA10*	0.46185	0.010369	*FAM171A1*	-1.2102	0.002908
HHLA1	-1.2202	2.16E-07	*CDC7*	-1.02	0.010373	*LOC101927556*	-2.4482	0.00292
ABHD2	0.84237	2.17E-07	*PHLDA2*	0.53435	0.010378	*SCARNA7*	0.64576	0.002938
TWSG1	-1.0837	2.52E-07	*RPL4*	0.31761	0.010431	*EMP3*	-1.4962	0.002943
SOGA1	-1.379	2.74E-07	*PDP1*	-0.5085	0.010501	*ZFAND3*	0.68959	0.002949

SMARCA2	1.00862	3.01E-07	*SLC12A2*	-0.3854	0.010547	*CD151*	0.51396	0.002966
NT5E	-0.907	3.18E-07	*TXNDC17*	0.79252	0.010557	*SLC41A2*	0.93235	0.002999
GSN	0.7965	3.28E-07	*ANXA6*	-1.0639	0.010588	*PTTG1*	-0.8237	0.003018
STK17B	-1.101	3.60E-07	*TLN2*	-0.8306	0.010597	*SEMA3A*	-0.7374	0.003047
RPL9P8	1.21284	3.67E-07	*RNU5D-1*	-1.1635	0.010603	*PGPEP1*	0.86741	0.0031
PRPF31	-0.8227	4.11E-07	*FEN1*	-0.5229	0.01062	*ARHGAP11A*	-0.5629	0.003137
SAMD4A	-1.6247	4.12E-07	*GCLC*	0.47285	0.010622	*RNPEPL1*	0.76535	0.003164
ANXA4	0.93355	4.17E-07	*NUDT4*	0.49844	0.010633	*ABLIM1*	0.50843	0.003185
DUSP1	-1.1471	4.97E-07	*ARHGDIA*	0.45977	0.010655	*CDCA2*	-0.704	0.003189
RMRP	0.63142	4.98E-07	*CDC25A*	-1.0205	0.010682	*SETD1A*	-0.6637	0.003194
CST3	0.87972	5.25E-07	*EML2*	0.68203	0.010699	*CCND1*	-0.3978	0.003196
SNAPC1	-1.3392	5.42E-07	*INF2*	-0.4084	0.010862	*ARHGEF26*	-1.3417	0.003216
SEC14L1	-1.0516	5.74E-07	*FLOT2*	0.53619	0.010892	*FAT4*	-1.2385	0.00324
DHCR24	0.7036	5.78E-07	*SNAI2*	-1.5497	0.010913	*PPP1R26*	-0.6402	0.003296
SNORA2C	1.78181	6.11E-07	*ZDBF2*	0.69473	0.010929	*MPRIP*	-0.3813	0.003337
CCT5	-0.6564	6.25E-07	*H2AC7*	0.98637	0.011001	*NLE1*	-1.043	0.003345
EPB41L2	-1.0161	6.29E-07	*ZNF551*	-0.7057	0.011104	*PRPF38A*	-0.6589	0.003346
TMPRSS4	1.22218	6.49E-07	*DGKE*	-0.6481	0.011111	*NRP1*	0.47138	0.003365
RPS19	0.64983	6.52E-07	*MED1*	-0.3898	0.01115	*ARPC2*	0.46192	0.003374
ZNF462	-1.2713	6.58E-07	*AOC1*	0.96913	0.011234	*GRHL2*	-0.493	0.003388
LAMB1	-0.8435	6.70E-07	*KCNK6*	0.63456	0.011244	*ZNF468*	1.12491	0.003409
ASPH	0.66404	7.34E-07	*RNA5SP141*	-1.1363	0.011283	*MDC1*	-0.5888	0.00341
ENOSF1	-0.9039	7.66E-07	*CTSS*	0.7754	0.011332	*CASP2*	-0.7697	0.00343
AKAP13	0.67061	7.96E-07	*KRT8*	-0.2928	0.011402	*TFPI*	0.52276	0.00344
LENG8	-0.7044	8.13E-07	*NAPG*	-0.4576	0.011423	*PLK1*	-0.6487	0.003487
PHACTR2	-1.0074	8.70E-07	*MSH6*	-0.414	0.011481	*ABCG2*	-1.0273	0.003525
RPL31	0.72536	8.97E-07	*HCLS1*	-1.0131	0.011494	*JPT2*	-0.5088	0.003547

SRP14	0.73853	9.10E-07	*ZFAS1*	0.49315	0.011598	*NRCAM*	1.27592	0.003565
FHL1	-1.8536	9.78E-07	*RALGDS*	0.72988	0.011608	*PABPC4*	-0.4674	0.003587
FGF19	-5.2144	1.00E-06	*ARL4C*	-0.8131	0.011619	*RPL21*	0.41726	0.003616
HIP1	-1.3028	1.03E-06	*DISP2*	1.03483	0.011642	*NUFIP2*	0.40627	0.00362
RND3	-0.7814	1.05E-06	*SH3TC1*	0.753	0.011673	*CAT*	0.62291	0.003632
CLMN	0.85827	1.05E-06	*CDC42*	0.40013	0.011686	*SLC26A2*	-1.2363	0.003661
MYL12A	-0.6074	1.24E-06	*FTH1*	0.31211	0.011729	*TM9SF3*	0.4161	0.003685
ANKRD33B	-2.9765	1.27E-06	*BST2*	-0.7045	0.011778	*HNRNPM*	-0.4024	0.003695
MT1E	-1.9117	1.27E-06	*PER1*	-0.8387	0.011784	*SOD2*	0.41016	0.003747
MYH15	-2.4436	1.52E-06	*DST*	-0.3228	0.011828	*RAP1GAP*	0.7005	0.00375
MYH14	0.77781	1.52E-06	*HPS3*	0.51365	0.011884	*SIPA1*	1.01732	0.003754
LINC00665	-1.1643	1.62E-06	*EPB41L1*	0.42897	0.01189	*KNSTRN*	-0.6561	0.00377
BCAS1	1.35816	1.62E-06	*SKIL*	0.41199	0.011902	*CRAMP1*	-0.8145	0.00378
MGST1	0.7639	1.74E-06	*DUXAP8*	-0.673	0.011912	*SLC37A2*	0.76578	0.0038
TUBB	-0.6371	1.93E-06	*NDUFV3*	-0.5901	0.011942	*NDUFV2*	-0.4728	0.003806
CLDN1	-1.0952	1.93E-06	*CSTB*	0.38913	0.011971	*KATNAL1*	-1.2845	0.003812
CAV2	-1.4056	1.97E-06	*CEP295*	-0.4781	0.011989	*TSR1*	-0.5028	0.003838
DYNC1H1	-0.5831	2.00E-06	*C9orf78*	0.56466	0.012008	*SNORD62A*	1.36582	0.003865
SNORD87	1.68606	2.02E-06	*EPC1*	-0.5483	0.012044	*CDCA7*	-0.866	0.00387
PYGL	-0.8877	2.06E-06	*MYO19*	-0.5074	0.012087	*CAVIN1*	-0.558	0.003894
OLFM4	-4.3971	2.09E-06	*SRGAP2C*	-0.6348	0.012123	*HNRNPA0*	-0.6207	0.003939
EPN1	-0.6694	2.24E-06	*MBTPS1*	-0.4058	0.012289	*SYK*	0.88195	0.003961
ID1	-0.954	2.25E-06	*OTULINL*	1.29432	0.012331	*FCGBP*	-1.2588	0.003979
KIRREL1	-1.3317	2.47E-06	*SCOC*	0.94942	0.012334	*BCLAF1*	-0.4236	0.003998
LCP1	-0.9236	2.54E-06	*DEPDC1B*	-0.9134	0.01235	*OAS3*	-0.5119	0.004
FLRT2	-1.6004	2.63E-06	*MCAM*	-1.2396	0.012372	*SMC1A*	-0.4131	0.004036
NEURL1	-2.9507	2.76E-06	*GBA3*	-2.5432	0.012413	*CTSB*	0.45617	0.004062

MTRNR2L2	1.96707	2.90E-06	*NUP50*	-0.4513	0.01242	*CIT*	-0.5433	0.004065
SLC16A1	-0.8983	2.92E-06	*HIC1*	-1.2671	0.012447	*PLEKHG2*	-0.826	0.004127
WDR1	0.65618	3.01E-06	*ODC1*	-0.3805	0.012511	*ZNF28*	0.84804	0.00414
ANXA1	-0.6226	3.18E-06	*SCARB1*	-0.7131	0.012659	*CHORDC1*	-0.5246	0.004156
NCL	-0.567	3.39E-06	*SDR16C5*	1.08499	0.012678	*BRMS1L*	-1.055	0.004158
PSMC1P1	-3.512	3.39E-06	*DOCK9*	0.4343	0.012806	*CCNA2*	-0.6967	0.004168
ALDH3A2	0.75986	3.44E-06	*RFWD3*	-0.5171	0.012818	*SPAG5*	-0.5578	0.004198
CCDC80	-1.2691	3.65E-06	*IFNGR2*	0.61244	0.012829	*GMDS*	0.73068	0.004203
KPNA2	-0.6922	3.98E-06	*IL1RL1*	1.62189	0.012837	*HLA-B*	0.41566	0.00423
KIF15	-1.1884	4.01E-06	*CENPE*	-0.4555	0.012841	*EIF3A*	-0.371	0.004234
TCOF1	-0.7901	4.20E-06	*DUSP16*	0.71511	0.012857	*LUC7L3*	-0.3921	0.004245
RAB7A	0.65351	4.23E-06	*MRPL19*	-0.4778	0.012863	*BBLN*	0.99332	0.004331
SAP18	0.92587	4.31E-06	*RACGAP1*	-0.5487	0.012867	*CCDC144B*	0.59966	0.004339
NRP2	0.94081	4.40E-06	*ITGA3*	-0.3299	0.01288	*GINS1*	-0.8269	0.004345
ARHGAP29	-0.6751	4.57E-06	*DNAJB2*	0.7566	0.01296	*SQLE*	-0.4248	0.004362
CYP1B1-AS1	-0.9802	5.24E-06	*ANKRD22*	0.82839	0.012973	*AATK*	-1.3908	0.004391
RARRES1	1.06477	5.26E-06	*PTPN11*	-0.3665	0.012974	*CCDC43*	-0.6235	0.004436
MYADM	-0.6789	5.32E-06	*MCM3*	-0.4053	0.012977	*MAML2*	-0.6735	0.004444
KLF10	-0.9689	5.65E-06	*POLE*	-0.4732	0.013023	*GRAMD2B*	-1.017	0.004487
LOXL2	-1.4719	5.70E-06	*LGALS8*	-0.5381	0.013048	*NFAT5*	-0.4327	0.004494
TWF1	0.78296	5.84E-06	*NCOR2*	0.35537	0.013083	*SLFN13*	-0.812	0.004533
AMOTL2	-0.7693	6.09E-06	*JAK1*	0.4388	0.013105	*CPSF2*	-0.5053	0.004547
LPIN2	-0.6793	6.67E-06	*ATP5F1D*	0.61435	0.013125	*PTX3*	-2.2044	0.004596
SNORD27	2.39183	6.81E-06	*PTPRM*	-0.4717	0.013135	*GSTM3*	0.98698	0.004602
BCAT1	0.89761	6.88E-06	*SERF1A*	-1.1342	0.013149	*CLIC4*	-0.5015	0.004611
KIFC1	-0.9954	6.89E-06	*EPHB2*	-0.6966	0.013161	*VRK1*	-0.539	0.004621
MSLN	-4.2979	6.99E-06	*CHD9*	-0.4837	0.013162	*SYNM*	-0.988	0.004623

DNAJA1	-0.5927	7.02E-06	*ISG15*	-0.5232	0.013189	*MICAL3*	-0.5829	0.004639
DEPDC1	-1.2429	7.06E-06	*BICC1*	-0.9789	0.013197	*GLG1*	-0.4218	0.004725
EEF1A2	-0.6305	7.25E-06	*SCN8A*	-1.1347	0.013222	*ATP2B4*	0.57595	0.004725
MCFD2	-0.6613	7.59E-06	*TNFAIP3*	0.65777	0.013256	*C21orf58*	-1.3414	0.004727
SLC38A2	-0.5937	7.70E-06	*SNORD99*	1.17953	0.013266	*PRPF38B*	-0.4748	0.00476
PEG10	-3.7843	7.73E-06	*PTPRU*	0.56798	0.013318	*AGRN*	-0.4027	0.00477
SLC7A5	-0.7135	7.80E-06	*STX2*	-1.1755	0.013367	*SLC9A3R1*	0.56205	0.004789
CD68	1.20931	7.95E-06	*SAMD9*	-0.457	0.013374	*DCTN1*	-0.4262	0.004799
RN7SK	0.52662	8.21E-06	*CDYL2*	1.30469	0.013448	*TINAGL1*	0.43714	0.004834
IRS1	-0.8285	8.52E-06	*COPG1*	0.38184	0.013546	*VTRNA2-1*	-1.4049	0.004855
MYH10	-0.7808	9.03E-06	*DENND4A*	0.55598	0.01355	*MCM4*	-0.4616	0.004881
MCM7	-0.8231	9.10E-06	*PLEKHA2*	0.49206	0.013661	*HSP90AA1*	-0.3259	0.004894
PLCXD2	-1.7727	9.15E-06	*PIK3C2B*	0.59776	0.013691	*SFPQ*	-0.3651	0.004902
RPL37A	0.66402	9.30E-06	*SPATA5*	-0.6612	0.013761	*ERBB3*	0.47295	0.004908
RN7SL3	-0.609	9.64E-06	*KCNQ1*	1.02586	0.013823	*HCG25*	1.25979	0.004935
FRMD3	-2.159	1.05E-05	*RALGAPA2*	0.41891	0.013861	*FSTL1*	-0.851	0.004957
TOPORS	-0.7758	1.08E-05	*TFDP2*	0.48941	0.013937	*GRPEL2*	-0.7811	0.004958
TBK1	0.74606	1.20E-05	*SMAD3*	0.38387	0.014009	*MAN1A1*	-0.7006	0.004964
SYT7	-1.4406	1.21E-05	*METRN*	-1.1717	0.014024	*RAB8A*	0.50159	0.004964
MYC	-0.7578	1.24E-05	*GATAD2B*	-0.5227	0.014053	*RPS18*	0.37105	0.004999
OAS2	-1.1024	1.28E-05	*FKBP3*	-0.5937	0.014078	*RPS12*	0.43092	0.005001
TRIM28	-0.6194	1.28E-05	*MUC5B*	-1.7339	0.014132	*SELENOT*	0.58523	0.005005
SEMA4B	0.77537	1.38E-05	*FN1*	0.49763	0.014143	*TRIM29*	0.55516	0.005042
KIAA1217	0.74315	1.38E-05	*SNORD60*	1.29175	0.014169	*RFC4*	-0.6837	0.005065
FAM83A	0.97002	1.42E-05	*NUDCD1*	-0.5347	0.014218	*GABARAP*	0.61483	0.005141
MIR205HG	-2.2559	1.45E-05	*ZNF134*	-0.6233	0.014319	*ALDH1A3*	-0.4875	0.005148
CRABP2	-1.0078	1.53E-05	*TPRXL*	1.20509	0.014346	*DGLUCY*	-0.8201	0.00521

PLK2	-0.7204	1.56E-05	*ANLN*	-0.3713	0.014367	*FANCD2*	-0.6619	0.005263
NCAPG	-1.0943	1.62E-05	*NOP14*	-0.4725	0.014377	*TMC4*	0.54735	0.00528
ND3	0.60143	1.64E-05	*SET*	-0.3147	0.014413	*LAS1L*	-0.6647	0.005285
PLCXD3	-2.7206	1.65E-05	*SEM1*	0.52072	0.014443	*PARVB*	-1.1967	0.005315
HJURP	-0.8882	1.66E-05	*ICA1*	0.5786	0.014519	*SPATA13*	0.58785	0.005328
PPARG	0.76312	1.68E-05	*HBP1*	0.63422	0.014551	*COL6A2*	-2.8379	0.005334
RPS11	0.57075	1.73E-05	*INTS8*	0.49556	0.014568	*PTMA*	-0.3398	0.005384
MDN1	-0.6329	1.73E-05	*C5orf22*	0.69159	0.014594	*ACADVL*	0.45724	0.005384
BASP1	-1.6041	1.77E-05	*CHD7*	0.42975	0.014671	*NIPSNAP2*	0.75132	0.005406
LINC01962	-0.8613	1.82E-05	*BPTF*	-0.332	0.014683	*MMP7*	1.33953	0.005409
MYL12B	-0.5367	1.86E-05	*SGSM2*	-0.6292	0.014689	*HPSE*	-1.5136	0.005432
CDC20	-0.8899	1.90E-05	*BCL2L2-PABPN1*	-0.553	0.014741	*UQCR11*	0.73119	0.005457
MMP14	0.93442	1.91E-05	*SRPRA*	0.44102	0.014758	*TSPAN1*	0.60105	0.00547
SSH3	0.96096	1.91E-05	*CDK12*	-0.3686	0.014904	*KIF18A*	-0.6871	0.005496
EFL1	0.96944	1.94E-05	*MATR3*	-0.3362	0.014926	*KATNB1*	-1.0517	0.00557
CKAP2L	-0.9558	2.06E-05	*SH3BGRL3*	0.51188	0.014928	*RIOK3*	0.53616	0.005578
RNU4-1	0.81649	2.11E-05	*SIGMAR1*	-0.4792	0.014942	*SPRY4*	-0.6679	0.005584
ZBED6CL	-1.1991	2.14E-05	*DBN1*	-0.4174	0.014953	*SNORD33*	2.42878	0.005585
MTHFD1	-0.7314	2.16E-05	*PLCD3*	0.51543	0.014992	*GFUS*	0.64622	0.005591
PELI2	1.6356	2.24E-05	*E2F7*	-0.7386	0.014993	*ELFN2*	0.85686	0.005606
IMPA2	-1.1492	2.44E-05	*MMS22L*	-0.61	0.015007	*DERL1*	0.54879	0.005622
CD109	-1.2161	2.45E-05	*CABLES1*	0.76441	0.015145	*SRGAP1*	-0.4902	0.005685
EIF4E2	0.83357	2.56E-05	*TUSC3*	0.80185	0.015147	*UBL5*	0.79203	0.005697
FERMT2	-1.4271	2.60E-05	*ZNF92*	-1.7788	0.015153	*AACSP1*	-2.6566	0.005758
NDST1	-0.9567	2.70E-05	*SLC35F6*	-0.51	0.015166	*RNFT2*	-0.9545	0.005768
IFI27	-0.8711	2.77E-05	*CD82*	0.63654	0.015241	*ANP32B*	-0.4061	0.005805
PPP4R1	-0.6281	2.78E-05	*WSB1*	0.44339	0.015256	*SRSF7*	-0.4591	0.005812

DUSP5	-0.7487	2.82E-05	*ZNF701*	1.05996	0.015339	*FST*	-2.0472	0.005835
NCAPD2	-0.6772	2.85E-05	*PIM3*	-0.556	0.015342	*CCDC86*	-0.6534	0.005935
LOC102724843	-7.8177	2.94E-05	*FOXP1*	0.59815	0.01546	*SLC6A14*	1.12707	0.005972
ST14	0.60709	2.95E-05	*ADARB1*	-0.9194	0.015471	*CTCF*	-0.528	0.005995
SNORD89	1.77973	2.97E-05	*POLR1E*	-0.7104	0.015532	*ARSD*	0.97307	0.005999
RPPH1	0.6144	3.02E-05	*TCP11L2*	0.87675	0.015588	*FMC1-LUC7L2*	-1.3958	0.006004
COX5B	0.83678	3.04E-05	*UBE2H*	0.39973	0.015601	*ERCC6L*	-1.0931	0.006005
YES1	-0.6344	3.05E-05	*HDGFL2*	-0.5571	0.015684	*PSMC3IP*	-0.8933	0.006042
AMOTL1	-0.688	3.07E-05	*LAMA1*	-1.2323	0.01569	*GOT2*	-0.5007	0.006047
SYAP1	0.6732	3.13E-05	*SERPINB6*	0.45993	0.015698	*MECOM*	0.56446	0.006064
CCDC18	-1.0935	3.16E-05	*CEACAM1*	0.52033	0.015712	*SPP1*	1.31511	0.006073
LOC102724951	-3.2885	3.17E-05	*FJX1*	-1.5098	0.015775	*NUP210*	-0.4789	0.00608
FXYD3	1.14178	3.17E-05	*NUDT9*	0.68836	0.015779	*FAM111A*	-0.5003	0.006183
MELK	-0.9464	3.19E-05	*BLVRB*	0.58564	0.015789	*ZBTB21*	-0.6446	0.006184
AURKA	-0.9445	3.22E-05	*NAPRT*	0.53163	0.015793	*TCP1*	-0.3923	0.006218
KIF4A	-0.9827	3.22E-05	*COL17A1*	0.84815	0.015837	*STOML2*	-0.5368	0.006233
MTSS2	-0.8702	3.29E-05	*TM4SF4*	-2.6343	0.015901	*MAP1LC3B*	-0.4787	0.006277
SIK1B	-1.1268	3.29E-05	*CACNA1C*	1.20351	0.015915	*COX6A1*	0.53247	0.006339
TPT1	0.50576	3.33E-05	*TTC9*	0.78102	0.01594	*RNU11*	-1.8181	0.006356
MAP3K20	-0.772	3.34E-05	*B4GALNT4*	1.27577	0.015942	*KDM6A*	-0.5663	0.006398
SMC5	0.73222	3.35E-05	*RAB3B*	-0.7917	0.015971	*SPDL1*	-0.6523	0.006407
SSRP1	-0.5789	3.36E-05	*TMEM47*	-0.9254	0.015991	*UACA*	-0.4218	0.006413
ZNF787	-1.0284	3.37E-05	*SNHG5*	0.50412	0.016032	*RNA5SP199*	-1.4789	0.006425
U2AF1	-0.7106	3.48E-05	*AKT3*	-0.5017	0.016047	*EZH2*	-0.6657	0.006426
SPARC	-2.9941	3.61E-05	*SLC28A3*	1.46322	0.016117	*RUNX1*	-0.5197	0.006459
AKR1C3	0.95228	3.62E-05	*SPCS2*	0.4945	0.016117	*TEP1*	0.54971	0.006483
MDK	0.76175	3.64E-05	*FABP5*	-0.5073	0.016152	*FAM111B*	-0.6831	0.006509

SNORD15B	0.64444	3.73E-05	*H2AC8*	-1.404	0.016197	*MAPK8IP1*	-1.63	0.006525
SREBF1	0.67428	3.90E-05	*PRR15*	0.72474	0.016294	*HERC1*	0.48614	0.006569
SNORD45A	1.84411	3.94E-05	*RRP7BP*	-0.7239	0.0164	*LMBRD2*	0.75685	0.006619
SMC4	-0.5783	4.06E-05	*CCDC85B*	-0.8444	0.01645	*POLR2A*	-0.377	0.006663
SNORA7A	1.44764	4.08E-05	*TUBB6*	-0.7396	0.016487	*ADCY5*	0.95548	0.006666
NIN	-0.7069	4.27E-05	*LATS2*	-0.6291	0.016515	*B4GALNT3*	0.75882	0.006694
NME7	1.30124	4.31E-05	*HEATR5A*	0.57375	0.016523	*GK5*	0.57886	0.006704
ID3	-1.7132	4.33E-05	*B4GALNT1*	-1.5692	0.016566	*KRI1*	-0.6419	0.006715
VCP	-0.5495	4.35E-05	*NUP155*	-0.4719	0.016568	*COL13A1*	-1.7343	0.006722
GAS5	0.75369	4.49E-05	*CDA*	-2.0363	0.016596	*SERBP1*	-0.3574	0.006756
GCNT3	1.12726	4.49E-05	*INSR*	0.67731	0.016698	*ECHDC2*	0.81112	0.006781
MALL	0.64714	4.55E-05	*TMEM245*	-0.4437	0.016703	*RPL5*	0.33798	0.006821
ZNF721	-2.3402	4.55E-05	*ITPR2*	0.4848	0.016716	*CA2*	1.22352	0.006864
IFIT1	-0.9586	4.86E-05	*GTDC1*	0.70465	0.016726	*SOCS3*	-0.9933	0.00689
CCNB1	-0.7485	4.93E-05	*LRP3*	1.27656	0.01678	*SEH1L*	-0.4239	0.030746
HSP90AB1	-0.4811	5.10E-05	*ENY2*	0.58074	0.016805	*TM7SF3*	0.48922	0.030791
CDCA8	-1.0516	5.20E-05	*ZNF367*	-0.8648	0.016819	*PRECSIT*	-0.8969	0.030831
PVR	-0.6787	5.38E-05	*WWC1*	-0.4219	0.016877	*MRPS6*	-0.5345	0.030834
NASP	-0.6078	5.46E-05	*SLC44A3-AS1*	-0.9096	0.016879	*A2M*	-1.5788	0.030912
HSPA4	-0.5414	5.54E-05	*SMS*	-0.4198	0.016886	*MGAT5B*	-1.2798	0.030958
NEAT1	-0.4938	5.55E-05	*CKAP5*	-0.3375	0.016927	*MRFAP1*	-0.3084	0.030966
STING1	-1.0439	5.74E-05	*NSA2*	-0.4125	0.016948	*ELF4*	0.55602	0.030978
CXCL5	-3.878	6.23E-05	*NES*	-1.0356	0.016996	*GTF3C4*	-0.4578	0.030995
HUWE1	-0.5108	6.26E-05	*ABHD4*	0.58736	0.017038	*RNASEH2C*	-0.6433	0.031056
LIPG	-1.0808	6.33E-05	*IFI44*	-0.578	0.01711	*PMPCA*	-0.4173	0.031106
PTPN14	-0.684	6.57E-05	*IGF2BP3*	-0.4368	0.017119	*DNTTIP2*	-0.3659	0.031119
RPS13	0.62906	6.61E-05	*MASTL*	-0.7086	0.017123	*DSE*	-0.7575	0.031146

ATAD2	-0.6012	6.71E-05	*ZNF160*	0.6176	0.017161	*LMO7*	0.28646	0.031182
PNN	-0.5301	6.72E-05	*PKIB*	1.04856	0.017179	*GXYLT1*	-0.4722	0.031188
ZNF703	1.05329	6.89E-05	*TFPI2*	-0.8003	0.017205	*APOL6*	-0.3093	0.03131
CBX5	-0.5814	7.00E-05	*KLF6*	-0.4027	0.017224	*TIAM1*	0.55143	0.031316
ANXA11	0.6584	7.09E-05	*FUCA1*	0.60918	0.017231	*LGR4*	0.46498	0.031386
RPL23AP42	0.65007	7.15E-05	*LIN7C*	-0.4827	0.017336	*IL4R*	0.55887	0.031538
HELLS	-0.7743	7.25E-05	*GEM*	1.15994	0.017345	*ZNF37A*	-0.521	0.031703
RAB12	-0.7242	7.30E-05	*THUMPD1*	-0.4489	0.017352	*PHTF2*	-0.6653	0.031752
FRMD6	-1.5165	7.34E-05	*IPO4*	-0.4972	0.017466	*KRT4*	-1.6309	0.031783
KIF22	-0.9171	7.34E-05	*ELL2*	-0.5758	0.017549	*CHD1L*	-0.6067	0.031829
DLGAP5	-0.8569	7.54E-05	*RANBP17*	0.74963	0.017583	*CAMK2N2*	-1.4707	0.031831
BCL2L15	1.4336	7.59E-05	*LIG3*	-0.4738	0.017627	*KIAA0513*	-0.8802	0.031837
CHMP1B	-0.711	7.78E-05	*SIAH2*	0.72757	0.017636	*TMED9*	0.35588	0.031846
TCAF1	-0.761	7.78E-05	*CNKSR3*	-0.6556	0.017663	*SDCBP*	0.34396	0.031943
CTPS1	-0.8799	7.83E-05	*ME2*	-0.6416	0.017735	*ZNF510*	0.73482	0.031988
RPL30	0.58752	7.92E-05	*ANXA2*	0.28641	0.017751	*VPS13C*	0.32766	0.032006
RNU5E-1	-1.022	8.44E-05	*LY6D*	-1.992	0.017881	*CACNB3*	0.86062	0.032027
NOP53	0.71915	8.49E-05	*APOBEC3B*	-0.7573	0.017916	*ZNF780A*	0.58794	0.032065
TNS3	-0.8107	8.55E-05	*HGS*	0.40668	0.017962	*SNORA70*	1.00808	0.032089
METTL4	-1.0457	8.62E-05	*SLC41A1*	-0.6563	0.017973	*RPL18*	0.2874	0.032095
COX8A	1.06775	8.62E-05	*PHLDA1*	-0.3409	0.018021	*SGO1*	-0.6495	0.032202
LMNB2	-0.6387	8.82E-05	*PPT1*	-0.4767	0.018092	*TUB*	-1.4189	0.032324
PDPR	-0.9487	9.03E-05	*UBC*	0.29439	0.018104	*PARP4*	0.32537	0.032347
NABP1	-0.7881	9.03E-05	*DKK3*	-1.4323	0.018142	*PLEKHA6*	0.475	0.03239
LIMCH1	-0.579	9.53E-05	*PAICS*	-0.412	0.018144	*LINC00273*	-0.58	0.032643
REEP3	0.8343	9.56E-05	*PDZD8*	0.3951	0.018221	*PTPN21*	-0.8871	0.032736
KIAA1522	0.57203	9.71E-05	*DDIAS*	-0.9239	0.018257	*ECH1*	0.39188	0.032793

MAP7D3	-1.052	9.89E-05	*ERVK3-1*	-0.4517	0.018276	*ZBTB44*	0.45392	0.032802
SIX4	-0.9881	0.000103	*ZNF326*	-0.5114	0.018322	*MMRN2*	-0.8037	0.032926
CALR	-0.4825	0.000103	*CMIP*	-0.4752	0.018384	*PKM*	-0.262	0.032998
CCND2	-3.1892	0.000103	*RSL1D1*	-0.3647	0.018429	*MCM2*	-0.3937	0.033038
ANKRD10	0.58794	0.000105	*PIGO*	-0.6105	0.018437	*LANCL3*	-1.4415	0.033131
DCDC2	-1.0895	0.000106	*MMD*	-0.9057	0.018475	*EWSR1*	-0.3189	0.033279
ANKRD12	-0.5894	0.000106	*GALNT18*	-1.17	0.018521	*PODXL*	-0.4136	0.033302
VAPA	-0.5201	0.000107	*H4C5*	0.88401	0.018521	*HMGCR*	-0.3499	0.03333
NCOA7	-0.7097	0.000107	*SPC25*	-0.8185	0.018543	*ZZEF1*	0.3826	0.03336
UQCRQ	0.63303	0.000111	*SLC22A18*	0.93206	0.018583	*ITGA1*	-0.6971	0.033511
SNORD15A	0.73756	0.000112	*HNRNPD*	-0.345	0.018799	*SNORA67*	1.5789	0.033518
NR3C1	-0.8351	0.000113	*ADRB2*	-0.9674	0.018941	*CUL5*	0.4441	0.033541
SLC44A2	-0.7434	0.000114	*SNORA53*	0.43446	0.018946	*MRPL45*	-0.4586	0.033763
SNORA8	1.9665	0.000115	*SLC4A8*	0.98895	0.018975	*DDX21*	-0.3037	0.033851
DEK	-0.5311	0.000117	*SHMT2*	-0.4337	0.018981	*RAB6A*	0.33283	0.033956
FLNA	-0.4986	0.000117	*ARPC1B*	0.45206	0.019007	*SH3BGRL2*	0.52773	0.033965
SERF2	0.569	0.000118	*PMAIP1*	-0.6289	0.019076	*LOC441666*	0.72267	0.03397
TMBIM1	0.70752	0.000118	*NPM1*	-0.2911	0.019083	*RRBP1*	-0.2891	0.03398
GOLM2	0.58355	0.000118	*RPL38*	0.35012	0.019196	*SOX12*	-0.7569	0.034006
TNS4	-0.7519	0.00012	*KDM5C*	0.42138	0.019235	*NUF2*	-0.7065	0.034051
TMED10	0.53353	0.000121	*RNU5E-6P*	-1.0193	0.019279	*U2AF2*	-0.3096	0.034081
ORMDL3	0.96803	0.000122	*SRCAP*	-0.3832	0.019287	*DUXAP9*	-0.5579	0.034103
SNORD96A	2.38632	0.000123	*POLQ*	-0.4945	0.019287	*CCT2*	-0.3314	0.034218
NR2F2	-0.6279	0.000124	*TMBIM6*	0.31219	0.019302	*GTF3C1*	-0.3602	0.034255
DIAPH1	-0.5273	0.000124	*TET3*	-0.4559	0.019355	*DHX15*	-0.3593	0.034304
NDUFB4	1.01909	0.000124	*CDK14*	-1.1128	0.019392	*UNC119*	0.73869	0.034315
HCAR1	-1.5016	0.000124	*EFEMP1*	-1.6327	0.01941	*SPICE1*	0.57457	0.034348

SCARNA2	-3.4616	0.000125	*ABCF1*	-0.3653	0.019542	*SLC39A11*	0.53814	0.034354
ITGB6	0.90622	0.000125	*IFIT2*	-0.5389	0.019575	*PLXNB2*	0.3144	0.034359
SREBF2	0.59044	0.000127	*RAP1GAP2*	0.67613	0.019587	*ZNF608*	-0.4675	0.03436
KLHL5	-0.8068	0.000127	*EMC10*	0.48539	0.019601	*ASCC2*	0.48272	0.034436
RPS6KA5	-1.0854	0.000127	*PRKCA*	0.39638	0.019653	*ULK1*	0.64398	0.034482
GPT2	1.11329	0.000128	*SOX7*	-1.2355	0.019659	*HMGXB4*	-0.4232	0.034513
EIF5AL1	1.64302	0.000134	*TFF2*	-1.7619	0.019663	*SLC7A2*	-1.1112	0.034535
SORCS2	-1.756	0.000137	*JPH1*	-0.9366	0.019705	*TPM4*	0.30007	0.034671
ALCAM	-0.6291	0.000145	*GSPT1*	-0.3352	0.019736	*AMD1*	-0.3695	0.034731
RNA5SP150	-1.6129	0.000147	*MND1*	-1.4325	0.019828	*TFAM*	-0.4806	0.034901
USP1	-0.7757	0.000152	*INCENP*	-0.434	0.019833	*CTSE*	-1.6896	0.03494
ERBB2	0.60062	0.000153	*CCNF*	-0.6871	0.019843	*JAG2*	-0.8889	0.034942
POLD4	1.01148	0.000154	*PLK4*	-0.7396	0.019883	*ZNHIT6*	-0.5003	0.035057
UBE2G2	-0.6886	0.000159	*NUDT21*	-0.4158	0.019892	*ZBTB37*	-0.6236	0.035087
PIGG	-2.1162	0.000159	*CHD4*	-0.3102	0.019995	*PTEN*	0.36833	0.035144
UCA1	-0.5815	0.00016	*UGT1A1*	0.99575	0.019997	*ARHGAP35*	-0.3137	0.035256
COL6A1	-0.9452	0.000163	*PSMC5*	-0.4027	0.020035	*ADM*	-0.7415	0.035405
TMC5	0.96984	0.000163	*COPE*	0.48944	0.02004	*C11orf1*	0.89235	0.035426
HSP90B1	-0.4587	0.000165	*HCP5*	0.90622	0.020145	*HOXC10*	-1.4065	0.035559
PTPRH	0.99222	0.000166	*IRF2BP2*	0.51405	0.020189	*KDM3B*	-0.3539	0.035569
IFI6	-0.9194	0.000172	*DIDO1*	-0.3996	0.020271	*EIF5B*	-0.3	0.03566
DHFR	-0.9046	0.000174	*RGS2*	0.85227	0.020357	*SLC9A1*	0.46378	0.035742
TNNT1	-0.9891	0.000174	*CABIN1*	-0.5303	0.020388	*PI4K2B*	-0.9093	0.03577
NXN	-1.5357	0.000175	*NUCKS1*	0.31268	0.020573	*NME1*	-0.3935	0.035779
MCM8	-0.9384	0.000176	*LINC01234*	-1.0286	0.020685	*RNA5-8SN2*	1.21049	0.035852
TJP3	0.70533	0.000176	*EDC4*	-0.5226	0.02069	*TCHP*	-0.6152	0.036007
SNORA49	1.00582	0.000177	*PARD3*	-0.3752	0.020723	*FAM214A*	0.65257	0.036029

MB21D2	-1.6269	0.000191	*RBM19*	-0.5284	0.020754	*MGME1*	-0.6409	0.036036
EGFR	-0.5776	0.000194	*NDUFA6*	0.45745	0.020756	*C3orf52*	0.6133	0.03605
SLC12A7	0.62363	0.000197	*LARS2*	-0.6027	0.020806	*DHX57*	-0.5331	0.036136
SLK	0.57016	0.000202	*AGAP2*	-1.556	0.020817	*VPS9D1-AS1*	-1.1587	0.036151
DDX58	-0.7718	0.000205	*CMPK2*	-1.0514	0.020817	*PCMTD1*	0.44832	0.036215
MAML1	0.72725	0.000205	*SLFN5*	-0.337	0.020833	*SMDT1*	0.88658	0.036235
PTP4A2	0.56387	0.00022	*TOLLIP*	0.68596	0.020855	*VPS4A*	-0.4715	0.036275
HNRNPA2B1	-0.4465	0.000221	*MKRN3*	-1.4803	0.020902	*GLO1*	-0.4347	0.036309
KYNU	1.07276	0.000222	*RNASEH1*	-0.4327	0.020907	*WDHD1*	-0.5161	0.036319
PRSS3	1.21542	0.000223	*PLEKHA7*	0.355	0.020929	*SNORA40*	-3.497	0.036408
FAM174B	1.26184	0.000224	*MYO10*	-0.4021	0.021008	*NOTCH2*	-0.3113	0.036506
TLN1	-0.5034	0.000228	*SPRY1*	-0.7895	0.021054	*GABBR2*	-1.3866	0.036541
SLC1A3	-1.0329	0.000231	*GPBP1L1*	0.40437	0.021057	*L2HGDH*	-0.4744	0.036555
ZDHHC20	0.63385	0.000232	*MYO1B*	-0.412	0.021067	*GAS6*	-0.7235	0.036559
TACSTD2	-0.5122	0.000233	*KDM5A*	0.3344	0.02115	*RNASEH2A*	-0.6634	0.036568
MBOAT7	-0.5983	0.000235	*MFSD6*	0.5299	0.021317	*TTC39A*	0.90754	0.036693
RNA5SP429	-2.3071	0.000235	*NRARP*	-0.9165	0.021378	*GPATCH4*	-0.431	0.03678
KRT18	-0.4391	0.000242	*SCAF4*	-0.4803	0.02142	*ADSL*	-0.38	0.036887
RBMS2	-0.746	0.000249	*APOL1*	-0.4742	0.021431	*LDLRAP1*	0.61538	0.036933
SRRM2	-0.4569	0.000249	*RPGRIP1L*	-0.7561	0.02157	*KRT20*	-0.9371	0.036977
MANSC1	0.98972	0.000249	*MIA2*	0.38379	0.021572	*JUN*	-0.3359	0.037008
IER3	-0.6204	0.000258	*GNL2*	0.40451	0.021575	*TAF1B*	-0.644	0.037061
TUBB4B	-0.4789	0.000262	*CFL2*	-0.7471	0.021576	*PTPRJ*	-0.3496	0.037169
G3BP1	-0.5545	0.000263	*HINT3*	-1.1723	0.021611	*MME*	-0.8276	0.037218
CHST12	-1.0809	0.000265	*ZC3H14*	-0.4504	0.021691	*BACE2*	-0.492	0.037252
TNFRSF11A	1.13965	0.000273	*GEMIN5*	-0.5764	0.021747	*DDX11*	-0.4162	0.037279
COX6B1	0.70355	0.000274	*OPA1*	0.35147	0.021777	*GATD3B*	-0.5314	0.037352

RAB5C	0.65271	0.000277	*ATP5F1C*	0.44162	0.021853	*SMAD4*	-0.6291	0.037356
VASP	0.61516	0.000285	*RPS24*	0.31774	0.021907	*ATR*	0.37578	0.037453
CCDC152	-2.1124	0.000288	*NANOS1*	-1.192	0.021945	*PLPP5*	0.83475	0.03746
ATAD5	-0.8345	0.00029	*PSMD7*	-0.3783	0.021977	*TMX1*	-0.4091	0.037545
LDLR	-0.5082	0.000294	*IMPDH2*	-0.3871	0.022017	*ETNK1*	0.39681	0.037656
SNORD46	1.29573	0.000295	*VAMP8*	0.57904	0.022058	*OGFR*	-0.5072	0.037671
H3-3B	-0.5136	0.000295	*RAB2A*	0.42536	0.022086	*NSG1*	-1.5501	0.038008
MCTS1	1.0589	0.000296	*CDKN3*	-0.678	0.022116	*SORBS3*	-0.6986	0.038086
RCN1	-0.532	0.000304	*ASAP1*	-0.3813	0.022184	*SPECC1L-ADORA2A*	-1.0341	0.038103
KMT5C	-1.3834	0.000305	*GPAT4*	0.54954	0.02224	*ECT2*	-0.3185	0.03816
IFIT3	-0.7649	0.000305	*SNORA73B*	0.39816	0.022259	*DENND10*	0.63135	0.038218
LASP1	-0.4555	0.000332	*KAT7*	-0.5007	0.022378	*NEDD1*	-0.6008	0.038237
SCARNA4	-1.9339	0.000337	*PDCD6IP*	0.3794	0.022543	*DNAJC6*	-1.1202	0.038456
FOSL1	-0.7241	0.000339	*LRRFIP1*	0.30996	0.02265	*POLE3*	-0.3946	0.038497
NFIB	-0.6653	0.000339	*ABL2*	-0.5181	0.022718	*CEMIP2*	0.3282	0.038705
SLC44A3	1.79268	0.000344	*BUB1B*	-0.5083	0.022725	*TRIP13*	-0.569	0.038813
ASXL1	-0.7095	0.000345	*SCAMP2*	0.51102	0.022776	*TBRG1*	0.54548	0.038897
UBE2C	-0.9092	0.000346	*BRSK2*	-1.3789	0.022786	*TMEM258*	0.71524	0.038934
ANKRD11	-0.4733	0.000348	*SNORA74D*	-0.9306	0.022791	*CARHSP1*	-0.6031	0.038951
SNORA48	1.49678	0.000356	*ASCC3*	-0.4081	0.022799	*KLHDC8B*	-1.1762	0.039047
CCT7	-0.5055	0.000359	*DCPS*	0.73801	0.022858	*KRT17*	-1.6414	0.039085
DENR	-0.6433	0.000363	*PAPSS2*	-0.768	0.022898	*GOLIM4*	-0.3863	0.039117
PPP1R16A	0.94144	0.000369	*DYNC2H1*	-0.7193	0.022923	*UNC93B1*	0.45236	0.039159
MUC4	-1.2827	0.000369	*MGP*	-0.9999	0.022927	*CDYL*	0.44218	0.039208
RCC1	-0.7642	0.000372	*HLA-A*	0.30172	0.022966	*MAGI3*	-0.6182	0.03927
ALPP	-2.7465	0.000381	*GPX1*	0.52292	0.023001	*ATP5MG*	0.38626	0.039287
TAGLN2	0.56386	0.000385	*LDAF1*	0.87086	0.023057	*CDKN2AIPNL*	-0.7494	0.039296

DIAPH3	-0.8407	0.000393	*FMNL3*	-0.8859	0.0232	*TMC6*	0.34001	0.039396
TMEM45B	0.79047	0.000398	*ARHGEF12*	0.3162	0.023325	*NIP7*	-0.5716	0.039399
NIBAN1	0.88743	0.000408	*POLA2*	-0.9653	0.023343	*LRP1*	0.46678	0.039424
SGCE	-1.1425	0.000412	*PISD*	-0.6399	0.023405	*UPK3BL1*	-1.8137	0.039572
LPP	0.52395	0.000415	*DNAJC3*	0.39075	0.023454	*CAPN1*	0.29691	0.039742
SNORA24	1.48817	0.000421	*VGLL4*	0.52486	0.023515	*DMXL2*	0.3876	0.039798
EPDR1	-1.5009	0.00043	*EZR*	-0.2952	0.023631	*SUZ12*	-0.3524	0.039856
SLC16A5	0.78032	0.000433	*CCPG1*	0.37004	0.023741	*ZFYVE1*	0.652	0.03996
MTHFD2	-0.5264	0.000435	*CLIP4*	-0.424	0.023748	*CARD6*	0.6527	0.040061
NLN	-0.7522	0.000436	*CORO1B*	0.45455	0.023838	*GTSE1*	-0.614	0.040068
ASPM	-0.5902	0.000438	*DUSP14*	-0.7656	0.023858	*UBALD2*	0.49722	0.040086
PPM1G	-0.5302	0.000439	*ADIPOR2*	0.36225	0.023899	*RBL1*	-0.6082	0.040097
KIF11	-0.7261	0.000443	*UBE2Q1*	0.48889	0.023924	*QSOX2*	-0.4684	0.04033
ZNF444	-1.0118	0.000451	*MDGA1*	-1.6094	0.023927	*SMU1*	-0.358	0.040389
DEF8	-0.8962	0.000451	*POFUT1*	-0.446	0.023952	*GLOD4*	0.44872	0.040502
CHAF1A	-0.7894	0.000459	*KANK1*	-0.5712	0.023965	*MKRN1*	0.39107	0.040566
TIMP1	0.72314	0.000473	*CDT1*	-0.7352	0.024078	*EIF2S3*	0.30051	0.040679
RAB11A	0.56709	0.000473	*SNORD17*	0.37672	0.024146	*BTG1*	0.43396	0.040734
ATXN1L	-0.8241	0.00048	*CDX2*	1.12135	0.024205	*TFPT*	-0.5547	0.040813
RRP1B	-0.6614	0.000481	*PLAAT3*	0.37436	0.024236	*MIS18BP1*	-0.4143	0.040815
SREK1	-0.5206	0.000487	*RREB1*	0.36367	0.024239	*MYBBP1A*	-0.4063	0.040874
HNRNPA3	-0.4788	0.000488	*CEP43*	-0.5291	0.024292	*COMMD6*	0.60072	0.041006
UQCRH	0.70208	0.000492	*PLS1*	0.43242	0.024296	*PCDH9*	-1.0922	0.041036
KIF14	-0.8593	0.000493	*SAV1*	-0.54	0.024309	*STRN*	-0.3442	0.041062
SCARNA13	0.94907	0.000494	*NOM1*	-0.5441	0.024329	*STAG2*	-0.3646	0.041076
CEP128	-1.0609	0.000499	*CHD8*	-0.3232	0.024332	*GNPNAT1*	0.46532	0.041102
VTRNA1-1	-1.0643	0.00051	*USP22*	0.36147	0.024348	*H1-5*	-0.3041	0.041111

PDIA4	-0.483	0.00051	*ABCC3*	0.36155	0.024387	*ZDHHC14*	-1.0494	0.041116
EIF4G1	-0.4242	0.000517	*ALDH3A1*	1.70185	0.02444	*TMSB4X*	-0.2786	0.041244
MACF1	-0.4297	0.000518	*RAD51D*	-0.7697	0.024448	*CKMT1A*	0.75732	0.041503
SYTL2	0.621	0.00052	*PSIP1*	-0.4585	0.024456	*UBB*	0.28038	0.04151
ITGB5	0.55886	0.000546	*PCYOX1L*	-0.9485	0.02449	*PPDPF*	0.3358	0.041573
POLR1G	-0.9092	0.000547	*RMC1*	0.73464	0.024509	*TRIM38*	0.39782	0.041663
SNORD21	1.96588	0.00055	*HPGD*	0.74129	0.024542	*MYO6*	0.31489	0.041674
EFNA5	-0.8493	0.000551	*BUB1*	-0.4324	0.024616	*GGH*	-0.5102	0.041756
WDR62	-0.8684	0.00056	*DNM1*	-0.7099	0.024688	*GBP2*	0.56162	0.041815
PSME1	-0.5019	0.000565	*EBNA1BP2*	-0.3804	0.024702	*EIF2AK2*	-0.2933	0.041918
TMEM106B	0.58307	0.000571	*SLC4A1AP*	-0.4583	0.02471	*SERP1*	0.35369	0.042003
GABRP	-0.8243	0.00058	*CCNI*	0.37871	0.024711	*PTGES*	0.47063	0.042111
CCT4	-0.5133	0.000593	*BMS1*	-0.362	0.024717	*RANBP1*	-0.3091	0.042132
HGSNAT	0.77285	0.000603	*ERLIN1*	-0.5637	0.024727	*UPK3B*	-0.9056	0.042142
CAPN8	0.75442	0.000612	*NLGN2*	-0.7887	0.024842	*CALM1*	-0.2976	0.042195
PCNX4	-0.6894	0.000618	*MIR4435-2HG*	-0.3992	0.024988	*DAP*	0.36487	0.042297
MCM5	-0.6465	0.000622	*LMO3*	1.19156	0.025046	*CKAP2*	-0.3805	0.042473
MXD1	0.86713	0.000622	*CWC27*	-0.4967	0.025104	*TRA2B*	-0.2806	0.042477
LSS	-0.6224	0.000623	*SRSF10*	-0.3683	0.025157	*SRSF2*	-0.349	0.042597
CAPG	0.75213	0.000658	*SORT1*	-0.4044	0.025265	*HOXA5*	-1.8149	0.042597
NPAS2	0.62834	0.00066	*LGALSL*	-0.652	0.025371	*AIF1L*	-0.4952	0.042697
YBX1	-0.4156	0.000663	*CFDP1*	-0.4131	0.025402	*SLC17A9*	-1.008	0.042723
UNC5B	1.41975	0.000663	*NSUN5P1*	-0.6077	0.025506	*HS2ST1*	-0.4984	0.042811
RABGAP1L	0.6649	0.000665	*CBS*	-0.4642	0.02551	*OBSCN*	-0.5636	0.042997
PLBD1	0.71353	0.00067	*ZNF605*	0.79454	0.025607	*SLC2A1*	-0.3388	0.043062
REPS2	1.34759	0.000679	*SPATS2L*	0.32159	0.025621	*ZNF706*	0.52101	0.043078
CARD9	-1.3107	0.000679	*RIPOR1*	-0.4917	0.025668	*MRPS9*	-0.44	0.04311

FAM83D	-0.89	0.000683	*ABCA12*	0.72963	0.025789	*HNMT*	0.64286	0.043133
H4C9	-1.1725	0.00069	*UQCRB*	0.36377	0.025792	*CENPU*	-0.6922	0.043222
STK24	0.53544	0.000715	*DEPTOR*	0.95195	0.025808	*SEC22A*	0.67449	0.043294
IGFBP4	-0.8151	0.000718	*SNORD14A*	1.3639	0.025862	*SCARNA6*	0.4991	0.043317
CHFR	0.98133	0.000721	*EIF4A3*	-0.4556	0.025887	*GANAB*	-0.2874	0.043357
IGFBP5	-1.529	0.000721	*NFATC3*	-0.4885	0.025932	*SERINC2*	0.78491	0.043455
TACC3	-0.5554	0.000722	*ERC1*	0.35824	0.025934	*CLDN9*	-1.4382	0.043524
CST6	-2.04	0.000722	*MYPN*	-1.6533	0.025972	*SLC40A1*	0.82913	0.04364
CAPN5	0.72927	0.000723	*MIER1*	-0.4175	0.02599	*EPS8*	0.29776	0.04381
FBXO5	-1.0241	0.00073	*ARIH1*	0.3969	0.026065	*C22orf46*	-0.4751	0.043848
BAZ1B	-0.5005	0.000731	*SNRPD2*	0.43032	0.026116	*DMBT1*	1.53553	0.043915
ADGRL2	-0.8266	0.000734	*SLC12A4*	-0.7678	0.026193	*NOS3*	-0.7139	0.043929
PPP2R1A	-0.5127	0.000742	*CREBRF*	0.55479	0.026231	*ATP5ME*	0.413	0.043999
FNTA	0.6015	0.000745	*NNT*	0.45318	0.026275	*LRRC8D*	-0.5173	0.044001
UNC13D	-0.6858	0.000745	*GSTP1*	0.31461	0.026399	*FBXO17*	-1.4237	0.044016
MAGED1	-0.7956	0.000749	*ALOX15*	-1.4662	0.026437	*IFITM10*	1.04219	0.044074
PPL	-0.492	0.000751	*EPB41L3*	1.14688	0.026458	*GNAI1*	-0.7047	0.044106
ST6GALNAC5	-1.9142	0.00076	*ARHGAP17*	-0.5562	0.026536	*DROSHA*	0.36675	0.044348
FBXO2	-1.2044	0.000768	*LMO4*	0.55479	0.026569	*AEBP2*	0.41045	0.0444
CHD2	0.45101	0.000773	*CDC25B*	-0.4242	0.026625	*BUB3*	-0.4366	0.044428
TICRR	-0.7934	0.000791	*NUAK2*	-1.0961	0.026728	*UBE2M*	0.53594	0.044486
LOC102723360	-2.1626	0.000792	*SLC7A11-AS1*	1.29247	0.026735	*SNX5*	-0.3436	0.044515
RAB9B	-0.727	0.000794	*ANP32E*	-0.4303	0.026992	*PER3*	0.52239	0.044667
NXPE3	-1.2436	0.0008	*RBM27*	-0.476	0.027014	*PITX1*	0.62092	0.044774
ATP1B1	-0.507	0.000805	*MAGEA6*	-1.9811	0.027071	*CKMT1B*	0.61955	0.044826
PHF19	-0.9293	0.000817	*H2BC17*	-0.5417	0.027187	*PLA2G4A*	0.84367	0.044841
PRR13	0.61905	0.000825	*NDUFA4*	0.55188	0.027202	*RPL34*	0.33143	0.044841

FARP1	0.52101	0.000846	*KIF1C*	-0.367	0.027227	*GEMIN4*	-0.5921	0.04497
NR4A2	-1.115	0.000865	*ARPC4*	0.44901	0.027346	*MZT2A*	0.60825	0.044975
PKMYT1	-1.3801	0.000878	*NOP56*	-0.3381	0.027439	*MISP*	0.42425	0.045127
CEACAM7	-1.4814	0.00088	*TM9SF2*	0.33944	0.02744	*GADD45GIP1*	-0.4187	0.045215
RPL32	0.47231	0.000883	*SPC24*	-0.7051	0.027441	*BTBD9*	0.68808	0.04539
NMT2	-0.9711	0.000888	*HEBP2*	0.46891	0.027447	*NRAS*	-0.449	0.045485
LDHA	-0.4259	0.000895	*GAPDH*	-0.2757	0.027486	*PPP6R1*	-0.2866	0.045514
NF2	-0.6842	0.000915	*AHCY*	-0.385	0.027491	*FAM168A*	-0.4158	0.045578
BIRC5	-0.6503	0.00092	*RTN4RL1*	-1.9927	0.027501	*RASA1*	-0.3412	0.045645
CENPO	-0.8895	0.000943	*USP3*	0.5206	0.027549	*GBP1*	-0.7215	0.045727
PRSS21	-2.3316	0.000956	*PDSS2*	0.65294	0.02757	*FANCG*	-0.7001	0.045906
NAGK	0.88849	0.000976	*PLOD1*	-0.4349	0.027634	*SLFN12*	-0.7383	0.045915
DTX4	0.60595	0.000989	*DLG1*	-0.3257	0.027658	*SEC23A*	-0.4095	0.045945
JADE2	-0.6215	0.000992	*GTF2A1*	-0.5215	0.02777	*GCC2*	0.32361	0.046005
RAB11FIP3	-0.9454	0.000992	*RHOD*	0.71578	0.027779	*SEPTIN3*	1.24271	0.046023
SMC2	-0.6482	0.001001	*PNPLA6*	-0.5698	0.027809	*GPR153*	0.71835	0.046102
ATP6V0E1	0.78637	0.001008	*ABCC5*	-0.5192	0.027833	*TLCD1*	0.88601	0.046123
ARSJ	-2.0315	0.001009	*SLC7A11*	-0.4216	0.028105	*ZNF316*	0.7241	0.046123
BRCA1	-0.615	0.00101	*PRKAG1*	0.5981	0.02821	*ZNF83*	0.6514	0.046186
PRRC2A	-0.47	0.001016	*MTBP*	-0.7705	0.028258	*GINS2*	-0.8225	0.04629
H2AC11	-0.6502	0.001021	*NDUFC2*	0.63809	0.028342	*ANKHD1-EIF4EBP3*	-0.488	0.046453
TNFRSF21	-0.4697	0.001023	*ETF1*	-0.3393	0.028434	*GRK3*	-0.6126	0.046569
EMILIN2	-1.5379	0.001023	*CLCN3*	0.4043	0.02847	*MTOR*	-0.3508	0.046636
ZC3H18	-0.6431	0.001042	*ARID5B*	-0.5726	0.028587	*RBM25*	-0.2769	0.046659
HOXA3	-1.1103	0.001045	*GLYR1*	-0.4588	0.028609	*PLEKHA5*	0.30506	0.046701
RPS28	0.68719	0.00105	*CHD1*	-0.3633	0.028626	*CLUAP1*	-0.5927	0.046819
RGPD6	0.58846	0.001054	*HNRNPR*	-0.3289	0.028676	*WDR43*	-0.3364	0.046835

LAMB3	0.54906	0.001063	*HMGN2*	-0.3071	0.02875	*EPS8L1*	0.45501	0.046996
RESF1	0.58283	0.001068	*FIGNL1*	-0.5777	0.028864	*MTFP1*	-0.7934	0.047097
AP1G2	0.61178	0.00107	*USP48*	0.3661	0.028886	*CEP85*	-0.5225	0.047155
NBEA	0.68331	0.001074	*SAMD12*	0.32242	0.028907	*KRT10*	0.73907	0.047231
ENG	-1.161	0.001085	*EEFSEC*	0.83996	0.028985	*SH3GLB2*	0.49693	0.047329
DFFA	-0.6192	0.001089	*COX7B*	0.53262	0.029028	*ATF3*	-0.5168	0.04752
CRELD2	-0.8726	0.001105	*SVIP*	0.65681	0.029039	*CYP4F12*	0.99127	0.047626
GATA2	-1.0634	0.001111	*PCTP*	0.61803	0.029047	*ZNF814*	-0.3966	0.047662
B2M	0.42617	0.001111	*SRGAP2B*	-0.479	0.029077	*EME2*	-0.6906	0.047836
NCAPG2	-0.7367	0.001113	*RNU5B-1*	-0.6368	0.029129	*SNORA79B*	0.744	0.047844
BRCA2	-0.7574	0.001116	*ARL14*	0.78421	0.029143	*PSRC1*	-0.7692	0.047867
PDE2A	1.31151	0.00113	*KIF13B*	0.44338	0.029153	*MICOS10*	0.45888	0.047876
SYNCRIP	-0.4525	0.001148	*ARFGEF1*	0.33917	0.029356	*TMBIM4*	0.75422	0.048163
TUBG1	-0.6566	0.00115	*PRSS12*	0.64735	0.029366	*ARMC5*	-0.9841	0.048165
CALU	-0.4824	0.001157	*HCFC1R1*	-0.874	0.029507	*DDX20*	-0.6056	0.048185
MSH2	-0.694	0.001177	*RAN*	-0.3707	0.029573	*RAD50*	-0.2975	0.048284
BRD8	-0.612	0.001222	*GRAMD1B*	-1.0305	0.029573	*ASB13*	0.89518	0.048296
CRAT	1.05435	0.001229	*PELP1*	-0.4361	0.029682	*FAR2*	0.70369	0.048351
DDX52	-0.5468	0.001234	*SLC39A14*	-0.445	0.02969	*NAA38*	0.66711	0.048435
SCRN1	-0.5227	0.001253	*NBPF1*	0.4442	0.029703	*PALM2AKAP2*	-0.3791	0.048444
DDX46	-0.4842	0.001254	*UBL7*	0.87258	0.029743	*LIMK1*	-0.552	0.048472
SGSM3	0.71519	0.001257	*RBIS*	0.64803	0.029754	*LTV1*	-0.3902	0.048669
SNORA63	1.05315	0.001267	*WDR6*	-0.4598	0.029851	*ABR*	0.35659	0.048683
MX2	-0.8252	0.001268	*KRT15*	0.58173	0.029872	*TP53BP2*	0.396	0.048717
GPX2	1.04866	0.001286	*PTPRF*	-0.3358	0.029961	*KRT80*	-0.4524	0.048733
HBEGF	-0.7605	0.00129	*LOC644669*	0.58147	0.029999	*CXCL16*	0.59318	0.048784
YWHAH	-0.6183	0.001309	*TAOK1*	0.30802	0.030003	*TSPAN18*	1.05152	0.048821

ARHGAP12	0.58592	0.001324	*STIP1*	-0.3058	0.030086	*PHF21A*	0.4975	0.04884
TUFM	-0.5047	0.001326	*RUVBL2*	-0.3759	0.030103	*E2F8*	-0.6645	0.048874
SLC4A4	-2.0146	0.001326	*MAGI1*	0.56676	0.030172	*CYCS*	0.32196	0.048913
FANCA	-0.9989	0.001329	*ENPP1*	-1.1965	0.030205	*ACTB*	-0.23	0.049134
PDIA6	-0.4258	0.001338	*PIMREG*	-0.9503	0.030215	*FLOT1*	-0.3153	0.049162
PHAX	-0.692	0.001348	*CPSF3*	-0.4205	0.030271	*ESF1*	-0.3819	0.049184
RSAD2	-0.8462	0.001352	*ATP5MK*	0.54215	0.0303	*KMT2D*	-0.2857	0.049202
MIR1248	-3.129	0.001352	*ZNF587B*	-0.4508	0.030376	*PELO*	-0.6255	0.049298
MIR3648-1	0.91564	0.00137	*GEN1*	-0.5588	0.03046	*CCNB2*	-0.444	0.049333
THSD7A	1.11812	0.001374	*ATXN2L*	-0.3651	0.030482	*SPATA6L*	0.79918	0.049352
SCEL	-0.707	0.001376	*ARL6IP5*	0.5856	0.030513	*TSC22D4*	-0.5127	0.049376
ITGB4	0.52232	0.001377	*TRNP1*	0.71606	0.030514	*UPF3B*	-0.4967	0.049604
SH3YL1	0.68448	0.001381	*PDAP1*	-0.3598	0.030522	*POLR2I*	0.5789	0.049623
FBLIM1	0.83864	0.001381	*FIBCD1*	1.08326	0.030552	*WWP2*	-0.4316	0.04965
SGK2	0.9892	0.001389	*NUP153*	-0.4028	0.030646	*MCM6*	-0.4039	0.049675
MAN2B1	0.90017	0.001394	*RERE*	0.37037	0.030654	*PES1*	-0.3624	0.049745
COX2	0.2322	0.049786	*B3GALT5*	0.55928	0.049941			

Table S5 Complete list of genes differentially expressed in response to 1,25(OH)$_2$D$_3$ supplementation in the quasi-mesenchymal pancreatic ductal adenocarcinoma subtype.

Gene ID	log2FC	p-value	Gene ID	log2FC	p-value	Gene ID	log2FC	p-value
ANO1	-4.80364	4.08E-39	*DNAAF11*	-2.25477	0.014045	*MXD4*	0.773081	0.005384
MUC3A	-3.31906	3.80E-31	*PLK2*	0.606546	0.014074	*CADM1*	-1.61311	0.005393
ALDH1A1	-4.92094	2.01E-26	*TUFM*	0.538614	0.014081	*BARX1*	-7.67706	0.005399
CTSE	-4.61625	6.76E-26	*NRCAM*	-2.32585	0.014141	*CDK6*	-0.85104	0.005428
CEACAM7	-8.58921	1.53E-25	*PTP4A1*	0.61449	0.014208	*SEZ6L2*	0.674952	0.005448
MUC6	-3.22523	1.17E-24	*CPZ*	0.926054	0.014222	*LOC644669*	-1.1931	0.005479
S100P	-3.97252	1.06E-23	*ELFN1*	-1.83285	0.014272	*NCLN*	0.702971	0.005516

PPP1R1B	-3.98658	8.55E-23	*TOM1*	0.677815	0.014368	*HSPBP1*	0.760532	0.005521
UGT1A6	-6.50236	5.53E-22	*MATN2*	-0.93202	0.014398	*SNORA7B*	1.285412	0.005522
RNA5S9	2.127882	1.90E-20	*GPR137*	0.748686	0.014408	*PRPF31*	0.623094	0.005538
OLFM4	-8.48667	5.25E-20	*ABO*	-0.77429	0.014411	*UBALD1*	0.97182	0.005549
KRAS	-2.36527	2.31E-19	*MRTFA*	-0.68871	0.01442	*TM4SF4*	-5.49494	0.005568
RNA5SP149	2.15259	1.25E-17	*NXN*	0.634681	0.014422	*CREB3L1*	-1.63495	0.005578
CAPN8	-5.57874	1.04E-16	*MINDY2*	-0.59321	0.014459	*SNORD60*	1.044436	0.005612
CCDC144B	-3.34383	2.64E-16	*ALG3*	0.633011	0.014548	*ZFP3*	-3.09732	0.005618
MUC5AC	-2.99647	1.47E-15	*ARHGEF38*	-1.33107	0.01457	*ZNF605*	-1.08624	0.005646
RNA5SP145	2.002679	1.54E-15	*ECHDC2*	-0.93086	0.014604	*PIBF1*	-0.81744	0.005678
TRIM29	-3.16312	1.62E-15	*ZNF792*	-1.42927	0.014625	*AKR1B1*	0.610257	0.005723
KRT13	-2.14809	6.53E-15	*POMK*	-0.5886	0.014678	*TRIM2*	-0.73768	0.005901
RNA5S1	1.618182	1.04E-12	*PDP1*	0.593567	0.014759	*RNU6-14P*	1.374954	0.005908
ALOX5	-3.22857	1.86E-12	*HRNR*	0.779286	0.01477	*ZNF598*	0.62829	0.005948
MXRA5	-5.03012	2.02E-12	*GSN*	-0.69751	0.014797	*LGALSL*	0.799175	0.006003
GPX2	-2.57067	9.44E-12	*CEACAM6*	-2.08381	0.014808	*SRP14*	0.586877	0.006038
MMP28	-6.23286	1.19E-11	*SH2B1*	0.71385	0.014831	*MYO6*	-0.70481	0.006061
VWDE	-3.69281	2.16E-11	*SNORA74D*	0.943769	0.014847	*NDUFV2*	0.696158	0.006063
SNORA44	2.244931	5.03E-11	*GRAMD1C*	-1.02345	0.014939	*ZNF813*	-1.57443	0.006069
SORBS1	-2.38164	6.12E-11	*STRAP*	-0.61349	0.014983	*ALG12*	0.75136	0.006085
BCAT1	-2.74298	7.44E-11	*STUB1*	0.56433	0.015035	*POR*	0.591071	0.006093
GJA5	-7.23784	8.67E-11	*PGAP6*	0.581052	0.015054	*GPR160*	-1.08898	0.006116
RNF128	-4.15191	1.03E-10	*LOC643201*	-3.50352	0.015153	*DROSHA*	-0.62109	0.006146
FYB1	-4.07871	2.10E-10	*ZNHIT2*	0.819778	0.015154	*NSMF*	0.705059	0.006234
GOLGA8A	-1.9077	2.14E-10	*PVR*	0.539677	0.015221	*MYG1*	0.90526	0.006318
RNA5SP481	2.562625	2.89E-10	*ISOC2*	0.63882	0.015249	*BAG6*	0.607039	0.006327
RNY4	1.421104	3.30E-10	*PRKCE*	0.78278	0.01528	*DNTTIP2*	0.593767	0.006341

PLA2G2F	-5.69215	3.57E-10	*ACTN1*	0.513385	0.015306	*UBASH3B*	-1.0061	0.006386
ALDH2	-1.95191	4.99E-10	*DHX38*	0.544464	0.01536	*NRARP*	0.89752	0.006395
ONECUT2	-2.17733	5.99E-10	*PHKG2*	0.671593	0.015367	*BAIAP2L2*	-1.01818	0.006424
PPARG	-1.59387	7.49E-10	*HINT1*	0.594412	0.015383	*FAM83F*	0.65809	0.006588
XIST	-6.26098	1.05E-09	*ATP6V1F*	0.692835	0.015451	*VASH1-AS1*	-2.98739	0.00662
DAPK1	-1.66287	1.21E-09	*LBH*	-1.65434	0.015489	*PPP2CA*	0.690646	0.006627
ERN2	-4.02737	1.76E-09	*ZNF600*	-1.24954	0.01561	*CAPN13*	-1.84133	0.006627
SLITRK6	-2.92175	2.11E-09	*CKMT1B*	-0.86727	0.015638	*CMIP*	0.642842	0.006696
LYPD2	-7.50606	3.00E-09	*RNPS1*	0.515864	0.015647	*ARHGAP27P1-BPTFP1-KPNA2P3*	-1.08476	0.006696
HPGD	-4.15256	5.47E-09	*SH3BGRL3*	0.587064	0.015663	*BHLHE41*	-2.50427	0.006766
SAA2	1.252497	5.73E-09	*DAXX*	0.579488	0.01569	*DNAJB1*	0.582477	0.006786
RNA5SP199	2.100936	6.59E-09	*TFPT*	0.744142	0.015695	*PLA2G2C*	-2.41433	0.006818
RN7SL4P	1.186985	6.64E-09	*TOPORS*	0.567227	0.015714	*UGT1A10*	-9.86654	0.006819
VILL	-3.22625	7.26E-09	*ANKRD36*	-0.55045	0.01575	*RHNO1*	-0.99796	0.006827
RNU6-17P	2.175594	7.34E-09	*SNORA10*	1.032241	0.015765	*NONO*	0.573513	0.00684
ANXA10	-4.88813	8.27E-09	*CORO7-PAM16*	3.076454	0.015766	*HRCT1*	1.536013	0.006878
G6PD	1.189283	8.30E-09	*SEL1L*	0.586773	0.015788	*SREBF1*	-0.63988	0.00688
SNORA18	1.420763	1.29E-08	*TYMS*	0.60806	0.015839	*GNAI2*	0.569905	0.006885
KLK10	-2.46702	1.32E-08	*ATP9A*	-0.61356	0.01588	*LGALS9*	-0.75259	0.006893
PAX7	-6.72997	2.36E-08	*DCXR*	0.651094	0.015887	*ANTXR2*	-0.76662	0.006895
SLCO1B3	-1.73323	2.71E-08	*CHN2*	-2.56966	0.01591	*MAP1LC3B*	0.643824	0.006931
ADAM23	-2.69714	4.52E-08	*RAD54B*	-0.9835	0.015948	*PLEKHA5*	-0.73015	0.00699
LOC117779438	-3.51447	5.42E-08	*SYTL4*	-0.76458	0.01606	*TGFB2*	0.920308	0.006995
PDE4D	-1.90208	5.77E-08	*CTSD*	0.469057	0.016096	*TMEM205*	0.704448	0.007007
SAA1	1.179919	5.89E-08	*AFAP1*	-0.58182	0.016134	*BMI1*	-0.88558	0.007014
GPRC5A	-1.31052	6.19E-08	*CLDN1*	0.589929	0.016147	*SLC25A22*	0.748174	0.007026
ADAM8	-2.92	7.20E-08	*NR5A2*	-1.34972	0.016152	*MIR4458HG*	-2.11265	0.007092

TESC	-3.19678	7.49E-08	*DMAC1*	0.789233	0.016262	*ADARB1*	0.755634	0.007125
SNORD22	1.158916	8.14E-08	*MED24*	0.588755	0.016301	*C19orf53*	0.669551	0.007129
SLC45A3	-2.08836	1.01E-07	*LRRN4*	-2.86707	0.016314	*TCIM*	-3.55237	0.007158
SLC44A4	-2.5048	1.03E-07	*H2AW*	0.792622	0.016322	*MLH3*	-0.78143	0.007215
SFRP1	-6.84234	1.12E-07	*HIP1*	0.657	0.016353	*ACOT13*	0.704787	0.007264
SH3TC1	-1.95853	1.14E-07	*KITLG*	-0.74165	0.016354	*OGFR*	0.634468	0.007295
C1orf116	-1.51521	1.28E-07	*CFDP1*	0.550942	0.016367	*SLC35A4*	0.670154	0.007315
PADI1	-1.98035	1.50E-07	*RPS6KA5*	0.645479	0.016384	*MPHOSPH6*	0.74056	0.007344
ETFRF1	-1.84286	1.56E-07	*FIZ1*	0.784904	0.016394	*EEF1A2*	0.741248	0.007384
SLC26A9	-3.41901	1.72E-07	*CTAGE4*	-1.3893	0.016435	*RNA5-8SN2*	0.684213	0.007406
CPVL	-2.15958	1.88E-07	*PDAP1*	0.521113	0.016505	*MATR3*	0.719781	0.007425
TNNI2	-5.33705	1.93E-07	*SNCG*	0.573477	0.016512	*CIAO2B*	0.760017	0.007457
KRT17	-5.07769	2.40E-07	*LITAF*	0.589813	0.016554	*CCNY*	0.64085	0.007458
CYP3A5	-1.70047	3.26E-07	*NOB1*	0.595192	0.016659	*RXYLT1*	-0.91211	0.007462
WNT7A	-4.40324	3.30E-07	*COQ9*	0.620348	0.016726	*PES1*	0.606666	0.007483
TM4SF18	-3.30272	3.98E-07	*MTFP1*	0.737105	0.016741	*NEK10*	-1.69608	0.00749
USP32P1	-3.01306	4.02E-07	*BMP3*	-2.16582	0.016742	*NDUFS8*	0.671204	0.007505
TMEM178B	-3.44869	4.53E-07	*TFDP2*	-0.58529	0.01684	*RNY3*	0.615981	0.00752
SPART	-2.30181	4.58E-07	*CTSL*	0.518583	0.016869	*MCFD2*	0.602492	0.007529
MUC1	-1.50671	5.79E-07	*SLC1A3*	0.625037	0.016876	*ATP6V1C2*	-1.56616	0.007564
WWC3	-3.05831	6.56E-07	*RPS15*	0.527675	0.016876	*VASN*	0.799553	0.007574
IL1RN	-2.74597	6.90E-07	*SLC38A2*	0.521748	0.016882	*FAM43A*	0.886263	0.007574
PTX3	1.697151	8.42E-07	*ENTPD5*	-0.74328	0.016882	*NME7*	0.906837	0.007582
SMARCA2	-1.42735	9.24E-07	*MANSC1*	-0.67096	0.016934	*PRKCA*	-0.69636	0.007616
SYT8	-3.21984	9.61E-07	*USF3*	-0.55733	0.016941	*IFITM3*	0.724421	0.007653
UGT1A7	-4.52606	1.01E-06	*CARHSP1*	0.636364	0.017086	*CST2*	-2.58591	0.007679
UBXN10	-4.82371	1.12E-06	*SHC1*	0.548128	0.0171	*FNTA*	-0.72589	0.007712

SNORA2C	1.478427	1.17E-06	*ITGB5*	-0.58066	0.017105	*PGM2L1*	0.630994	0.00774
TSPYL5	-5.91924	1.25E-06	*EHBP1*	0.554539	0.017136	*ADRB2*	0.837372	0.007794
CEACAM5	-3.82816	1.29E-06	*SLC12A7*	0.508133	0.017218	*RGS2*	-1.19794	0.0078
CALB2	1.287536	1.39E-06	*ISG15*	0.560837	0.01727	*NQO1*	0.560033	0.007859
G0S2	1.49888	1.44E-06	*ANKRD11*	0.48871	0.017279	*PDE9A*	0.761868	0.00786
ITGB6	-1.72702	1.48E-06	*TANC1*	-0.54453	0.017339	*TNFAIP2*	0.706912	0.007923
SRGAP1	-1.52476	1.73E-06	*LRP2*	-1.82356	0.017352	*SNORD62A*	1.056486	0.00793
FXYD3	-1.62614	1.81E-06	*FAU*	0.531645	0.017366	*EPHA2*	-0.68804	0.007961
TFF2	-6.52885	2.03E-06	*AATF*	0.498553	0.017391	*CDH1*	0.552719	0.007971
GALNT5	-1.4568	2.04E-06	*CASP1*	1.030968	0.017414	*COL4A1*	-1.40488	0.007972
UGT1A1	-3.15338	2.27E-06	*STAC*	-3.02241	0.017472	*CEBPD*	0.745226	0.008028
SNORA70	1.586687	2.28E-06	*FARP1*	-0.54519	0.017474	*GATM*	-1.27229	0.00807
CXCL1	1.180968	2.34E-06	*CXCL3*	1.044887	0.017524	*LAMA3*	-0.92182	0.008081
GSTM3	-1.89557	2.35E-06	*ANXA4*	-0.53593	0.017524	*NAMPT*	0.631495	0.008086
EPAS1	1.068993	2.61E-06	*GALNT10*	0.584572	0.017557	*GPR153*	-1.29881	0.008206
CHFR	-1.98397	2.75E-06	*HOXB8*	-2.23066	0.017573	*CARD9*	0.947074	0.008228
FADS2	-1.48818	3.62E-06	*POLR3H*	0.603478	0.017604	*ZDBF2*	-3.04102	0.008272
RNA5SP202	1.604725	4.12E-06	*NNT*	-0.6862	0.01762	*KLF5*	-0.64078	0.0083
CXCL5	-5.15408	4.54E-06	*UBE2D2*	0.706468	0.017632	*SSR4*	0.765991	0.008347
HSD17B2	-2.23119	4.78E-06	*RNF24*	0.571615	0.017659	*FLNA*	0.659326	0.008403
STARD13	-2.02339	4.85E-06	*WDR91*	0.797471	0.017763	*FOSB*	0.781005	0.008436
FBP1	-6.00225	5.04E-06	*MFSD12*	0.631176	0.01777	*DIXDC1*	-1.41926	0.008535
MUC5B	-1.13667	5.09E-06	*SNORD116-8*	1.401462	0.01777	*RNU2-1*	0.721202	0.008551
CCN1	1.059631	5.25E-06	*POLR2C*	0.562092	0.017807	*ESPL1*	-0.90953	0.008573
RNA5SP141	1.58909	5.26E-06	*MED14*	-0.59891	0.017994	*ADGRF5*	-1.22609	0.008627
PAG1	-1.42256	5.61E-06	*TEX15*	-2.08923	0.018012	*CALU*	0.537799	0.008628
ARL14	-2.22446	6.49E-06	*SNORD17*	0.604259	0.018031	*RCC1*	0.630695	0.008689

COL17A1	-2.21836	6.57E-06	*MANF*	0.584535	0.018137	*CHMP2A*	0.604026	0.008751
AATK	-2.11288	6.67E-06	*PLEK2*	-0.92242	0.018221	*PYROXD1*	-0.94568	0.008771
CCDC144A	-1.74662	6.80E-06	*RPP25*	-1.18586	0.018285	*ALG14*	0.905576	0.008788
HNF1B	-2.28579	7.15E-06	*NIBAN1*	0.610536	0.018294	*ZNF488*	-1.92168	0.008792
SNORA80E	1.524186	7.32E-06	*LXN*	-0.96611	0.018328	*IL17C*	1.530406	0.008807
LINC01819	-3.20422	9.54E-06	*PDE2A*	0.804277	0.018362	*GAPDH*	0.513493	0.008808
MT2A	1.077865	9.57E-06	*SNRPB*	0.50881	0.01837	*NPNT*	-3.66826	0.008812
TNIP1	0.909209	9.88E-06	*TGIF1*	0.641657	0.018472	*RNU6-5P*	0.692702	0.008815
INSR	-2.15232	1.01E-05	*ATP6V0B*	0.63943	0.018508	*TBC1D16*	0.614178	0.00886
WFDC2	1.292029	1.06E-05	*SSH1*	0.570323	0.018571	*SERP1*	-0.59847	0.008895
NFKBIA	1.05676	1.08E-05	*RFX3*	-0.76165	0.018588	*NBEA*	-0.91459	0.008938
SNORA23	1.170249	0.000012	*DPP9*	0.560668	0.018641	*RNU6ATAC*	0.896582	0.00894
FLNC	-3.66514	1.24E-05	*MIR210HG*	-1.31384	0.018666	*SLC37A2*	0.852325	0.008967
SH3PXD2B	1.008486	1.25E-05	*EHD2*	0.654053	0.01872	*HLA-V*	-1.09076	0.008993
PCSK9	-3.44948	1.39E-05	*TMSB10*	0.537102	0.018759	*PLCXD1*	-0.91238	0.009042
MSLN	-2.9286	1.41E-05	*KIAA1549L*	-1.19862	0.018761	*SOCS3*	0.827112	0.009071
PRSS3	-2.70618	1.58E-05	*NBDY*	0.7496	0.018893	*ZNF558*	-1.69194	0.009102
HID1	-1.31665	1.63E-05	*BCLAF1*	0.496573	0.018924	*BNC2*	-2.49941	0.009103
PLXDC2	-3.57881	0.000019	*EPHB3*	0.636235	0.018983	*RHOC*	0.605806	0.009111
AKAP12	1.142426	1.94E-05	*TMEM208*	0.75079	0.018989	*EIF4A1*	0.513907	0.009155
FAM13A	-1.5384	1.97E-05	*NCOA7*	0.540215	0.018998	*PLEKHS1*	-1.45194	0.009157
NRP2	-1.48924	2.04E-05	*USP48*	-0.51339	0.01904	*LRCH1*	-0.79194	0.009187
SCUBE1	-1.93812	2.07E-05	*SFMBT1*	0.663121	0.019089	*SPNS2*	-0.76308	0.009207
SNORD14C	2.448377	2.11E-05	*ZNHIT1*	0.653905	0.019099	*PDPR*	0.624845	0.009255
ZBTB7C	-3.01015	2.32E-05	*TLR4*	-1.07325	0.019221	*RPL23*	0.549486	0.009285
SH3RF1	-1.23442	2.41E-05	*KDM7A*	-0.84942	0.019248	*RNU4-2*	0.689975	0.00929
PI3	1.0666	2.41E-05	*MYO10*	0.49135	0.019261	*FRMD4A*	-1.03155	0.009357

VSIG2	-4.96315	2.56E-05	*HINT2*	0.796562	0.019302	*MEST*	0.769355	0.009472
SLC16A5	-1.1428	2.59E-05	*ST3GAL4*	-0.76732	0.019321	*PRORP*	0.757163	0.009475
SPINK4	-5.45838	2.62E-05	*SNORD13*	0.96487	0.019379	*FKBP4*	-0.59341	0.009482
TMEM47	-1.89686	2.65E-05	*GIMAP1*	-2.23355	0.019399	*NECTIN3*	-0.9137	0.009684
CAPNS1	0.977146	2.79E-05	*KCNN4*	-0.95098	0.019432	*PARD3*	0.581729	0.009698
KIF13B	-1.2219	2.84E-05	*TXNDC12*	0.60565	0.019452	*CD81*	0.603191	0.009702
FTL	0.90306	2.89E-05	*ANKRD36B*	-0.63496	0.019457	*LMNB2*	0.577648	0.009804
STMN3	1.01394	3.16E-05	*SNRPD2*	0.540886	0.019472	*CNN3*	0.58511	0.009869
ALDH3A1	-1.36873	3.25E-05	*TMEM132A*	0.620196	0.019566	*GUCY1A2*	-2.73622	0.009896
NPHP3-ACAD11	-5.14162	3.36E-05	*TCEA2*	0.71588	0.019572	*ZHX3*	0.712276	0.00991
GLIPR1	1.279779	3.39E-05	*PHLDB1*	-0.6329	0.019579	*G3BP1*	0.597064	0.009933
RNA5SP150	1.527923	3.62E-05	*KBTBD8*	-2.46301	0.019626	*PGD*	0.593827	0.010072
BTBD16	-4.63125	3.91E-05	*VPS13B*	-0.53954	0.019688	*USP28*	-0.815	0.010109
LINC00472	-1.22513	4.01E-05	*NFIX*	0.693928	0.019786	*SNHG1*	0.615876	0.010165
ZNF229	-3.5022	0.000041	*RAPGEF4*	-2.50013	0.019822	*SNAPC1*	0.675803	0.010266
SGK2	-1.84904	4.15E-05	*ZMAT2*	0.559014	0.019858	*TAF7*	0.550974	0.010278
TBC1D4	1.018989	4.16E-05	*GPR39*	-1.16754	0.019873	*TAPBP*	0.54189	0.010278
MUC16	-4.0403	4.51E-05	*MERTK*	0.882195	0.019894	*MT1E*	0.889779	0.010322
ZNF354C	-3.57516	5.02E-05	*RPL29*	0.495352	0.019901	*NUAK2*	0.941256	0.010399
UGT1A4	-6.47332	5.16E-05	*FGF19*	-4.85892	0.019922	*ITGA6*	-0.55225	0.010413
KLK6	-4.12843	5.88E-05	*NCKAP5*	1.246257	0.019949	*PER3*	-0.83722	0.01043
SNORD33	1.464819	6.08E-05	*DDIAS*	-0.875	0.019951	*CFAP20*	0.714052	0.010492
SNORA24	1.371464	6.25E-05	*KCNK6*	-0.80248	0.01996	*SNORA21*	-2.68433	0.010512
SNORD15A	0.888215	6.33E-05	*TNC*	0.826273	0.019987	*TMA7*	0.620384	0.010527
CXCL8	1.23942	6.51E-05	*MEX3C*	0.667958	0.020001	*ZNF700*	-1.49583	0.010597
RPS29	1.030792	6.55E-05	*VAPA*	0.652016	0.020023	*DCP1B*	-1.23415	0.010632
ITGBL1	-1.83075	6.55E-05	*ADAMTS9*	-1.21808	0.020085	*PLAT*	-2.39397	0.010698

HOTAIRM1	-4.07035	6.86E-05	*HDAC5*	0.599837	0.020086	*STMN1*	0.587225	0.010714
LRRC61	1.161418	7.04E-05	*UBE2G2*	0.516692	0.02012	*MARVELD1*	0.642477	0.010792
RNA5SP298	1.333748	7.13E-05	*NDUFB10*	0.594619	0.020129	*MCRIP1*	0.779135	0.010795
SERPINB9	1.017333	7.45E-05	*INPP1*	-0.84695	0.02015	*PODXL2*	0.697815	0.010798
ANKRD33B	1.059541	7.55E-05	*FRMD3*	0.836947	0.020179	*MTSS2*	0.621805	0.010803
FAM83A	-1.58144	7.64E-05	*CSDE1*	0.507614	0.020259	*RACK1*	0.505522	0.010844
MIR1248	2.402629	8.04E-05	*ZNF737*	-1.12974	0.020347	*USP14*	0.6946	0.010851
CHST6	-1.83143	8.09E-05	*GAMT*	1.018502	0.020435	*ERICH5*	-3.25304	0.010881
ICAM1	0.957214	8.18E-05	*MAGEA6*	0.94969	0.020448	*RIMKLA*	0.884847	0.010915
KDM5A	-0.93265	8.21E-05	*B3GALT5*	-3.23691	0.020469	*ENGASE*	-1.03949	0.011006
MON2	-1.01761	8.57E-05	*TMEM18*	0.651845	0.020556	*FBLIM1*	-0.73017	0.011035
SNORD16	1.614079	0.000088	*DCTN1*	0.477903	0.020559	*LPCAT4*	-0.82761	0.01108
MYH14	-2.89566	9.03E-05	*RPL9P8*	-0.93877	0.020591	*SPICE1*	-0.85746	0.01109
S100A4	-1.11903	9.16E-05	*LRG1*	0.603114	0.020629	*MIRLET7IHG*	-0.83535	0.011107
SNORD96A	1.939455	0.000094	*GDF15*	0.668782	0.020641	*LOC441666*	-1.3809	0.011126
KLK11	-3.1307	9.65E-05	*CES2*	0.562892	0.020679	*RPL18A*	0.524113	0.011208
FAM174B	-3.05169	9.73E-05	*KRT19P1*	-2.82688	0.020819	*FHL1*	0.863275	0.011233
CRAT	-1.57814	9.85E-05	*ADGRE5*	0.571918	0.020913	*ZNF559*	-1.82686	0.011308
SNORD116-17	3.239313	0.000105	*SNRNP27*	0.569064	0.020979	*LINC00894*	-1.13612	0.011322
POF1B	-1.97564	0.000105	*NPTN*	0.532467	0.021006	*EPN1*	0.694627	0.011328
ITPRID2	-0.78027	0.000108	*RBCK1*	0.605003	0.021048	*ERGIC3*	0.528473	0.011348
ABHD17C	-1.29935	0.00011	*AMOTL2*	0.518118	0.021063	*SNN*	0.855216	0.011422
CFB	0.91908	0.000114	*MMD*	0.715849	0.021155	*ZFP14*	-1.06046	0.011461
CST1	-8.07313	0.000114	*NAPG*	0.66259	0.021247	*PPL*	0.545257	0.011537
SNORD45A	1.174812	0.000115	*EIF3C*	0.479895	0.021313	*IER3*	0.532851	0.011555
TINAGL1	-1.16367	0.000121	*AHNAK*	-0.47764	0.021339	*TIMP1*	0.677572	0.011615
IDH2	0.967423	0.000122	*EIF2S2*	0.49169	0.02135	*SF3A1*	0.689773	0.011651

MICU3	-4.52971	0.000123	*FAM156B*	-2.14346	0.021411	*TUBG1*	0.577659	0.011715
SNORD8	1.018221	0.000129	*TULP3*	-0.68537	0.021414	*RAB8A*	0.587152	0.011728
TNIK	-1.23227	0.00013	*DNAJA2*	0.505522	0.021455	*CYBA*	0.653195	0.011766
EPS8L3	-2.67697	0.000138	*MROH2A*	-3.11272	0.021473	*ZNF10*	-2.43805	0.011784
RGPD2	-2.55975	0.000138	*DEF8*	0.724061	0.021482	*FOS*	-0.6191	0.011832
CDC42EP1	-1.06344	0.000141	*RPL36*	0.537526	0.021521	*MTHFD2*	0.604465	0.011918
COL4A3	-2.43319	0.000142	*GNG2*	-1.36934	0.021558	*LGALS1*	0.638123	0.011973
PLBD1	-1.03877	0.000143	*NBPF3*	-0.71087	0.021578	*RNU5E-1*	0.923379	0.011993
PSME1	0.851995	0.000145	*RASD2*	0.973783	0.021604	*ITK*	-1.67788	0.01201
RANBP17	-1.9518	0.000146	*APBA2*	-1.67332	0.021606	*SESTD1*	-0.82486	0.012036
LOC101928120	3.044592	0.000146	*CENPB*	0.540225	0.021628	*NAA38*	0.744964	0.012064
NINJ1	1.00291	0.000149	*ZNF100*	-1.36908	0.021694	*PFDN1*	0.703665	0.012163
IL1A	1.068105	0.000155	*PISD*	0.62499	0.021776	*PABPN1*	0.536006	0.0122
PTGS2	1.13876	0.000169	*EDAR*	-1.88532	0.021842	*ZBTB40*	-0.60129	0.012296
MMP19	-3.14551	0.000171	*RAB30*	-0.974	0.021863	*HSPA4*	0.567478	0.012365
SNORA81	0.988723	0.000188	*GBP1*	0.746947	0.021887	*IMPA2*	0.734956	0.012409
AGR3	-5.10509	0.00019	*PEG10*	0.504142	0.021987	*IL7R*	-1.36359	0.012429
FRY	-2.73016	0.000196	*KLF10*	0.531589	0.02204	*SELENOO*	0.676925	0.012434
PEDS1-UBE2V1	-4.03769	0.000207	*EDN1*	1.05821	0.022043	*ARHGAP40*	1.066115	0.012442
SNORA65	1.166649	0.000217	*B4GALT5*	0.510773	0.022059	*RRP1B*	0.559976	0.012469
LYZ	-1.71184	0.000218	*FADS3*	0.603811	0.022079	*ZNF528*	-1.23109	0.012483
IL1B	0.95319	0.000225	*PLEKHH2*	-0.77123	0.022102	*UBAP1*	0.570045	0.012537
SNORA54	1.641641	0.000228	*ILDR1*	-2.1656	0.022164	*ELMO3*	0.795678	0.012599
ZNF570	-2.31225	0.000239	*LRIG3*	-0.87139	0.022166	*HOXA10*	-2.08463	0.012613
PLAU	0.800041	0.000242	*NDUFA2*	0.675121	0.022287	*EPHX1*	0.623791	0.01268
B4GALT1	0.794206	0.000248	*MSMO1*	-0.68333	0.022305	*FUCA1*	0.579966	0.01273
UGT1A9	-5.76429	0.000253	*DEXI*	0.753997	0.022362	*SIX1*	-1.51648	0.012752

RTL10	1.050384	0.000254	*APOL6*	0.5671	0.02239	*ASNS*	0.71694	0.012804
ELFN2	-1.79495	0.000254	*PRKACA*	0.546695	0.02241	*GAK*	-0.70482	0.012811
DHRS9	-1.84162	0.00026	*SCAMP4*	0.558274	0.022534	*SNORA40*	1.428542	0.012816
CLGN	1.049949	0.000264	*PRSS21*	0.794957	0.022637	*CSF1*	0.801592	0.01282
SLC7A5	0.815322	0.00027	*KCNQ1*	-1.12581	0.02269	*METTL7A*	-0.87919	0.012857
PHLDB2	0.935521	0.000273	*SLC5A1*	-2.06129	0.02284	*TRIM28*	0.704205	0.013059
SERPINB5	-1.41358	0.000278	*RNASEK-C17orf49*	1.532212	0.022934	*SIRPA*	0.670698	0.013064
CEMIP2	-0.77972	0.00029	*NOMO2*	0.566941	0.02294	*SNORD99*	0.93928	0.013085
CCND2	-3.67803	0.000296	*ADAM9*	-0.5564	0.022946	*SPATA13*	-0.72066	0.013086
RASGRF1	-2.62389	0.000307	*RPS15A*	0.503965	0.02296	*C4BPB*	-1.22587	0.013141
CCDC77	-1.19531	0.000348	*IGSF10*	1.452154	0.023061	*SREK1*	0.547488	0.013146
RALBP1	0.827962	0.000358	*ENG*	0.69199	0.023084	*PIEZO1*	0.580662	0.01319
VTRNA1-1	1.208698	0.000362	*IFI27L2*	0.992541	0.023085	*FAM118A*	-0.78716	0.013214
TMEM45B	-1.30148	0.000373	*DNAI7*	-1.68569	0.023228	*PSMD7*	0.526782	0.013215
PDE4C	-8.35233	0.000377	*PLBD2*	0.555299	0.023271	*RNA5SP429*	0.637809	0.013243
MECOM	-1.17877	0.000396	*KIF3A*	0.538006	0.023278	*PPP1R15A*	0.582178	0.013247
CKMT1A	-1.73701	0.000399	*IRAK2*	0.619635	0.023325	*TWSG1*	0.582178	0.013259
ZDHHC20	-1.07006	0.000411	*TMSB4XP4*	2.418035	0.023382	*TICAM2*	-2.75585	0.013266
LCP1	0.951543	0.000414	*FHOD1*	0.60556	0.023399	*UBE2S*	0.67559	0.013277
ID3	1.245595	0.000417	*PSMB8*	0.644003	0.023445	*NCAM1*	-2.3094	0.013363
MUCL3	-3.12937	0.000417	*PSME3IP1*	0.568958	0.023457	*KRTCAP2*	0.739235	0.013395
RPS2	0.803077	0.000436	*MCC*	0.572709	0.023606	*TUBB3*	0.680008	0.01345
INTS8	-0.89103	0.000456	*CARNS1*	-1.55864	0.023622	*RTN4RL1*	0.911483	0.013453
KNL1	-0.83974	0.000457	*KIRREL3*	-1.52954	0.023628	*BCL2L15*	-1.0205	0.013519
TMC1	-1.88289	0.000459	*UBB*	0.446186	0.023668	*SHROOM2*	-1.63103	0.013736
MGAM2	-2.55479	0.000474	*RYR1*	-1.50861	0.023735	*PDP2*	0.729602	0.013747
HP	1.567875	0.000495	*SIGMAR1*	0.532603	0.023875	*HOXB-AS3*	-1.91199	0.01385

AKR1B10	-1.0797	0.000499	*RPL36AL*	0.513652	0.023901	*SDR16C5*	-1.50351	0.013878
SNORA11	2.038089	0.000501	*SLC7A11-AS1*	-1.0942	0.023931	*SNORA47*	1.411393	0.01388
TMBIM1	-0.8088	0.000507	*FAM126B*	-0.66164	0.023933	*HBEGF*	0.654461	0.013899
GPT2	-1.70962	0.000509	*PBX1*	-0.71533	0.023936	*RASL11A*	-1.8315	0.0139
SOD2	0.754375	0.000514	*TXN*	0.529056	0.023949	*CYP2B7P*	1.255181	0.013902
MDFIC	-2.34515	0.000526	*PKD1*	0.564193	0.023958	*PLAC8*	-0.72262	0.013945
SLPI	0.837283	0.000529	*MMP15*	0.572302	0.023975	*PTTG1IP*	0.528924	0.013967
ZNF91	-2.11865	0.000539	*MRPL28*	0.596174	0.024008	*TNFAIP3*	0.757187	0.013983
SNHG17	0.78837	0.000546	*DCAF11*	0.586841	0.024024	*RAB12*	0.646998	0.013991
TACSTD2	0.778329	0.000548	*CDC25B*	0.526323	0.024063	*PIK3R2*	0.663873	0.014013
GRHL1	-1.04051	0.000555	*CTPS1*	0.569875	0.024074	*TAP1*	0.576863	0.014026
MAST4	-1.0003	0.000589	*TUBA1A*	0.772206	0.02411	*NRG3*	-2.8081	0.014036
TRIM31	-4.47144	0.000618	*P4HA2*	0.491271	0.024189	*FAM20C*	0.782763	0.037278
PIK3C2G	-3.18211	0.000633	*PROSER1*	-0.67997	0.024206	*ZMYM6*	-0.70805	0.037512
LDB3	-2.58724	0.000655	*MAGEA2B*	1.807518	0.024212	*MAN1A1*	0.475037	0.037543
INPP5D	-1.99621	0.000658	*ISYNA1*	0.664501	0.024218	*ARRB1*	-0.49225	0.037554
CXCL2	1.27481	0.00066	*SARDH*	0.889206	0.024253	*SNORD104*	0.849376	0.037563
HGSNAT	-1.13368	0.000665	*PARM1*	-0.8158	0.024322	*MAPK12*	0.582022	0.0376
SNORA20	0.939176	0.000698	*CHST12*	0.633222	0.024388	*GATA6*	-0.97632	0.03761
CYP4F12	-2.40415	0.000699	*MCTS1*	0.678443	0.024477	*PDZK1IP1*	0.815571	0.037695
DOCK8	-1.16865	0.000714	*PTPRB*	-0.83118	0.024506	*WWC1*	0.516405	0.037718
HLA-C	0.656553	0.000733	*FAM3B*	-2.66363	0.024588	*KRT6B*	1.605317	0.037754
SIK1B	0.935079	0.000734	*ZNF285*	-1.81457	0.024635	*SHMT2*	0.499156	0.037993
CALD1	0.869757	0.000753	*COX7A2*	0.574149	0.02464	*NDRG1*	-0.69929	0.038078
ZNF83	-1.56189	0.000767	*YWHAG*	0.472346	0.024685	*BBLN*	0.564839	0.038129
SNORA7A	1.13214	0.000781	*KARS1*	0.511206	0.024766	*TRIB3*	0.633915	0.038131
U2AF1	0.769461	0.000783	*ADD2*	-1.59551	0.024767	*LGALS3*	0.485224	0.038158

EPHB2	0.92252	0.000788	*C11orf98*	0.592017	0.024781	*BTBD11*	0.838027	0.038174
SPTSSA	0.921116	0.000798	*NOP56*	0.518614	0.024837	*TAF13*	0.658335	0.03818
PKIA	-5.31701	0.000805	*PSMC1*	0.569526	0.025003	*MCUR1*	0.52667	0.038239
ADAM19	-2.15581	0.000814	*HNRNPA0*	0.534649	0.025059	*SPIN1*	0.523226	0.038274
ZNF845	-1.74937	0.00083	*NOMO1*	0.544267	0.025066	*ADAM32*	-0.58681	0.038403
SSPN	-1.63496	0.00083	*DBN1*	0.576823	0.025068	*GSPT2*	-1.95859	0.038434
PIP5K1B	-4.51165	0.00084	*BORCS8-MEF2B*	1.453091	0.025103	*SNRPC*	0.486103	0.03844
CLMN	0.693705	0.000841	*GRN*	0.461806	0.025191	*ZFP36L1*	-0.4872	0.038472
CHMP1B	0.725189	0.000854	*ST3GAL6*	-1.2479	0.025197	*PDXK*	0.463486	0.038494
SNHG11	1.178724	0.000868	*LOC105373159*	-1.28668	0.025265	*ERV3-1*	0.594614	0.038628
B4GALNT3	-1.4861	0.000885	*CRIP2*	0.63564	0.025276	*NCL*	0.397212	0.03871
RAPGEF3	-1.78937	0.000889	*NAXE*	0.59095	0.025284	*PSD3*	-0.59728	0.038745
MAOA	-1.45187	0.000897	*HIRIP3*	0.780501	0.025356	*SNORA52*	1.358842	0.038749
SLC43A3	-1.52361	0.000916	*ZNFX1*	0.484863	0.025498	*DUSP23*	-1.956	0.03875
LAD1	-1.11911	0.000946	*MAX*	0.655028	0.025509	*PPP1R12B*	-0.59306	0.038791
THBD	1.051175	0.000947	*ZDHHC11B*	-1.25155	0.025516	*ATXN2L*	0.479094	0.039021
GLS	-0.77801	0.00097	*UQCRH*	0.545193	0.025558	*TIMP3*	-0.78364	0.039049
UCP2	-2.66118	0.000972	*CLDN3*	-0.84242	0.025564	*SOX5*	-1.92502	0.039144
RGPD8	-1.07832	0.000972	*GLB1L2*	-0.83479	0.025613	*AGPAT3*	0.480081	0.039231
CDR2L	-1.05584	0.000977	*DST*	-0.51893	0.025761	*ID1*	0.512991	0.039241
GPX3	0.946532	0.000983	*SHISA5*	0.560441	0.025894	*DNAJC8*	0.456108	0.039245
VAC14	0.822637	0.000984	*PAQR4*	0.725853	0.025905	*STK17B*	0.527836	0.03931
RSAD2	-0.85131	0.000998	*SLFN5*	0.572696	0.025917	*SREK1IP1*	0.546485	0.039429
ZDHHC2	-1.18666	0.001019	*NUDT21*	0.523211	0.025924	*GSTZ1*	0.659303	0.039435
OSBPL5	0.801732	0.001033	*ERBB3*	-0.55486	0.02596	*MTCH2*	0.490874	0.03944
ADAMTS17	-3.18367	0.001046	*AKT1*	0.500517	0.026006	*CENATAC*	-0.67062	0.039445
POLR2L	0.806888	0.001053	*CHRNA7*	-1.37412	0.026027	*AUP1*	0.4432	0.039446

ZNF680	-1.9152	0.001058	*IFI44*	-0.67945	0.026108	*DLEU1*	-0.55964	0.039506
PADI2	1.24295	0.001067	*RNU5B-1*	0.614698	0.026134	*EMILIN2*	0.758706	0.03963
RPL28	0.772662	0.001079	*TMEM106C*	0.560939	0.026188	*SAMD4A*	0.620792	0.039632
EPS8	-0.84388	0.001096	*CEBPB*	0.587049	0.026292	*ATP1B3*	-0.51229	0.039644
SNORA48	1.091112	0.001143	*PXYLP1*	-0.84371	0.026327	*RASSF6*	-0.74938	0.039742
RAB31	0.824096	0.001164	*IL4R*	0.660539	0.026342	*ERP27*	-2.27864	0.039751
SERF2	0.738774	0.0012	*CFAP44*	-0.64945	0.026366	*BMS1P10*	-1.09755	0.039754
AMFR	0.892168	0.00121	*KCNAB1*	-1.28745	0.0264	*TULP4*	0.518654	0.039804
TFPI2	-8.04685	0.001211	*GET3*	0.614636	0.026465	*PDE7B*	-2.11132	0.039813
OGFRL1	0.753025	0.001239	*CRABP2*	0.596555	0.026525	*FAM3C*	0.486019	0.039877
TXNRD1	0.630443	0.001239	*RPL32*	0.459959	0.026616	*PSMC5*	0.482656	0.039878
RIPK3	-3.69731	0.001243	*DUS4L-BCAP29*	0.932519	0.026633	*LOC105369760*	0.838233	0.039968
CYP4F3	-1.79485	0.001254	*SNORA62*	0.687516	0.026659	*SNORA8*	0.871587	0.04003
DERA	-0.98738	0.001261	*FBXL14*	-0.76334	0.026685	*ABHD2*	-0.54725	0.040069
LY75-CD302	-3.23623	0.001342	*MRPS24*	0.744485	0.026697	*PDE6B*	-1.49093	0.040105
SKIL	-0.72847	0.001351	*GADD45A*	0.625037	0.026827	*BASP1*	0.601123	0.04013
C6orf223	-2.96449	0.001369	*TSHZ2*	-1.55553	0.026834	*SCRN2*	0.662576	0.040148
RPS5	0.756399	0.00137	*APOL3*	0.810619	0.026866	*MRPS15*	0.505479	0.040153
CD14	1.662672	0.001381	*EEF2*	0.482711	0.026925	*IL18*	-0.69007	0.040212
GPX1	0.740951	0.001406	*RNF40*	0.482918	0.026991	*MAP4*	0.444138	0.040304
SP140L	0.738339	0.001443	*CREBBP*	0.462864	0.027033	*ARHGAP25*	1.135074	0.040339
RNU6-36P	1.494225	0.001474	*ETF1*	0.498304	0.027043	*PPP6R1*	0.480602	0.040429
CAMK2N1	-1.04154	0.001475	*ZNF365*	-1.95415	0.027072	*MAN2A1*	0.508965	0.040442
SARM1	-1.50916	0.001475	*PPP4R1*	0.596182	0.02709	*DYNLL2*	0.455891	0.040457
CCN2	1.00147	0.00148	*RNF152*	-1.1223	0.027214	*FAAP20*	0.581842	0.040514
GYG2	-3.59249	0.001483	*MAP2K2*	0.486283	0.027274	*RIC8A*	0.477966	0.04053
PIM1	-1.34599	0.001485	*NDUFA11*	0.634949	0.027325	*BRD3*	0.53238	0.040534

ZNF787	0.810464	0.001491	*ASAH2B*	0.948967	0.02733	*CETN2*	0.572762	0.040553
SDCBP2	-1.50088	0.001501	*BAP1*	0.522774	0.027387	*SMIM11A*	-1.05002	0.040607
SNORA3B	1.024935	0.001501	*CPSF2*	0.551223	0.027549	*PAX8-AS1*	-0.49733	0.040648
FGF14	-2.48093	0.001502	*AGPAT1*	0.539952	0.027551	*RPS27*	0.485642	0.040683
MYL12B	0.73919	0.001518	*NSG1*	-1.35654	0.027557	*NECTIN1*	-0.65506	0.040771
SNORA67	1.594303	0.001558	*SOX7*	0.865202	0.027666	*DNAJC15*	-0.86595	0.040823
SERPINB1	0.707255	0.001566	*SREBF2*	-0.45903	0.027707	*GTF2A1*	0.497465	0.040832
RPL23AP42	0.788316	0.00157	*TNNT1*	0.649821	0.027767	*DDIT4*	0.468335	0.040851
PRXL2A	-0.8837	0.001601	*ZNF891*	-0.86583	0.027819	*MRPL37*	0.512341	0.040869
UBA52	0.734966	0.001637	*CTSA*	0.475245	0.028258	*ZNF607*	-1.1224	0.04096
SLC9A2	-1.17184	0.001647	*LIMA1*	-0.50035	0.02831	*RPL6*	0.42363	0.040981
EPSTI1	-1.77837	0.001654	*PMEPA1*	-3.28795	0.028413	*LAMTOR5*	0.614751	0.040997
DUSP5	0.695221	0.001706	*KIRREL1*	0.606208	0.028443	*COX6B1*	0.503269	0.041108
FGFR2	-1.70308	0.001709	*SRA1*	0.586712	0.028457	*PSMD2*	0.423926	0.041126
ARHGAP42	-0.98512	0.001718	*SNORD116-3*	1.293761	0.028496	*MIR663A*	-0.53573	0.041204
AOC1	-2.33357	0.001727	*SNORA25*	0.9276	0.028504	*MEIS3*	0.691031	0.041248
ITGB4	-0.63717	0.001733	*EIF4A3*	0.545128	0.028508	*ENY2*	0.508893	0.04129
FTH1	0.716595	0.001733	*INSIG2*	-0.6962	0.028551	*HMGA1*	0.404608	0.041292
ZNF160	-1.51451	0.001742	*UBC*	0.430941	0.028583	*G6PC3*	0.521729	0.041393
PRNP	0.684328	0.00175	*ZNF668*	0.946312	0.028633	*YY1*	0.521864	0.041535
SQSTM1	0.641148	0.001769	*LCN2*	0.600256	0.028681	*CTNNAL1*	0.487857	0.041584
PADI3	0.780085	0.001781	*PSMB10*	0.74557	0.028688	*MZF1*	-0.7578	0.041622
GSTM4	-1.87371	0.001792	*SERPINA1*	0.890308	0.028693	*C9orf72*	0.792511	0.041638
ZNF30	-2.7749	0.001829	*ATP5F1D*	0.632257	0.028755	*IMPDH2*	0.458949	0.041695
ADCY5	-3.93497	0.001843	*RNF14*	0.54788	0.028814	*YWHAB*	0.431288	0.041745
ZNF808	-2.10685	0.001859	*AIF1L*	0.605832	0.028861	*SNORA84*	1.055972	0.041764
COPE	0.714119	0.001862	*NFATC3*	0.500514	0.028959	*STING1*	0.629888	0.041811

JPH2	-2.1833	0.001864	*CDC42SE2*	0.515978	0.029006	*LRRC8C*	0.672273	0.041937
GJB4	-3.37035	0.001922	*PIK3AP1*	0.800204	0.029135	*USH2A*	-1.75902	0.041955
FOXM1	-0.74126	0.001947	*DNAH12*	-1.4243	0.029142	*VWA5A*	-0.83913	0.041957
RABGAP1L	-0.73348	0.001961	*DISP2*	-0.77959	0.029209	*ZNF114*	0.924763	0.041959
EPHA4	-1.21666	0.001967	*RNF43*	-2.70289	0.029231	*ALAS1*	0.468996	0.041976
ZNF440	-1.47085	0.001976	*ATR*	-0.52043	0.029231	*IL20RA*	-1.19082	0.04199
SERPINE2	-0.97524	0.001977	*DSE*	0.616514	0.029236	*CEP126*	-0.84779	0.042024
TSC22D2	-0.70566	0.00202	*RAB13*	0.553644	0.029294	*PLSCR1*	-0.54916	0.042069
ALDH3B1	0.703938	0.002033	*KCTD3*	-0.60216	0.02932	*HNRNPC*	0.437724	0.042143
FOXP1	-0.84759	0.002051	*CSTB*	0.551019	0.029371	*MBD3*	0.540603	0.042241
BCAS1	-1.39934	0.002064	*ABL1*	0.528553	0.029386	*BRD7*	0.472536	0.042263
ALDH3A2	-0.67785	0.002068	*NAPSA*	-2.46956	0.029406	*RPL38*	0.511862	0.042278
IGFBP5	-1.86696	0.002121	*KLHL5*	0.522553	0.029423	*SART1*	0.510203	0.042346
FBLN1	-1.4794	0.002125	*COLGALT1*	0.477587	0.029663	*PSMB7*	0.484123	0.0424
EIF5AL1	1.168101	0.002131	*MYADM*	0.503462	0.029683	*C1S*	0.709	0.042407
TOP1	0.602793	0.002172	*AHCY*	0.474764	0.029702	*ADIRF*	-6.43239	0.04246
TREM1	1.087712	0.002192	*RIN3*	-1.3078	0.029759	*PLEKHG3*	0.54047	0.042506
ST8SIA3	-4.25398	0.002206	*OFD1*	-0.63161	0.029826	*CYC1*	0.495593	0.042645
LPIN2	0.857622	0.002229	*ADIPOR2*	-0.56707	0.029857	*ECI1*	0.541314	0.042774
MCTP1	1.069287	0.002249	*C6orf62*	0.474316	0.029862	*FAM89B*	0.70949	0.042777
RPL19	0.607169	0.002273	*BMP4*	-0.83182	0.029862	*CSNK1A1*	0.446439	0.042968
SCARNA1	1.404858	0.002277	*ANP32E*	0.5195	0.029866	*TBC1D2*	0.592125	0.043062
ZNF880	-2.44809	0.002288	*CEP128*	0.624723	0.029871	*WNK1*	-0.46221	0.04311
SNORD46	1.024779	0.002306	*TNFSF15*	0.558604	0.029954	*CAVIN2*	0.818686	0.043138
GDA	-0.999	0.002334	*TRDMT1*	-0.96168	0.029956	*LINC01485*	-1.65036	0.043285
ARFGEF3	-0.80864	0.002344	*EFNA1*	0.7907	0.029957	*RNF167*	0.496017	0.043345
IRAG2	-4.70186	0.002348	*PLIN3*	0.529282	0.030035	*FGD4*	-0.55191	0.04337

FZD3	-1.16447	0.002424	*RASA4B*	0.861393	0.030087	*C4A*	0.718355	0.043404
CREG2	-1.53298	0.00244	*ZNF888*	-1.02342	0.030141	*MTRNR2L1*	0.669367	0.043431
RNF43	-0.91325	0.002466	*KIAA0930*	0.555641	0.030252	*KCNRG*	-2.57746	0.043432
TMEM97	-1.06605	0.002483	*PSMA4*	0.477157	0.030333	*USP11*	0.495971	0.043439
HLA-A	0.608698	0.002486	*PPFIBP2*	-0.63326	0.030375	*LRRC4*	1.268335	0.043486
CAPN5	-0.98522	0.002505	*CUTA*	0.585538	0.030397	*SDF4*	0.464908	0.043592
LYPD3	-1.85914	0.002514	*COMT*	0.543647	0.030427	*PPP2R5E*	0.525795	0.043621
RPL36A	0.667428	0.002529	*LONP1*	0.512328	0.030504	*RPL17-C18orf32*	0.783297	0.043715
CARD6	-1.12938	0.002539	*SNORA17B*	0.824652	0.030588	*DDX21*	0.417432	0.04373
SNORD10	0.833264	0.002566	*USPL1*	-0.69674	0.030614	*LSR*	0.498845	0.043751
NEFL	-2.86441	0.002602	*VDAC1*	0.490265	0.030642	*SNORA37*	1.441696	0.043843
CACNA1C	-2.05104	0.00261	*BSG*	0.459566	0.030802	*NBPF10*	-0.51912	0.043872
PPP2R2C	-1.41533	0.002612	*MMRN2*	0.642512	0.030943	*TOMM34*	0.508018	0.043904
BAG3	0.662939	0.002612	*AHDC1*	0.548464	0.031019	*SNORA1*	1.11089	0.043964
SEMA4G	-1.67252	0.002631	*ISM1*	1.466906	0.031142	*PSMA3*	0.496409	0.043967
NPC1L1	-3.09701	0.002636	*FKBP8*	0.492657	0.031211	*RPL9*	0.54534	0.043981
HLA-E	0.626904	0.002643	*ATP5IF1*	0.540815	0.031234	*ERP29*	0.460523	0.044039
RNU5A-1	0.837262	0.002684	*CKB*	0.679307	0.031366	*AK6*	0.612889	0.044041
EGR1	0.896519	0.002689	*RIPOR1*	0.594241	0.031481	*KCTD5*	0.606671	0.044095
RGPD6	-0.67617	0.002693	*C15orf48*	0.727167	0.031612	*TUBB*	0.408607	0.044124
RPL37P6	1.87558	0.002706	*DLC1*	0.789855	0.031638	*ZNF253*	-2.02537	0.044198
MCTP2	-1.0868	0.002732	*MBD2*	0.527589	0.031646	*MYO5C*	-0.45029	0.04433
ALKBH7	1.121053	0.002757	*ZKSCAN1*	0.477211	0.031679	*PINK1*	-0.61042	0.044336
HLA-B	0.612749	0.002784	*OTUD3*	-0.66167	0.031777	*NRIP2*	-1.28195	0.044472
MYC	0.660726	0.002812	*HR*	-1.04842	0.031788	*CCL2*	1.072912	0.044531
CPNE2	0.821306	0.002842	*CDYL2*	-1.52808	0.031817	*ZBTB21*	0.588758	0.044592
ZC3H12A	0.738019	0.002847	*FAT1*	-0.46876	0.031833	*CLTA*	0.467567	0.04462

IGSF9B	-1.64519	0.002857	*PPP4C*	0.528152	0.031864	*ADAM12*	1.715945	0.044663
CCDC191	-1.00582	0.002892	*CNOT3*	0.614902	0.031874	*ASPM*	-0.46229	0.044699
CRYBG2	-1.05584	0.002927	*FAHD1*	0.567112	0.031968	*GJB3*	-0.92794	0.044718
CAVIN1	0.737151	0.00294	*PHF23*	0.566957	0.031989	*MYO7A*	0.608404	0.044798
ANKRD10	-0.66195	0.002942	*HNF4A*	-0.90764	0.03203	*IFIT2*	0.446234	0.044802
CTSV	-1.11347	0.00295	*SYNE3*	0.703481	0.032052	*SMPD1*	0.658125	0.04482
FXYD5	0.784138	0.002979	*ARMH4*	-1.86163	0.032098	*PIM3*	0.5685	0.044861
APRT	0.781894	0.003009	*SLC16A10*	-1.32482	0.032187	*CRKL*	0.470097	0.044865
IRF1	0.852348	0.003043	*TTC1*	0.489083	0.032266	*PRSS8*	0.497944	0.044883
ARL10	-1.27865	0.003049	*ARL6IP4*	0.492844	0.032363	*ATG2B*	-0.61099	0.044889
TBK1	-0.69597	0.00307	*TMSB4X*	0.488834	0.032379	*PERP*	-0.53717	0.044916
IFITM2	0.83038	0.003076	*AKNA*	-0.73165	0.032382	*DNPH1*	0.778205	0.044951
MRPS34	0.752693	0.003077	*RNF123*	0.566689	0.032384	*ZNF460*	0.527042	0.044966
ERC1	-0.72528	0.003089	*CCT7*	0.473199	0.032458	*TM2D2*	-0.72354	0.045018
BORCS5	1.270445	0.003116	*SNORA49*	0.590329	0.032473	*TRPM8*	-1.59087	0.045046
MGAT3	-3.103	0.003253	*TSC22D4*	0.565249	0.032588	*EIF4H*	0.433184	0.04509
CD274	0.931704	0.003267	*JUNB*	0.575486	0.032664	*DPP3*	0.53175	0.045103
RHOV	0.880065	0.003352	*HEG1*	0.720542	0.032687	*FYN*	0.606267	0.045129
IQSEC3	-2.89191	0.003371	*LIF*	0.638378	0.032718	*LENG1*	0.614157	0.045184
AMZ2	0.677211	0.003377	*GBA*	0.618906	0.032736	*MAN2A2*	-0.54452	0.0452
SLC39A4	-1.27139	0.003386	*ZNF581*	0.661012	0.032952	*ZFP36L2*	-0.55884	0.04521
RNA5SP335	1.960835	0.003398	*BLOC1S1*	0.632143	0.032995	*MAPK1*	0.46243	0.045241
MPZL2	-0.90394	0.003462	*NIPAL2*	-0.9289	0.03303	*SNORD116-16*	1.158247	0.045416
CHN2	-1.38602	0.003489	*DNAH5*	-0.92738	0.033039	*GUCY1A1*	-1.37664	0.045498
MELTF	0.730911	0.003497	*NEDD8*	0.519517	0.033103	*IGFN1*	1.421259	0.045516
ITFG2	-1.0157	0.003508	*ABCA4*	-2.05413	0.033108	*RPS2P46*	-2.50421	0.045547
KLHDC7A	-1.67617	0.003531	*HCLS1*	0.745341	0.033112	*KIAA1143*	0.551824	0.045623

CD83	0.983075	0.003596	*XBP1*	-0.56581	0.033142	*CABIN1*	0.506732	0.045631
FAM227A	-1.09683	0.003607	*INAVA*	-0.67099	0.033205	*CD82*	0.511228	0.045655
IL6	1.285953	0.003613	*RBM27*	0.507195	0.033266	*MKNK2*	0.494151	0.04575
SLC4A2	0.68769	0.003625	*LINC00632*	-0.92627	0.03327	*NDUFA3*	0.612463	0.045763
ABCG2	-1.02342	0.003644	*SMARCD2*	0.515893	0.033286	*GM2A*	0.554377	0.045861
FCGRT	-1.52924	0.003651	*ATG9B*	-1.47407	0.033454	*SLC2A4RG*	0.53136	0.046015
CST4	-9.54636	0.003653	*MEGF9*	-0.70704	0.033454	*LIMK1*	0.525358	0.046092
KICS2	-1.2617	0.003689	*COX8A*	0.609968	0.033502	*RBM8A*	0.453615	0.046106
LASP1	0.613511	0.003703	*DDX60*	-0.67994	0.03355	*COL4A4*	-0.86073	0.046157
RSL1D1	0.623172	0.003715	*EIF6*	0.542869	0.03356	*HOXA13*	-2.16765	0.04618
SUMF1	-0.94028	0.003754	*PGLS*	0.594655	0.033588	*ASDURF*	-3.18237	0.046189
SEMA5A	-2.06726	0.003789	*SNORA64*	1.243812	0.033604	*MTHFD1*	0.495136	0.046196
EIF3CL	-6.232	0.003795	*PCNX3*	0.471406	0.033629	*NUDT16L1*	0.678823	0.046242
LINC00205	0.773904	0.003799	*MOCOS*	-0.71889	0.033679	*FTSJ3*	0.436162	0.046331
ECHDC3	-3.28487	0.003815	*ARHGEF17*	0.538647	0.033759	*TM7SF2*	0.491842	0.046409
MESP1	2.002511	0.003816	*FUT9*	-1.71538	0.034102	*SNTB1*	0.559009	0.046429
ZNF28	-1.32623	0.003847	*LINC02381*	-1.67101	0.034227	*IFI30*	0.635798	0.046455
GATA3	-1.30918	0.003861	*B3GNT5*	0.488239	0.034244	*SRM*	0.542928	0.046506
MYL12A	0.753233	0.003878	*TSEN34*	0.610623	0.034286	*XPC*	-0.50145	0.046598
S100A9	0.731499	0.003881	*PPM1G*	0.43574	0.034307	*HLA-DRB1*	0.502226	0.046602
TMEM39A	-0.88038	0.003894	*ARTN*	1.530665	0.034397	*CD2AP*	-0.41607	0.046626
CASC9	1.049877	0.003902	*STAMBP*	0.512359	0.034441	*EIF3FP3*	0.825488	0.046639
RPS14	0.664005	0.00391	*UCA1*	0.498806	0.03447	*LOC102724434*	-1.70545	0.046726
PDK1	-0.96039	0.003961	*PRR15*	-0.77577	0.034542	*ZNF682*	-2.48972	0.046786
SYT7	0.802867	0.003989	*PCBP1*	0.453365	0.03461	*TMTC1*	-0.97148	0.046839
CD74	0.610669	0.004001	*B3GNT7*	-1.25573	0.034681	*RNF166*	0.885572	0.046929
PNPLA3	-1.18773	0.004026	*FDFT1*	-0.45095	0.034703	*TTC5*	0.553626	0.046978

TM4SF1	-0.8535	0.004045	*DYNLT1*	0.550475	0.034866	*NABP1*	0.494544	0.04701
HSPA9	0.643371	0.004048	*JAK1*	0.468228	0.034894	*ABHD4*	-0.53171	0.047326
RIOK3	-0.72398	0.004052	*SNORD71*	1.371179	0.034897	*PHACTR3*	-1.6124	0.047373
HIF1A	0.669413	0.004068	*PSMB3*	0.502369	0.034965	*NMT1*	0.419281	0.047382
FLRT3	-1.1945	0.004103	*KIF1C*	0.521697	0.034987	*LINC02449*	-0.86267	0.0475
UBLCP1	0.721607	0.004106	*GBP4*	0.630629	0.034999	*SLC16A14*	0.660799	0.047522
PSME2	0.684591	0.004126	*DUXAP10*	0.490114	0.035063	*PDE3A*	-1.15129	0.047589
IKBKB	-0.77817	0.004152	*SARS1*	0.488833	0.035072	*LARP6*	0.637439	0.047603
CNTRL	-0.85439	0.004192	*CRIM1*	0.481136	0.035162	*AFAP1-AS1*	0.58153	0.04767
ALCAM	0.662656	0.00421	*DCAF4*	-0.77321	0.035163	*MON1B*	0.493756	0.047733
LSAMP	-1.4228	0.004221	*DHCR24*	0.462835	0.035176	*RASSF2*	-0.95386	0.047775
HOXB3	-1.05031	0.004259	*RPSA*	0.424324	0.035323	*H2BC7*	-1.428	0.047834
CA5B	-0.96482	0.004282	*ACTG1*	0.405768	0.035341	*GTF3A*	-0.50081	0.047889
SLC40A1	-1.35903	0.004285	*USF2*	0.528168	0.035348	*WASF3*	-1.76224	0.047944
HMOX1	0.784556	0.00429	*PHAX*	0.552981	0.035452	*ELOB*	0.523875	0.047968
DDX11L2	-3.42147	0.004375	*ACO2*	0.475904	0.035483	*AOPEP*	-0.76805	0.047983
RPL14	0.581394	0.004387	*BORA*	-0.85269	0.035538	*TNFRSF1A*	0.470511	0.047994
IK	0.579974	0.004408	*H1-3*	0.591087	0.035661	*EIF4G1*	0.398503	0.048113
ALDH1L2	0.992015	0.00445	*KRBA2*	-0.60132	0.035674	*TXNIP*	-0.47973	0.0482
ANKRD12	0.733732	0.004571	*RAB15*	-0.69734	0.035773	*FAM50A*	0.468866	0.048219
RPL5	0.57136	0.00458	*ZNF274*	-0.62279	0.035867	*RABL6*	0.453145	0.048367
PTMS	0.712805	0.004594	*PPP1R3E*	-0.99512	0.035876	*DDA1*	0.620105	0.048442
KIAA0408	5.722235	0.004606	*ZNF750*	-1.7521	0.0359	*LOC101927556*	0.841707	0.048488
RAB3D	0.664415	0.004665	*MMP24OS*	0.530869	0.035905	*ZNF317*	0.549031	0.048503
NSA2	0.669296	0.004695	*MID1IP1*	0.535298	0.035973	*SNORD116-24*	1.28078	0.048557
MUC20	-0.74876	0.004702	*RAPH1*	-0.53453	0.03599	*TLN1*	0.397739	0.048582
CARD11	-1.02329	0.004708	*SLC22A18*	0.641707	0.036046	*ZNF860*	-1.13273	0.048689

MUC13	-1.52687	0.004728	*LAIR1*	0.750113	0.036055	*FECH*	0.619362	0.048714
CITED2	0.715704	0.004739	*EFEMP1*	-1.83652	0.036071	*FERMT2*	0.607277	0.048735
RPL13	0.625126	0.004768	*HERC3*	-0.87287	0.036096	*THG1L*	0.607705	0.048763
DMRTA1	-1.97319	0.004787	*SLC35F6*	0.525148	0.036105	*TRERF1*	-0.54921	0.04879
TECR	0.65259	0.004883	*CBFB*	0.543961	0.036248	*ZSWIM6*	0.468195	0.048831
ZNF585B	-0.9832	0.004898	*TMF1*	-0.60217	0.036251	*PIGO*	0.546555	0.048878
RNF187	0.678097	0.004908	*ELL3*	0.945362	0.036261	*TMC6*	0.511445	0.048882
DNAJA1	0.605377	0.004959	*ATIC*	0.484713	0.036298	*IDH3B*	0.500969	0.049014
PSMA6	0.632266	0.004978	*PPP1R26*	0.543243	0.036386	*CTNNB1*	0.403014	0.049118
RN7SL1	0.702121	0.004999	*P4HB*	0.403277	0.036433	*SNORA36A*	1.374006	0.049135
RPS27A	0.575552	0.005013	*TPD52L2*	0.461082	0.036458	*ASAP3*	0.620602	0.049206
DCAF12	0.6535	0.005071	*TNKS1BP1*	0.521161	0.036515	*ST6GALNAC3*	1.31522	0.049303
AIG1	0.751186	0.00508	*HOXA1*	-1.91703	0.036527	*SDC1*	0.492468	0.049308
C5orf24	0.690525	0.005127	*OLFML2A*	-0.95258	0.036656	*COBL*	-0.60556	0.049327
PLEKHA6	-0.6991	0.005129	*CCT5*	0.477404	0.036696	*RPLP2*	0.424508	0.049354
RAB11FIP3	0.738335	0.005145	*PTPRM*	0.60615	0.036762	*SLC1A4*	0.53865	0.049448
LRP3	-2.69695	0.005162	*LONRF2*	-0.73069	0.036787	*MTPN*	0.433274	0.04948
FABP4	-3.78789	0.005173	*BCL2L14*	-1.12885	0.036808	*DKC1*	0.451979	0.049494
XDH	0.606731	0.005178	*TESK1*	0.550216	0.036826	*CARD19*	0.668745	0.049517
GAS2L3	-0.87847	0.005233	*VPS13A*	-0.45982	0.036856	*IGBP1*	0.483282	0.049527
MB	1.107981	0.005247	*ATP5F1E*	0.462191	0.036866	*EFCAB2*	0.831716	0.049663
SORL1	-0.70951	0.005254	*GET1-SH3BGR*	-1.91235	0.036874	*H4C14*	0.495643	0.049747
DGKA	-0.85703	0.005275	*GSDMB*	-0.60632	0.036888	*BCKDK*	0.577683	0.049814
DYNLRB1	0.716813	0.005298	*RNU4-1*	0.524185	0.03691	*RPL4P4*	-2.03944	0.04982
RNF181	0.731704	0.005306	*MLLT10*	-0.55726	0.036951	*STK24*	0.417022	0.049851
AXL	0.728353	0.005332	*ARHGAP24*	1.225796	0.037049	*LOC102723996*	0.640044	0.049897
PRSS22	0.782372	0.005343	*HNF1A-AS1*	-1.09323	0.037056	*TIGAR*	0.706358	0.049916

RAP2B	-0.67495	0.005348	*MBOAT7*	0.586331	0.037127	*ECT2*	-0.41726	0.049939
C5orf15	0.505699	0.049982	*SDC4*	0.465513	0.049989			